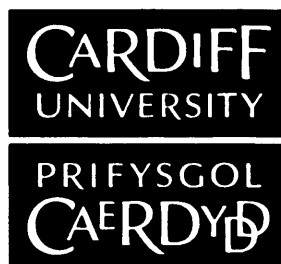


**Cardiff University**  
**School of Chemistry**



**EXPANDED RING CARBENES – SYNTHESIS,  
COORDINATION AND CATALYSIS**

**Thesis submitted for the degree of Doctor of Philosophy by:**

**Manuel Iglesias Alonso**

**Supervisors: Dr. A. Dervisi, Dr. I. A. Fallis, Prof. K. J. Cavell**

**Department of Chemistry**

**Cardiff University**

**July 2008**

UMI Number: U585105

All rights reserved

INFORMATION TO ALL USERS

The quality of this reproduction is dependent upon the quality of the copy submitted.

In the unlikely event that the author did not send a complete manuscript and there are missing pages, these will be noted. Also, if material had to be removed, a note will indicate the deletion.



UMI U585105

Published by ProQuest LLC 2013. Copyright in the Dissertation held by the Author.  
Microform Edition © ProQuest LLC.

All rights reserved. This work is protected against  
unauthorized copying under Title 17, United States Code.



ProQuest LLC  
789 East Eisenhower Parkway  
P.O. Box 1346  
Ann Arbor, MI 48106-1346

## ***ACKNOWLEDGEMENTS***

Firstly, I would like to thank my supervisors: Professor Kingsley J. Cavell for all his good advice, infinite patience and especially for setting an example for me to follow, Dr Nancy Dervisi for always being available whenever I needed her help or guidance and Dr Ian Fallis for his support in the difficult beginnings.

Especial thanks must go to Dr Dirk J. Beetstra who gave a big boost to this project when it was most needed.

I am lucky to say that it is impossible to name all those who have been of help, who supported me and with whom I shared enjoyable moments in Cardiff. However, I could not fail to thank the old crew: Lino, Grazia, Frenchie, Dave, Debs, Eugene, Caterina, Dirk, Mark, Eli, Txell and those who joined us later: Vincenzo, Richard, Anabel, Paula, Massimo, Vero and Niek for all the good moments in the pub, parties, trips... and even at the department.

My thanks also go to all the past and present members of lab 2.94 (2.91) who I worked with. It was a pleasure to work with you guys.

I can not thank enough Vane for standing me for so many years, especially during the writing-up of this thesis, and my siblings, Bea, Silvia and Iván, for having done so since the moment of their birth.

Finally, I would like to dedicate this thesis to my parents for the extraordinary efforts that they had to make to bring us up.

## ABBREVIATIONS

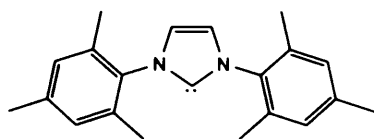
Å	Angstroms
acac	Acetylacetonate
Ar	Aryl
Atm	Atmosphere
Av	Average
bs	Broad singlet
bd	Broad doublet
bt	Broad triplet
Bu	Butyl
ca	<i>Circa</i>
CAAC	Cyclic alkyl(amino)carbene
cm	Centimetre
C <sub>NHC</sub>	Carbenic carbon
COD	1,5-Cyclooctadienyl
conc	Concentrated
Cy	Cyclohexyl
d	Doublet
δ	Chemical shift (in ppm)
DCE	Dichloroethane
DCM	Dichloromethane
dd	Doublet of doublets
ddd	Doublet of doublets of doublets
DIPP	Diisopropylphenyl
DME	Dimethoxyethane
DMF	N,N'-Dimethylformamide
DMSO	Dimethylsulphoxide
<i>e.g.</i>	<i>Exempli gratia</i> (for example)
Eq	Equivalent
ES-MS	Electrospray mass spectrometry
<i>et al.</i>	<i>Et alii</i> (and others)

Et <sub>2</sub> O	Diethyl ether
g	Gram
h	Hour or heptet
HOMO	Highest occupied molecular orbital
HPLC	High pressure liquid chromatography
HRMS	High resolution mass spectrometry
hν	Irradiation with light
Hz	Hertz
<i>i</i> -Pr	<i>Iso</i> -propyl
IR	Infrared spectroscopy
K[HMDS]	Potassium hexamethyldisilazide
L	Ligand
LDA	Lithium diisopropylamide
LUMO	Lowest unoccupied molecular orbital
m	Multiplet
<i>m</i>	<i>Meta</i>
m.p.	Melting point
MCPBA	<i>Meta</i> -Chloroperoxybenzoic acid
Me	Methyl
Mes	Mesityl (1,3-trimethylphenyl)
mg	Milligram
MHz	Megahertz
min	Minute
ml	Millilitre
mmol	Millimol
ν	Wavenumber
nbe	Norbornene
NBS	<i>N</i> -Bromosuccinimide
<i>n</i> -BuLi	<i>n</i> -Butyllithium
NHC	N-heterocyclic carbene
nm	Nanometres
NMR	Nuclear magnetic resonance
<i>o</i>	Ortho

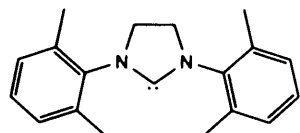
OAc	Acetate
ORTEP	Oak-Ridge thermal ellipsoid plot
°C	Degrees Celsius
<i>p</i>	Para
p	Pentet
Ph	Phenyl
ppm	Parts per million
<i>p</i> -TsOH	<i>Para</i> -toluenesulphonic acid
q	Quartet
quint	Quintet
R	Alkyl or aryl
rbf	Round bottom flask
RCM	Ring closure metathesis
ref	Reference
ROMP	Ring opening metathesis polymerisation
rt	Room temperature
s	Singlet
sept	Septet
t	Triplet
<i>t</i> -Bu	<i>Tert</i> -butyl
THF	Tetrahydrofurane
TLC	Thin layer chromatography
TMS	Trimethylsilyl
TOF	Turnover frequency
Tol	Tolyl
TON	Turnover number
Ts	Tosyl ( <i>p</i> -toluenesulfonyl)
UV	Ultraviolet
Xyl	Xylyl

## Carbenes

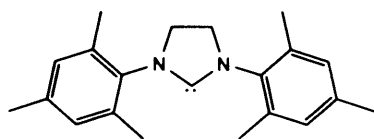
**IMes**



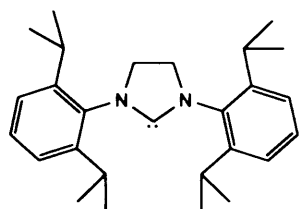
**5-Xyl**



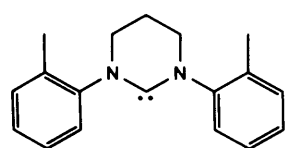
**5-Mes**



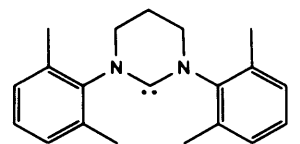
**5-DIPP**



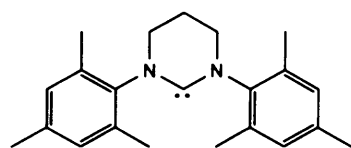
**6-Tol<sup>o</sup>**



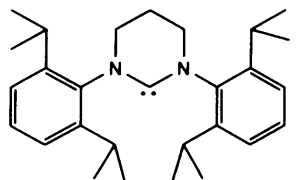
**6-Xyl**



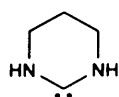
**6-Mes**



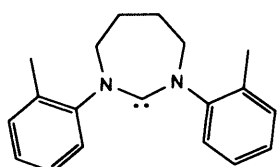
**6-DIPP**



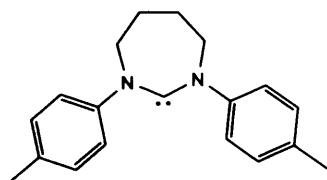
**6-H**



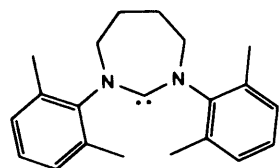
**7-Tol<sup>o</sup>**



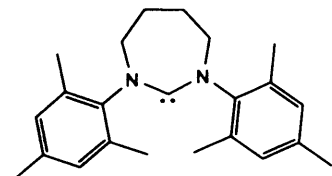
**7-Tol<sup>P</sup>**



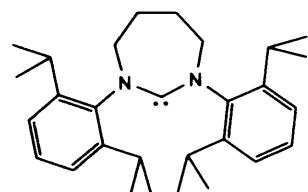
**7-Xyl**



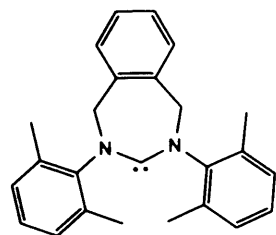
**7-Mes**



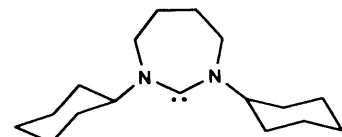
**7-DIPP**



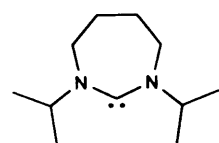
**Xyl7-Xyl**



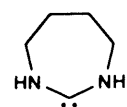
**7-Cy**



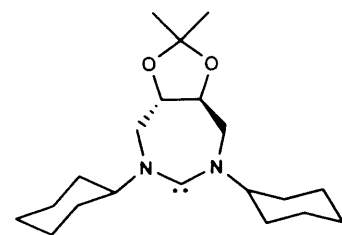
**7-<sup>i</sup>Pr**



**7-H**

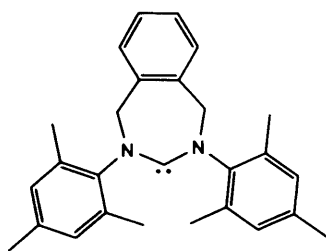


**7-DIOC**

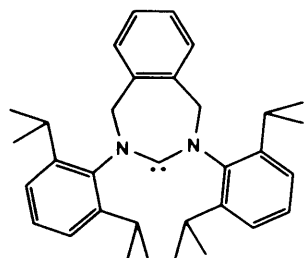




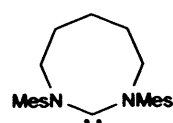
**Xyl7-Mes**



**Xyl7-DIPP**



**8-Mes**



## ***ABSTRACT***

The work presented in this thesis is mainly concerned with the synthesis, metal coordination and applications of expanded (larger than five-membered) N-heterocyclic carbenes.

Chapter two describes the spectroscopic and solid state properties of novel 7-membered carbenes and their parent azolium salts bearing a simple or substituted butane backbone with Cy, *i*-Pr, DIPP, Mes, Xyl and *o*-Tol N-substituents. A new method for the synthesis of saturated azolium salts, using K<sub>2</sub>CO<sub>3</sub> as a mild base for the deprotonation of the corresponding formamidines, reacted with di-electrophiles under aerobic conditions, is also presented.

In chapters three and four the syntheses, solid-state and solution studies of their silver, rhodium, iridium and platinum complexes are discussed. Expansion of the ring provides carbenes with N-C<sub>NHC</sub>-N angles close to the sp<sup>2</sup> angle (120°), which consequently forces the N-substituents to bend towards the metal centre. Additionally, expanded carbenes were found to be more basic than their five-membered analogues.

Chapter five describes the synthesis of seven-membered azolium salts with an alkenic function in the C(5)-C(6) position. The olefinic backbone was further functionalised by Diels-Alder reaction with cyclopentadiene. The rhodium complexes, [Rh(NHC)(CO)acac], of these carbenes are also presented in this chapter.

The greater donor abilities and wide NCN angles of the expanded carbenes make them interesting candidates for the study of their catalytic applications. In the sixth chapter results are presented from the catalytic performance of 7-NHC rhodium and iridium complexes in the transfer hydrogenation of ketones. The rhodium complexes of 5-, 6- and 7-membered carbenes were also tested as catalysts in olefin hydrogenation reactions with molecular hydrogen.

## TABLE OF CONTENTS

<b>1. Introduction</b> .....	<b>1</b>
<i>1.1. Definition of a carbene</i> .....	<b>2</b>
<i>1.2. Historical overview</i> .....	<b>2</b>
<i>1.3. Ground-state spin multiplicity of carbenes</i> .....	<b>5</b>
<i>1.3.1. Factors that can dictate the ground-state multiplicity of carbenes</i> .....	<b>5</b>
<i>1.3.1.1. Electronic factors</i> .....	<b>5</b>
<i>1.3.1.2. Steric Effects</i> .....	<b>7</b>
<i>1.3.2. Effects of the ground-state multiplicity in the reactivity of carbenes</i> .....	<b>7</b>
<i>1.3.2.1. Reactivity and stability of triplet carbenes</i> .....	<b>8</b>
<i>1.3.2.2. Reactivity and stability of singlet carbenes</i> .....	<b>11</b>
<i>1.4 Types of aminocarbenes</i> .....	<b>18</b>
<i>1.5. N-heterocyclic carbenes</i> .....	<b>21</b>
<i>1.5.1. Electronic properties</i> .....	<b>21</b>
<i>1.5.2. Steric properties</i> .....	<b>23</b>
<i>1.5.3. Coordination chemistry of NHC's</i> .....	<b>24</b>
<b>2. Synthesis of novel expanded-ring N-heterocyclic carbenes</b> .....	<b>30</b>
<i>2.1. Introduction</i> .....	<b>31</b>
<i>2.2. Results and Discussion</i> .....	<b>34</b>
<i>2.2.1. Synthesis of azolium salts from diamines</i> .....	<b>34</b>
<i>2.2.1.1. Synthesis of the diamines <i>N,N'</i>-dicyclohexyl-1,4-diaminobutane (2.4) and (-)-trans-4,5-Bis[<i>N</i>-Cyclohexyl]-2,2-dimethyl-1,3-dioxolan (2.5)</i> .....	<b>34</b>
<i>2.2.1.2. Synthesis of 1,3-diazepan-2-ylidene derivatives 7-Cy·HPF<sub>6</sub> and DIOC-Cy·HPF<sub>6</sub></i> .....	<b>39</b>
<i>2.2.1.3. X-Ray analysis</i> .....	<b>41</b>
<i>2.2.1.4. Deprotonation experiments of 1,3-diazepan-2-ylidene derivatives 7Cy·HPF<sub>6</sub> and DIOC-Cy·HPF<sub>6</sub></i> .....	<b>45</b>
<i>2.2.1.5. Synthesis of <i>N,N</i>-dihydrodiazepene salts</i> .....	<b>46</b>
<i>2.2.2. A new method of ring-closure</i> .....	<b>47</b>
<i>2.2.2.1. Synthesis of halide salts</i> .....	<b>47</b>
<i>2.2.2.2. Exchange of the counter anion - Formation of tetrafluoroborate salts</i> .....	<b>50</b>

2.2.2.3. <i>Solution NMR studies</i> .....	52
2.2.2.4. <i>Isolation of free carbenes</i> .....	53
2.2.2.5. <i>Properties and structure of expanded free carbenes</i> .....	55
<b>2.3. Experimental</b> .....	<b>59</b>
2.3.1. <i>Synthesis of azolium salts from diamines</i> .....	60
2.3.1.1. <i>First approach</i> .....	60
2.3.1.2. <i>Second approach</i> .....	62
2.3.2. <i>New method</i> .....	67
2.3.3. <i>Isolation of free carbenes</i> .....	83
<b>3. Synthesis and structure of silver (I) carbenes</b> .....	<b>87</b>
3.1. <i>Introduction</i> .....	88
3.2. <i>Results and Discussion</i> .....	91
3.2.1. <i>Synthesis of silver (I) carbenes</i> .....	91
3.2.2. <i>Solid-state structure of silver (I) carbenes</i> .....	93
3.2.2.1. <i>Changes upon coordination</i> .....	93
3.2.2.2. <i>Comparison between 5-, 6-, and 7-membered silver (I) carbenes</i> .....	95
3.2.2.3. <i>Effects of the substitution on the backbone in the solid-state structure of silver (I) carbenes</i> .....	98
3.2.3. <i>Behaviour of silver (I) carbenes in solution</i> .....	100
3.2.4. <i>Expanded carbenes as transfer agents</i> .....	103
3.3. <i>Experimental</i> .....	104
<b>4. Complexes of expanded-ring N-heterocyclic carbenes</b> .....	<b>110</b>
4.1. <i>Introduction</i> .....	111
4.2. <i>Results and discussion</i> .....	114
4.2.1. <i>Complexation of cyclohexyl derivatives</i> .....	114
4.2.1.1. <i>Synthesis of the [Pt(7-Cy)(nbe)<sub>2</sub>] complex</i> .....	114
4.2.1.2. <i>Solid state structure of the [Pt(7-Cy)(nbe)<sub>2</sub>] complex</i> .....	115
4.2.1.3. <i>Rhodium(I) and Iridium(I) COD complexes</i> .....	117
4.2.1.4. <i>Solid state structures of Rh(I) and Ir(I) COD complexes</i> .....	120
4.2.1.5. <i>Rhodium(I) and Iridium(I) biscarbonyl complexes</i> .....	124
4.2.1.6. <i>Solid state structure of Rh(I) and Ir(I) biscarbonyl complexes</i> .....	126

4.2.1.7. <i>Solution NMR studies</i> .....	127
4.2.2. <i>Complexation of aromatic derivatives</i> .....	129
4.2.2.1. <i>Rh(I)COD complexes</i> .....	129
4.2.2.2. <i>Rhodium(I) carbonyl complexes</i> .....	134
<b>4.3. <i>Experimental</i></b> .....	<b>137</b>
<b>5. <i>Functionalisation of the carbene backbone</i></b> .....	<b>147</b>
<b>5.1. <i>Introduction</i></b> .....	<b>148</b>
<b>5.2. <i>Results and discussion</i></b> .....	<b>151</b>
5.2.1. <i>Synthesis and deprotonation experiments of 1,3-Bis-(2,4,6-trimethylphenyl)-4,7-dihydro-3H-[1,3]diazepin-1-ium tetrafluoroborate (5.7) and 1,3-Bis-(2,6-diisopropylphenyl)-4,7-dihydro-3H-[1,3]diazepin-1-ium tetrafluoroborate (5.8)</i> .....	151
5.2.2. <i>Reactivity of the alkenic backbone</i> .....	154
5.2.2.1. <i>Attempts of epoxidation</i> .....	155
5.2.2.2. <i>Reactivity towards Diels-Alder cycloaddition</i> .....	159
5.2.3. <i>Coordination chemistry of the functionalised amidinium salts 5.11 and 5.12</i> .....	163
5.2.3.2. <i>Synthesis of silver complexes</i> .....	163
5.2.3.2. <i>Synthesis of rhodium complexes</i> .....	163
5.2.3. <i>Self-catalytic-hydrogenation of complex 5.15</i> .....	171
<b>5.3. <i>Experimental</i></b> .....	<b>173</b>
<b>6. <i>Catalytic Hydrogenation and Transfer Hydrogenation reactions</i></b> .....	<b>181</b>
<b>6.1. <i>Introduction</i></b> .....	<b>182</b>
6.1.1. <i>Reduction of ketones</i> .....	182
6.1.1.1. <i>Direct hydrogen transfer</i> .....	183
6.1.1.2. <i>Hydridic route</i> .....	183
6.1.2. <i>Reduction of alkenes</i> .....	186
<b>6.2. <i>Results and discussion</i></b> .....	<b>188</b>
6.2.1. <i>Transfer hydrogenation</i> .....	188
6.2.2. <i>Catalytic hydrogenation of alkenes</i> .....	192
<b>6.3. <i>Experimental</i></b> .....	<b>195</b>

***APPENDIX 1: Crystallographic data (CIF files) on CD at the back of the thesis.***

# Chapter

# 1

## Introduction



Figure 1.1. Ground-state multiplicity of carbenes.

<b>1.1. Definition of a carbene</b> .....	<b>2</b>
<b>1.2. Historical summary</b> .....	<b>2</b>
<b>1.3. Ground-state spin multiplicity of carbenes</b> .....	<b>5</b>
1.3.1. Factors that can dictate the ground-state multiplicity of carbenes.....	5
1.3.1.1. Electronic factors.....	5
1.3.1.2. Steric Effects.....	7
1.3.2. Effects of the ground-state multiplicity in the reactivity of carbenes.....	7
1.3.2.1. Reactivity and stability of triplet carbenes.....	8
1.3.2.2. Reactivity and stability of singlet carbenes.....	11
<b>1.4 Types of aminocarbenes</b> .....	<b>18</b>
<b>1.5. N-heterocyclic carbenes</b> .....	<b>21</b>
1.5.1. Electronic properties.....	21
1.5.2. Steric properties.....	23
1.5.3. Coordination chemistry of NHC's.....	24

Ernst, J. H., *J. Am. Chem. Soc.* 1978, 100, 2535. (c) Miller, W. M., *J. Am. Chem. Soc.* 1971, 93, 2416.

\* Fischer, S. O., *Magnol. A. Organ. Chem. Int. Ed. Engl.* 1962, 1, 280.

**Chapter 1. Introduction.****1.1. Definition of a carbene.**

Carbenes are neutral, divalent carbon species linked to two adjacent groups by covalent bonds, possessing only six electrons in its valence shell and two unshared electrons. A free carbene may have two different spins in the ground state, singlet (when the two nonbonding electrons are in the same orbital with antiparallel spins) or triplet (when the two nonbonding electrons are in different orbitals with parallel spins) (Figure 1.1).

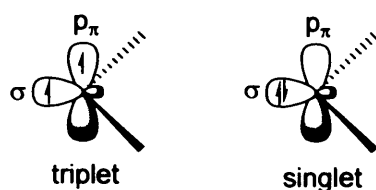
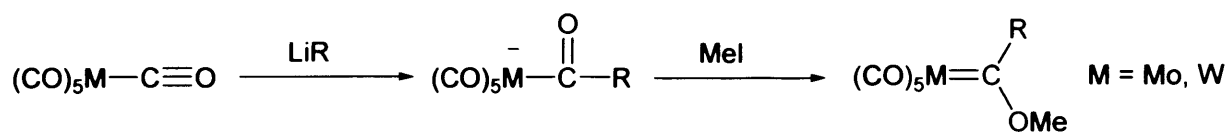


**Figure 1.1.** Ground-state multiplicity of carbenes.

**1.2. Historical overview.**

The first carbene complexes were synthesised in 1915 by Chugaev.<sup>1</sup> However, they were not recognised as such until in 1970,<sup>2</sup> six years after Fischer had synthesised the first carbene complexes to be so formulated.<sup>3</sup> They were formed by alkylation of a carbonyl complex followed by methylation (Scheme 1.1).



**Scheme 1.1.** Preparation of the first carbene complexes by Fischer.

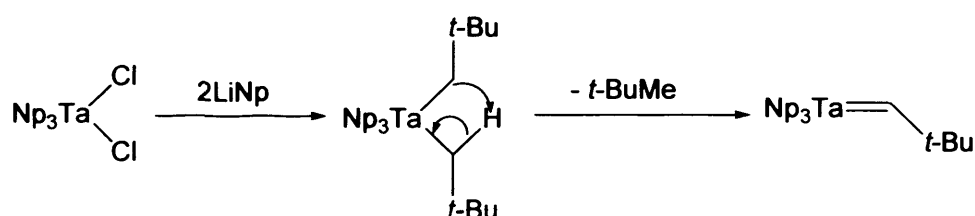
<sup>1</sup> Chugaev, L.; Skanavy-Grigorizeva, M. *J. Rus. Chem. Soc.* **1915**, 47, 776.

<sup>2</sup> (a) Rouschias, G.; Shaw, B. L., *Chem. Commun.*, **1970**, 183. (b) Burke, A.; Balch, A. L.; Enemark, J. H. *J. Am. Chem. Soc.* **1970**, 92, 2555. (c) Butler, W. M.; Enemark, J. H. *Inorg. Chem.* **1971**, 10, 2416.

<sup>3</sup> Fischer, E. O.; Maasbol, A. *Angew. Chem., Int. Ed. Engl.* **1964**, 3, 580.



Fischer carbenes coordinate to the metal almost exclusively via  $\sigma$ -donation from the lone pair because the  $p$  orbital on the carbenic carbon barely accepts any electron density from the metal  $d_{\pi}$  orbitals. Therefore, the electron density donated from the lone pair is not compensated by  $\pi$ -backdonation from the metal, leaving the carbenic carbon positively charged. As a consequence of this, Fischer type carbenes are considered to be electrophilic carbenes. Their counterpart, the nucleophilic carbenes, were not discovered until 1974,<sup>4</sup> when Schrock, in an attempt to make  $\text{Ta}(\text{Np})_5$  ( $\text{Np} = \text{CH}_2\text{CMe}_3$  or neopentyl), isolated  $\text{Np}_3\text{Ta}=\text{CH}(t\text{-Bu})$ , the first Schrock type carbene (Scheme 1.2).



**Scheme 1.2.** Preparation of the first Schrock type carbene.

The formation of the carbene complex probably goes via  $\text{Ta}(\text{Np})_5$ , however, the steric strain created by the five bulky neopentyl groups coordinated to the metal centre leads this complex to undergo an  $\alpha$ -proton abstraction.

In between the discovery of Fischer and Schrock carbene complexes Wanzlick<sup>5</sup> and Öfele<sup>6</sup> reported independently the first NHC metal complex. Despite the fact that Wanzlick never accomplished his purpose, the isolation of a free carbene, he established the basis for its synthesis and postulated the equilibrium carbene-enetetramine.<sup>7</sup> This equilibrium was a source of controversy for almost forty years,<sup>8</sup> until Hahn and co-workers observed for the

<sup>4</sup> Schrock, R.R. *J. Am. Chem. Soc.* **1974**, *96*, 6796.

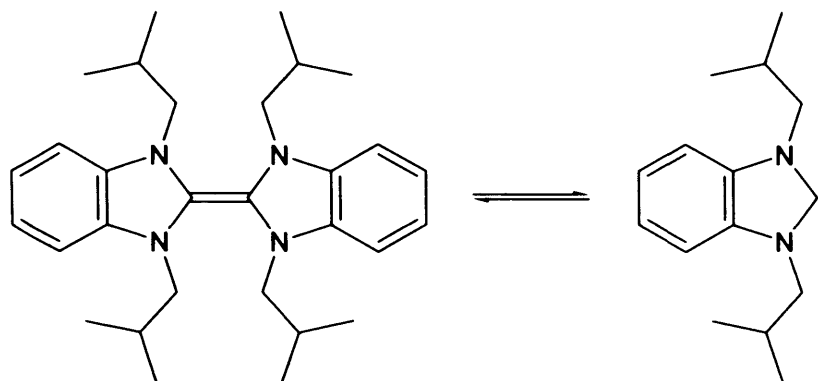
<sup>5</sup> Wanzlick, H.W.; Schönherr, H.-J. *Angew. Chem., Int. Ed. Engl.* **1968**, *7*, 141.

<sup>6</sup> (a) Öfele, K. *J. Organomet. Chem.* **1968**, *12*, 42. (b) Öfele, K. *Angew. Chem., Int. Ed. Engl.* **1970**, *9*, 739. (c) Öfele, K. *J. Organomet. Chem.* **1970**, *22*, C9.

<sup>7</sup> Wanzlick, H.-W. *Angew. Chem.* **1962**, *74*, 129; *Angew. Chem. Int. Ed. Engl.* **1962**, *1*, 75.

<sup>8</sup> (a) Liu, Yufa; Lemal David M. *Tetrahedron Letters* **2000**, *41*, 599. (b) Winberg, H. E.; Carnahan, J. E.; Coffman, D. D.; Brown, M. *J. Am. Chem. Soc.* **1965**, *87*, 2055. (c) Cardin, D. J.; Doyle, M. J.; Lappert, M. F. *J. Chem. Soc. Chem. Commun.* **1972**, 927.

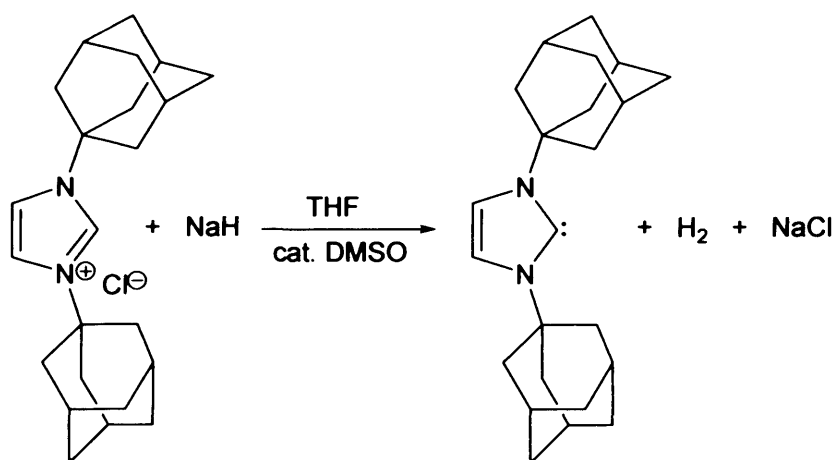
first time evidence for an equilibrium between an N-heterocyclic carbene and its dimer<sup>9</sup> (Scheme 1.3).



**Scheme 1.3.** First evidence of Wanzlick equilibrium.

The isolation and crystallographic characterisation of the first stable N-heterocyclic carbene by Arduengo<sup>10</sup> in 1991 led to increasing attention in the use of these carbenes as ancillary ligands.

Arduengo's carbene was prepared by deprotonation of the correspondent imidazolium salt with KH and a catalytic amount of dimethyl sulfoxide (Scheme 1.4). The single crystal suitable for X-ray diffraction studies was grown by cooling a toluene solution of the free carbene.



**Scheme 1.4.** Synthesis of the first crystalline free carbene.

<sup>9</sup> Hahn, F. Ekkehardt; Wittenbecher, Lars; Le Van, Duc ; Fröhlich Roland *Angew. Chem. Int. Ed.* **2000**, *39*, 541.

<sup>10</sup> Arduengo III, A.J.; Harlow, R.L.; Kline, M.A. *J. Am. Chem. Soc.* **1991**, *113*, 361.

### 1.3. Ground-state spin multiplicity of carbenes.

The main division that is used to classify carbenes is whether the two electrons are paired (singlet carbenes) or unpaired (triplet carbenes). Triplet carbenes are diradicals, which can be described by the electron configuration  $\sigma^1 p_\pi^1$  ( $^3B_1$  state). On the other hand, singlet carbenes can be described by two different  $^1A_1$  electronic configurations:  $\sigma^2$  and  $p_\pi^2$ , being the former being the most stable in the majority of cases<sup>11</sup> (Figure 1.2).

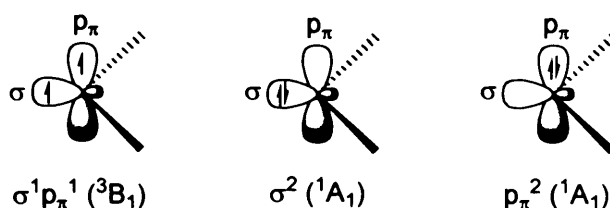


**Figure 1.2.** Ground-state electronic configuration of carbenes.

The difference in energy between the  $\sigma$  and the  $p_\pi$  orbitals determines the ground-state multiplicity of the carbene. According to Hoffmann, a  $\sigma$ - $p_\pi$  gap larger than 2 eV is needed to obtain a singlet carbene, whilst values below 1.5 eV lead to the triplet ground-state.<sup>12</sup>

#### 1.3.1. Factors that can dictate the ground-state multiplicity of carbenes.

The stability and ground-state of carbenes is derived from a combination of steric and electronic factors. Therefore, the nature of the substituents adjacent to the carbene core plays an important role in the reactivity of carbenes.

##### 1.3.1.1. Electronic factors.

Electronic factors can be divided into inductive effects and mesomeric effects. The inductive effects are a consequence of the electronegativity of the substituents. The highly electronegative substituents stabilise the  $\sigma$ -nonbonding orbital by withdrawing electron density whereas the  $p_\pi$  orbital remains unchanged. Therefore, the  $\sigma$ - $p_\pi$  gap is increased and

<sup>11</sup> Bourissou, D.; Guerret, O.; Gabbai, F. P.; Bertrand, G. *Chem. Rev.*, **2000**, *100*, 39.

<sup>12</sup> Gleiter, R.; Hoffmann, R. *J. Am. Chem. Soc.* **1968**, *90*, 1475.

the singlet state is favoured. On the contrary,  $\sigma$ -electron-donating substituents (low electronegativity) induce a small  $\sigma$ - $p_x$  gap which favours the triplet state.

Mesomeric effects often play a more important role than inductive effect in most carbenes.<sup>13</sup> Bertrand and co-workers in their review on stable carbenes<sup>11</sup> classify the substituents interacting with the carbene centre into two types,  $\pi$ -electron-donating groups and  $\pi$ -electron-withdrawing groups, which they call X and Z, respectively. As a result of this, carbenes were classified according to their substituents:

(X,X)-Carbenes, which are predicted to be bent singlet carbenes (Figure 1.3.a).

(Z,Z)-Carbenes, which are predicted to be singlet carbenes even though they are linear (Figure 1.3.b).

(X,Z)-Carbenes, which are predicted to be quasy-linear singlet carbenes (Figure 1.3.c).

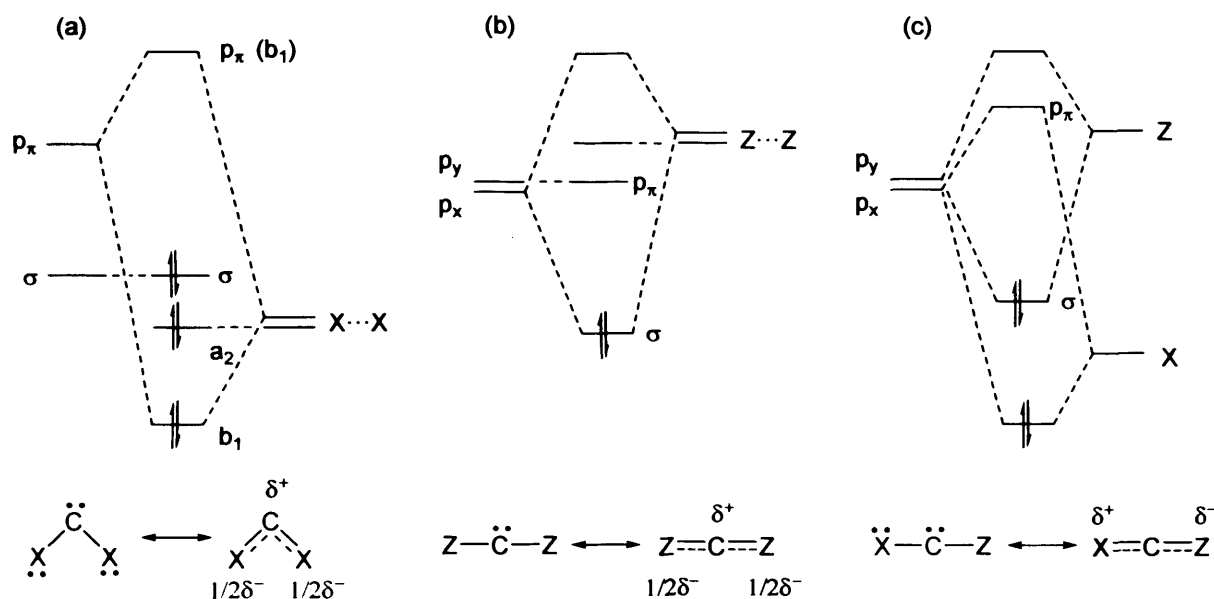


**Figure 1.3.** Perturbation orbital diagrams showing the influence of the mesomeric effects.<sup>11</sup>

As a result of the above explanation it can be concluded that mesomeric effects stabilise singlet carbenes.

<sup>13</sup> (a) Hoffmann, R.; Zeiss, G. D.; Van Dine, G. W. *J. Am. Chem. Soc.* **1968**, *90*, 1485. (b) Baird, N. C.; Taylor, K. F. *J. Am. Chem. Soc.* **1978**, *100*, 1333.

## 1.3.1.2. Steric Effects.

The increase of the steric hindrance around the carbene core stabilises kinetically all types of carbenes by preventing dimerisation. Furthermore, the linearity or non-linearity of the carbene influences the ground-state spin multiplicity, being crucial when electronic effects are negligible.

The linear geometry implies a  $sp$ -hybridized carbene centre with two nonbonding degenerate orbitals ( $p_x$  and  $p_y$ ). Bending the molecule breaks its degeneracy, and the carbon atom adopts an  $sp^2$ -type hybridisation: the  $p_y$  orbital remains almost unchanged (it is usually called  $p_\pi$ ), while the orbital that starts as pure  $p_x$  orbital is stabilized since it acquires  $s$  character (therefore it is usually called  $\sigma$ ) (Figure 1.4). The linear geometry is an extreme case, most carbenes are bent and their frontier orbitals will be systematically called  $\sigma$  and  $p_\pi$ .<sup>11</sup>

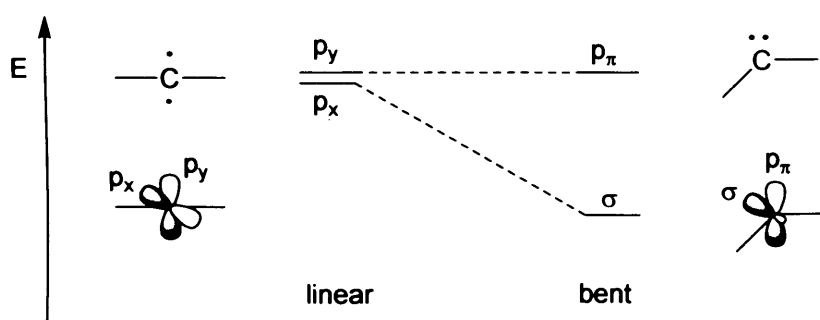


**Figure 1.4.** Relationship between the carbene bond angle and the nature of the frontier orbitals.

Figure 1.4 illustrates the decrease of the  $\sigma$ - $p_\pi$  gap as the carbene bond angle is expanded and the corollary electronic stabilization of the triplet relative to the singlet state. Therefore, the bending of the molecule destabilises the triplet state.

## 1.3.2. Effects of the ground-state multiplicity in the reactivity of carbenes.

The reactivity and stability of carbenes is decisively influenced by their ground-state multiplicity. Triplet carbenes react according to what is expected for radicals, whereas singlet carbenes can behave as nucleophiles through the non-bonding electron pair or as electrophiles, accepting electron density *via* the vacant orbital.

## 1.3.2.1. Reactivity and stability of triplet carbenes.

The low thermodynamic stability of triplet carbenes has prevented their crystallographic characterisation. Despite the fact that the synthesis of a triplet carbene stable in solution at ambient temperature remains elusive, Tomioka and co-workers have made considerable progress in this field. They synthesised a triplet carbene indefinitely stable at 130 K in liquid solution and, moreover, indefinitely stable at ambient temperature in solid state.<sup>14</sup> This was achieved by steric protection of the carbene, which led to its kinetic stabilisation, and by delocalising the unpaired electrons with adjacent aromatic systems, lowering the thermodynamic energy of the species (Figure 1.5).

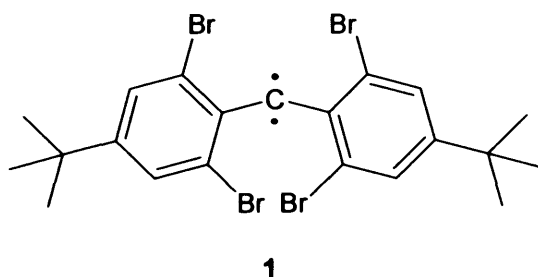
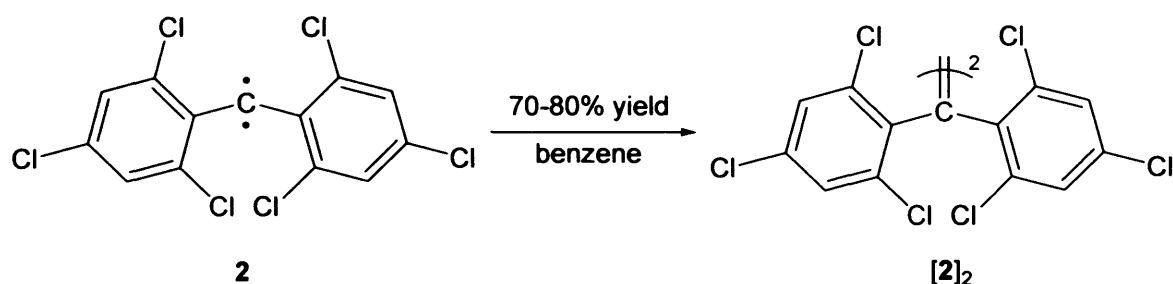


**Figure 1.5.** Stable triplet carbene synthesised by Tomioka *et al.*

When Tomioka's carbene **1** is dissolved in dry and degassed benzene it gives only small amounts of carbene dimers. However, when the steric hindrance around the carbene core is reduced, e. g. polychlorinated diphenylcarbene **2**, the proportion of dimer increases<sup>15</sup> (Scheme 1.4).

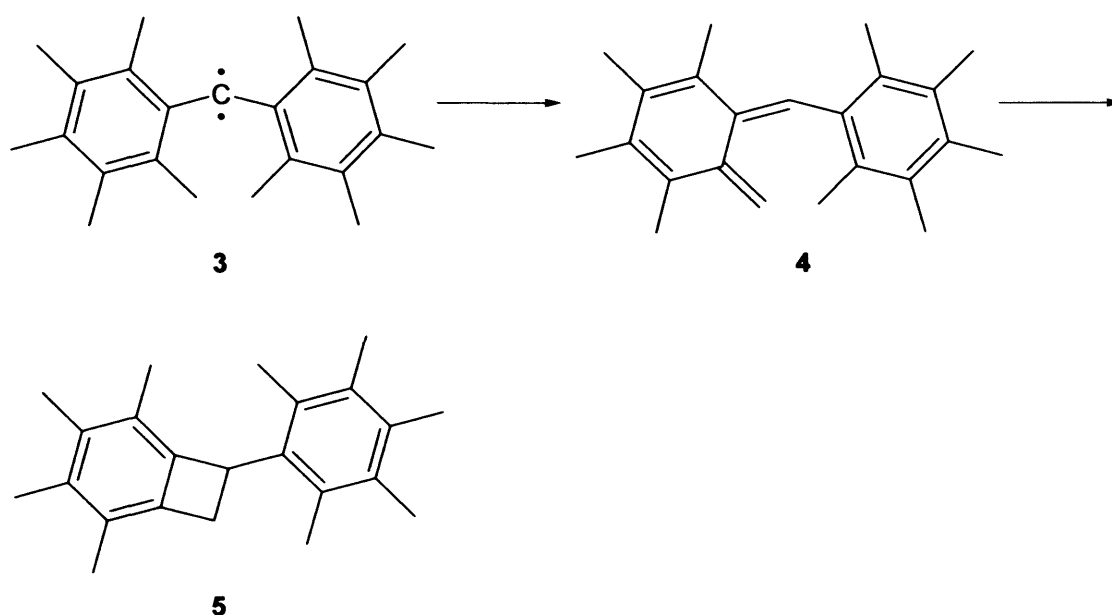
<sup>14</sup> (a) Tomioka, H.; Watanabe, T.; Hirai, K.; Furukawa, K.; Takui, T.; Itoh, K. *J. Am. Chem. Soc.* **1995**, *117*, 6376. (b) Tomioka, H.; Hattori, M.; Hirai, K.; Murata, S. *J. Am. Chem. Soc.* **1996**, *118*, 8723. (c) Furukawa, K.; Takui, T.; Itoh, K.; Watanabe, T.; Hirai, K.; Tomioka, H. *Mol. Cryst. Liq. Cryst.* **1996**, *278*, 271.

<sup>15</sup> (a) Braun, W.; Bass, A. M.; Pilling, M. *J. Chem. Phys.* **1970**, *52*, 5131. (b) Laufer, A. H. *Res. Chem. Intermed.* **1981**, *4*, 225.



**Scheme 1.4.** Dimerisation of triplet carbene **2**.

If the steric hindrance at the carbene core is enough to prevent dimerisation, other decomposition mechanisms can take place. For instance, *ortho* alkyl substitution in, at least, one of the aromatic rings usually leads to intramolecular H-abstraction<sup>16,17</sup> or C-H insertion of the carbene (Scheme 1.5).<sup>16,18</sup>



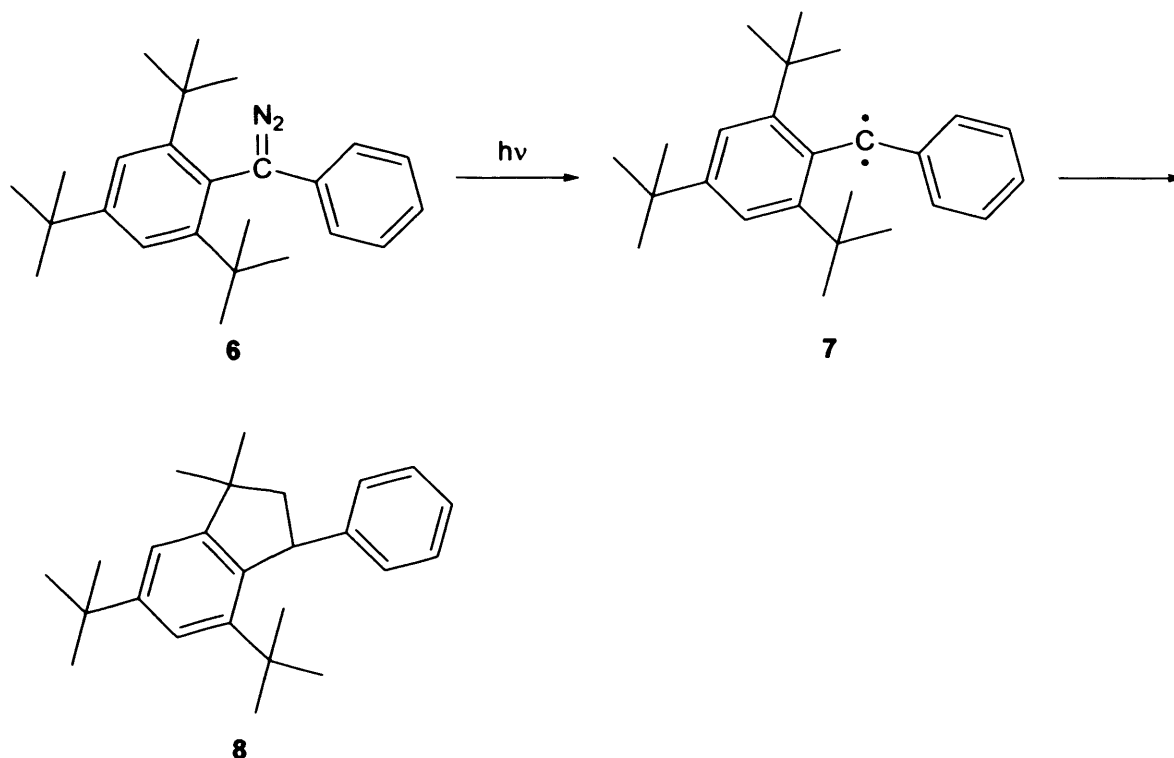
**Scheme 1.5.** Intramolecular H-abstraction of one of the *ortho* methyls followed by electrocyclicisation of the transient species **4**.

<sup>16</sup> (a) Tomioka, H.; Okada, H.; Watanabe, T.; Banno, K.; Komatsu, K.; Hirai, K. *J. Am. Chem. Soc.* **1997**, *119*, 1582. (b) Sander, W.; Kirschfeld, A.; Kappert, W.; Muthusamy, S.; Kiselewsky, M. *J. Am. Chem. Soc.* **1996**, *118*, 6508.

<sup>17</sup> Tomioka, H.; Okada, H.; Watanabe, T.; Hirai, K. *Angew. Chem., Int. Ed. Engl.* **1994**, *33*, 873.

<sup>18</sup> Hirai, K.; Komatsu, K.; Tomioka, H. *Chem. Lett.* **1994**, 503.

Irradiation of **6** at room temperature affords **8**, which is most probably the result of the C-H insertion of transient carbene **7** into one of the *t*-butyl groups at an *ortho* position (Scheme 1.6).



**Scheme 1.6.** Intramolecular insertion of the carbene into a C-H bond.

The reactivity of diaryl carbenes against different species can be tested by *in situ* generation of the carbene.

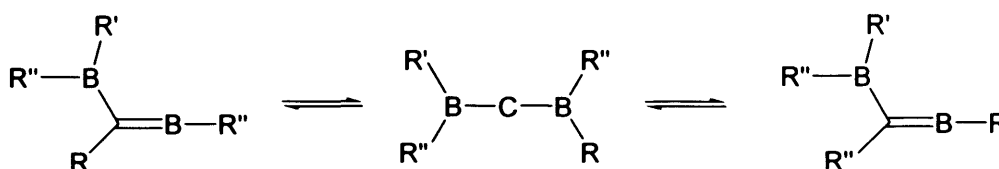
Photolysis of the diazo precursors in presence of oxygen or methanol affords the corresponding oxidised ketones<sup>16,19</sup> or methanol insertion adducts (Scheme 1.7).

<sup>19</sup> (a) Tomioka, H.; Mizutani, K.; Matsumoto, K.; Hirai, K. *J. Org. Chem.* **1993**, *58*, 7128. (b) Tomioka, H.; Hirai, K.; Nakayama, T. *J. Am. Chem. Soc.* **1993**, *115*, 1285. (c) Tomioka, H.; Nakajima, J.; Mizuno, H.; Sone, T.; Hirai, K. *J. Am. Chem. Soc.* **1995**, *117*, 11355.



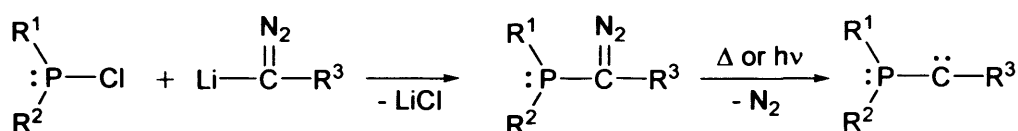


(Z,Z)-carbenes have not yet been isolated, 1,2-migration being the most common decomposition pathway<sup>20</sup> (Scheme 1.9).



**Scheme 1.9.** 1,2-migration in a (Z,Z)-carbene.

The phosphinosilylcarbene isolated by Bertrand *et al.* in 1988, represented the first example of a stable (X,Z)-carbene,<sup>21</sup> and, what is more, the first example of a stable carbene. Unfortunately, this carbene did not show any ability as a ligand for transition metals (Scheme 1.10).



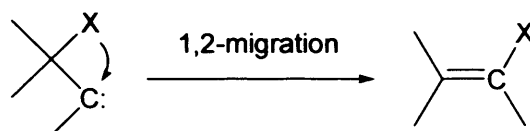
**Scheme 1.10.** Synthesis of the first stable carbene ( $R^1 = R^2 = {}^i\text{Pr}_2\text{N}$ ;  $R^3 = \text{SiMe}_3$ ).

The most widely studied (X,X)-carbenes are the aminocarbenes and, among them, N-heterocyclic carbenes are the most successful due to their high stability and excellent performance as a ligands for catalytic systems. Most aminocarbenes can be isolated as stable solids in absence of moisture. The stability of these carbenes results from thermodynamic stabilisation by mesomeric (+M) as well as inductive (-I) effects, and kinetic stabilisation due to the shielding of the carbene centre by bulky N-substituents.

<sup>20</sup> (a) Menzel, M.; Winckler, H. J.; Ablelom, T.; Steiner, D.; Fau, S.; Frenking, G.; Massa, W.; Berndt, A. *Angew. Chem., Int. Ed. Engl.* **1995**, *34*, 1340. (b) Fau, S.; Frenking, G. *J. Mol. Struct. (THEOCHEM)* **1995**, *338*, 117.

<sup>21</sup> Igau, A.; Grutzmacher, H.; Baceiredo, A.; Bertrand, G., *J. Am. Chem. Soc.* **1988**, *110*, 6463.

One of the main decomposition pathways for singlet carbenes is the previously mentioned 1,2-migration. This reaction entails the intramolecular 1,2-migration of one of the groups adjacent to carbene core (X) *via* concerted mechanism<sup>22</sup> (Scheme 1.11).



**Scheme 1.11.** Representation of a generic 1,2-migration.

Similar decomposition products were observed for N-heterocyclic carbenes with electrophilic substituents on the nitrogens,<sup>23</sup> however, the mechanism of the reaction has proved to take place *via* intermolecular reaction.<sup>23,24</sup> This behaviour is a consequence of the nucleophilic nature of singlet carbenes, which makes them reactive against electrophiles<sup>25</sup> (Scheme 1.12.a) or Lewis acids<sup>26</sup> (Scheme 1.12.b).

<sup>22</sup> (a) Nickon, A. *Acc. Chem. Res.* **1993**, *26*, 84. (b) Storer, J. W. Hook, K. N. *J. Am. Chem. Soc.* **1993**, *115*, 10426. (c) Sulzbach, H. M.; Platz, M. S.; Schaefer, H. F., III; Hadad, C. M. *J. Am. Chem. Soc.* **1997**, *119*, 5682. (d) Keating, A. E.; Garcia-Garibay, M. A.; Houk, K. N. *J. Am. Chem. Soc.* **1997**, *119*, 10805. (e) Ford, F.; Yuzawa, T.; Platz, M. S.; Matzinger, S.; Fülischer, M. *J. Am. Chem. Soc.* **1998**, *120*, 4430.

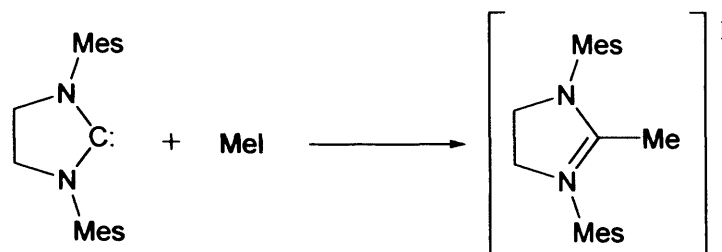
<sup>23</sup> Solé, S.; Gornitzka, H.; Guerret, O.; Bertrand, G. *J. Am. Chem. Soc.* **1998**, *120*, 9100.

<sup>24</sup> (a) McGibbon, G. A.; Heinemann, C.; Lavorato, D. J.; Schwarz, H. *Angew. Chem., Int. Ed. Engl.* **1997**, *36*, 1478. (b) Maier, G.; Endres, J.; Reisenauer, H. P. *Angew. Chem., Int. Ed. Engl.* **1997**, *36*, 1709. (c) Wacker, A.; Pritzkow, H.; Siebert, W. *Eur. J. Inorg. Chem.* **1998**, 843. (d) Wacker, A.; Pritzkow, H.; Siebert, W. *Eur. J. Inorg. Chem.* **1999**, 789.

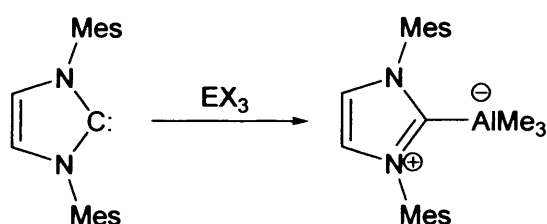
<sup>25</sup> (a) Arduengo, A. J., III; Davidson, F.; Dias, H. V. R.; Goerlich, J. R.; Khasnis, D.; Marshall, W. J.; Prakasha, T. K. *J. Am. Chem. Soc.* **1997**, *119*, 12742. (b) Teles, J. H.; Melder, J. P.; Ebel, K.; Schneider, R.; Gehrler, E.; Harder, W.; Brode, S.; Enders, D.; Breuer, K.; Raabe, G. *Helv. Chim. Acta* **1996**, *79*, 61.

<sup>26</sup> (a) Arduengo, A. J., III; Gamper, S. F.; Tamm, M.; Calabrese, J. C.; Davidson, F.; Craig, H. A. *J. Am. Chem. Soc.* **1995**, *117*, 572. (b) Arduengo, A. J., III; Dias, H. V. R.; Calabrese, J. C.; Davidson, F. *J. Am. Chem. Soc.* **1992**, *114*, 9724. (c) Li, X. W.; Su, J.; Robinson, G. H. *J. Chem. Soc., Chem. Commun.* **1996**, 2683. (d) Kuhn, N.; Henkel, G.; Kratz, T.; Kreutzberg, J.; Boese, R.; Maulitz, A. H. *Chem. Ber.* **1993**, *126*, 2041. (e) Singaram, B.; Cole, T. E.; Brown, H. C. *Organometallics* **1984**, *3*, 774.

(a)

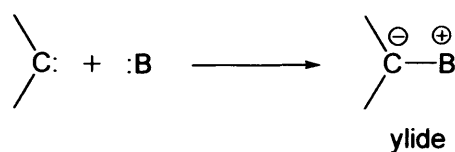


(b)



**Scheme 1.12.** Reactivity of singlet carbenes against electrophiles<sup>25a</sup> (a) or Lewis acids<sup>26b</sup> (b).

On the other hand, the vacant  $p_{\pi}$  orbital at the carbene carbon enables the carbene to act as an electrophile. Transient electrophilic carbenes react with Lewis bases to give ylides<sup>27</sup> (Scheme 1.13).



**Scheme 1.13.** Formation of ylides from transient electrophilic carbenes ( $B = \text{PR}_3, \text{AsR}_3, \text{O}=\text{CR}_2, \text{N}\equiv\text{CR}$ ).

<sup>27</sup> (a) Wang, J. L.; Toscano, J. P.; Platz, M. S.; Nikolaev, V.; Popik, V. *J. Am. Chem. Soc.* **1995**, *117*, 5477. (b) Jackson, J. E.; Soundararajan, N.; Platz, M. S.; Liu, M. T. H. *J. Am. Chem. Soc.* **1988**, *110*, 5595. (c) Toscano, J. P.; Platz, M. S.; Nikolaev, V. Popic, V. *J. Am. Chem. Soc.* **1994**, *116*, 8146. (d) Goumri, S.; Polishchuk, O.; Gornitzka, H.; Bacciredo, A.; Bertrand, G. *Angew. Chem., Int. Ed. Engl.* **1999**, *38*, 3727. (e) De March, P.; Huisgen, R. *J. Am. Chem. Soc.* **1982**, *104*, 4952 and 4953. (f) Padwa, A.; Hornbuckle, S. F. *Chem. Rev.* **1991**, *91*, 263. (g) Janulis, E. P.; Wilson, S. R.; Arduengo A. J., III *Tetrahedron Lett.* **1984**, 405.

When the steric hindrance around the carbene core allows the approach, singlet carbenes can react with themselves or other carbenes to form CC double bonds. In the case of singlet carbenes the formation of the double bond is believed to entail the attack of the  $\sigma$  lone pair of one singlet carbene on the vacant  $p_x$ -orbital of a second carbene by a nonleast-motion pathway<sup>28</sup> (Figure 1.6). The fact that the dimerisation does not proceed by a least-motion pathway<sup>29</sup> brings about an activation energy for this process.<sup>30</sup> This barrier arises from electronic factors, mainly because the non-least motion pathway leads to an excited state of the dimer, and steric factors, due to the repulsion between the two carbenes. Interestingly, this activation energy can be reduced by the use of catalytic amounts of a Lewis acid.<sup>29b, 31</sup>

On the other hand, the thermodynamic stability of the dimer against the free carbene depends as well on electronic and steric factors. Namely, the loss of aromaticity and the increasing steric bulk about the carbene core are unfavourable factors for the formation of the dimer.<sup>30b</sup>

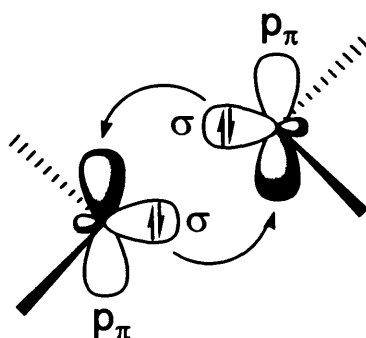


**Figure 1.6.** Schematic representation of the dimerisation of singlet carbene.

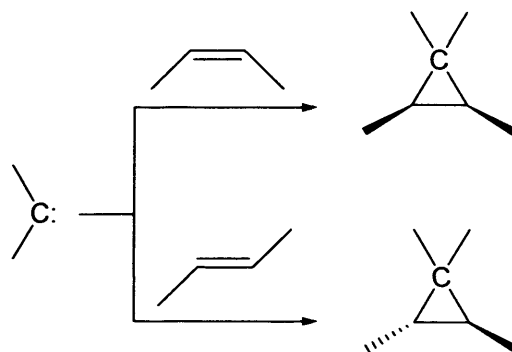
<sup>28</sup> (a) Carter, E. A.; Goddard, W. A., III *J. Phys. Chem.* **1986**, *90*, 998. (b) Trinquier, G.; Malrieu, J. P. *J. Am. Chem. Soc.* **1987**, *109*, 5303. (c) Malrieu, J. P.; Trinquier, G. *J. Am. Chem. Soc.* **1989**, *111*, 5916. (d) Jacobsen, H.; Ziegler, T. *J. Am. Chem. Soc.* **1994**, *116*, 3667.

<sup>29</sup> (a) Hoffmann, R.; Gleiter, R.; Mallory, F. B. *J. Am. Chem. Soc.* **1970**, *92*, 1460. (b) Alder, Roger W.; Blake, Michael E. *Chem. Commun.* **1997**, 1513.

<sup>30</sup> (a) Ohta, K.; Davidson, E. R.; Morokuma, K. *J. Am. Chem. Soc.* **1985**, *107*, 3466. (b) Taton, T. A.; Chen, P. *Angew. Chem., Int. Ed. Engl.* **1996**, *35*, 1011.

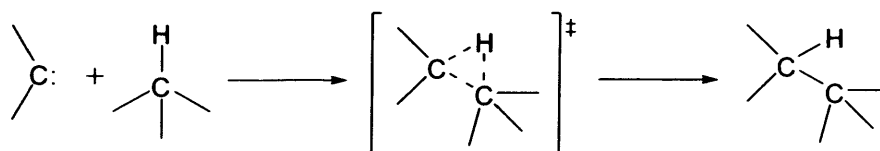
<sup>31</sup> Arduengo, A. J., III; Goerlich, J. R.; Marshall, W. J. *Liebigs Ann.* **1997**, 365.

Like triplet carbenes, singlet carbenes react with alkenes to yield the corresponding cyclopropane derivatives, although by entirely different mechanisms. Unlike triplet carbenes, the product of the cyclopropanation reaction of singlet carbenes retains the stereochemistry about the double bond, which suggests a concerted process<sup>32</sup> (Scheme 1.14).



**Scheme 1.14.**

Similarly, triplet and singlet carbenes can be inserted into unpolarised C-H bonds, following a radical mechanism in the case of triplet carbenes. However, as a consequence of the spin conservation rule, the insertion of a singlet carbene must be a one-step process involving a three-center cyclic transition state<sup>33</sup> (Scheme 1.15). In the case of stable singlet carbenes, this reaction does not proceed unless drastic conditions are used.<sup>21, 32a</sup>



**Scheme 1.15.** C-H insertion of a singlet carbene.

<sup>32</sup> (a) Igau, A.; Baceiredo, A.; Trinquier, G.; Bertrand, G. *Angew. Chem., Int. Ed. Engl.* **1989**, *28*, 621. (b) Skell, P. S.; Garner, A. Y. *J. Am. Chem. Soc.* **1956**, *78*, 3409 and 5430. (c) Skell, P. S.; Woodworth, R. C. *J. Am. Chem. Soc.* **1956**, *78*, 4496 and 6427. (d) Skell, P. S. *Tetrahedron* **1985**, *41*, 1427. (e) Keating, A. E.; Merrigan, S. R.; Singleton, D. A.; Houk, K. N. *J. Am. Chem. Soc.* **1999**, *121*, 3933.

<sup>33</sup> Bethell, D. *Adv. Phys. Org. Chem.* **1969**, *7*, 153.

Recently, Bertrand and co-workers published the insertion of (alkyl)(amino)carbenes into an H-H bond.<sup>34</sup> The author proposed a nucleophilic activation, which involves the interaction of the carbene's lone pair of electrons with an H<sub>2</sub> antibonding orbital in the transition state. This interaction causes the polarisation of the H<sub>2</sub> molecule, which ultimately triggers the nucleophilic attack of the negatively polarised hydrogen atom on the carbene's unoccupied p<sub>π</sub> orbital (Figure 1.7).

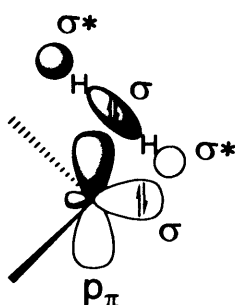
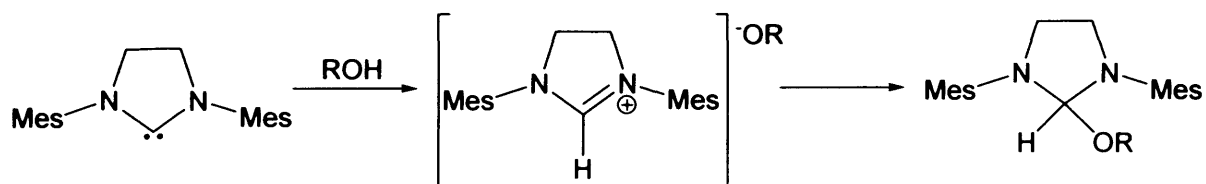


**Figure 1.7.** Schematic representation of H<sub>2</sub> on a carbene carbon.

A more commonly observed reaction for singlet carbenes is the insertion into polarised X-H bonds. For example, alcohols react with N-heterocyclic carbenes to give the 1,1-addition product. Unlike insertions into unpolarised C-H bonds, this reaction is better explained as the result of a stepwise mechanism, involving the protonation of the carbene by the alcohol followed by nucleophilic addition of the alkoxide<sup>35</sup> (Scheme 1.16).



**Scheme 1.16.** Insertion of IMes into the O-H bond of an alcohol.<sup>35b</sup>

<sup>34</sup> Frey, Guido D.; Lavallo, Vincent; Donnadiu, Bruno; Schoeller, Wolfgang W.; Bertrand, G. *Science*, **2007**, *316*, 439.

<sup>35</sup> (a) Enders, D.; Breuer, K.; Raabe, G.; Runsink, J.; Teles, J. H.; Melder, J. P.; Ebel, K.; Brode, S. *Angew. Chem., Int. Ed. Engl.* **1995**, *34*, 1021. (b) Csihony, Szilárd; Culkin, Darcy A.; Sentman, Alan C.; Dove, Andrew P.; Waymouth, Robert M.; Hedrick, James L. *J. Am. Chem. Soc.* **2005**, *127*, 9079.

Singlet carbenes, especially aminocarbenes, have proven to be excellent ligands for transition metals. Carbene complexes of every transition metal have been published, Ru, Pd, Rh and Ir being the most successful due to their vast catalytic applications.

#### 1.4 Types of aminocarbenes.

The first stable carbene, synthesised by Arduengo<sup>10</sup> in 1991, was based on an imidazole framework. In principle the stabilisation arising from the two nitrogens adjacent to the carbene carbon and the electronic delocalisation were believed to be indispensable for the stability of the carbene. This groundbreaking discovery sparked great interest in this field, leading to the synthesis of a vast number of imidazol-ylidene carbenes, which are still nowadays the most widely studied type of carbenes (Figure 1.8).

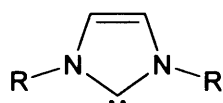


**Figure 1.8.** Unsaturated 5-membered carbene derived from an imidazolium salt.

Four years later, in 1995, Arduengo again published the synthesis of the first stable saturated 5-membered carbene. The saturation of the backbone results in slightly wider N-C<sub>NHC</sub>-N angles,<sup>36</sup> a significant increase of the basicity<sup>37</sup> and a higher tendency for dimerisation.

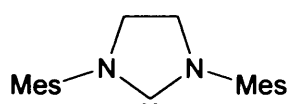


**Figure 1.9.** Imidazolin-2-ylidene isolated by Arduengo *et. al.* in 1995.

The stability of imidazolin-2-ylidene carbenes disproves the prerequisite of cyclic 6 $\pi$ -electron delocalisation for the synthesis of stable carbenes (Figure 1.9).

<sup>36</sup> Arduengo, III, A. J.; Goerlich, Jens R.; Marshall, William J. *J. Am. Chem. Soc.* **1995**, *117*, 11027.

<sup>37</sup> (a) Alder, R.W.; Allen, P.R.; Williams, S.J. *Chem. Commun.* **1995**, 1267; (b) Kim, Y.J.; Streitwieser, A. *J. Am. Chem. Soc.* **2002**, *124*, 5757.



This conclusion broadened the scope for the design of new carbenes, allowing for the synthesis of more exotic carbenes and more importantly the tuning of the steric and electronic properties of carbenes. The most prominent examples are expanded NHC's (6- and 7-membered, **13**<sup>38</sup> and **14**<sup>39</sup> respectively), acyclic aminocarbenes (**15**<sup>40</sup>) and CAAC's (cyclic alkyl(amino)carbenes) (**16**<sup>41</sup>) (Figure 1.10).

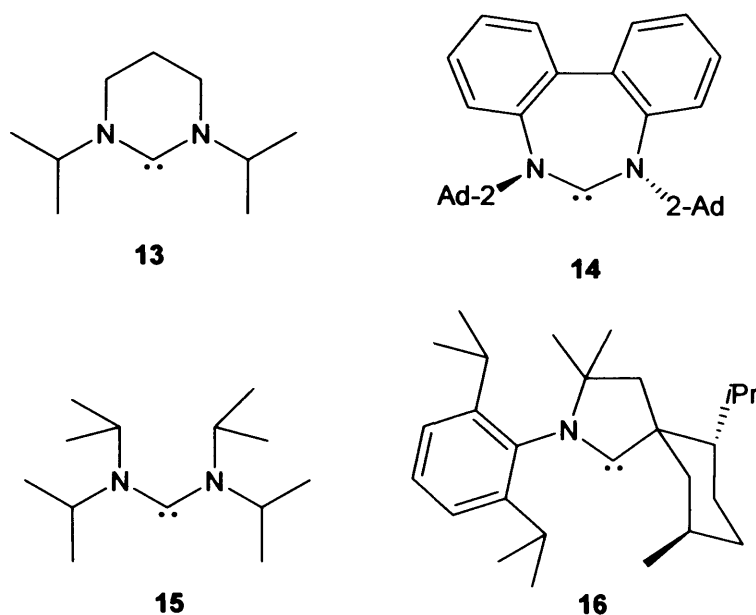


**Figure 1.10.** Examples of aminocarbenes without  $6\pi$ -electron delocalised backbones.

The replacement of one of the nitrogen atoms of the imidazol-2-ylidene with an oxygen atom or a sulphur atom gives the corresponding oxazol-2-ylidene or thiazol-2-ylidene, respectively (Figure 1.11).

<sup>38</sup> Herrmann, W.; Schneider, S. K.; Öfele, K.; Sakamoto, M.; Herdtweck, E. *J. Organomet. Chem.* **2004**, *689*, 2441

<sup>39</sup> Scarborough, C. C.; Grady, M. J. W.; Guzei, I. A.; Gandhi, B. A.; Bunel, E. E.; Stahl, S. S. *Angew. Chem., Int. Ed.* **2005**, *44*, 5269

<sup>40</sup> Denk, K.; Sirsch, P.; Herrmann, W. A. *J. Organomet. Chem.* **2002**, *649*, 219.

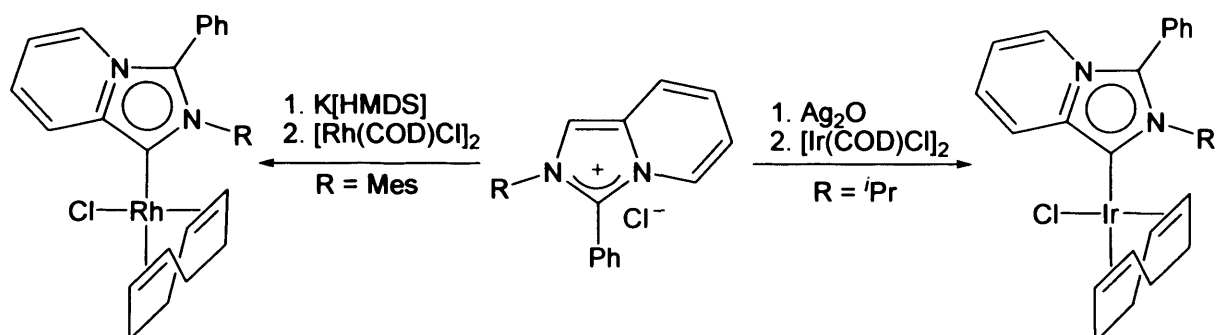
<sup>41</sup> Lavallo, V.; Canac, Y.; Präsang, C.; Donnadiou, B.; Bertrand, G. *Angew. Chem. Int. Ed.* **2005**, *44*, 5705.



**Figure 1.11.** Depiction of generic oxazol-2-ylidene and thiazol-2-ylidene carbenes.

Thiazol-2-ylidenes exist in a proton catalysed chemical equilibrium with their dimers,<sup>42</sup> however oxazol-2-ylidenes are not stable but can be generated by metal template synthesis.<sup>43</sup>

The most acidic proton in imidazolium salts is that at the C<sup>2</sup>, therefore C<sup>2</sup>-coordinated metal imidazol-2-ylidenes are referred to as normal carbenes. Conversely, N-heterocyclic carbenes derived from imidazolium salts bound to the metal through the C<sup>4</sup> or C<sup>5</sup> have been recently described and are referred to as abnormal carbenes. The abnormally bound carbene complex can be obtained selectively by blocking the C<sup>2</sup> position, which prevents the formation of C<sup>2</sup>-coordinated species (Scheme 1.17).<sup>44</sup>



**Scheme 1.17.** Synthesis of an abnormal carbene complex using an imidazolium salt blocked in the C<sup>2</sup> position.

<sup>42</sup> Arduengo, III, A. J.; Goerlich, J. R.; Mashall, W. J. *Liebigs Ann.* **1997**, 365.

<sup>43</sup> (a) Ruiz, J.; García, G.; Mosquera, M. E. G.; Perandones, B. F.; Gonzalo, M. P.; Vivanco, M. J. *Am. Chem. Soc.* **2005**, *127*, 8584. (b) Tamm, M.; Hahn, F. E. *Coord. Chem. Rev.* **1999**, *182*, 175. (c) Basato, M.; Michelin, R. A.; Mozzon, M.; Sgarbossa, P.; Tassan, A. *J. Organomet. Chem.* **2005**, *690*, 5414.

<sup>44</sup> (a) Alcarazo, M.; Roseblade, S. J.; Cowley, A. R.; Fernández, R.; Brown, J. M.; Lassaletta, J. M. *J. Am. Chem. Soc.* **2005**, *127*, 3290. (b) Roseblade, S. J.; Ros, A.; Monge, D.; Alcarazo, M.; Álvarez, E.; Lassaletta, J. M.; Fernández, R. *Organometallics* **2007**, *26*, 2570.

Abnormal carbenes as well as CAAC's feature enhanced donor capabilities due to the presence of a single nitrogen atom adjacent to the carbene carbon. Interestingly, a new kind of N-heterocyclic carbene with no nitrogens adjacent to the carbene carbon atom has been recently reported by Raubenheimer *et. al.*<sup>45</sup> and Han and Huynh.<sup>46</sup> This new type of NHC's are known as remote N-heterocyclic carbenes (*r*NHC's) (Figure 1.12).

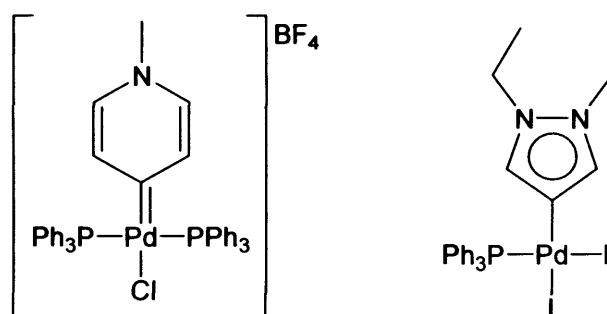


Figure 1.12. Examples of *r*NHC's.

## 1.5. N-heterocyclic carbenes.

### 1.5.1. Electronic properties.

N-heterocyclic carbenes can be classified as (X,X)-carbenes and the interactions of the  $\pi$ -electrons of the nitrogens with the empty  $p_{\pi}$ -orbital at the carbene carbon atom result in a four-electron-three-center  $\pi$ -system where the N–C bonds acquire partial double bond character. Therefore, the structure can be described by three main resonance structures (Figure 1.13).

<sup>45</sup> (a) Meyer, W. H.; Deetlefs, M.; Pohlmann, M.; Scholz, R.; Esterhuysen, M.W.; Julius, G. R.; Raubenheimer, H. G. *Dalton Trans.* **2004**, 413. (b) Schneider, S. K.; Julius, G. R.; Loschen, C.; Raubenheimer, H. G.; Frenking, G.; Herrmann, W. A. *Dalton Trans.* **2006**, 1226. (c) Schneider, S. K.; Roembke, P.; Julius, G. R.; Loschen, C.; Raubenheimer, H. G.; Frenking, G.; Herrmann, W. A. *Eur. J. Inorg. Chem.* **2005**, 2973. (d) Raubenheimer, H. G.; Cronje, S. *Dalton. Trans.* **2008**, 1265. (e) Schuster, O.; Raubenheimer, H. G. *Inorg. Chem.* **2006**, 45, 7997.

<sup>46</sup> (a) Han, Y.; Huynh, H. V. *Chem. Commun.* **2007**, 1089. (b) Han, Y.; Huynh, H. V.; Tan, G. K. *Organometallics* **2007**, 26, 6581.

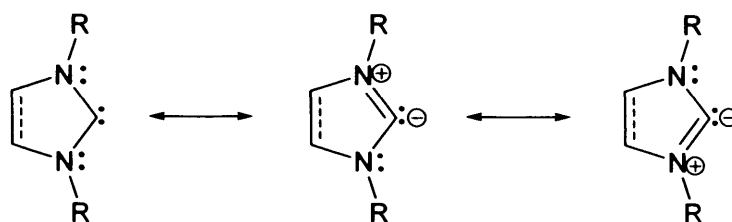


**Figure 1.13.** Resonance structures of heterocyclic five-membered carbenes.

The two nitrogen atoms donate electron density to the carbene's empty  $p_\pi$  orbital by mesomeric effect and withdraw electron density from the  $\sigma$ -nonbonding orbital by inductive effect (Figure 1.14). This results in an increase of the  $\sigma$ - $p_\pi$  gap and, therefore, a stabilisation of the singlet carbene.

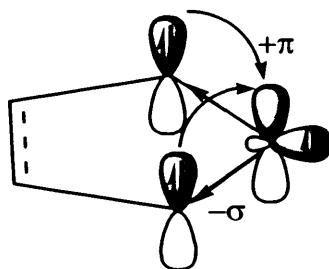


**Figure 1.14.** Electronic effects in N-heterocyclic carbenes.

The stability of N-heterocyclic carbenes stems mainly from the electronic effects above explained, even though steric hindrance also plays an important role. Steric protection of the carbene certainly enhances its stability, but it is not a crucial factor.<sup>47</sup> The aromaticity of the 6- $\pi$ -electron five-membered carbene was believed to play an important role in the carbene stability.<sup>48</sup> However, the independent studies by Apeloig and Frenking discarded aromaticity as the major stabilising effect.<sup>49</sup> This explains why saturated N-heterocyclic carbenes can also be isolated. More recent theoretical and experimental reports suggest that a certain degree of aromaticity would confer some thermodynamic stability, yet

<sup>47</sup> Arduengo A.J. III.; Dias, H.V.R.; Harlow, R.L.; Kline, M.; *J. Am. Chem. Soc.* **1992**, *114*, 5530.

<sup>48</sup> Cioslowski, *J. Int. J. Quantum Chem., Quantum Chem. Symp.* **1993**, *27*, 309.

<sup>49</sup> (a) Heinemann, C.; Müller, T.; Apeloig, Y.; Schwarz, H. *J. Am. Chem. Soc.* **1996**, *118*, 2023. (b) Boehme, C.; Frenking, G. *J. Am. Chem. Soc.* **1996**, *118*, 2039.

significantly smaller than in traditional systems like benzene.<sup>50</sup> This might account for the higher stability towards dimerisation observed for unsaturated carbenes.<sup>8a, 29b</sup>

### 1.5.2. Steric properties.

The steric bulkiness of carbenes can not be quantified by Tolman's cone angle due to the "fence" or "fan" type shape associated with N-heterocyclic carbenes. Consequently, a new model was defined by Nolan *et al.* in order to quantify the steric factors characterising NHC's.<sup>51</sup> The steric hindrance of NHC's was conceptualised as "the percent of the volume occupied by ligand atoms in a sphere centered on the metal ( $\%V_{\text{Bur}}$ )."<sup>52</sup> Importantly, this new model makes possible the comparison not only with other carbenes, but also with tertiary phosphines.

The volume of the sphere represents the space around the metal atom that must be shared by the different ligands upon coordination. The radius of the sphere was arbitrary decided to be 3 Å and the C or P atom of the DFT optimized geometries of free ligand was positioned 2 Å from the putative metal centre. A representation of this model is depicted in Figure 1.15.

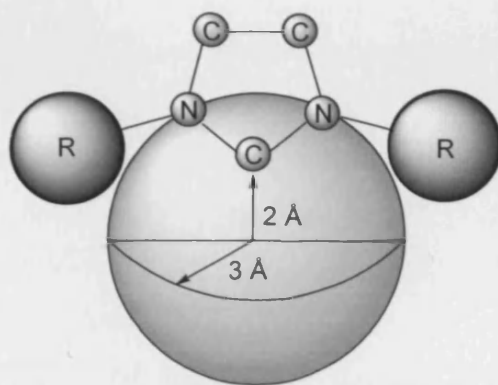


**Figure 1.15.** Sphere dimensions for steric parameter determination.<sup>51a</sup>

<sup>50</sup> Lehmann, J.F.; Urquhart, S.G.; Ennios, L.E.; Hitchcock, A.P.; Hatano, K.; Gupta, S.; Denk, M.K. *Organometallics* **1999**, *18*, 1862.

<sup>51</sup> (a) Hillier, Anna C.; Sommer, William J.; Yong, Ben S.; Petersen, Jeffrey L.; Cavallo, Luigi; Nolan, Steven P. *Organometallics* **2003**, *22*, 4322. (b) Viciu, Mihai S.; Navarro, Oscar; Germaneau, Romain F.; Kelly, Roy A., III; Sommer, William; Marion, Nicolas; Stevens, Edwin D.; Cavallo, Luigi; Nolan, Steven P. *Organometallics* **2004**, *23*, 1629.

<sup>52</sup> Díez-González, Silvia; Nolan, Steven P. *Coord. Chem. Rev.* **2007**, *251*, 874.

### 1.5.3. Coordination chemistry of NHC's.

The most widely used method for the synthesis of carbene complexes is *via* ligand substitution at the metal centre. This method requires the free carbene to be a stable species or at least a reactive intermediate which allows the synthesis of the complex by *in situ* generation of the ligand.

Generally, free carbenes are produced and isolated, or generated *in situ*, by deprotonation of the corresponding salt using an external base like NaOAc, NaH, KO<sup>t</sup>Bu, LDA or K[HMDs]. The use of an external base can be avoided by reacting the salt with a metal precursor containing basic ligands such as [Pd(OAc)<sub>2</sub>]<sup>53</sup> or [(COD)Ir(μ-OR)<sub>2</sub>Ir(COD)].<sup>54</sup> Additionally, free carbenes derived from azolium frameworks can also be prepared by other methods such as thermal decomposition of 2-alkoxyimidazolines, 2-alkoxyimidazolidines<sup>55</sup> and 2-(pentafluorophenyl)imidazolidines<sup>56</sup> or reductive desulfurisation of thiones<sup>57</sup> with potassium or sodium/potassium alloy (Scheme 1.18).

---

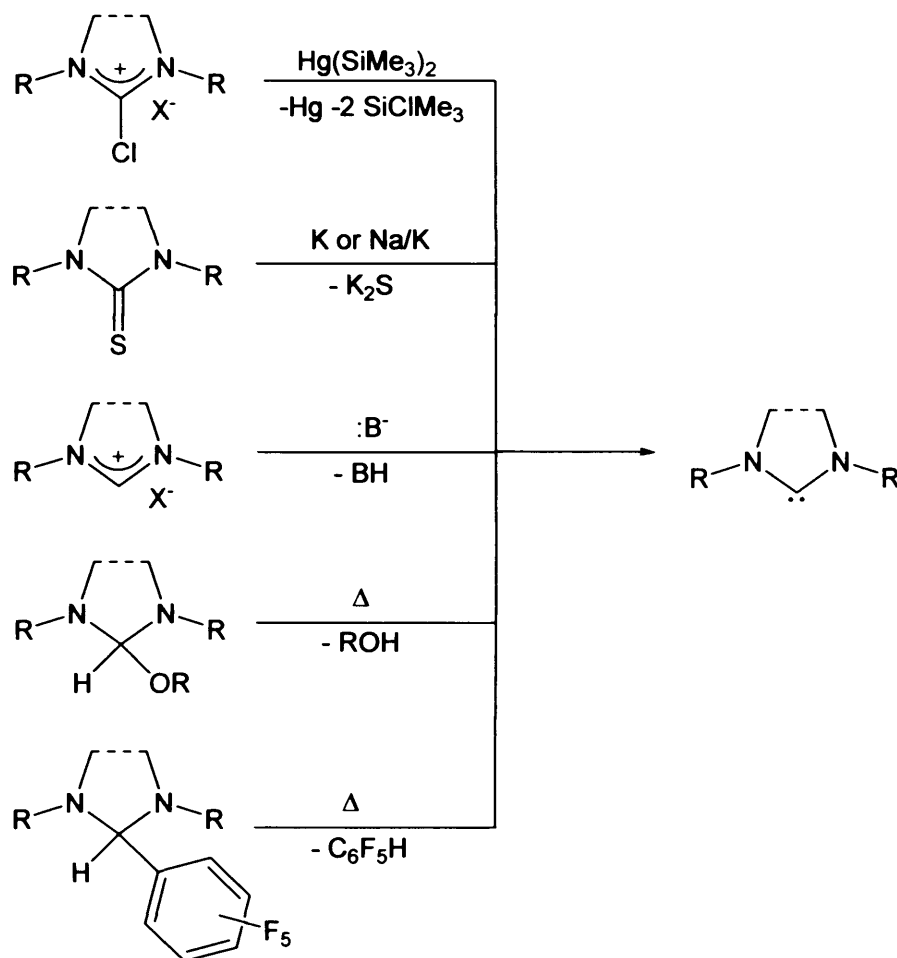
<sup>53</sup> (a) Hahn, F. E.; Foth, M. *J. Organomet. Chem.* **1999**, *585*, 241. (b) Herrmann, W. A.; Elison, M.; Fischer, J.; Köcher, C.; Artus, G. R. *J. Angew. Chem. Int. Ed. Engl.* **1995**, *34*, 2371. (c) Herrmann, W. A.; Reisinger, C.-P.; Spiegler, M. *J. Organomet. Chem.* **1998**, *557*, 93.

<sup>54</sup> (a) Köcher, C.; Herrmann, W. A. *J. Organomet. Chem.* **1997**, *532*, 261. (b) Hahn, F. E.; Holtgrewe, C.; Pape, T.; Martin, M.; Sola, E.; Oro, L. A. *Organometallics* **2005**, *24*, 2203.

<sup>55</sup> Scholl, M.; Ding, S.; Lee, C.W.; Grubbs, R. H. *Org. Lett.* **1999**, *1*, 953.

<sup>56</sup> (a) Nyce, G. W.; Cishony, S.; Waymouth, R. M.; Hedrick, J. L. *Chem. Eur. J.* **2004**, *10*, 4073. (b) Blum, A. P.; Ritter, T.; Grubbs, R. H.; *Organometallics* **2007**, *26*, 2122.

<sup>57</sup> (a) Denk, M. K.; Thadani, A.; Hatano, K.; Lough, A. J. *Angew. Chem. Int. Ed. Engl.* **1997**, *36*, 2607. (b) Hahn, F. E.; Wittenbecher, L.; Boese, R.; Bläser, D. *Chem. Eur. J.* **1999**, *5*, 1931.



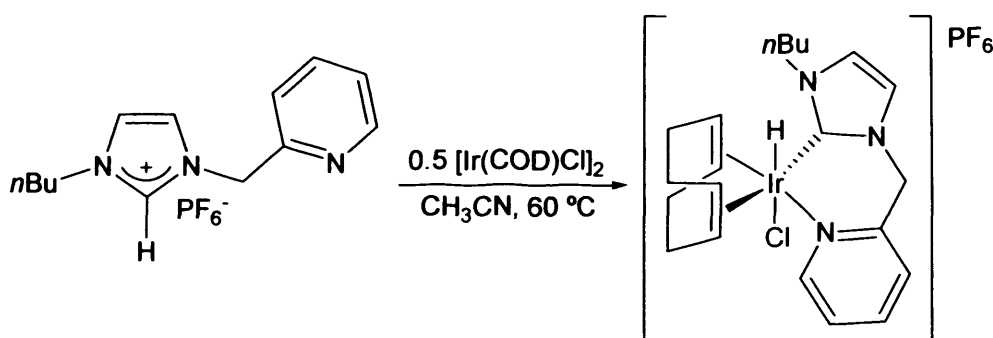
**Scheme 1.18.** Summary of methods for the preparation of free carbenes.

An important method for the synthesis of carbene complexes is the transfer from silver (I) to a number of transition metals as it makes possible the preparation of complexes not accessible otherwise and does not require the use of Schlenk techniques. This method will be discussed in more detail in *Chapter 3*.

In 2001 Cavell and Yates showed theoretically and experimentally that the oxidative addition of the C<sup>2</sup>-X bond (X = halogen) of imidazolium cations to electron rich d<sup>10</sup> metals proceeds readily. However, the oxidative addition of C<sup>2</sup>-H bonds is sluggish and no product is experimentally observed for C<sup>2</sup>-C<sub>Alkyl</sub> bonds.<sup>58</sup> These results paved the way for the application of oxidative addition as an efficient method for the synthesis of carbene complexes.

<sup>58</sup> (a) McGuinness, D. S.; Cavell, K. J.; Yates, B. F. *Chem. Commun.* **2001**, 355.(b) McGuinness, D. S.; Cavell, K. J.; Yates, B. F.; Skelton, B.W.; White, A. H. *J. Am. Chem. Soc.* **2001**, *123*, 8317. (c) Graham, D. C.; Cavell, K. J.; Yates, B. F. *Dalton Trans.* **2007**, 4650.

The studies by Peris *et. al.* on the oxidative addition of N-(2-pyridylmethyl)imidazolium cations to iridium (I) showed that the formation of the corresponding chelate complex is favoured by initial coordination of the nitrogen atom at the pyridyl substituent (Scheme 1.19).<sup>59</sup> Additionally, chelation stabilises carbene complexes prone to undergo reductive elimination. This has been rationalised as a consequence of the rigid conformation of chelate ligands, which prevents optimal orbital overlap during the reductive elimination.<sup>60</sup>



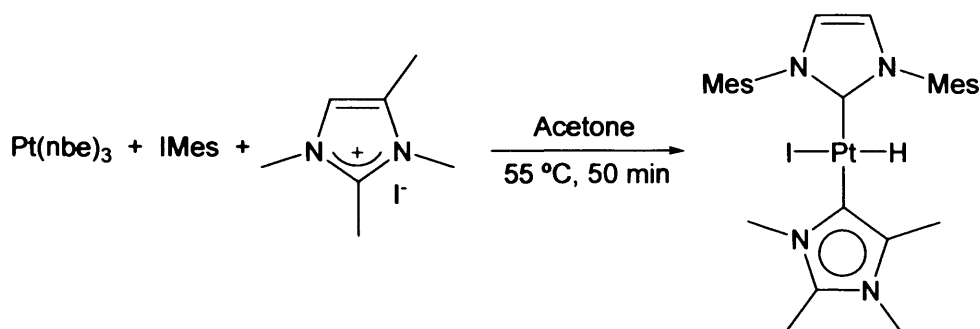
**Scheme 1.19.** Synthesis of a chelate carbene complex by oxidative addition of a C<sup>2</sup>-H bond.

Interestingly, Cavell and co-workers showed that the preparation of abnormal carbene complexes can also be achieved by oxidative addition of the C<sup>4</sup>-H bond of C<sup>2</sup> blocked imidazolium cations to Pt<sup>0</sup>. The abnormal carbene complex is obtained by reaction of the blocked imidazolium salt, with Pt(nbe)<sub>3</sub> and IMes in acetone (Scheme 1.20). The authors propose the initial formation of a [Pt(IMes)(nbe)<sub>2</sub>] complex, an electron rich intermediate, which subsequently undergoes oxidative addition of the C<sup>4</sup>-H bond of the imidazolium salt.

<sup>59</sup> Mas-Marzá, E.; Sanaffl, M.; Peris, E. *Inorg. Chem.* **2005**, *44*, 9961.

<sup>60</sup> McGuinness, D. S.; Saendig, N.; Yates, B. F.; Cavell, K. J. *J. Am. Chem. Soc.* **2001**, *123*, 4029.  
b) Graham, D. C.; Cavell, K. J.; Yates, B. F. *Dalton Trans.* **2005**, 1093. c) Graham, D. C.; Cavell, K. J.; Yates, B. F. *Dalton Trans.* **2006**, 1768.





**Scheme 1.20.** Synthesis of an abnormally bound carbene complex by oxidative addition of the  $\text{C}^4\text{-H}$  bond.

The template synthesis of carbenes, first reported by Chugaev in 1925,<sup>61</sup> has been improved thanks to the contribution of various research groups like Beck *et. al.*,<sup>62</sup> Fehlhhammer *et. al.*,<sup>63</sup> and more recently Liu *et. al.*<sup>64</sup> and especially Hahn *et. al.*<sup>65</sup> Nowadays this method is of special interest for the preparation of macrocyclic carbenes or oxazolidin-2-ylidenes, which are not accessible by standard methods and usually entails the metallation of a functionalised isocyanide followed by a nucleophilic attack on the coordinated carbon atom (Scheme 1.21).

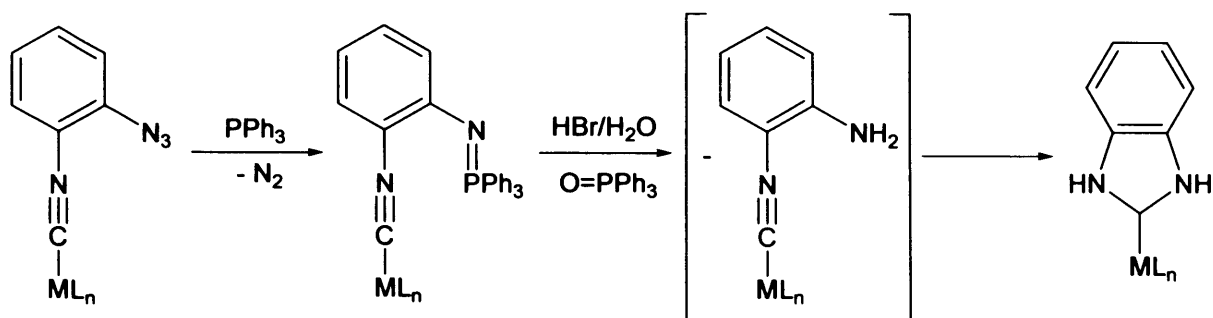
<sup>61</sup> Chugaev, L.; Skanawy-Grigorjewa, M.; Posnjak, A. *Z. Anorg. Allg. Chem.* 1925, 148, 37

<sup>62</sup> Beck, W.; Weigand, W.; Nagel, U.; Schaal, M. *Angew. Chem. Int. Ed. Engl.* 1984, 23, 377.

<sup>63</sup> (a) Fehlhhammer, W. P.; Bartel, K.; Petri, W. *J. Organomet. Chem.* 1975, 87, C34. (b) Bär, E.; Völkl, A.; Beck, F.; Fehlhhammer, W. P.; Robert, A. *J. Chem. Soc. Dalton Trans.* 1986, 863. (c) W. Fehlhhammer, P.; Zinner, G.; Beck, G.; Fuchs, J. *J. Organomet. Chem.* 1989, 379, 277. (d) Kunz, R.; Le Grel, P.; Fehlhhammer, W. P. *J. Chem. Soc. Dalton Trans.* 1996, 3231.

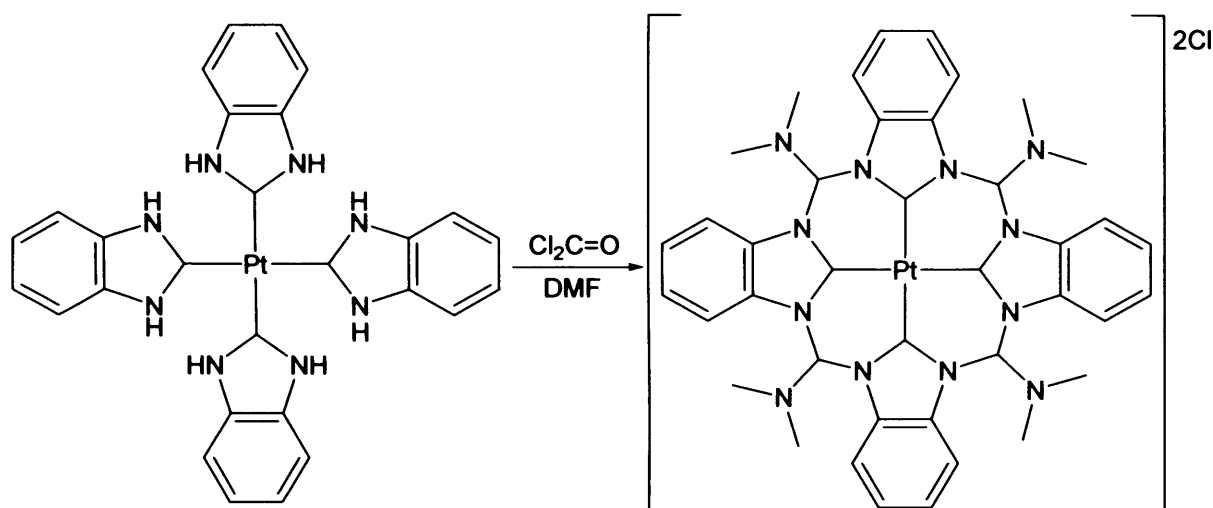
<sup>64</sup> (a) Liu, C.-Y.; Chen, D.-Y.; Lee, G.-H.; Peng, S.-M.; Liu, S.-T. *Organometallics* 1996, 15, 1055. (b) Ku, R.-Z.; Chen, D.-Y.; Lee, G.-H.; Peng, S.-M.; Liu, S.-T. *Angew. Chem. Int. Ed. Engl.* 1997, 36, 263.

<sup>65</sup> (a) Hahn, F. E. *Angew. Chem. Int. Ed. Engl.* 1993, 32, 650. (b) Hahn, F. E.; Tamm, M. *Chem. Commun.* 1993, 842. (c) Hahn, F. E.; Tamm, M.; Lügger, T. *Angew. Chem. Int. Ed. Engl.* 1994, 33, 1356. (d) Hahn, F. E.; Tamm, M. *Organometallics* 1995, 14, 2597. (e) Hahn, F. E.; Tamm, M. *Chem. Commun.* 1995, 569. (f) Glaser, M.; Spies, H.; Lügger, T.; Hahn, F. E. *J. Organomet. Chem.* 1995, 503, C32. (g) Hahn, F. E.; Langenhahn, V.; Meier, N.; Lügger, T.; Fehlhhammer, W. P. *Chem. Eur. J.* 2003, 9, 704. (h) Hahn, F. E.; Langenhahn, V.; Lügger, T.; Pape, T.; Le Van, D. *Angew. Chem. Int. Ed.* 2005, 44, 3759.



**Scheme 1.21.** Template-controlled cyclization of 2-azidophenyl isocyanide.

A remarkable example that illustrates the potential of this method is the synthesis of the tetracarbeno macrocycle reported by Hahn and co-workers (Scheme 1.22).<sup>65h</sup>



**Scheme 1.22.** Template synthesis of a tetracarbeno macrocycle.

To date, research has mainly focused on five-membered carbenes, leaving six- and seven-membered ring carbenes relatively unexplored. The work presented in this thesis will focus on the synthesis and characterisation of expanded (larger than 5-membered) saturated carbenes complexes. The good donor ability and large  $N-C_{CHN}-N$  angles featured by expanded carbenes make them very interesting for use as ligands in catalytic systems. The wide  $N-C_{NHC}-N$  angles force the  $N$ -substituents to come closer to the metal centre, which should induce a higher selectivity and allow a better transmission of information from the ligand to the substrate. The design and synthesis of chiral carbenes *via* backbone

substitution is, therefore, an appealing enterprise. However, the available literature methods for the synthesis of expanded carbenes are poorly reproducible or low yielding, consequently, a new synthetic methodology which made possible the synthesis of expanded carbenes in good yields needed to be developed.

# Chapter

# 2

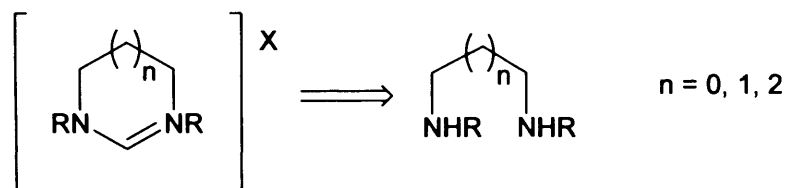
## Synthesis of novel expanded-ring N-heterocyclic carbenes

<b>2.1. Introduction</b> .....	31
<b>2.2. Results and Discussion</b> .....	34
2.2.1. Synthesis of azolium salts from diamines.....	34
2.2.1.1. Synthesis of the diamines <i>N,N'</i> -dicyclohexyl-1,4-diaminobutane (2.4) and (-)- <i>trans</i> -4,5-Bis[ <i>N</i> -Cyclohexyl]-2,2-dimethyl-1,3-dioxolan (2.5) .....	34
2.2.1.2. Synthesis of 1,3-diazepan-2-ylidene derivatives <i>7</i> -Cy·HPF <sub>6</sub> and <i>DIOC</i> -Cy·HPF <sub>6</sub> .....	39
2.2.1.3. X-Ray analysis.....	41
2.2.1.4. Deprotonation experiments of 1,3-diazepan-2-ylidene derivatives <i>7</i> Cy·HPF <sub>6</sub> and <i>DIOC</i> -Cy·HPF <sub>6</sub> .....	45
2.2.1.5. Synthesis of <i>N,N</i> -dihydrodiazepene salts.....	46
2.2.2. A new method of ring-closure.....	47
2.2.2.1. Synthesis of halide salts.....	47
2.2.2.2. Exchange of the counter anion - Formation of tetrafluoroborate salts.....	50
2.2.2.3. Solution NMR studies.....	52
2.2.2.4. Isolation of free carbenes.....	53
2.2.2.5. Properties and structure of expanded free carbenes.....	55
<b>2.3. Experimental</b> .....	59
2.3.1. Synthesis of azolium salts from diamines .....	60
2.3.1.1. First approach.....	60
2.3.1.2. Second approach.....	62
2.3.2. New method.....	67
2.3.3. Isolation of free carbenes.....	83

## Chapter 2. Synthesis of novel expanded-ring N-heterocyclic carbenes.

### 2.1. Introduction.

The wide interest in the synthesis of azolium salts arises from their central role as carbene precursors, by far the most frequently used, and their numerous applications as ionic liquids. To date research has largely focused on five-member ring carbenes. Examples of “expanded ring” six-membered<sup>1</sup> and seven-membered carbenes<sup>1a, 2</sup> have also been reported although to a lesser extent. In virtually all cases the carbene ring (whether, 5-, 6-, or 7-membered) is formed by the reaction of diamines (or diimines) with a formyl unit to close the ring (Scheme 2.1).

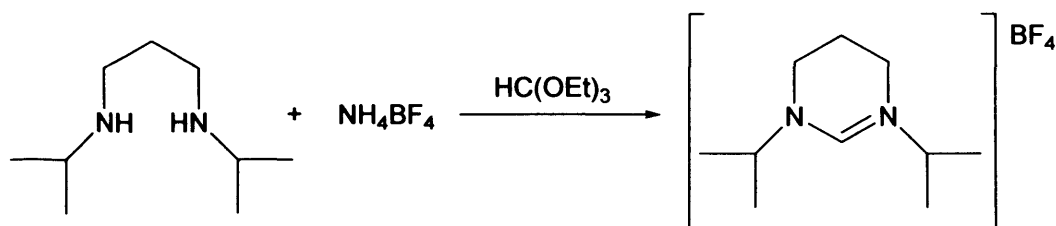


**Scheme 2.1.** Classical synthesis of saturated carbene precursors.

<sup>1</sup> (a) Alder, R. W.; Blake, M. E.; Bortolotti, C.; Bufali, S.; Butts, C. P.; Linehan, E.; Oliva, J. M.; Orpen, A. G.; Quayle, M. J. *Chem. Commun.* **1999**, 241; (b) Bazinet, P.; Yap, G. P. A.; Richeson, D. S. *J. Am. Chem. Soc.* **2003**, *125*, 13314.; (c) Mayr, M.; Wurst, K.; Ongania, K.-H.; Buchmeiser, M. R. *Chem. Eur. J.* **2004**, *10*, 1256; (d) Herrmann, W; Schneider, S. K.; Öfele, K.; Sakamoto, M.; Herdtweck, E. *J. Organomet. Chem.* **2004**, *689*, 2441; (e) Jazzar, R.; Liang, H.; Donnadiou, B.; Bertrand, G. *J. Organomet. Chem.* **2006**, *691*, 3201; (f) Bazinet, P.; Ong, T.-G.; O’Brien, J. S.; Lavoie, N.; Bell, E.; Yap, G. P. A.; Korobkov, I.; Richeson, D. S. *Organometallics* **2007**, *26*, 2885.

<sup>2</sup> (a) Scarborough, C. C.; Grady, M. J. W.; Guzei, I. A.; Gandhi, B. A.; Bunel, E. E.; Stahl, S. S. *Angew. Chem., Int. Ed.* **2005**, *44*, 5269; (b) Scarborough, C. C.; Popp, B. V.; Guzei, I. A.; Stahl, S. S. *J. Organomet. Chem.*, **2005**, *690*, 6143; (c) Rogers, M. M.; Wendlandt, J. E.; Guzei, I. A.; Stahl, S. S. *Org. Lett.* **2006**, *8*, 2257; (d) Iglesias, M.; Beestra, D. J.; Stasch, A.; Horton, P. N.; Hursthouse, M. B.; Coles, S. J.; Cavell, K. J.; Dervisi, A.; Fallis, I. A. *Organometallics* **2007**, *26*, 4800.

In the case of saturated azolium salts, this additional carbon atom is usually inserted by reaction of a diamine with triethylorthoformate and an ammonium (Scheme 2.2) salt,<sup>1a</sup> or formaldehyde followed by N-bromosuccinamide.<sup>1c</sup>



**Scheme 2.2.** Synthesis of the first expanded carbene.

This synthetic methodology is often poorly reproducible or low yielding when applied to the synthesis of expanded carbenes, which has limited the availability of the very basic and relatively unexplored 6- and, especially, 7-membered ring carbenes.<sup>2d</sup>

The biphenyl carbene, reported by Stahl<sup>2a</sup> and coworkers in 2005, represents the first example of a seven-membered ring N-heterocyclic carbene. The amidinium salt **2.1** (Figure 2.1) was synthesised in 65% yield, however, attempts to obtain the aromatic N-substituted analogues were unsuccessful, probably due to the lower basicity of the diaryl amines together with the entropic and enthalpic cost arising from the cyclisation of a seven-membered ring.

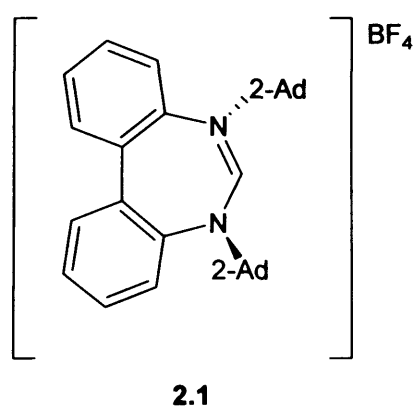
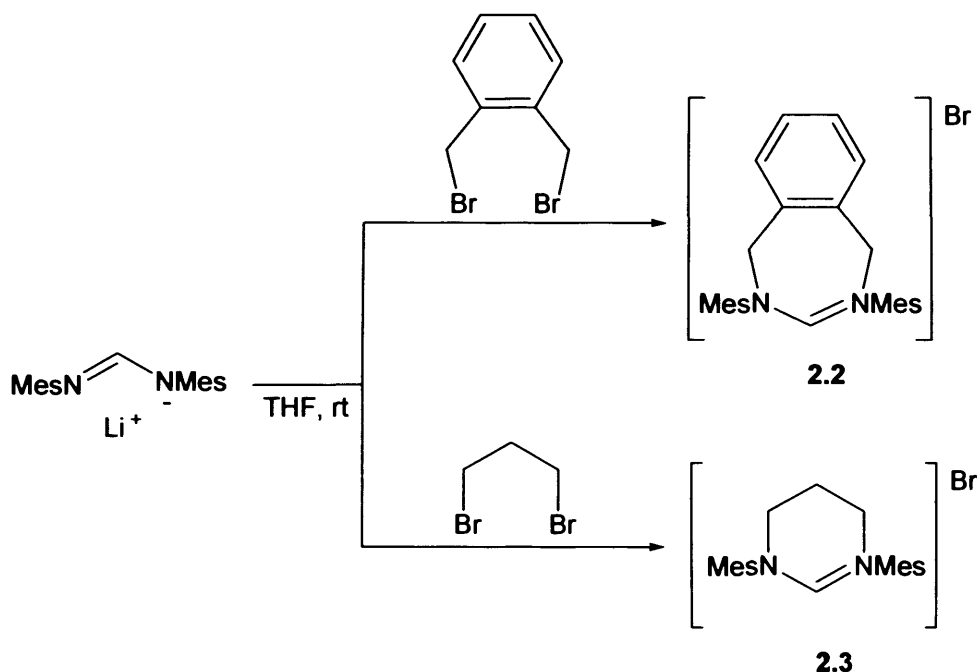


**Figure 2.1.** First example of a seven-membered amidinium salt presented by Stahl *et al.*

The new method of ring-closure, recently published by Bertrand *et al.*,<sup>1e</sup> in which an amidine fragment is first prepared and the ring is closed with a dibromohydrocarbyl unit (Scheme 2.2) using BuLi as base and THF as the solvent, offers a potentially very useful

synthetic methodology. This new approach was proved to be very efficient for the synthesis of a range of azolium salts, which included the seven membered-ring salt **2.2**, and also a better yielding synthesis of the six membered **2.3** previously reported by Herrmann *et al.*<sup>1d</sup> as examples (Scheme 2.3).



**Scheme 2.3.** New method of ring-closure reported by Bertrand *et al.*

It is commonly accepted that saturated expanded carbenes, as well as acyclic diaminocarbenes<sup>3</sup> are more basic than their five-membered equivalents. Theoretical calculations<sup>4</sup> showed that the main factor determining the basicity of the carbene is the NCN angle, more than electron delocalisation or substitution on the backbone. Therefore, expanded-ring systems were synthesised to provide carbenes with large NCN angles. Some of these carbene precursors were built with peripheral (backbone) substitution in order to force the NCN angle even closer to linearity.

<sup>3</sup> a) Merceron, N.; Miqueu, K.; Baccaredo, A.; Bertrand, G. *J. Am. Chem. Soc.* **2002**, *124*, 6806; b) Teuma, E.; Lyon-Saunier, C.; Gornitzka, H.; Mignani, G.; Baccaredo, A.; Bertrand, G. *J. Organomet. Chem.* **2005**, *690*, 5541.

<sup>4</sup> Magill, A. M.; Cavell, K.J.; Yates, B.F. *J. Am. Chem. Soc.* **2004**, *126*, 8717.

## 2.2. Results and Discussion.

### 2.2.1. Synthesis of azolium salts from diamines.

The initial efforts in the area of expanded ring NHCs concentrated on the synthesis of 1,3-diazepan-2-ylidene derivatives **7-Cy**·HPF<sub>6</sub> and **DIOC-Cy**·HPF<sub>6</sub> (Figure 2.2). The first of the two azolium salts to be synthesised was **7-Cy**·HPF<sub>6</sub>, which represents the first example of a completely saturated, unsubstituted, seven-membered carbene precursor. The next carbene precursor (**DIOC-Cy**·HPF<sub>6</sub>) was prepared in order to study whether the added strain of the *trans*-fused dioxolane ring on the carbene backbone would result in larger NCN angles and possibly increased basicity. These salts were synthesised using the classic methodology, i.e. by addition of a formyl unit to the corresponding diamines.

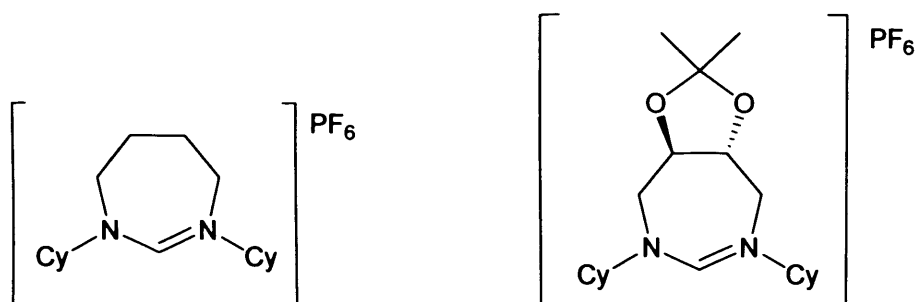
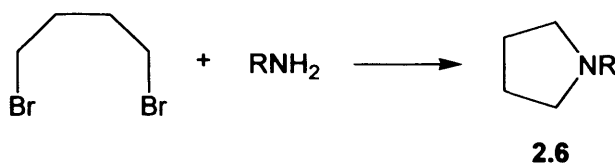


**Figure 2.2.** Target amidinium salts.

#### 2.2.1.1. Synthesis of the diamines *N,N'*-dicyclohexyl-1,4-diaminobutane (**2.4**) and (-)-*trans*-4,5-Bis[*N*-Cyclohexyl]-2,2-dimethyl-1,3-dioxolan (**2.5**).

Direct amination to the secondary amine is a deceptively simple synthetic approach because the monosubstituted product (secondary amine) is more nucleophilic than the reactant (primary amine), which leads ultimately to formation of the tertiary amine. More importantly, in this case, intramolecular reaction leads to formation of the corresponding pyrrolidine (**2.6**). The formation of the five-membered ring is entropically and thermodynamically favoured, in consequence, **2.6** is the main product of the reaction, even when the reaction is performed in absence of solvent to force the intermolecular reaction (Scheme 2.4).





**Scheme 2.4.** Direct amination of 1,4-dibromobutane.

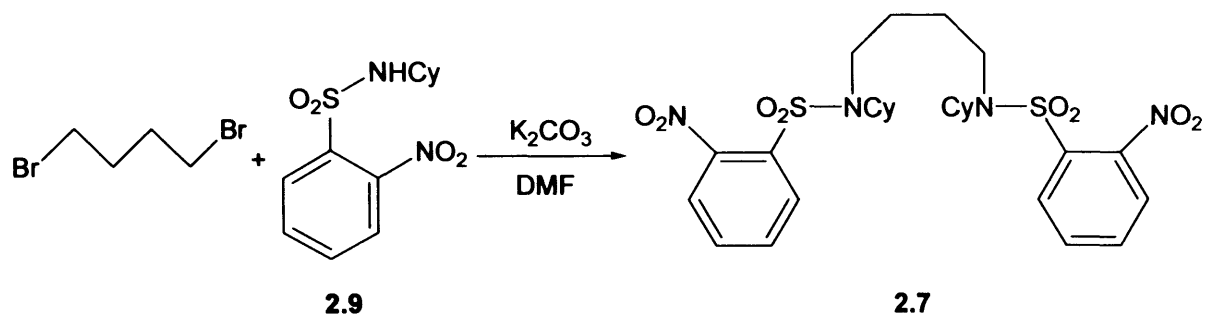
Diamines **2.4** and **2.5** were first synthesised using sulfonamides as nucleophiles (Schemes 2.5 and 2.6). These sulfonamides are protecting and activating groups; their use avoids the formation of tertiary amines (Scheme 2.4) and allows the use of milder conditions with improved yields.<sup>5</sup>

The protected amines **2.7** and **2.8** were synthesised by the reaction of 1,4-dibromobutane (Scheme 2.5) and (-)-*trans*-4,5-Bis[*tosyloxymethyl*]-2,2-dimethyl-1,3-dioxolan (Scheme 2.6), respectively, with N-Cyclohexyl-2-nitro-benzenesulfonamide (**2.9**) and an excess of potassium carbonate in dry dimethylformamide at 80°C. The reaction mixture is diluted with water and the product extracted with diethyl ether. Evaporation of the solvent affords the product as a white solid. Crystals of **2.7** suitable for X-ray single-crystal diffraction were obtained by slow evaporation of a chloroform solution of the compound (Figure 2.3). When performed on a scale smaller than 5 mmol of the di-electrophile [(-)-*trans*-4,5-Bis[*tosyloxymethyl*]-2,2-dimethyl-1,3-dioxolan (**2.10**) or 1,4-dibromobutane the reaction was completed overnight in good yields. However, attempts to scale up the reaction always resulted in a considerable increase of the reaction time and drop of the yield.

The secondary amines **2.4** and **2.5** were synthesised by deprotection of sulfonamides **2.7** and **2.8**, respectively. The corresponding sulphonamide is reacted overnight with an equimolar amount of thiophenol at 80°C. The resulting reaction mixture is acidified with hydrochloric acid in order to form the hydrochloride, which is extracted with water. The aqueous layer is basified with NaOH until it remains basic (pH = 8) to litmus paper and the free amine is extracted with dichloromethane.

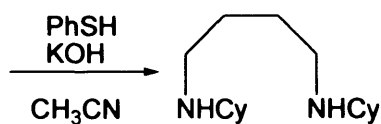
---

<sup>5</sup> Kurosawa, Wataru; Kan, Toshiyuki; Fukuyama, Torhu *Organic Syntheses Coll.* Vol. 10, p.482; Vol. 79, p.186.



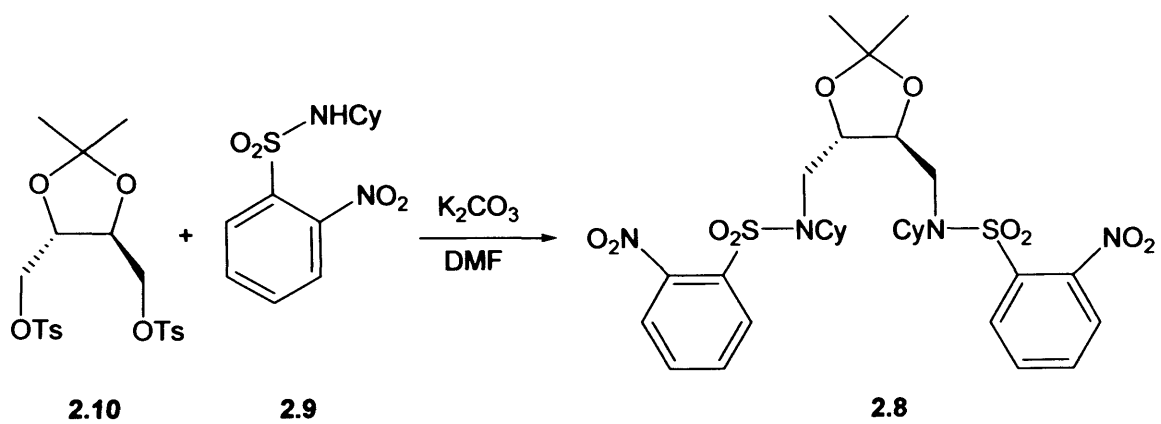
2.9

2.7



2.4

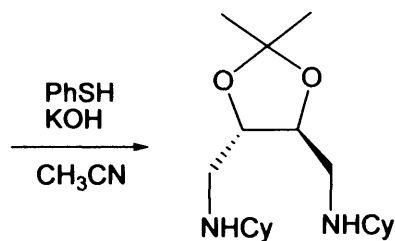
Scheme 2.5. Synthesis of diamine 2.4.



2.10

2.9

2.8



2.5

Scheme 2.6. Synthesis of diamine 2.5.

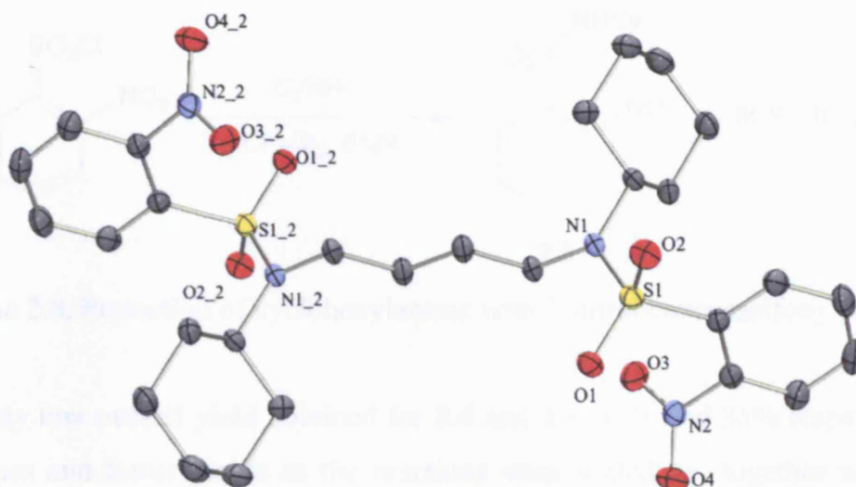
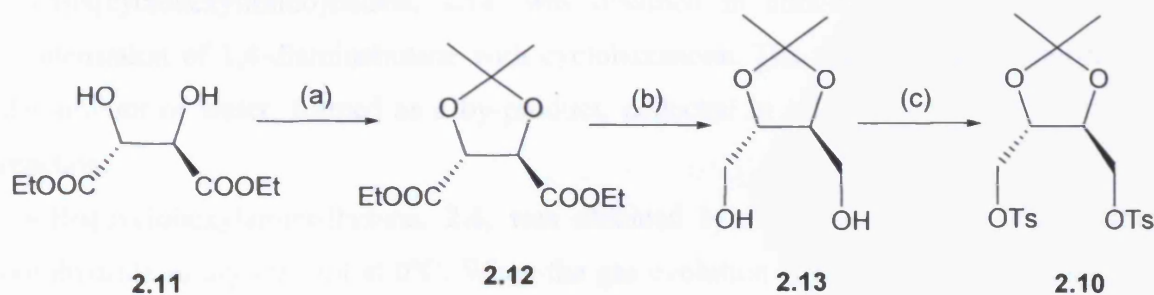


**Figure 2.3.** ORTEP ellipsoid plots at 50% probability of the molecular structure of **2.7**. Hydrogens have been omitted for clarity.

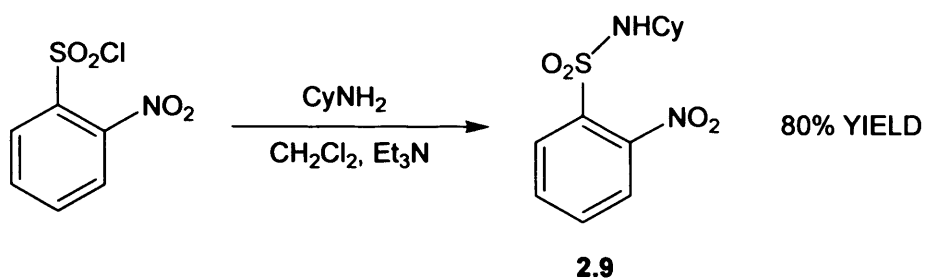
The ditosylate tartrate derivative **2.10**, in Scheme 2.6, was prepared by literature methods from the commercial available (-)-*trans*-4,5-diethyl-2,3-isopropylidene-L-tartrate (**2.11**) in three steps<sup>6</sup> (Scheme 2.7).



**Scheme 2.7.** Preparation of the tartrate ditosylate. Reagents and condition: (a) Acetone (1.1 eq), Tos-OH (cat), in  $\text{CHCl}_3$  / molecular sieves, 2.5 h reflux (b)  $\text{LiAlH}_4$  (3 eq) /  $\text{Et}_2\text{O}$ , 6 h reflux (c) Tos-Cl (1 eq), 18 h  $-25^\circ\text{C}$ .

N-Cyclohexyl-2-nitro-benzenesulfonamide (**2.9**) was obtained in good yields by reaction of cyclohexylamine with 2-nitrobenzenesulfonylchloride at ambient temperature (Scheme 2.8).

<sup>6</sup> Murder, Barry A.; Brown, John; Chaloner, Penny A.; Nicholson, Philip N.; Parker, David *Synthesis* **1979**, 5, 350.



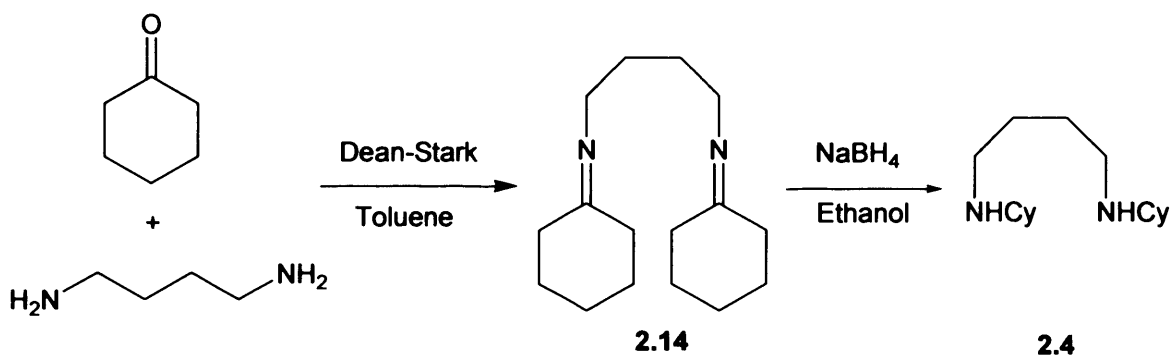
**Scheme 2.8.** Protection of cyclohexylamine with 2-nitrobenzenesulfonylchloride.

The relatively low overall yield obtained for **2.4** and **2.5**, 45% and 35% respectively, long reaction times and lower yields as the reactions were scaled up, together with the long synthesis, especially in the case of **2.5**, and the use of large amounts of thiophenyl for the deprotection represented an important drawback concerning the synthesis of the salts in large scale. Therefore, a new synthetic approach was proposed for the synthesis of the target diamines.

This new approach entails the formation of the corresponding diimine, **2.14** or **2.15**, followed by reduction with  $\text{NaBH}_4$ . The overall yields obtained for amines **2.4** and **2.5** are 75% and 76% respectively.

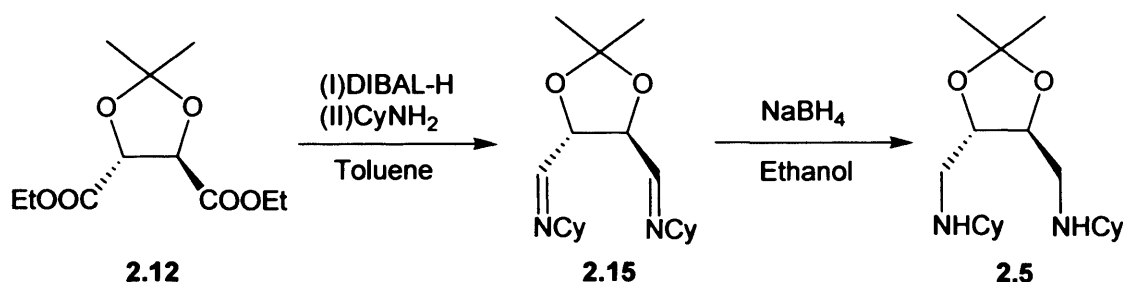
1,4-Bis[cyclohexylimino]butane, **2.14**, was obtained in almost quantitative yields by condensation of 1,4-diaminobutane with cyclohexanone. The reaction was monitored by the amount of water, formed as a by-product, collected in a Dean-Stark trap during the reaction.

1,4-Bis[cyclohexylamino]butane, **2.4**, was obtained by reduction of **2.14** with sodium borohydride in dry ethanol at  $0^\circ\text{C}$ . When the gas evolution was finished the reaction was stirred for one more hour. The residue obtained after evaporation of ethanol was dissolved in water and extracted with diethyl ether (Scheme 2.9).



**Scheme 2.9.** Synthesis of diamine **2.4** via imine intermediate.

The tartrate diester derivative **2.12** was converted to the tartrate diimine, **2.15**, by reduction to the aldehyde with DIBAL-H and *in situ* condensation with cyclohexylamine. The reaction mixture is kept at  $-78^{\circ}\text{C}$  until the cyclohexylamine is added to avoid direct reduction of the ester to the alcohol. Reduction of **2.15** with sodium borohydride to affords diamine **2.5** as was described for **2.4** (Scheme 2.10).



**Scheme 2.10.** Synthesis of diamine **2.5** via reductive amination.

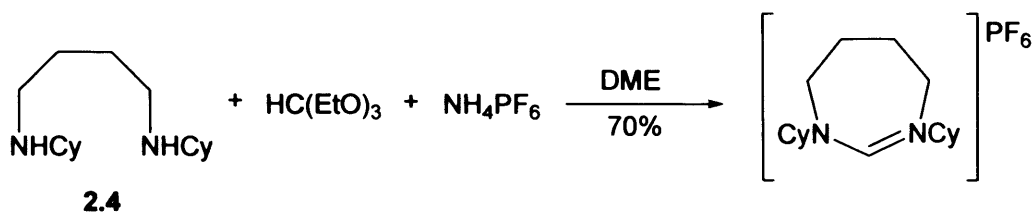
This new approach means a significant improvement in the synthesis of compound **6** and especially **7**. In both cases the number of steps was reduced, yields were improved and reaction times were significantly shorter.

#### 2.2.1.2. Synthesis of 1,3-diazepan-2-ylidene derivatives 7-Cy-HPF<sub>6</sub> and DIOC-Cy-HPF<sub>6</sub>.

Ring closure of diamines **2.4** and **2.5** was attempted using triethyl orthoformate as co-solvent according to literature methods.<sup>7</sup> In the first case (7-Cy-HPF<sub>6</sub>) this method led to low yields (10-20%) and in the second (DIOC-Cy-HPF<sub>6</sub>) no product was isolated.

In order to ensure the high dilution conditions required for these systems, two equivalents of triethylorthoformate were reacted with the corresponding cyclohexyl diamine (**2.4** or **2.5**) in DME. The reaction mixture was refluxed for 3h at  $120^{\circ}\text{C}$ . The solvent was evaporated *in vacuo* and the residue crystallised from a mixture of dichloromethane / diethyl ether, affording the amidinium salt 7-Cy-HPF<sub>6</sub> (Scheme 2.11) in overall yields of 70%. Crystals suitable for X-Ray analysis were obtained by layering hexanes on a dichloromethane solution of the amidinium salt.

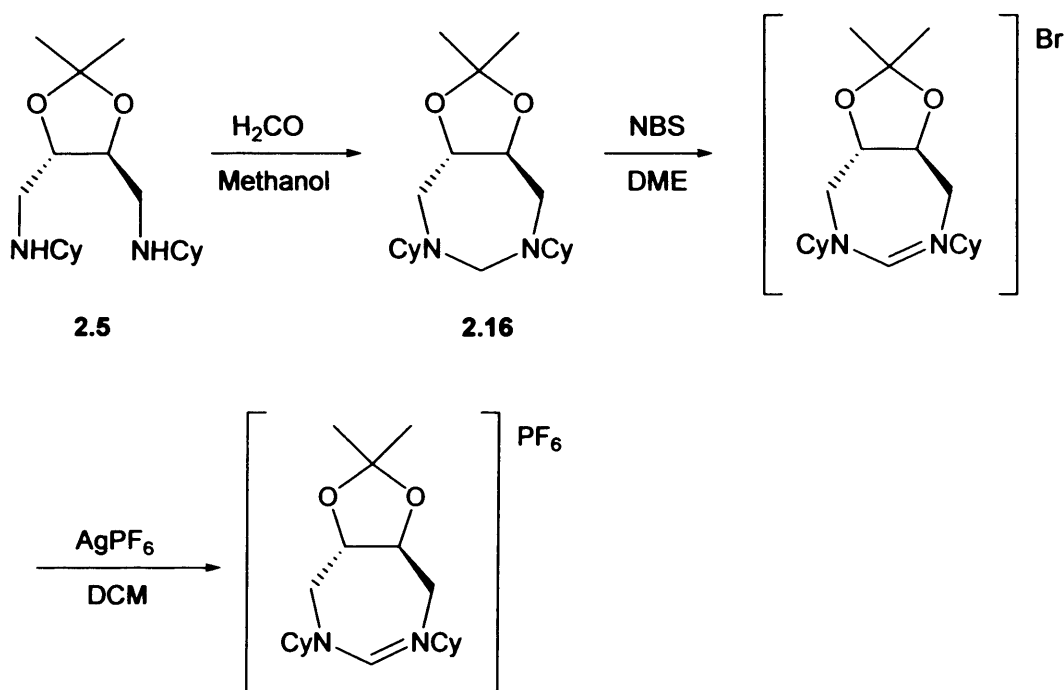
<sup>7</sup> (a) Scarborough, Christopher C.; Grady, Michael J. W.; Guzei, Ilia A.; Gandhi, Bhaves A.; Bunel, Emilio E.; Stahl, Shannon S. *Angew. Chem. Int. Ed.* **2005**, *44*, 5269; (b) Saba, S.; Brescia, A.; Kaloustian, M. K. *Tetrahedron Letters* **1991**, *32*, 5031.



**Scheme 2.11.** Synthesis of amidinium salt **7-Cy·HPF<sub>6</sub>**.

The next target in the 1,3-diazepan-ylidene series was the carbene precursor **DIOC-Cy·HPF<sub>6</sub>**. Unfortunately, despite dilution of the system with DME, the yield of cyclisation drops dramatically to values lower than 10%. This might be a consequence of the further strain originated from the dioxolane ring on the backbone, which prevents the molecule from taking the right conformation for ring closure.

The preferred route for the ring-closure of the tartrate derivative is shown in Scheme 2.12, although low yields of the amidinium salt **7-Cy·HBr** were obtained (in 10-20% yield).



**Scheme 2.12.** Synthesis of amidinium salt **DIOC-Cy·HPF<sub>6</sub>**.

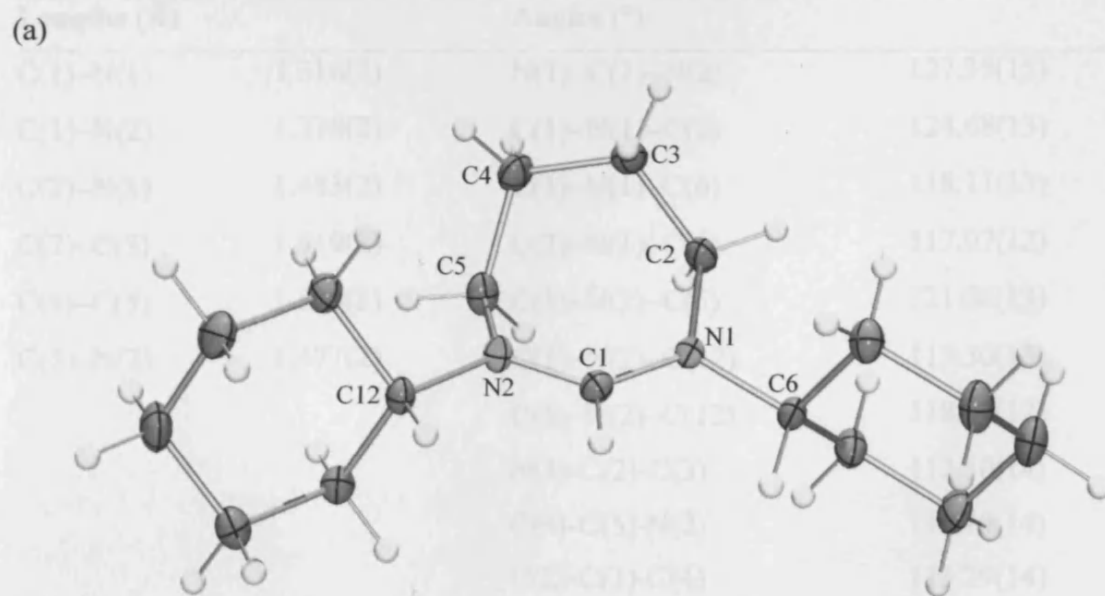
Diamine **2.5** on treatment with formaldehyde in methanol at 50°C forms the methylene intermediate **2.16**. When **2.16** is reacted with N-bromosuccinamide in DME at ambient temperature, the bromide salt **DIOC-Cy·HBr** precipitates out of the DME solution after 2-3h. Filtration of the solid affords **DIOC-Cy·HBr** as a white waxy solid in 10-20% yield. It

is noteworthy that attempts to purify the crude reaction mixture by chromatography on silica gel resulted always in decomposition of the amidinium salt. Treatment of **DIOC-Cy**·HBr with AgPF<sub>6</sub> formed its PF<sub>6</sub><sup>-</sup> analogue. Crystals suitable for X-ray diffraction were obtained by crystallisation from a mixture of chloroform / diethyl ether (2:1).

### 2.2.1.3. X-Ray analysis.

Singe-crystal X-ray diffraction data were collected for salts **7-Cy**·HPF<sub>6</sub> and **DIOC-Cy**·HPF<sub>6</sub>; their ORTEP plots are shown in Figure 2.4. The solid state structure of **5** reveals an unusually large NCN angle at 135.90(10)° compared to a value of 127.35(15)° for the non-substituted 7-membered ring of **7-Cy**·HPF<sub>6</sub>. The corresponding value for the biaryl derivative **2.1** is even smaller at 124.2(3)°, and that of the xylene derived salt, **2.2**, at 127.50(14)°.

The amidinium ring of salt **7-Cy**·HPF<sub>6</sub> adopts a chair conformation with the C3 and C4 above or below the NCN plane. This is the expected conformation of minimum energy for an unsubstituted, seven-membered ring. Differently, in **DIOC-Cy**·HPF<sub>6</sub>, the *trans* substitution on the backbone forces the ring to adopt a rigid twisted-chair conformation, with the C3 above and the C4 below the NCN plane.



(b)

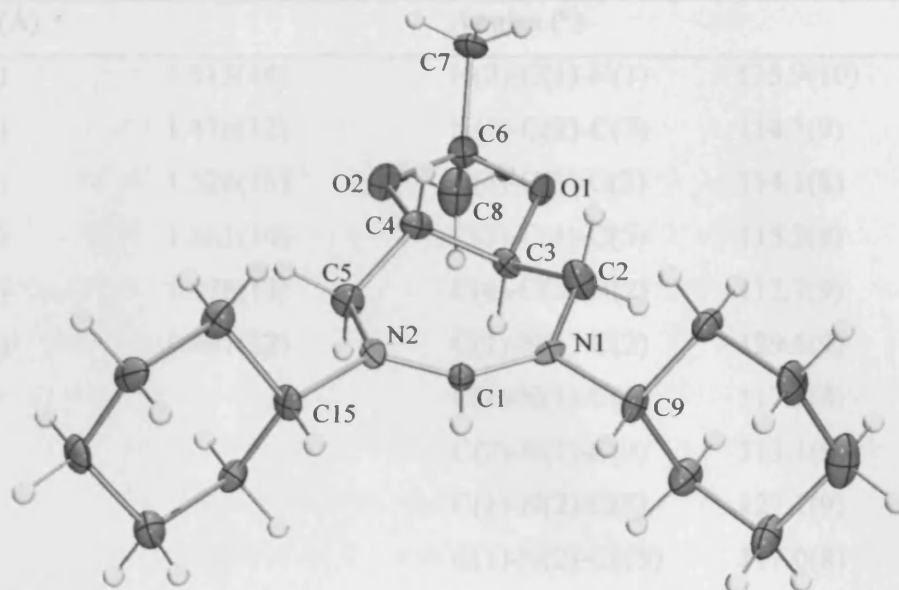


**Figure 2.4.** ORTEP ellipsoid plot at 30% probability of the amidinium cations **7-Cy-HPF<sub>6</sub>** (Figure 2.4.a) and **DIOC-Cy-HPF<sub>6</sub>** (Figure 2.4.b). Counteranions have been omitted for clarity.

**Table 2.1.** Selected bond lengths (Å) and angles (°) for **7-Cy-HPF<sub>6</sub>**.

Lengths (Å)		Angles (°)	
C(1)–N(1)	1.316(2)	N(1)–C(1)–N(2)	127.35(15)
C(1)–N(2)	1.318(2)	C(1)–N(1)–C(2)	124.68(13)
C(2)–N(1)	1.483(2)	C(1)–N(1)–C(6)	118.11(13)
C(2)–C(3)	1.519(2)	C(2)–N(1)–C(6)	117.07(12)
C(4)–C(5)	1.516(2)	C(1)–N(2)–C(5)	121.26(13)
C(5)–N(2)	1.477(2)	C(1)–N(2)–C(12)	119.30(13)
		C(5)–N(2)–C(12)	118.84(12)
		N(1)–C(2)–C(3)	112.50(14)
		C(4)–C(5)–N(2)	113.19(14)
		C(2)–C(3)–C(4)	113.29(14)
		C(5)–C(4)–C(3)	111.52(13)



**Table 2.2.** Selected bond lengths (Å) and angles (°) for **DIOC-Cy-HPF<sub>6</sub>**.

Lengths (Å)		Angles (°)	
C(1)-N(1)	1.313(14)	N(2)-C(1)-N(1)	135.9(10)
C(2)-N(1)	1.476(12)	N(1)-C(2)-C(3)	114.3(9)
C(2)-C(3)	1.520(13)	C(4)-C(3)-C(2)	114.1(8)
C(3)-C(4)	1.461(14)	C(3)-C(4)-C(5)	115.2(8)
C(4)-C(5)	1.476(13)	C(4)-C(5)-N(2)	112.7(9)
C(5)-N(2)	1.497(12)	C(1)-N(1)-C(2)	129.6(9)
		C(1)-N(1)-C(9)	117.3(8)
		C(2)-N(1)-C(9)	113.1(9)
		C(1)-N(2)-C(5)	127.1(9)
		C(1)-N(2)-C(15)	117.0(8)
		C(5)-N(2)-C(15)	115.0(9)

The torsional angle ( $\beta$ ) between the planes defined by the C2-N1...N2-C5 atoms functions as a mechanism to release the steric tension caused by the expansion of the ring. The twisting of the ring in the amidinium salt **7-Cy-HPF<sub>6</sub>** results in a torsional angle of 23.3°, whereas in **5** the two C-N...N planes deviate from planarity by only 9.9° (Figure 2.5).

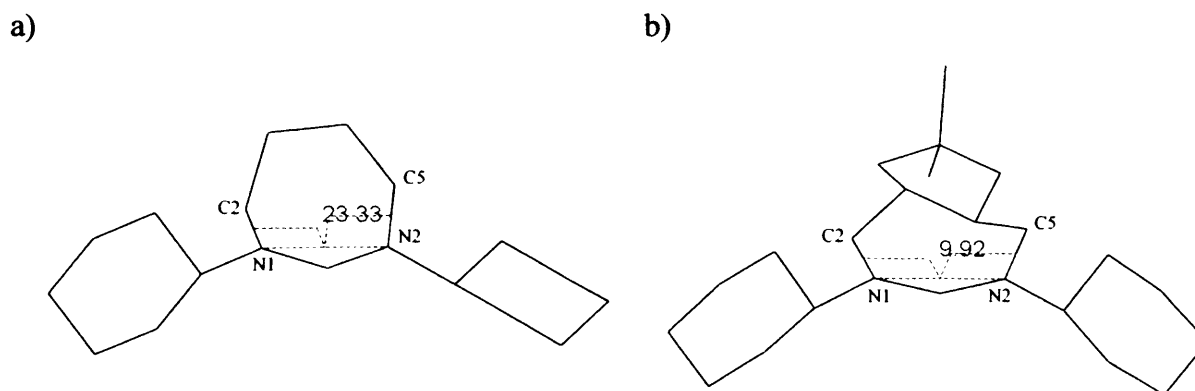


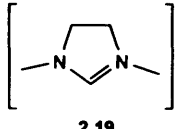
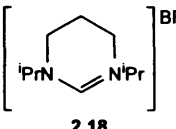
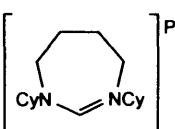
**Figure 2.5.** Mercury representation of the torsional angle ( $\alpha$ ) in the amidinium cations **7-Cy-HPF<sub>6</sub>** (3.3°, Figure 2.4.a) and **DIOC-Cy-HPF<sub>6</sub>** (9.9°, Figure 2.4.b). Hydrogen atoms and counteranions are omitted for clarity.

The conformation of **DIOC-Cy-HPF<sub>6</sub>**, locked due to the *trans* substitution on the backbone, prevents **DIOC-Cy-HPF<sub>6</sub>** from realising its annular strain by twisting the ring. This leaves **DIOC-Cy-HPF<sub>6</sub>** with only two alternatives to discharge its ring strain: enlargement of the N-C-N angle or tetrahedral deviation of the ring carbon atoms.

In the amidinium salt **7-Cy-HPF<sub>6</sub>** the C2 and C5 carbon ring angles range from 111.5 to 113.3° while in **DIOC-Cy-HPF<sub>6</sub>** an even more strained ring is observed as indicated from the corresponding angle range, 112.6 - 116.0°. This fact, together with the larger N-C-N angle observed for the tartrate derivative **DIOC-Cy-HPF<sub>6</sub>** (8.5° wider than **7-Cy-HPF<sub>6</sub>**), illustrates the strain caused in the structure by the dioxolane substitution on the backbone.

When the saturated, unsubstituted, seven-membered salt **7-Cy-HPF<sub>6</sub>** is compared against similar six- (**2.18**)<sup>1a</sup> and five-membered (**2.19**)<sup>8</sup> carbene precursors, a widening of the N-C-N angle is observed as the size of the ring is increased (Table 2.3). It is noteworthy the large increase of the N-C-N angle between the five-membered ring **2.19** and the expanded carbenes **2.18** and **7-Cy-HPF<sub>6</sub>** (9.7 and 12.1°, respectively). However, the expansion of the ring from a six- to a seven- membered does not lead to a significant augment of the N-C-N angle. In this case, the additional strain arising from the expansion of the ring results in an increase of the torsion angle ( $\beta$ ) and a tetrahedral deviation of the ring carbon atoms. In the amidinium salt **2.18** the C2 and C3 carbon ring angles range from 108.8 to 109.1° and the torsion angle ( $\beta$ ) is 1.7° (Table 2.3).

**Table 2.3.** Influence of the ring size in the structure of azolium salts.

			
	<b>2.19</b>	<b>2.18</b>	<b>7-Cy-HPF<sub>6</sub></b>
NCN angle (°)	115.3	125.0	127.4
C2-N1...N2-C5 ( $\beta$ ) (°)	-	1.7	23.3
NC2C3 (°)	-	108.8 -109.1	111.5 – 113.3

<sup>8</sup> Arduengo, A. J., III; Goerlich, J. R.; Marshall, W. J. *J. Am. Chem. Soc.* **1995**, *117*, 11027.

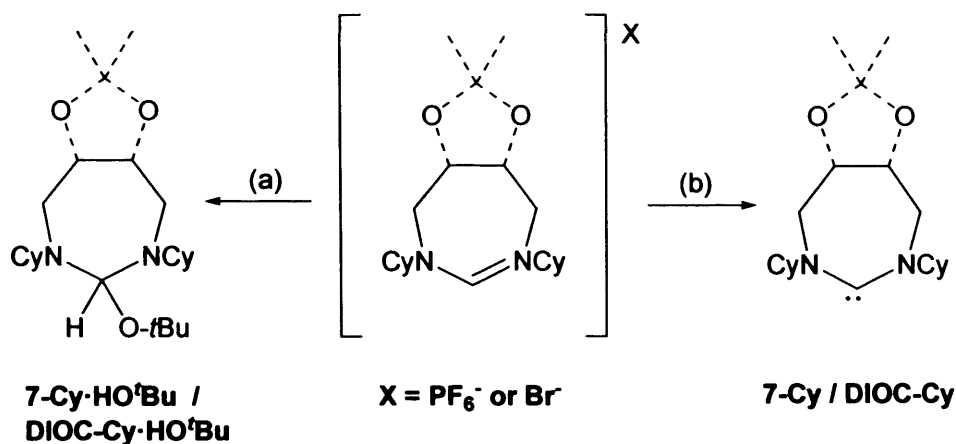
#### 2.2.1.4. Deprotonation experiments of 1,3-diazepan-2-ylidene derivatives **7-Cy**·HPF<sub>6</sub> and **DIOC-Cy**·HPF<sub>6</sub>

The amidinium salts **7-Cy**·HPF<sub>6</sub> and **DIOC-Cy**·HPF<sub>6</sub> are the first saturated seven-membered rings NHC precursors reported to date. Initial attempts to prepare the free carbenes **7-Cy** and **DIOC-Cy** using potassium *tert*-butoxide as the base afforded only the corresponding *t*-butoxide adducts **7-Cy**·HO<sup>t</sup>Bu and **DIOC-Cy**·HO<sup>t</sup>Bu (Scheme 2.13). In complexation studies with [Ir(COD)Cl]<sub>2</sub> these alcohol adducts did not react further even after heating for one day to 80°C; starting materials were recovered instead. The use of potassium hydride or a combination of potassium hydride/potassium *tert*-butoxide in order to deprotonate salts **7-Cy** and **DIOC-Cy** was also unsuccessful. The 1,3-dicyclohexyl-2-diazepanylidene carbene **7-Cy** was formed only after treatment of the amidinium salt with the amide base, KN(SiMe<sub>3</sub>)<sub>2</sub>, in aromatic solvents. The same base however left salt **DIOC-Cy**·HPF<sub>6</sub> unchanged. The dioxolane carbene **DIOC-Cy** was generated only after treatment of the bromide salt with the stronger amide base LDA [LiN(<sup>t</sup>Pr)<sub>2</sub>].

Attempts at the isolation of the free carbenes afforded **7-Cy** as a yellow oil and led to decomposition of **DIOC-Cy**. Free carbene **7-Cy** was characterised by proton and carbon NMR, whereas a <sup>13</sup>C NMR spectrum could not be recorded for carbene **DIOC-Cy** as it was rather unstable in solution; the formed carbene was used immediately in metallation reactions. Perhaps the more characteristic spectroscopic evidence in the formation of **7-Cy** is the carbene carbon shift in <sup>13</sup>C NMR (C<sub>6</sub>D<sub>6</sub>), which is significantly deshielded at 251.2 ppm. This value is notably higher than the ones reported for tetrahydropyrimid-2-ylidenes and even acyclic carbenes, appearing in the range of 236 – 243 ppm.<sup>9, 1a</sup>

---

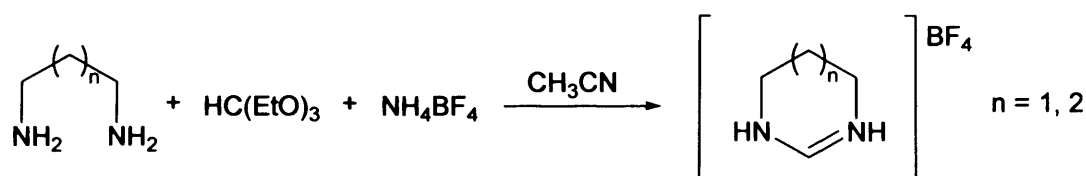
<sup>9</sup> Otto, M.; Conejero, S.; Canac, Y.; Romanenko, V. D.; Rudzevitch, V.; Bertrand, G. *J. Am. Chem. Soc.* **2004**, *126*, 1016.



**Scheme 2.13.** (a) 1 eq.  $\text{KO}^t\text{Bu}$  in toluene, (b) 1eq.  $\text{KN}(\text{SiMe}_3)_2$  in toluene for **7-Cy**, 1eq.  $\text{LiN}(\text{}^i\text{Pr})_2$  in toluene for **DIOC-Cy**.

#### 2.2.1.5. Synthesis of N,N-dihydrodiazepene salts.<sup>10</sup>

The N,N-dihydro-derivatives **6-H** $\cdot\text{BF}_4$  and **7-H** $\cdot\text{BF}_4$  were obtained by ring-closure of the commercially available 1,3-diaminopropane or 1,4-diaminobutane, respectively, with triethyl orthoformate and ammonium tetrafluoroborate in acetonitrile (Scheme 2.14).



**Scheme 2.14.** Synthesis of N,N-dihydrodiazepene salts **6-H** $\cdot\text{BF}_4$  and **7-H** $\cdot\text{BF}_4$ .

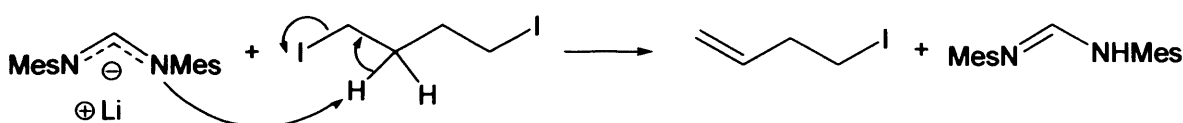
The N-alkylation of **6-H** $\cdot\text{BF}_4$  and **7-H** $\cdot\text{BF}_4$  shows potential for the synthesis of novel ionic liquids, like the commercially available 1-butyl-3-methylimidazolium tetrafluoroborate.<sup>11</sup> Moreover, these compounds provide us with a stepping stone for the synthesis of asymmetric carbene precursors.

<sup>10</sup> Compounds synthesised and characterised by James Wixey, B.Sc. Research Project, Cardiff University 2008.

<sup>11</sup> Alcantara, R.; Canoira, L.; Guilherme-Joao, P.; Perez-Mendo, J. P. *Applied Catalysis, A: General* **2001**, 218(1-2), 269.

### 2.2.2. A new method of ring-closure.

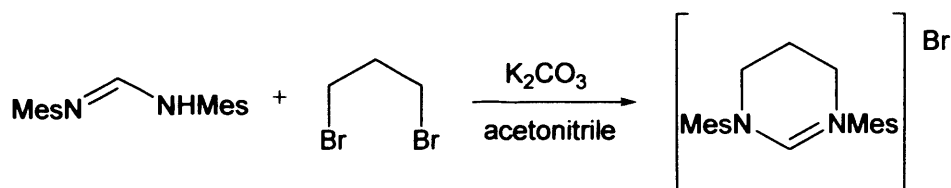
The applicability of the “reverse” “click”-process reported by Bertrand<sup>1c</sup> is, unfortunately, limited by the nature of the di-electrophile. For example, the ring-closure of 1,4-diiodobutane with the lithium salt of a formamidine leads to low yields for the formation of the azolium salt, mainly due to HI-elimination (Scheme 2.15). Moreover, the use of *n*-Buli requires the utilization of Schlenk techniques, which limits the scale-up of the reaction. Therefore, a variation of this method was proposed in the hope of broadening its scope.



**Scheme 2.15.** Proposed decomposition pathway.

#### 2.2.2.1. Synthesis of halide salts.

The main difference with Bertrand’s method lies in the use of a softer base, in this case potassium carbonate, in order to obtain a less basic nucleophile. As an example, 1,3-dibromopropane was refluxed with dimesitylformamidine and half an equivalent of potassium carbonate in acetonitrile for 4h, affording the ring-closed product (**6-Mes**·HBr) in a 82% yield after recrystallisation (Scheme 2.16). Note that Bertrand and co-workers reported a 50% yield using the lithium salt.

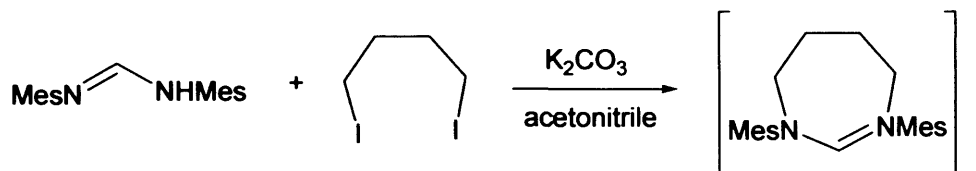


**Scheme 2.16.** Preparation of amidinium salt **6-Mes**·HBr.

Moreover, Bertrand reported that the synthesis of the five-membered anolgue is not feasible starting from 1,2-dibromoethane due to HBr-elimination. The use of potassium carbonate as base affords this salt as white crystals in a 75% yield.

This synthetic approach has also proved to be an effective method for the synthesis of seven-membered salts. As an example, 1,4-diiodobutane and dimesityl formamidine were

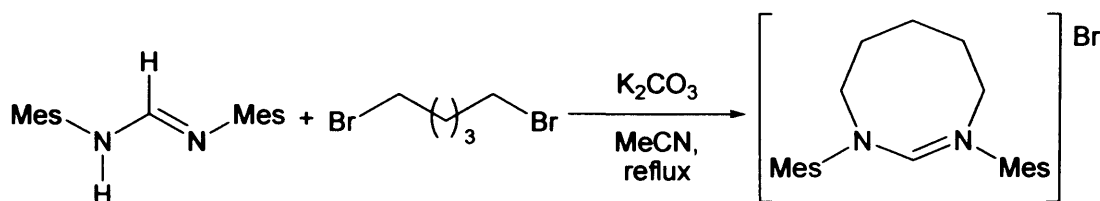
refluxed overnight in presence of potassium carbonate to afford 7-Mes·HI in 89% yield (30 g scale; Scheme 2.17).



**Scheme 2.17.** Preparation of amidinium salt 7-Mes·HI.

The reaction proceeds rapidly for the larger ring sizes and lesser sterically congested amidines [for example 1,4-diodobutane and N,N'-bis(2,4,6-trimethylphenyl)amidine], while increasing steric congestion and/or decreasing the ring size results in longer reaction times [1,2-dibromopropane and N,N'-bis(2,6-diisopropylphenyl)amidine require extended periods of reflux]. The solvent and excess of dihalide precursor were removed *in vacuo*, and the resulting mixture was dissolved in dichloromethane, and filtered to remove the potassium salts. Addition of diethyl ether to the dichloromethane solutions results in crystallisation of the product. Salts prepared in this way were obtained in high yields (70-90%).

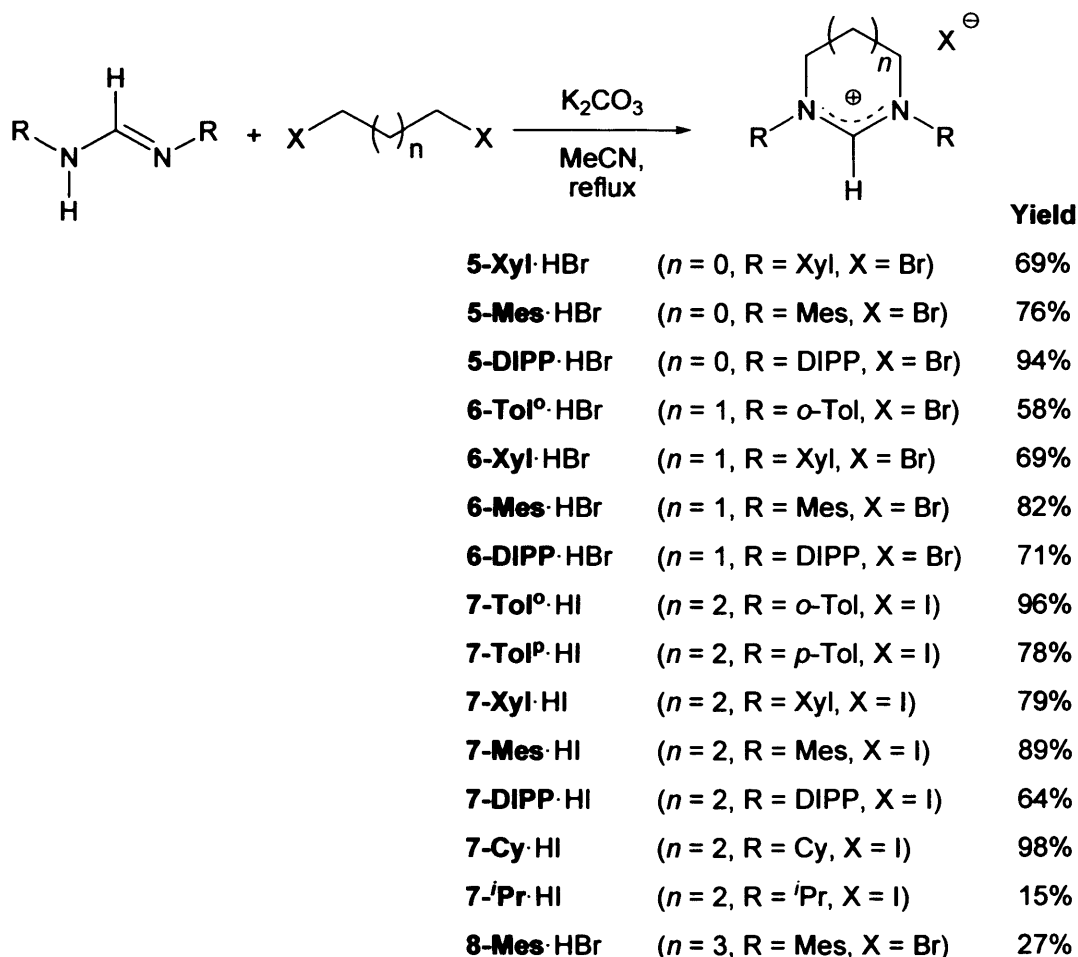
The use of this method in high dilution conditions also made possible the synthesis of the first 8-membered carbene precursor, 8-Mes·HBr as a white crystalline material, although in low yields (Scheme 2.18).<sup>10</sup>



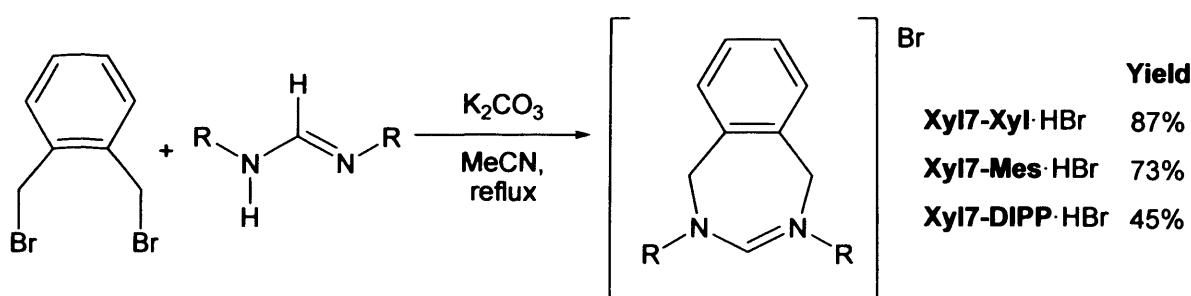
**Scheme 2.18.** Synthesis of 8-Mes·HBr.

In order to prove the versatility of this method we have synthesised a wide range of salts using a variety of di-electrophiles and formamidines<sup>12</sup> (Schemes 2.19 and 2.20).

<sup>12</sup> (a) Tamaoki, A.; Yamamoto, K.; Maeda, K.; Jpn. Kokai Tokkyo Koho, Patent JP 55049353, 1980. (b) Roberts, R.M. *J. Org. Chem.* **1949**, *14*, 277. (c) Cotton, F.A.; Haefner, S.C.; Matonic,



**Scheme 2.19.** Synthesis of 5, 6, 7 and 8-membered saturated NHC ligands (*n* = 0 - 3, X = Br, I)

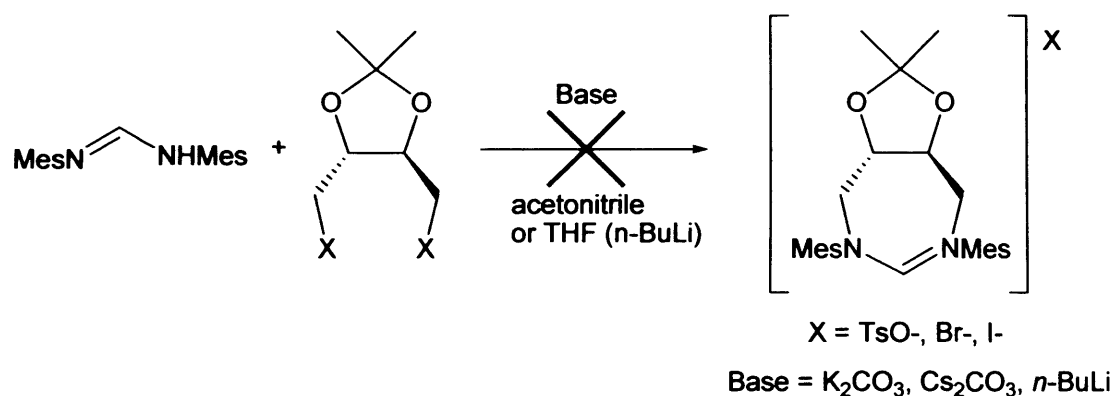


**Scheme 2.20.** Synthesis and structures of benzo-diazepanyl NHC salts.

It is noteworthy that, despite the versatility of this method, attempts of ring-closing the tartrate derivative were unsuccessful. Reaction of the formamidines with half an equivalent

J.H.; Wang X.; Murillo, C.A. *Polyhedron* **1997**, *16*, 541. (d) Krahulic, Kelly E.; Enright, Gary D.; Parvez, Masood; Roesler, Roland *J. Am. Chem. Soc.* **2005**, *127*, 4142.

of potassium carbonate in acetonitrile against different leaving groups (TsO-, Br-, and I-)<sup>6,13,14</sup> did not lead to formation of the desired amidinium salt. Similar results were obtained when a stronger base was used (Cs<sub>2</sub>CO<sub>3</sub> or *n*-BuLi). Neither caesium carbonate in acetonitrile nor *n*-BuLi in THF (Bertrand's methodology) resulted in the formation of any amidinium salt (Scheme 2.21).



**Scheme 2.21.** Failed ring-closure of the tartrate derivative.

This unexpected result can be rationalised as a consequence of the use of a weak nucleophile (formamidine) and the ether effect. According to this theory, the repulsion between the non-bonding electron pairs on the oxygen atoms beta to the electrophile and the approaching nucleophile electronically deactivates the nucleophilic attack.

#### 2.2.2.2. Exchange of the counter anion - Formation of tetrafluoroborate salts.

All the halide salts obtained by this method were converted into the BF<sub>4</sub> salts dissolving them either in acetone or acetonitrile, depending on the solubility of the halide salt, followed by addition of 1 equivalent of NaBF<sub>4</sub> in water solution (Scheme 2.20 and 2.21). The solvent was removed *in vacuo*, the product dissolved in dichloromethane, separated from the remaining water and dried with magnesium sulphate. Slow addition of ether to the dichloromethane solutions affords the salts in virtually quantitative yields. The exchange of

<sup>13</sup> Tani, Kazuhide; Suwa, Kenichi; Tanigawa, Eiji; Ise, Tomokazu; Yamagata, Tsuneaki; Tatsuno, Yoshitaka; Otsuka, Sei *J. Organomet Chem.* **1989**, 370, 203.

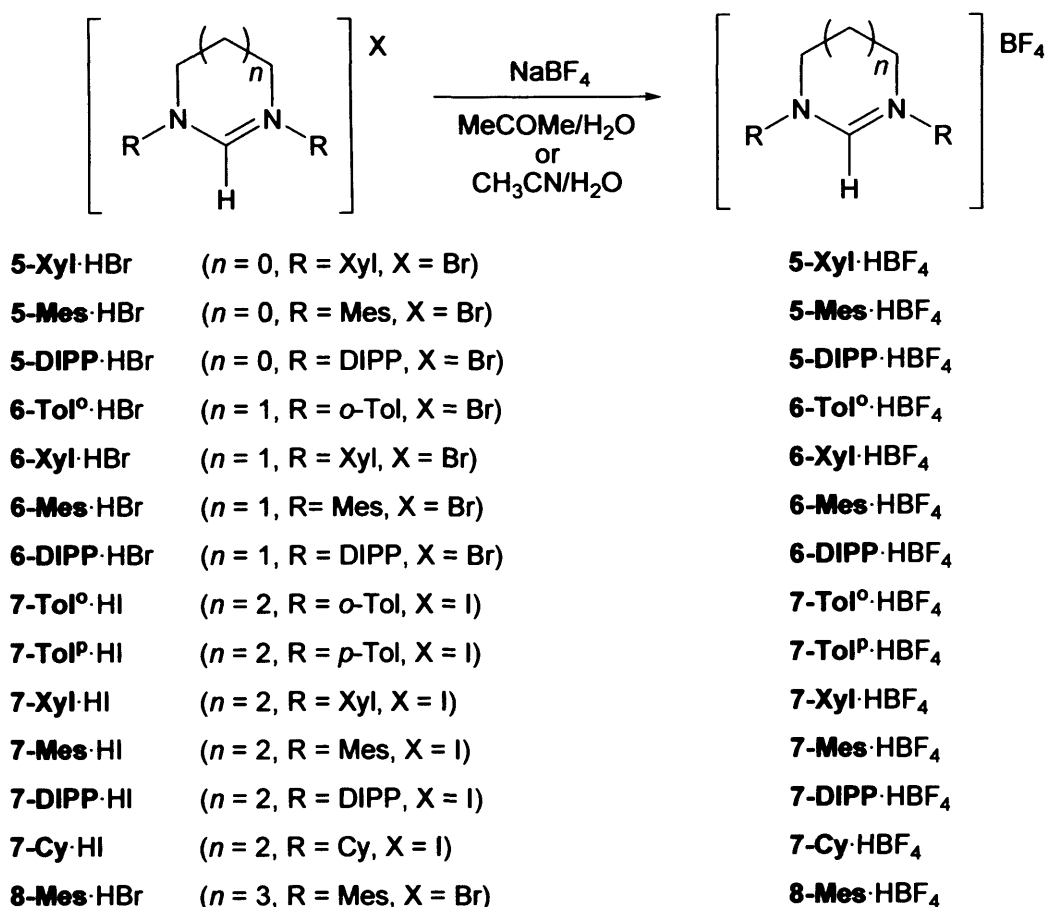
<sup>14</sup> Khanapure, Subhash P.; Najafi, Nahid; Manna, Sukumar; Yang, Jing-Jing; Rokach, Joshua *J. Org. Chem.* **1995**, 60, 7548.



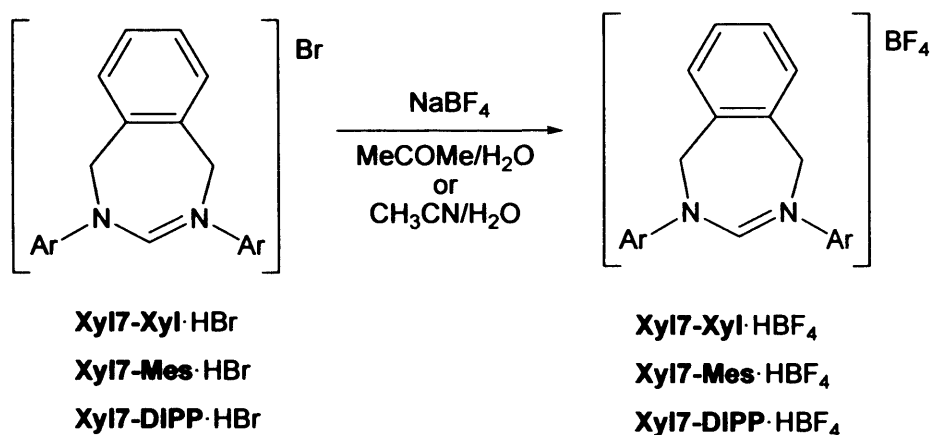
the counter anion results in small shifts in  $^1\text{H}$  NMR and  $^{13}\text{C}$  NMR, following no apparent pattern.

The tetrafluoroborate salts, shown in Scheme 2.22 and 2.23, are also possible to obtain in a one pot synthesis from the corresponding formamidines, without prior isolation of the intermediate amidinium halides.

A suspension of the formamidine with one equivalent of the dihalide, and half an equivalent of potassium carbonate was refluxed in acetonitrile until the ring-closure is finished (disappearance of the  $\text{ICH}_2$ - protons at 3.3 ppm and arising of  $\text{NCH}_2$ - protons at around 4.5 ppm peaks in  $^1\text{H}$  NMR). At the end of the reaction a solution of sodium tetrafluoroborate in water was added and the reaction mixture stirred for 15 min at ambient temperature. Evaporation *in vacuo* of the solvent resulted in the precipitation of the solid in the remaining water. The product is dissolved in dichloromethane and the residual water separated. Slow addition of diethyl ether to the dichloromethane solution results in the crystallisation of the product.



**Scheme 2.22.** Synthesis of tetrafluoroborate salts.



**Scheme 2.23.** Synthesis of tetrafluoroborate salts.

### 2.2.2.3. Solution NMR studies.

In the  $^1\text{H}$  NMR spectra of the  $\text{BF}_4^-$  salts ( $\text{CDCl}_3$  solvent) the  $\text{C}_2\text{-H}$  of the amidinium shifts upfield with increasing ring size, indicating reduced acidity for this hydrogen, and as a corollary, the increased basicity of the conjugate base – the free carbene. A similar trend is not evident in the  $^{13}\text{C}$  NMR for the amidinium carbon (the 5- and the 7-membered rings are shifted downfield when compared to the 6-membered rings) (Table 2.4).

**Table 2.4.**  $^1\text{H}$  ( $^{13}\text{C}$ ) NMR data in  $\text{CDCl}_3$  for the  $\text{C}_{\text{NHC}}\text{-H}$  ( $\text{C}_{\text{NHC}}$ ).

R =	Mes	Xyl	DIPP	Tol <sup>o</sup>	Tol <sup>p</sup>
7-R·HI	7.22 (157.8)	7.28 (157.6)	7.27 (157.0)	7.41 (156.3)	7.58 (156.5)
6-R·HBr	7.57 (153.5)	7.68 (153.3)	7.55 (152.8)	7.72 (153.7)	-
5-R·HBr	8.92 (159.0)	9.20 (159.0)	8.10 (158.0)	-	-
7-R·HBF <sub>4</sub>	7.21 (158.2)	7.28 (158.0)	7.29 (157.3)	7.36 (156.5)	7.50 (155.1)
6-R·HBF <sub>4</sub>	7.52 (154.0)	7.83 (154.3)	7.57 (153.1)	7.55 (153.3)	-
5-R·HBF <sub>4</sub>	7.96 (158.9)	8.16 (160.1) <sup>a</sup>	7.66 (160.0) <sup>a</sup>	-	-

<sup>a</sup>NMR data in DMSO

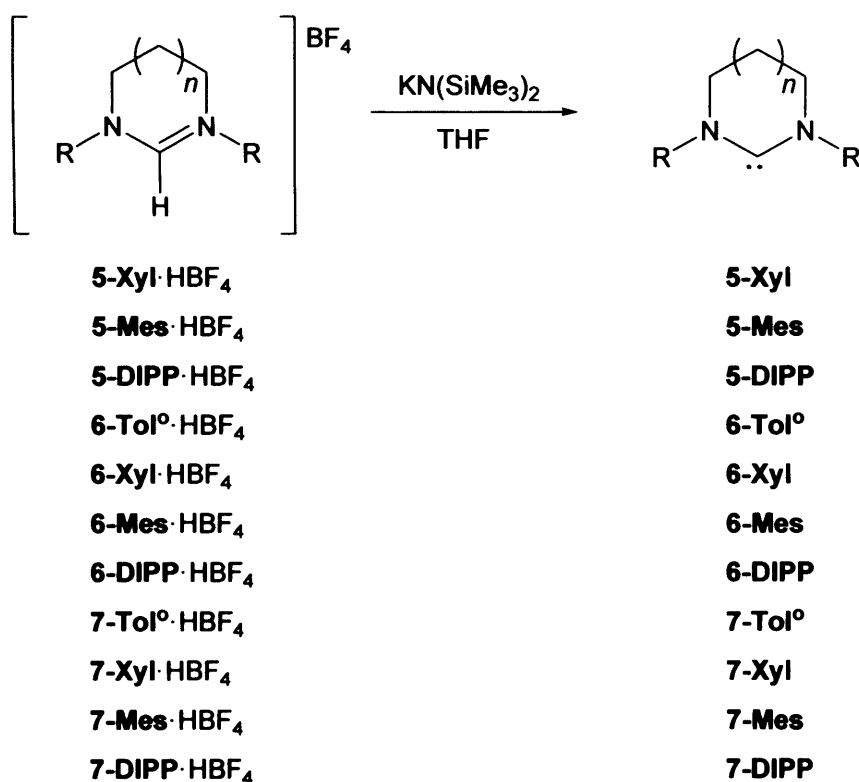
The methylene protons of the benzo-diazepanyl salts, **Xyl7-Mes·HBr**, **Xyl7-Xyl·HBr** and **Xyl7-DIPP·HBr**, are not visible at ambient temperature in  $^1\text{H}$  NMR spectra at 400 MHz in  $\text{CDCl}_3$ . However, they occur as broad singlets in acetonitrile- $d_3$ . This is indicative of a fluxional process caused by the flipping of the benzylic ring on the backbone. The

exchange rate between the two extreme conformations, comparable with the NMR timescale, causes coalescence of the peaks that belong to the two different conformers.

When the solvent used for the  $^1\text{H}$  NMR experiment is deuterated acetonitrile, a broad singlet attributable to the protons of the methylene group emerges at  $\delta = 5.3\text{-}5.5$  ppm, consistent with the chemical shift expected for benzylic protons.

#### 2.2.2.4. Isolation of free carbenes.

Many of the free carbenes generated from the  $\text{BF}_4$ -salts are surprisingly stable and could, in general, be isolated in good yield as crystalline solids (Scheme 2.24). The carbenes were prepared in THF using  $\text{KN}(\text{SiMe}_3)_2$  as the base and were isolated from THF/hexane as white microcrystalline solids and dried *in vacuo*.



**Scheme 2.24.** Deprotonation of tetrafluoroborate salts.

In contrast with the reactivity of the majority of the  $\text{HBF}_4$ -salts, deprotonation of **7-Tol<sup>o</sup>·HBF<sub>4</sub>** with 1 equivalent of  $\text{KN}(\text{SiMe}_3)_2$  led to formation of the corresponding carbene and a 44% of the base adduct, **7-Tol<sup>o</sup>·HN(SiMe<sub>3</sub>)<sub>2</sub>** (Figure 2.6). On the contrary, its six-

membered equivalent (**6-Tol**<sup>0</sup>·HBF<sub>4</sub>) shows only the formation of free carbene **6-Tol**<sup>0</sup>. This can be a consequence of the higher basicity of 7-membered carbenes or a higher electrophilicity of their carbenic carbons, due to a less effective electron donation from the nitrogen atoms. On the other hand, the different behaviour arising from the nature of the aromatic substituent is presumably due to the less sterically demanding *o*-tolyls, which allows the base, or nucleophile, to reach the carbene core.

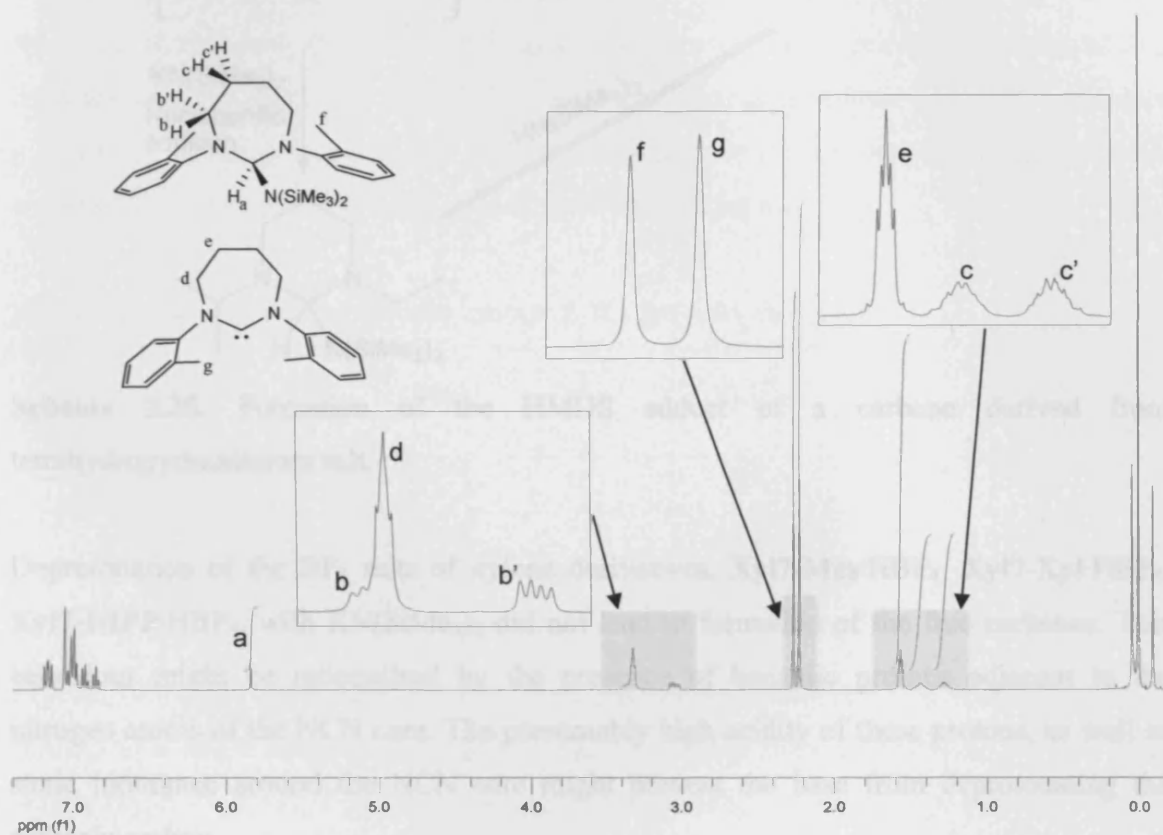
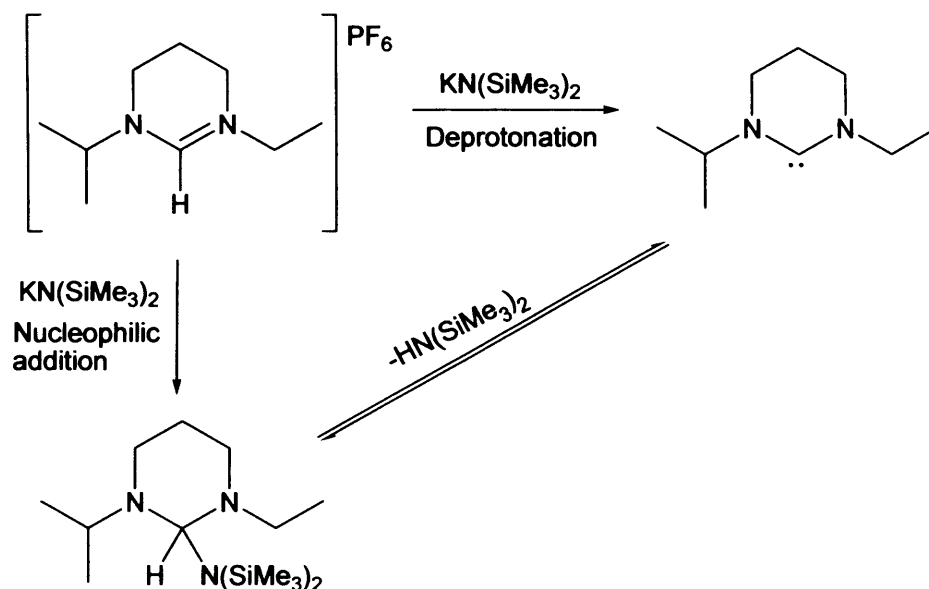


**Figure 2.6.** <sup>1</sup>H NMR (C<sub>6</sub>D<sub>6</sub>) obtained from the attempted deprotonation of **7-Tol**<sup>0</sup>·HBF<sub>4</sub> with K[HMDS], showing formation of **7-Tol**<sup>0</sup>·HN(SiMe<sub>3</sub>)<sub>2</sub> in 44% yield.

A similar behaviour has been previously reported by Alder and co-workers for tetrahydropyrimidinium salts.<sup>15</sup> The authors reported a competitive nucleophilic attack of the HMDS anion coming from the base (K[HMDS]) in the C<sub>NHC</sub>-H deprotonation of the azolium salt, which generates the HMDS adduct. Interestingly, the base adduct was proved

<sup>15</sup> (a) Lloyd-Jones, Guy C.; Alder, R. W.; Owen-Smith, Gareth J. J. *Chem. Eur. J.* **2006**, *12*, 5361.  
 (b) Alder, R. W.; Chaker, L.; Paolini, F. P. V. *Chem. Commun.* **2004**, 2172.

to be in equilibrium with the free carbene and the corresponding protonated base (H[HMDS]) (Scheme 2.25).



**Scheme 2.25.** Formation of the HMDS adduct of a carbene derived from tetrahydropyrimidinium salt.

Deprotonation of the BF<sub>4</sub> salts of xylene derivatives, **Xyl17-Mes**·HBF<sub>4</sub>, **Xyl17-Xyl**·HBF<sub>4</sub>, **Xyl17-DIPP**·HBF<sub>4</sub>, with KN(SiMe<sub>3</sub>)<sub>2</sub> did not lead to formation of the free carbenes. This behaviour might be rationalised by the presence of benzylic protons adjacent to the nitrogen atoms of the NCN core. The presumably high acidity of these protons, as well as steric hindrance around the NCN core might prevent the base from deprotonating the carbenic carbon.

It is worth mentioning that none of the free carbenes previously described showed traces of the formation of dimeric species, as would be expected for such bulky carbenes.

#### 2.2.2.5. Properties and structure of expanded free carbenes.

The free carbenes of the 7-membered ring species show intriguing structural and electronic properties. For the 7-membered rings the carbene carbon <sup>13</sup>C NMR shift is observed at around 258-260 ppm (Table 2.5). This shift is at considerably lower field than that for 5 and 6 member ring carbenes, which commonly occur in the region 235-245 ppm. It is only for acyclic NE-aminocarbenes (E = O, S) that such significant low field shifts for the

carbene carbon has previously been noted (for examples of N, O carbenes the chemical shift is 262-278 and for NS = 297).<sup>16,17</sup> In a comprehensive computational study looking at specific features of diaminocarbenes, Alder ascribes the large down-field shift in acyclic N, S carbenes to the paramagnetic contribution to the isotropic shielding constant.<sup>17</sup> In turn, he attributes the origin of this large paramagnetic contribution as stemming from the singlet-triplet gap brought about by the relatively poor interaction between the S( $\pi$ ) orbital and the C<sub>carbene</sub>( $\pi^*$ ) orbital and the consequential reduced donation of electron density from the S into the carbene  $\pi^*$  orbital. Extending this argument to the present 7-membered ring carbenes would suggest that there is less effective electron donation, from the N atoms to the carbene C, and hence a higher triplet contribution to the electronic structure of these carbenes when compared to the 5- and 6-membered carbenes.

**Table 2.5.** <sup>13</sup>C shifts of the carbene carbon in the free carbene in C<sub>6</sub>D<sub>6</sub>.

R Ring size	Mes	Xyl	DIPP
7	257.3	258.8	260.2
6	244.9	244.5	245.1
5	241.2	242.0	244.0

Crystals of **7-Mes** and **6-Mes**<sup>18</sup> suitable for single-crystal X-ray diffraction were grown by cooling a saturated solution of the free carbene in diethyl ether to 4°C; their ORTEP plots are shown in Figures 2.7 and 2.8, respectively. The solid state crystal structure of **7-Mes** represents the first one obtained for a 7-membered ring carbene. Selected bond lengths (Å) and angles (°) for **7-Mes** and **6-Mes** are displayed in Tables 2.6 and 2.7, respectively.

**7-Mes** features a slightly larger NCN angle than **6-Mes**, 116.6(4) and 114.65(13) respectively, and consequently C<sub>NHC</sub>-N-C<sub>Mes</sub> angle increases from *ca.* 115.2 in the seven- to *ca.* 117.1 in six-membered carbene. However, the most remarkable differences derived from the extra tension arising from the expansion of the ring in the solid state crystal structure of these two carbenes is the C<sub>ring</sub>-N...N-C<sub>ring</sub> torsion angle ( $\beta$ ), which increases

<sup>16</sup> Alder, R. W.; Blake, M. E.; Oliva, J. M. *J. Phys. Chem.* **1999**, *103*, 11200.

<sup>17</sup> Alder, R. W.; Butts, C. P.; Orpen, A. G. *J. Am. Chem. Soc.* **1998**, *120*, 11526.

<sup>18</sup> Crystals of **6-Mes** were obtained from Dr. Dirk Beetstra in our group.

from 0.0° in **6-Mes** to 25.4° in **7-Mes**, and the deviation from the ideal tetrahedral angle, which ranges from 111.4 to 113.5° in **7-Mes** and from 108.4 to 108.9° in **6-Mes**.

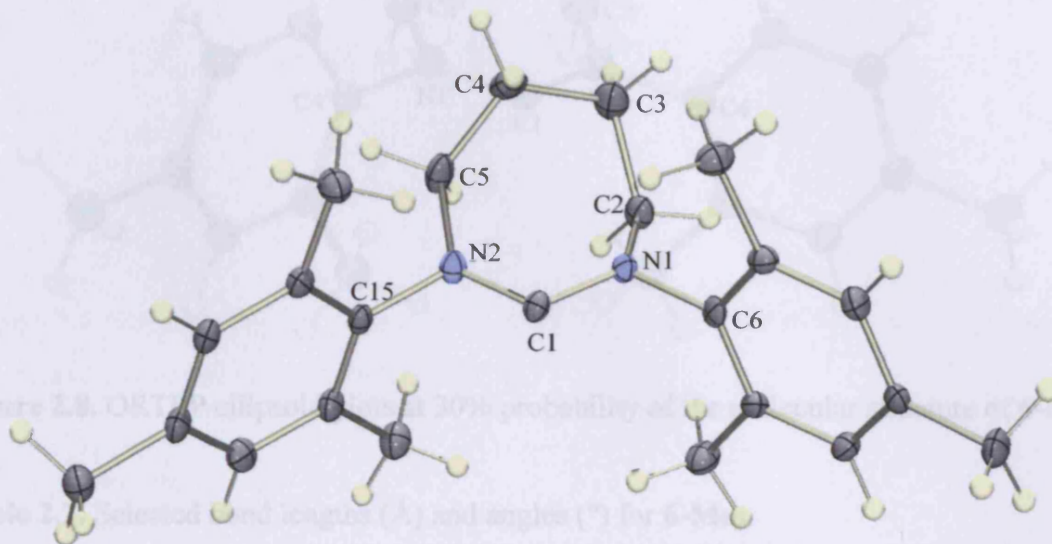


**Figure 2.7.** ORTEP ellipsoid plots at 30% probability of the molecular structure of **7-Mes**.

**Table 2.6.** Selected bond lengths (Å) and angles (°) for **7-Mes**.

Lengths (Å)		Angles (°)	
C(1)–N(2)	1.346(5)	N(1)–C(1)–N(2)	116.6(4)
C(1)–N(1)	1.349(5)	C(1)–N(1)–C(2)	126.9(4)
C(2)–N(1)	1.483(5)	C(1)–N(1)–C(6)	115.5(3)
C(2)–C(3)	1.507(7)	C(2)–N(1)–C(6)	115.5(3)
C(4)–C(5)	1.525(7)	C(1)–N(2)–C(5)	130.6(4)
C(5)–N(2)	1.502(6)	C(1)–N(2)–C(15)	115.0(4)
C(15)–N(2)	1.438(5)	C(5)–N(2)–C(15)	114.0(3)
C(6)–N(1)	1.444(5)	N(1)–C(2)–C(3)	113.5(4)
		C(4)–C(5)–N(2)	112.6(4)
		C(2)–C(3)–C(4)	111.4(4)
		C(5)–C(4)–C(3)	112.7(4)

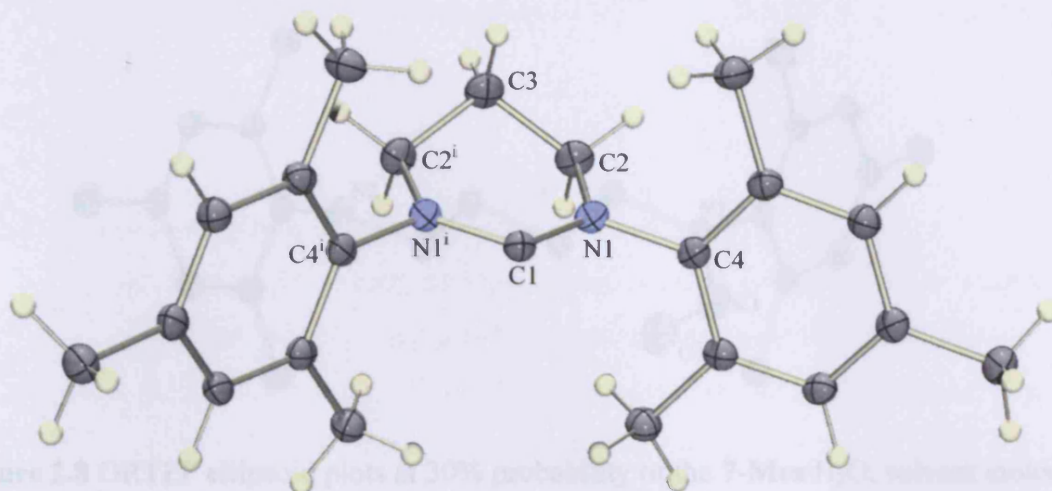


**Figure 2.8.** ORTEP ellipsoid plots at 30% probability of the molecular structure of **6-Mes**.

**Table 2.7.** Selected bond lengths (Å) and angles (°) for **6-Mes**.

Lengths (Å)		Angles (°)	
C(1)–N(1)	1.3464(12)	N(1)–C(1)–N(1) <sup>i</sup>	114.65(13)
N(1)–C(4)	1.4381(15)	C(1)–N(1)–C(4)	117.08(9)
N(1)–C(2)	1.4809(14)	C(1)–N(1)–C(2)	126.28(10)
C(1)–N(1)	1.3464(12)	C(4)–N(1)–C(2)	116.52(9)
		N(1)–C(2)–C(3)	108.88(10)
		C(2)–C(3)–C(2) <sup>i</sup>	108.37(14)

In order to identify the decomposition product of expanded carbenes, one drop of water was added to a diethyl ether solution of free carbene **7-Mes**. Concentration of volatiles under reduced pressure and cooling of the hexane solution afforded colourless crystals suitable for single-crystal X-ray diffraction, which shows the formation of the formamide **7-Mes**·H<sub>2</sub>O (Figure 2.8). This result was also confirmed by <sup>1</sup>H NMR, where the resonance for the formamide proton occurs as a singlet at *ca.* 8 ppm.



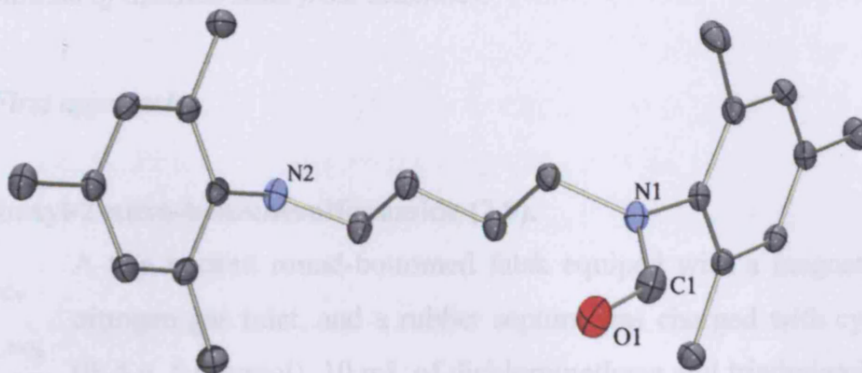


**Figure 2.8** ORTEP ellipsoid plots at 30% probability of the 7-Mes·H<sub>2</sub>O, solvent molecules and hydrogens have been omitted for clarity.

### 2.3. Experimental.

#### General Remarks.

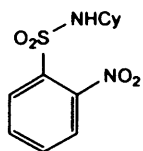
The solvents (dichloromethane, acetonitrile, diethylether, acetone) were used as purchased. The amidines bis(2,6-diisopropylphenyl)formamidine, bis(2,6-dimethylphenyl)formamidine, bis(2,4,6-trimethylphenyl)formamidine were synthesised according to literature methods.<sup>19</sup> All other reagents (1,2-dibromoethane, 1,3-dibromopropane, 1,4-diiodobutane, 2,6-dimethylaniline, 2,4,6-trimethylaniline, 2,6-diisopropylaniline, triethylorthoformate and sodium tetrafluoroborate were used as received. <sup>1</sup>H and <sup>13</sup>C NMR spectra were obtained on Bruker Avance AMX 400, 500 or Jeol Eclipse 300 spectrometers. The chemical shifts are given as dimensionless  $\delta$  values and are frequency referenced relative to TMS. Coupling constants *J* are given in hertz (Hz) as positive values regardless of their real individual signs. Mass spectra and high-resolution mass spectra were obtained in electrospray (ES) mode unless otherwise reported, on a Waters Q-TOF micromass spectrometer.

<sup>19</sup> Taylor, Edward C.; Ehrhart, Wendell A. *J. Org. Chem.* **1963**, *28*, 1108.

### 3.3.1. Synthesis of azolium salts from diamines.

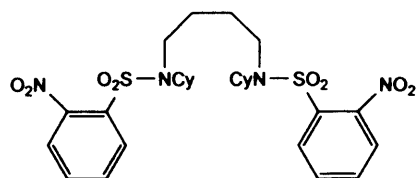
#### 2.3.1.1. First approach.

#### N-Cyclohexyl-2-nitro-benzenesulfonamide (2.9).



A two necked round-bottomed flask equipped with a magnetic stirring bar, nitrogen gas inlet, and a rubber septum was charged with cyclohexylamine (0.5 g, 5.0 mmol), 10 mL of dichloromethane and triethylamine (0.7 ml, 5.0 mmol). The mixture was stirred and cooled in an ice bath while 2-Nitrobenzenesulfonylchloride (1.00 g, 4.5 mmol) was added over a period of 5 min. After 5 min, the ice bath was removed and the reaction mixture was allowed to warm to room temperature, stirred for 30 min, and then quenched with 10 mL of 1M hydrochloric acid. The aqueous layer was extracted with two 25 ml portion of dichloromethane, and the combined organic extracts were washed with 5 ml of brine, dried over magnesium sulphate, filtered and concentrated under reduced pressure to give 1.30 g (3.9 mmol, 79%) of N-Cyclohexyl-2-nitro-benzenesulfonamide as a white solid.  $^1\text{H}$  NMR (400 MHz,  $\text{CDCl}_3$ , rt):  $\delta$  8.13-7.61 (4H, m, Ar-CH), 5.16 (1H, bd,  $^3J_{\text{HH}} = 7.4$ , NH), 3.28 (1H, m, Cy-CH), 1.75-0.85 (10H, m, Cy- $\text{CH}_2$ );  $^{13}\text{C}$  NMR (400 MHz,  $\text{CDCl}_3$ , rt):  $\delta$  135.7 (s, Ar-C), 133.7 (s, Ar-C), 133.3 (s, Ar-CH), 131.1 (s, Ar-CH), 125.8 (s, Ar-CH), 54.0 (s, Cy-CH), 34.2 (s, Cy- $\text{CH}_2$ ), 25.5 (s, Cy- $\text{CH}_2$ ), 24.9 (s, Cy- $\text{CH}_2$ ); MS (ES):  $m/z$  323.0481 ( $[\text{MK}]^+$ ;  $\text{C}_{12}\text{H}_{16}\text{N}_2\text{O}_4\text{SK}$  requires 323.0468).

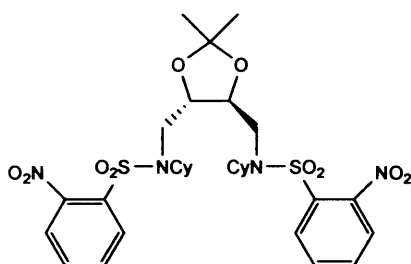
#### 1,4-Bis[N-Cyclohexyl-2-nitro-benzenesulfonamide]butane (2.7).



A pressure tube equipped with a magnetic stirring bar and a nitrogen gas inlet was charged with 0.6 mL (5.0 mmol) of 1,4-dibromobutane, 4.20 g (30.0 mmol) of potassium carbonate and 25 mL of dry dimethylformamide. To the stirred mixture was added 2.90 g (10.0 mmol) of N-Cyclohexyl-2-nitro-benzenesulfonamide over a period of 5 min and the resulting mixture was heated to 80°C overnight. The reaction mixture was allowed to cool to room temperature, diluted with 50 ml of water and extracted with three 60 ml portions of chloroform. The combined organic extracts were washed with brine (50 mL), dried over magnesium sulphate, filtered, and concentrated under reduced pressure to give 2.55 g of a white solid (4.6 mmol, 91%).  $^1\text{H}$

NMR (400 MHz, CDCl<sub>3</sub>, rt):  $\delta$  7.97-7.45 (8H, m, Ar-CH), 3.65-3.52 (2H, m, Cy-CH), 3.17 (4H, t,  $^3J_{\text{HH}} = 6.5$ , NCH<sub>2</sub>), 2.75-1.15 (14H, m, Cy-CH<sub>2</sub>); <sup>13</sup>C NMR (100 MHz, CDCl<sub>3</sub>, rt):  $\delta$  148.4 (s, Ar-C), 134.6 (s, Ar-C), 133.7 (s, Ar-CH), 132.0 (s, Ar-CH), 131.0 (s, Ar-CH), 124.4 (s, Ar-CH), 58.6 (s, NCH<sub>2</sub>), 44.0 (s, Cy-CH), 29.8 (s, Cy-CH<sub>2</sub>), 26.4 (s, Cy-CH<sub>2</sub>), 25.6 (s, Cy-CH<sub>2</sub>); MS (ES):  $m/z$  623.2228 ([MK]<sup>+</sup>; C<sub>28</sub>H<sub>39</sub>N<sub>4</sub>O<sub>8</sub>S<sub>2</sub> requires 623.2209).

**(-)-trans-4,5-Bis[N-Cyclohexyl-2-nitro-benzenesulfonamide-N-methyl]-2,2-dimethyl-1,3-dioxolan (2.8).**



A pressure tube equipped with a magnetic stirring bar and a nitrogen gas inlet was charged with 0.50 g (1.0 mmol) of (-)-trans-4,5-Bis[*tosyloxymethyl*]-2,2-dimethyl-1,3-dioxolan, 0.83 g (6.0 mmol) of potassium carbonate and 5 mL of dry dimethylformamide. To the stirred mixture 2.0

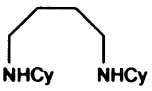
mmol of the cyclohexyl sulphonamide was added over a period of 5 min and the resulting mixture was heated in an 80°C oil bath overnight. The reaction mixture was allowed to cool to room temperature, diluted with 10 ml of water and extracted with three 15 ml portions of diethyl ether. The combined organic extracts were washed with brine (10 mL), dried over magnesium sulphate, filtered, and concentrated under reduced pressure to give 0.49 g (-)-trans-4,5-Bis[N-Cyclohexyl-2-nitro-benzenesulfonamide-N-methyl]-2,2-dimethyl-1,3-dioxolan as a white solid (0.7 mmol, 70%). <sup>1</sup>H NMR (400 MHz, CDCl<sub>3</sub>, rt):  $\delta$  8.09-7.50 (8H, m, Ar-CH), 3.84-3.60 (4H, m, NCH<sub>2</sub>), 3.28-3.15 (2H, m, Cy-CH), 1.88-1.25 (10H, m, Cy, CH<sub>2</sub>), 1.25 (6H, s, CH<sub>3</sub>); <sup>13</sup>C NMR (100 MHz, CDCl<sub>3</sub>, rt):  $\delta$  148.4 (s, Ar-C), 134.4 (s, Ar-C), 133.6 (s, Ar-CH), 132.2 (s, Ar-CH), 131.3 (s, Ar-CH), 124.4 (s, Ar-CH), 110.2 (s, C(CH<sub>3</sub>)<sub>2</sub>), 80.3 (s, CHO), 59.0 (s, Cy-CH), 46.9 (s, NCH<sub>2</sub>), 33.0 (s), 30.8 (s), 27.4 (s), 26.5 (s), 25.6 (s), 26.4 (s); MS (ES):  $m/z$  717.2252 ([MNa]<sup>+</sup>; C<sub>31</sub>H<sub>42</sub>N<sub>4</sub>O<sub>10</sub>S<sub>2</sub>Na requires 717.2240).

**1,4-Bis[cyclohexylamino]butane (2.4) and N-(((4S,5S)-5-((cyclohexylamino)methyl)-2,2-dimethyl-1,3-dioxolan-4-yl)methyl) cyclohexanamine (2.5).**

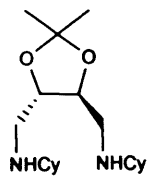
A pressure tube with a magnetic stirring bar and a nitrogen gas inlet was charged with 0.55 ml (5 mmol) of thiophenol and 3 ml of acetonitrile. The mixture was cooled in an ice bath and 10 M aqueous sodium hydroxide solution (0.5 ml, 5.0 mmol) was added over a period of 10 min. After 5 min, the ice bath was removed, and 2.0 mmol of the corresponding

sulphonamide were added over a period of 10 min. The reaction mixture is heated to 80°C overnight. The reaction mixture is allowed to cool to room temperature, diluted with 5 ml of water, and extracted with three 5 ml portions of dichloromethane. The combined organic layers were washed with brine, dried over magnesium sulphate and concentrated under reduced pressure. The residue is diluted in 10 ml of dichloromethane, and 5 ml of HCl (1M), added in order to form the hydrochloride, which is extracted into the aqueous layer. The aqueous layer is basified with NaOH (1M) until the aqueous layer remains basic (pH = 8) to litmus paper. The free amine is extracted with three 10 ml portions of dichloromethane, washed with brine, dried over magnesium sulphate, filtrated, and concentrated under reduced pressure to yield a white solid in a 50% yield in both cases.

**1,4-Bis[cyclohexylamino]butane (2.4).**

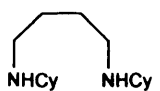
 <sup>1</sup>H NMR (400 MHz, CDCl<sub>3</sub>, rt): δ 2.57 (4H, m, NCH<sub>2</sub>), 2.35 (2H, m, NCH), 1.60 (14H, m, CH<sub>2</sub>), 1.1 (10H, m, CH<sub>2</sub>); <sup>13</sup>C NMR (400 MHz, CDCl<sub>3</sub>, rt): δ 57.3 (s, Cy-CH), 47.2 (s, NCH<sub>2</sub>), 34.0 (s, Cy-CH<sub>2</sub>), 28.7 (s, Cy-CH<sub>2</sub>), 26.5 (s, Cy-CH<sub>2</sub>), 25.5 (s, NCH<sub>2</sub>CH<sub>2</sub>); MS (ES): *m/z* 253.2641 ([MH]<sup>+</sup>; C<sub>16</sub>H<sub>33</sub>N<sub>2</sub> requires 253.2644).

**N-(((4S,5S)-5-((cyclohexylamino)methyl)-2,2-dimethyl-1,3-dioxolan-4-yl)methyl)cyclohexanamine (2.5).**

 <sup>1</sup>H NMR (400 MHz, CDCl<sub>3</sub>, rt): δ 3.78 (2H, m, OCH), 2.74 (4H, m, NCH<sub>2</sub>), 2.35 (2H, m, NCH), 1.81 (4H, m, CH<sub>2</sub>), 1.66 (4H, m, CH<sub>2</sub>), 1.55 (2H, m, CH<sub>2</sub>), 1.32 (6H, s, CH<sub>3</sub>), 1.18 (6H, m, CH<sub>2</sub>), 1.01 (4H, m, CH<sub>2</sub>); <sup>13</sup>C NMR (400 MHz, CDCl<sub>3</sub>, rt): δ 107.7 (s, C(CH<sub>3</sub>)<sub>2</sub>), 81.0 (s, CHO), 56.0 (s, NCH), 48.5 (s, NCH<sub>2</sub>), 32.5 (s), 32.4 (s), 26.2 (s), 25.1 (s), 24.0 (s); MS (ES): *m/z* 325.2853 ([MH]<sup>+</sup>; C<sub>19</sub>H<sub>37</sub>N<sub>2</sub>O<sub>2</sub> requires 325.2855).

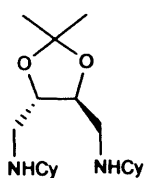
**2.3.1.2. Second approach.**

**1,4-Bis[cyclohexylamino]butane (2.4).**

 1,4-Butanediamine (5 ml, 50.0 mmol) and cyclohexanone (10 ml, 100.0 mmol) were dissolved in toluene (30 ml) in a 100 ml flask equipped with a Dean-Stark. The reaction mixture was heated to 140°C for 3h (until 1.8 ml of water was

collected in the Dean-Stark). Evaporation of toluene afforded 12.40 g of 1,4-bis[cyclohexylimino]butane (**2.14**) as a yellow oil (99%) which was used without further purification in the synthesis of the corresponding diamine.  $^1\text{H}$  NMR (400 MHz,  $\text{CDCl}_3$ , rt):  $\delta$  1.40-1.60 (m, 16H), 2.10-2.25 (m, 8H), 3.25 (m, 4H). 1,4-Bis[cyclohexylimino]butane (12.40 g, 50.0 mmol) was dissolved in 100 mL of dry ethanol in a 250 mL rbf, sodium borohydride (3.77 g, 100.0 mmol) was added in small portions over a period of 2h. When the gas evolution subsided the reaction was stirred further for an hour. The residue obtained after evaporation of the volatiles was dissolved in 100 mL of water and extracted with diethyl ether (3 x 100 mL). The combined organic fractions were washed with brine (50 mL), dried over magnesium sulphate, filtered and concentrated under reduced pressure until white crystals started to precipitate out of the solution. The flask was stored in the fridge overnight, after filtration 9.50 g of the diamine were obtained as white crystals (37.5 mmol, 75%).  $^1\text{H}$  NMR (400 MHz,  $\text{CDCl}_3$ , rt):  $\delta$  2.57 (4H, m,  $\text{NCH}_2$ ), 2.35 (2H, m,  $\text{NCH}$ ), 1.60 (14H, m,  $\text{CH}_2$ ), 1.1 (10H, m,  $\text{CH}_2$ );  $^{13}\text{C}$  NMR (400 MHz,  $\text{CDCl}_3$ , rt):  $\delta$  57.3 (s,  $\text{Cy-CH}$ ), 47.2 (s,  $\text{NCH}_2$ ), 34.0 (s,  $\text{Cy-CH}_2$ ), 28.7 (s,  $\text{Cy-CH}_2$ ), 26.5 (s,  $\text{Cy-CH}_2$ ), 25.5 (s,  $\text{NCH}_2\text{CH}_2$ ); MS (ES):  $m/z$  253.2641 ( $[\text{MH}]^+$ ;  $\text{C}_{16}\text{H}_{33}\text{N}_2$  requires 253.2644).

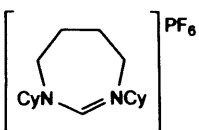
**N-(((4S,5S)-5-((cyclohexylamino)methyl)-2,2-dimethyl-1,3-dioxolan-4-yl)methyl)cyclohexanamine (2.5).**



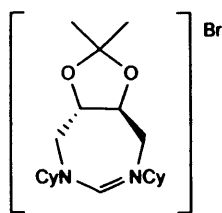
A solution of (4R,5R)-(-)-diethyl 2,3-*O*-isopropylidene-*L*-tartrate (10.0 mmol) in dry toluene (30 ml) was placed in an acetone/dry ice bath and a 1M solution of DIBAL-H (20 ml) in toluene was added dropwise using a syringe over a period of 1h under nitrogen. The resulting solution was stirred at -78°C for 3h. After completion of the reaction, cyclohexylamine (2.3 ml, 20.0 mmol) was added in one portion, and the reaction mixture was allowed to warm to room temperature while stirring overnight. To the reaction mixture 25 ml of water were added slowly and the mixture stirred for 15 minutes. The precipitate formed was filtered off, and the filtrate was washed with water (3 x 20 ml) and brine (20 ml), dried over magnesium sulphate, filtered and concentrated under reduced pressure to afford 3.20 g of **2.16** as an orange oil (99%).  $^1\text{H}$  NMR (400 MHz,  $\text{CDCl}_3$ ):  $\delta$  7.55 (2H, m,  $\text{N=CH}$ ), 4.28 (2H, m,  $\text{OCH}$ ), 2.95 (2H, m,  $\text{Cy-CH}$ ), 1.49-1.75 (10H, m), 1.40 (6H, s,  $\text{CH}_3$ ), 1.05-1.36 (10H, m);  $^{13}\text{C}$  NMR (400 MHz,  $\text{CDCl}_3$ ):  $\delta$  156.7 (s,  $\text{N=CH}$ ), 110.3 (s,  $\text{C}(\text{CH}_3)_2$ ), 79.1 (s,  $\text{CHO}$ ), 68.4 (s,  $\text{Cy-CH}$ ), 32.9 (s), 31.9 (s), 25.8 (s), 24.4 (s), 23.5 (s). Without further purification, the crude diimine (3.2 g,

10 mmol) was dissolved in 25 ml of dry ethanol in 100 ml rbf and sodium borohydride (0.75 g, 20 mmol) was added in small portions over a period of 2h. When the gas evolution had subsided the reaction was stirred further for another hour. The residue obtained after evaporation of ethanol was dissolved in 100 ml of water, extracted with 3 x 25 ml of diethyl ether. The combined organic layers were washed with brine (25 ml), dried over magnesium sulphate, filtered and concentrated under reduced pressure to afford 4.9 g of the diamine as a white waxy solid (7.6 mmol, 75.6%). <sup>1</sup>H NMR (400 MHz, CDCl<sub>3</sub>, rt): δ 3.78 (2H, m, OCH), 2.74 (4H, m, NCH<sub>2</sub>), 2.35 (2H, m, NCH), 1.81 (4H, m, CH<sub>2</sub>), 1.66 (4H, m, CH<sub>2</sub>), 1.55 (2H, m, CH<sub>2</sub>), 1.32 (6H, s, CH<sub>3</sub>), 1.18 (6H, m, CH<sub>2</sub>), 1.01 (4H, m, CH<sub>2</sub>); <sup>13</sup>C NMR (400 MHz, CDCl<sub>3</sub>, rt): δ 107.7 (s, C(CH<sub>3</sub>)<sub>2</sub>), 81.0 (s, CHO), 56.0 (s, Cy-CH), 48.5 (s, NCH<sub>2</sub>), 32.5 (s), 32.4 (s), 26.2 (s), 25.1 (s), 24.0 (s, CH<sub>2</sub>); MS (ES): *m/z* 325.2853 ([MH]<sup>+</sup>; C<sub>19</sub>H<sub>37</sub>N<sub>2</sub>O<sub>2</sub> requires 325.2855).

### 1,3-dicyclohexyl-1,3-diazepan-2-ylideneium-hexafluorophosphate.

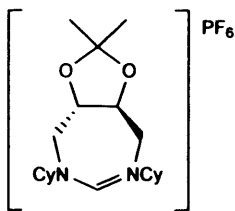
 1,4-Dicyclo-hexylaminebutane (3.00 g, 12.0 mmol), ammonium hexafluorophosphate (1.95 g, 12.0 mmol) and triethylorthoformate (4 ml, 24.0 mmol) were dissolved in 150 mL of DME. The reaction was heated to 120°C for 3h, after which time the solvent was evaporated under reduced pressure. The remaining residue was dissolved in chloroform and any insoluble impurities were filtered off. Evaporation of the solvent afforded 4.60 g of a white solid (11.3 mmol, 94%). Recrystallization from a mixture chloroform / diethyl ether (2:1) afforded 3.50 g of white crystals (8.4 mmol, 70%). <sup>1</sup>H NMR (400 MHz, CDCl<sub>3</sub>, rt): δ 7.60 (1H, s, NCHN), 3.60 (4H, m, NCH<sub>2</sub>), 3.41 (2H, m, Cy-CH), 2.02 (4H, m, CH<sub>2</sub>), 1.86 (4H, m, CH<sub>2</sub>), 1.77 (4H, m, CH<sub>2</sub>), 1.58 (2H, m, CH<sub>2</sub>), 1.39 (8H, m, CH<sub>2</sub>), 1.04 (2H, m, CH<sub>2</sub>); <sup>13</sup>C NMR (400 MHz, CDCl<sub>3</sub>, rt): δ 156.4 (s, NCN), 57.2 (s, Cy-CH), 44.7 (s, NCH<sub>2</sub>), 31.1 (s, CH<sub>2</sub>), 25.5 (s, CH<sub>2</sub>), 25.4 (s, CH<sub>2</sub>), 25.2 (s, CH<sub>2</sub>); MS (ES): *m/z* 263.2495 ([M-PF<sub>6</sub>]<sup>+</sup>; C<sub>17</sub>H<sub>31</sub>N<sub>2</sub> requires 263.2487).

**9,9-(dimethyl-8,10-dioxolanyl)methyl)-1,3-dicyclohexyl-diazepan-2-ylidenium-bromide (DIOC-Cy-HBr).**



The dioxolane diamine **2.5** (0.50 mg, 1.5 mmol) was dissolved in methanol (30 ml) and treated with an aqueous formaldehyde solution (36.5 %, 0.2 ml, 2.26 mmol). The reaction mixture was stirred at 50°C in a pressure tube overnight. Evaporation of the solvent afforded **2.16** as a pale yellow oil (0.50 g, 1.5 mmol) which was used without further purification in the next step. <sup>1</sup>H NMR (400 MHz, CDCl<sub>3</sub>): δ 0.95-1.25 (m, 10H), 1.32 (s, 6H), 1.55-1.85 (m, 10H), 2.45 (m, 2H), 2.55 (m, 2H), 3.15 (m, 2H), 3.55 (s, 1H), 3.88 (m, 2H). **2.16** (0.50 g, 1.5 mmol) was dissolved in dimethoxyethane and N-bromosuccinimide (0.27 g, 1.5 mmol) was added in small portions at 0°C. The reaction mixture was stirred for 3h at room temperature. A pale yellow precipitate formed, which was filtered off, washed with hexane and dried *in vacuo* to yield 0.10 g (0.15 mmol, 18%) of the bromide salt as a pale yellow powder. <sup>1</sup>H NMR (250 MHz, CDCl<sub>3</sub>, rt): δ 9.42 (1H, s, NCHN), 4.45 (2H, m, OCH), 3.74 (4H, m, NCH<sub>2</sub>), 3.08 (2H, m, Cy-CH), 2.10 – 1.40 (16H, m, CH<sub>2</sub>), 1.40 (6H, s, CH<sub>3</sub>), 1.05 (4H, m, CH<sub>2</sub>); <sup>13</sup>C NMR (100 MHz, DEPT, CDCl<sub>3</sub>, rt): δ 157.3 (s, NCHN), 113.3 (s, C(CH<sub>3</sub>)<sub>2</sub>), 76.5 (s, OCH), 69.4 (s, Cy-CH), 46.9 (s, NCH<sub>2</sub>), 31.0 (s, CH<sub>2</sub>), 30.9 (s, CH<sub>2</sub>), 26.8 (s, CH<sub>3</sub>), 25.0 (s, CH<sub>2</sub>), 24.93 (s, CH<sub>2</sub>), 24.88 (s, CH<sub>2</sub>); MS (ES): *m/z* 335.2704 ([M-Br]<sup>+</sup>; C<sub>20</sub>H<sub>35</sub>N<sub>2</sub>O<sub>2</sub> requires 335.2699).

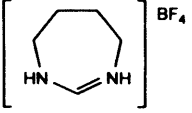
**9,9-(dimethyl-8,10-dioxolanyl)methyl)-1,3-dicyclohexyl-diazepan-2-ylidenium-hexafluorophosphate.**



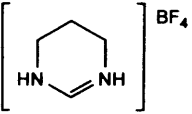
The dioxolane diamine **2.5** (0.50 g, 1.5 mmol), ammonium hexafluorophosphate (0.25 g, 1.54 mmol) and triethylorthoformate (0.5 ml, 3.1 mmol) were dissolved in 25 mL of DME. The reaction was heated to 90°C and left running overnight. Subsequently, volatiles were evaporated under reduced pressure and the slurry obtained was dissolved in chloroform (30 ml) and the insoluble impurities were filtered off. Evaporation of the solvent produced a yellow oil which was recrystallized from chloroform / diethyl ether (2:1) to afford 70 mg of white crystals (0.21 mmol, 10%). <sup>1</sup>H NMR (250 MHz, CDCl<sub>3</sub>): δ 7.80 (1H, s, NCHN), 3.78 (4H, m, OCH and NCH<sub>2</sub>), 3.56 (2H, m, Cy-CH), 3.15 (2H, m, NCH<sub>2</sub>), 2.05-1.05 (26H, m, Cy-CH<sub>2</sub> and CH<sub>3</sub>); <sup>13</sup>C NMR (400 MHz, CDCl<sub>3</sub>): δ 154.4 (s, NCHN), 112.1 (s, C(CH<sub>3</sub>)<sub>2</sub>), 74.9 (s, OCH), 70.1 (s, NCH), 46.5 (s,

NCH<sub>2</sub>), 29.8 (s, Cy-CH<sub>2</sub>), 29.7 (s, Cy-CH<sub>2</sub>), 24.9 (s, CH<sub>3</sub>), 24.1 (s, Cy-CH<sub>2</sub>), 24.0 (s, Cy-CH<sub>2</sub>), 23.8 (s, Cy-CH<sub>2</sub>); MS (ES): *m/z* 335.2687 ([M-PF<sub>6</sub>]<sup>+</sup>; C<sub>20</sub>H<sub>35</sub>N<sub>2</sub>O<sub>2</sub> requires 335.2699)

#### 4,5,6,7-tetrahydro-1H-1,3-diazepin-3-ium tetrafluoroborate.<sup>10</sup>

 The reaction was performed on a scale of, 5.0 ml of triethylorthoformate (30.0 mmol), 3.0 ml of 1,4-diaminobutane (30.0 mmol) and 3.14 g NH<sub>4</sub>BF<sub>4</sub> (30.0 mmol) in 45 ml of acetonitrile. Solution heated under reflux for 4 days at 95°C. The solution was filtered to remove any solid impurities and the filtrate collected. The acetonitrile was then removed *in vacuo*. The remaining residue was redissolved in a minimum amount of DCM and added to an excess of ether to precipitate out a white crystalline material which was then collected via filtration, washed with 2x5 ml of diethyl ether. The crystalline material was then dried *in vacuo* to yield 2.64 g of 7-H·BF<sub>4</sub> (11.1 mmol, 37%). <sup>1</sup>H NMR (CDCl<sub>3</sub>, 400 MHz, rt): δ 7.85 (2H, bs, NH), 7.65 (1H, m, NCHN), 3.45 (4H, m, NCH<sub>2</sub>), 1.9 (4H, m, NCH<sub>2</sub>CH<sub>2</sub>). <sup>13</sup>C NMR (CDCl<sub>3</sub>, 400 MHz, rt): δ 155.0 (s, NCHN), 46.2 (s, NCH<sub>2</sub>), 26.5 (s, NCH<sub>2</sub>CH<sub>2</sub>). LRMS calculated for C<sub>5</sub>H<sub>11</sub>N<sub>2</sub>: 99.137, found 99.09.

#### 3,4,5,6-tetrahydropyrimidin-1-ium tetrafluoroborate.<sup>10</sup>

 The reaction was performed on a scale of, 1.7 ml of triethylorthoformate (10.0 mmol), 0.9 ml of 1,4-diaminopropane (10.0 mmol) and 0.10 g NH<sub>4</sub>BF<sub>4</sub> (10.0 mmol) in 20.0 ml of acetonitrile. Solution heated under reflux for 4 days at 95°C. The solution was filtered to remove any solid impurities and the filtrate collected. The acetonitrile was then removed *in vacuo*. The remaining residue was redissolved in a minimum amount of DCM and added to an excess of ether to precipitate out a white crystalline material which was then collected via filtration, washed with 2x5mL of ether. The crystalline material was then dried *in vacuo* to yield 0.48 g of 6-H·BF<sub>4</sub>(2.8 mmol, 28%). <sup>1</sup>H NMR (CD<sub>3</sub>CN, 400 MHz, rt): δ 7.80 (1H, bs, NCHN), 3.37 (4H, m, NCH<sub>2</sub>), 2.35 (2H, m, NCH<sub>2</sub>CH<sub>2</sub>) ppm. <sup>13</sup>C NMR (CDCl<sub>3</sub>, 500 MHz, rt): δ 122.5 (s, NCHN), 43.25 (s, NCH<sub>2</sub>), 23.0 (s, NCH<sub>2</sub>CH<sub>2</sub>). LRMS calculated for C<sub>4</sub>H<sub>9</sub>N<sub>2</sub>: 85.04, found 85.07.

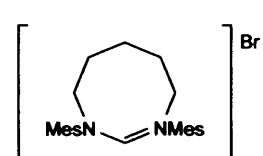


### 2.3.2. New method.

#### General protocol for the synthesis of the halide salts.

A mixture of 1 mmol of amidine, 0.5 mmol of  $K_2CO_3$  and 1-4 mmol of dihalide in 25 mL of acetonitrile is heated under reflux. At the end of the reaction, the volatiles are removed *in vacuo* and the residue freed of residual solvent by stirring with 3 portions of 5 mL of dichloromethane which were subsequently pumped off. The residue is dissolved in 5 mL of dichloromethane and filtered through a short column (0.5 cm) of silica. Ether is slowly added to the resulting dichloromethane solution until the product starts crystallizing.

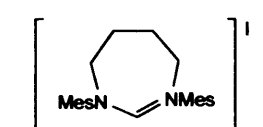
#### 1,3-Bis-(2,4,6-trimethylphenyl)- 3,4,5,6,7,8-hexahydro-1,3-diazocin-1-ium bromide.<sup>10</sup>



The reaction was performed on a scale of, 0.28 g of N,N'-di(mesityl)formamidine (1.0 mmol), 0.23 ml of 1,5-diaminopentane (1.0 mmol) and 0.08 g  $K_2CO_3$  (1.0 mmol) in 20 ml of acetonitrile.

Solution heated under reflux at 95°C for 2.5 weeks until the ring closure was fully complete (from  $^1H$ -NMR results). The solution was filtered to remove solid impurities and the acetonitrile removed *in vacuo*. The remaining residue was re-dissolved in a minimum amount of DCM added to an excess of ether to precipitate out a white crystalline material. This was collected and washed with 2x5 mL of ether. The crystalline material was then dried *in vacuo* to yield 0.11 g of **8-Mes·HBr** (0.3 mmol, 27%).  $^1H$  NMR ( $CDCl_3$ , 400 MHz, rt):  $\delta$  7.33 (1H, s, NCHN), 6.85 (4H, s, Ar-CH), 4.53 (4H, m, NCH<sub>2</sub>), 2.35 (12H, s, Ar-*o*-CH<sub>3</sub>), 2.25 (6H, s, Ar-*p*-CH<sub>3</sub>), 2.2 (4H, m, NCH<sub>2</sub>CH<sub>2</sub>), 1.67 (2H, m, NCH<sub>2</sub>CH<sub>2</sub>CH<sub>2</sub>).  $^{13}C$  NMR ( $CDCl_3$ , 500 MHz, rt):  $\delta$  158.0 (s, NCHN), 142.0 (s, Ar-C), 139.8 (s, Ar-C), 133.5 (s, Ar-C), 130.5 (s, Ar-CH), 54.0 (s, NCH<sub>2</sub>), 28.0 (s, NCH<sub>2</sub>CH<sub>2</sub>), 21.0 (s, Ar-*p*-Me and NCH<sub>2</sub>CH<sub>2</sub>CH<sub>2</sub>), 18.4 (s, Ar-*o*-CH<sub>3</sub>). LRMS calculated for C<sub>24</sub>H<sub>33</sub>N<sub>2</sub>: 349.50, found 349.25.

#### 1,3-Bis-(2,4,6-trimethylphenyl)-4,5,6,7-tetrahydro-3H-[1,3]diazepin-1-ium iodide.

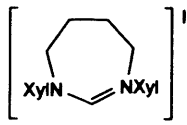


The reaction was performed on a 71.0 mmol scale of N,N'-di(mesityl)formamidine (19.90 g), 5.0 g of  $K_2CO_3$  (36.0 mmol) and 22.00 g of 1,4-diiodobutane (71.0 mmol) in 1 l of acetonitrile. The

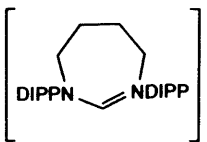
solution was heated under reflux for 5 hours to yield 29.20 g (63.0 mmol, 89%) of white, crystalline material.  $^1H$  NMR ( $CDCl_3$ , 400 MHz, rt):  $\delta$  7.22 (1H, s, NCHN), 6.92 (4H, s,

Ar-CH), 4.49 (4H, t,  $^3J_{\text{HH}} = 5.4$ , NCH<sub>2</sub>), 2.53 (4H, p,  $^3J_{\text{HH}} = 5.4$ , NCH<sub>2</sub>CH<sub>2</sub>), 2.37 (s, 12H, *o*-CH<sub>3</sub>), 2.24 (s, 6H, *p*-CH<sub>3</sub>); <sup>13</sup>C NMR (CDCl<sub>3</sub>, 100 MHz, rt):  $\delta$  157.8 (s, NCHN), 140.3 (s, Ar-C), 139.2 (s, Ar-C), 133.5 (s, Ar-C), 130.2 (s, Ar-CH), 55.1 (s, NCH<sub>2</sub>), 25.0 (s, NCH<sub>2</sub>CH<sub>2</sub>), 20.8 (s, *p*-CH<sub>3</sub>), 18.4 (s, *o*-CH<sub>3</sub>); MS (ES): *m/z* 335.2477 ([M - I]<sup>+</sup>; C<sub>23</sub>H<sub>31</sub>N<sub>2</sub> requires 335.2487).

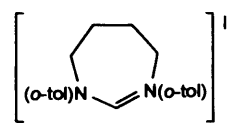
### 1,3-Bis-(2,6-dimethylphenyl)-4,5,6,7-tetrahydro-3H-[1,3]diazepin-1-ium iodide .

 The reaction was performed on a 43.3 mmol scale of N,N'-di(xylyl)formamidine (10.93 g), 5.8 ml of 1,4-diiodobutane (13.63 g, 44.0 mmol), 3.01 g of K<sub>2</sub>CO<sub>3</sub> (22.5 mmol) in 0.50 ml of acetonitrile. The solution was heated under reflux for 5 hours to yield 14.85 g (34.2 mmol, 79%) of white, crystalline material. <sup>1</sup>H NMR (CDCl<sub>3</sub>, 400 MHz, rt):  $\delta$  7.28 (1H, s, NCHN), 7.23 (2H, dd,  $^3J_{\text{HH}} = 6.8$ ,  $^3J_{\text{HH}} = 8.5$ , *p*-CH), 7.15 (4H, d,  $^3J_{\text{HH}} = 7.6$ , *m*-CH), 4.61 (4H, t,  $^3J_{\text{HH}} = 5.6$ , NCH<sub>2</sub>), 2.58 (4H, t,  $^3J_{\text{HH}} = 5.6$ , NCH<sub>2</sub>CH<sub>2</sub>), 2.46 (12H, s, *o*-CH<sub>3</sub>); <sup>13</sup>C NMR (CDCl<sub>3</sub>, 100 MHz, rt):  $\delta$  157.6 (s, NCHN), 141.6 (s, Ar-C), 134.0 (s, Ar-C), 130.2 (s, Ar-CH), 129.7 (s, Ar-CH), 55.2 (s, NCH<sub>2</sub>), 25.1 (s, NCH<sub>2</sub>CH<sub>2</sub>), 18.7 (s, CH<sub>3</sub>); MS (ES): *m/z* 307.2168 ([M - I]<sup>+</sup>; C<sub>21</sub>H<sub>27</sub>N<sub>2</sub> requires 307.2174).

### 1,3-Bis-(2,6-diisopropylphenyl)-4,5,6,7-tetrahydro-3H-[1,3]diazepin-1-ium iodide.

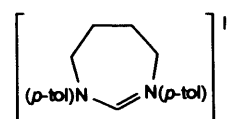
 The reaction was performed on a 11.0 mmol scale of N,N'-bis(diisopropylphenyl)formamidine (4.00 g), 0.78 mg of K<sub>2</sub>CO<sub>3</sub> (5.6 mmol), 1.6 ml of 1,4-diiodobutane (3.76 g, 12.1 mmol) in 400 ml of acetonitrile. The solution was heated under reflux for 17 hours to yield 3.87 g (7.1 mmol, 64%) of white, crystalline material. <sup>1</sup>H NMR (CDCl<sub>3</sub>, 400 MHz, rt):  $\delta$  7.40 (2H, t,  $^3J_{\text{HH}} = 7.8$ , *p*-CH), 7.27 (1H, s, NCHN), 7.23 (4H, d,  $^3J_{\text{HH}} = 7.8$ , *m*-CH), 4.63 (4H, bs, NCH<sub>2</sub>), 3.20 (4H, sept.,  $^3J_{\text{HH}} = 6.8$ , CH(CH<sub>3</sub>)<sub>2</sub>), 2.60 (4H, bs, NCH<sub>2</sub>CH<sub>2</sub>), 1.39 (12H, d,  $^3J_{\text{HH}} = 6.8$ , CH(CH<sub>3</sub>)<sub>2</sub>), 1.24 (12H, d,  $^3J_{\text{HH}} = 6.8$ , CH(CH<sub>3</sub>)<sub>2</sub>); <sup>13</sup>C NMR (CDCl<sub>3</sub>, 100 MHz, rt):  $\delta$  157.0 (s, NCHN), 144.7 (s, Ar-C), 138.7 (s, Ar-C), 130.9 (s, Ar-CH), 125.3 (s, Ar-CH), 56.4 (s, NCH<sub>2</sub>), 28.9 (s, CH(CH<sub>3</sub>)<sub>2</sub>), 25.1 (s, CH(CH<sub>3</sub>)<sub>2</sub>), 24.7 (s, NCH<sub>2</sub>CH<sub>2</sub>), 24.6 (s, CH(CH<sub>3</sub>)<sub>2</sub>); MS (ES): *m/z* 419.3426 ([M - I]<sup>+</sup>; C<sub>29</sub>H<sub>43</sub>N<sub>2</sub> requires 419.3426).

**1,3-Bis-(2-methylphenyl)-4,5,6,7-tetrahydro-3H-[1,3]diazepin-1-ium iodide.**



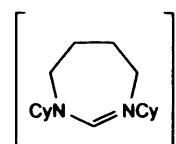
The reaction was performed on a 20.0 mmol scale of N,N'-di(*o*-tolyl)formamidine (4.48 g), 1.38 g. K<sub>2</sub>CO<sub>3</sub> (10.0 mmol) and 6.51 g. 1,4-diiodobutane (21.0 mmol) in 50 ml acetonitrile. The solution was heated under reflux overnight to yield 7.80 g (19.2 mmol, 96%) of white, crystalline material. <sup>1</sup>H NMR (CDCl<sub>3</sub>, 400 MHz, rt): δ 7.72 (2H, bs, *o*-CH), 7.41 (1H, s, NCHN), 7.26-7.22 (6H, m, *m,p*-CH), 4.50 (4H, bs, NCH<sub>2</sub>), 2.46 (4H, bs, NCH<sub>2</sub>CH<sub>2</sub>), 2.39 (6H, s, CH<sub>3</sub>); <sup>13</sup>C NMR (CDCl<sub>3</sub>, 100 MHz, rt): δ 156.3 (s, NCHN), 141.8 (s, ipsoC), 131.8 (s, C<sub>*o*</sub>-tolCH<sub>3</sub>), 130.7 (s, CH<sub>*o*</sub>-tol), 129.1 (s, CH<sub>*o*</sub>-tol), 127.2 (s, CH<sub>*o*</sub>-tol), 126.8 (s, CH<sub>*o*</sub>-tol), 55.0 (s, NCH<sub>2</sub>) 24.4 (s, NCH<sub>2</sub>CH<sub>2</sub>), 13.1 (s, CH<sub>3</sub>); MS (ES): *m/z* 279.1859 ([M - I]<sup>+</sup>; C<sub>19</sub>H<sub>23</sub>N<sub>2</sub> requires 279.1861).

**1,3-Bis-(4-methylphenyl)-4,5,6,7-tetrahydro-3H-[1,3]diazepin-1-ium iodide.**



The reaction was performed on a 20.0 mmol scale of N,N'-di(*p*-tolyl)formamidine (4.48 g), 1.38 g. K<sub>2</sub>CO<sub>3</sub> (10.0 mmol) and 6.51 g 1,4-diiodobutane (21.0 mmol) in 50 mL acetonitrile. The solution was heated under reflux overnight to yield 6.30 g (15.5 mmol, 78%) of white, crystalline material. <sup>1</sup>H NMR (CDCl<sub>3</sub>, 400 MHz, rt): δ 7.58 (1H, s, NCHN), 7.50 (4H, d, <sup>3</sup>J<sub>HH</sub> = 8.3, *o*-CH), 7.15 (4H, d, <sup>3</sup>J<sub>HH</sub> = 8.3, *m*-CH), 4.50 (4H, t, <sup>3</sup>J<sub>HH</sub> = 5.5, NCH<sub>2</sub>), 2.35 (4H, m, NCH<sub>2</sub>CH<sub>2</sub>), 2.27 (6H, s, CH<sub>3</sub>); <sup>13</sup>C NMR (CDCl<sub>3</sub>, 100 MHz, rt): δ 156.5 (s, NCHN), 141.8 (s, ipsoC<sub>*p*</sub>-tol), 140.1 (s, C<sub>*p*</sub>-tolCH<sub>3</sub>), 131.0 (s, CH<sub>*p*</sub>-tol), 125.0 (s, CH<sub>*p*</sub>-tol), 56.0 (s, NCH<sub>2</sub>) 25.5 (s, NCH<sub>2</sub>CH<sub>2</sub>), 21.5 (s, CH<sub>3</sub>); MS (ES): *m/z* 279.1852 ([M - I]<sup>+</sup>; C<sub>19</sub>H<sub>23</sub>N<sub>2</sub> requires 279.1861).

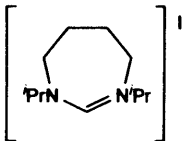
**1,3-Bis-(4-methylphenyl)-4,5,6,7-tetrahydro-3H-[1,3]diazepin-1-ium iodide.**



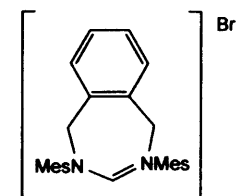
The reaction was performed on a 7.1 mmol scale of N,N'-di(cyclohexyl)formamidine (1.48 g), 0.50 g K<sub>2</sub>CO<sub>3</sub> (3.5 mmol) and 2.20 g. 1,4-diiodobutane (7.2 mmol) in 20 ml acetonitrile. The solution was heated under reflux for 2 days. The solution was filtered to remove any solid impurities and the filtrate collected. The acetonitrile was then removed *in vacuo*. The remaining residue was re-dissolved in a mixture 1:5 DCM/toluene and cooled to -4°C. Filtration of the precipitate yielded 2.7 g (6.9 mmol, 98%) of white waxy solid. <sup>1</sup>H NMR (CDCl<sub>3</sub>, 400 MHz, rt): δ 8.65 (1H, s, NCHN), 3.84 (4H, m, NCH<sub>2</sub>), 3.64 (2H, m, Cy-CH), 2.04 (4H, m,

CH<sub>2</sub>), 1.92 (4H, m, CH<sub>2</sub>), 1.75 (4H, m, CH<sub>2</sub>), 1.58 (2H, m, CH<sub>2</sub>), 1.41 (8H, m, CH<sub>2</sub>), 1.08 (2H, m, CH<sub>2</sub>); <sup>13</sup>C NMR (400 MHz, CDCl<sub>3</sub>): δ 154.4 (s, NCN), 63.8 (s, Cy-CH), 42.6 (s, NCH<sub>2</sub>), 31.2 (s, CH<sub>2</sub>), 28.8 (s, CH<sub>2</sub>), 23.2 (s, CH<sub>2</sub>), 22.9 (s, CH<sub>2</sub>); MS (ES): *m/z* 263.2471 ([M-PF<sub>6</sub>]<sup>+</sup>; C<sub>17</sub>H<sub>31</sub>N<sub>2</sub> requires 263.2487).

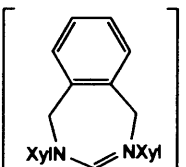
**1,3-Diisopropyl-4,5,6,7-tetrahydro-3H-[1,3]diazepin-1-ium iodide.**

 The reaction was performed on a scale of, 1.88 g of N,N'-di(isopropyl)formamidine (10.0 mmol), 3.20 g of 1,4-Diiodobutane (10.5 mmol) and 0.68 g K<sub>2</sub>CO<sub>3</sub> (4.9 mmol) in 20 ml of acetonitrile. Solution heated under reflux for 4 days at 95°C. The solution was filtered to remove any solid impurities and the filtrate collected. The acetonitrile was then removed *in vacuo*. The remaining residue was re-dissolved in a minimum amount of DCM and added to an excess of ether to precipitate out a white crystalline material which was then collected via filtration, washed with 2x5 mL of ether. The crystalline material was then dried *in vacuo* to yield 0.45 g of 7-<sup>i</sup>Pr-HI (1.5 mmol, 15%). <sup>1</sup>H NMR (CDCl<sub>3</sub>, 400 MHz, rt): δ 8.90 (1H, s, NCHN), 4.4 (2H, m, <sup>i</sup>Pr-CH), 3.5 (4H, m, NCH<sub>2</sub>), 2.1 (4H, m, NCH<sub>2</sub>CH<sub>2</sub>), 1.25 (12H, d, <sup>i</sup>PrCH<sub>3</sub>). <sup>13</sup>C NMR (CDCl<sub>3</sub>, 400 MHz, rt): δ 156.5 (s, NCHN), 68.5 (s, <sup>i</sup>Pr-CH), 43.0 (s, NCH<sub>2</sub>), 25.0 (s, NCH<sub>2</sub>CH<sub>2</sub>), 21.0 (s, <sup>i</sup>PrCH<sub>3</sub>'s). LRMS calculated for C<sub>11</sub>H<sub>23</sub>N<sub>2</sub>: 183.294, found 183.186.

**2,4-Bis-(2,4,6-trimethylphenyl)-4,5-dihydro-1H-benzo[e][1,3]diazepin-2-ium bromide.<sup>1c</sup>**

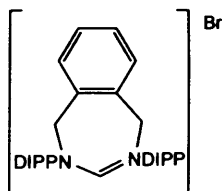
 The reaction was performed on a 35.8 mmol scale of N,N'-di(mesityl)formamidine (10.03 g), 36.0 mmol of α,α'-dibromo-*o*-xylene (9.49 g), 2.49 g. of K<sub>2</sub>CO<sub>3</sub> (18.0 mmol) in 500 ml of acetonitrile. The solution was heated under reflux for 5 hours to yield 12.42 g (26.2 mmol, 73%) of white, crystalline material.

**2,4-Bis-(2,6-dimethylphenyl)-4,5-dihydro-1H-benzo[e][1,3]diazepin-2-ium bromide.**

 The reaction was performed on a 7.9 mmol scale of N,N'-di(xylyl)formamidine (2.00 g), 2.09 g of α,α'-dibromo-*o*-xylene (7.9 mmol), 0.56 g of K<sub>2</sub>CO<sub>3</sub> (4.05 mmol) in 75 ml of acetonitrile. The

solution heated under reflux for 5 hours to yield 3.00 g (6.9 mmol, 87 %) of white, crystalline material.  $^1\text{H}$  NMR ( $\text{CDCl}_3$ , 400 MHz, rt):  $\delta$  7.42 (2H, dd,  $^3J_{\text{HH}} = 3.3$ ,  $^3J_{\text{HH}} = 5.5$ , Xy-CH), 7.27 (2H, dd,  $^3J_{\text{HH}} = 3.3$ ,  $^3J_{\text{HH}} = 5.5$ , Xy-CH), 7.22 (2H, t,  $^3J_{\text{HH}} = 7.5$ , *p*-CH), 7.19 (1H, s, NCHN), 7.13 (4H, br.d,  $^3J_{\text{HH}} = 7.6$ , *m*-CH), 2.35 (12H, br.s,  $\text{CH}_3$ ) (The  $\text{NCH}_2$ -groups are not observed at RT);  $^{13}\text{C}$  NMR ( $\text{CDCl}_3$ , 100 MHz, rt):  $\delta$  155.6 (s, NCHN), 142.5 (s, Ar-C), 134.9 (s, Ar-C), 130.1 (s, Ar-CH), 130.0 (s, Ar-CH), 129.5 (s, Ar-CH), 129.3 (s, Ar-CH), 57.7 (s,  $\text{NCH}_2$ ), 18.9 (s,  $\text{CH}_3$ ) (One Ar-C not observed,  $\text{NCH}_2$  is not visible in  $^{13}\text{C}$  DEPT experiment);  $^1\text{H}$  NMR ( $\text{CD}_3\text{CN}$ , 400 MHz, rt):  $\delta$  7.65 (1H, s, NCHN), 7.56 (2H, dd,  $^3J_{\text{HH}} = 3.4$ ,  $^3J_{\text{HH}} = 5.5$ , Xy-CH), 7.50 (dd,  $^3J_{\text{HH}} = 3.4$ ,  $^3J_{\text{HH}} = 5.5$ , 2H, Xy-CH), 7.32 (dd,  $^3J_{\text{HH}} = 6.7$ ,  $^3J_{\text{HH}} = 8.4$ , 2H, Xy-*p*-CH), 7.25 (4H, bd,  $^3J_{\text{HH}} = 7.4$ , Xy-*m*-CH), 5.46 (4H, bs,  $\text{NCH}_2$ ), 2.31 (12H, s,  $\text{CH}_3$ ),  $^{13}\text{C}$  NMR ( $\text{CD}_3\text{CN}$ , 100 MHz, rt):  $\delta$  158.2 (s, NCHN), 143.2 (s, Ar-C), 135.6 (s, Ar-C), 135.4 (s, Ar-C), 131.1 (s, Ar-CH), 130.9 (s, Ar-CH), 130.2 (s, Ar-CH), 130.0 (s, Ar-CH), 56.4 (s,  $\text{NCH}_2$ ), 18.5 (s,  $\text{CH}_3$ ). MS (ES):  $m/z$  355.2158 ( $[\text{M} - \text{Br}]^+$ ;  $\text{C}_{25}\text{H}_{27}\text{N}_2$  requires 355.2174).

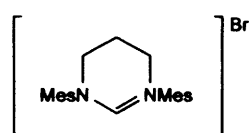
**2,4-Bis-(2,6-diisopropylphenyl)-4,5-dihydro-1H-benzo[e][1,3]diazepin-2-ium bromide.**



The reaction was performed on a 11.0 mmol scale of N,N'-bis(diisopropylphenyl)formamidine (4.00 g), 760 mg  $\text{K}_2\text{CO}_3$  (5.5 mmol) and 2.90 g  $\alpha,\alpha'$ -dibromo-*o*-xylene (11.0 mmol) in 400 ml acetonitrile. The solution was heated under reflux for 48 hours to yield 2.67 g (4.9 mmol, 45%) of white, crystalline material.  $^1\text{H}$  NMR ( $\text{CDCl}_3$ , 400 MHz, rt):  $\delta$  7.90 (1H, s, NCHN), 7.59-7.55 (2H, m, Xy-CH), 7.56-7.45 (4H, m, Xy-CH and *p*-CH), 7.37 (4H, d,  $^3J_{\text{HH}} = 7.7$ , *m*-CH), 1.97 (4H, h,  $^3J_{\text{HH}} = 2.5$  Hz,  $\text{CH}(\text{CH}_3)_2$ ), 1.33 (12H, t,  $^3J_{\text{HH}} = 6.7$ ,  $\text{CH}(\text{CH}_3)_2$ ), 1.18 (12H, t,  $^3J_{\text{HH}} = 6.7$ ,  $\text{CH}(\text{CH}_3)_2$ ) (The  $\text{NCH}_2$ -groups are not observed at rt);  $^{13}\text{C}$  NMR ( $\text{CDCl}_3$ , 100 MHz, rt):  $\delta$  155.0 (s, NCHN), 139.5 (s, Ar-C), 134.4 (s, Ar-C), 130.8 (s, Ar-CH), 129.8 (s, Ar-CH), 129.2 (s, Ar-CH), 125.2 (s, Ar-CH), 58.8 (s,  $\text{NCH}_2$ ), 28.6 (s,  $\text{CH}(\text{CH}_3)_2$ ), 25.3 (s,  $\text{CH}(\text{CH}_3)_2$ ), 24.6 (s,  $\text{CH}(\text{CH}_3)_2$ );  $^1\text{H}$  NMR ( $\text{CD}_3\text{CN}$ , 400 MHz, rt):  $\delta$  7.87 (s, 1H, NCHN), 7.55 (2H, dd,  $^3J_{\text{HH}} = 3.4$ ,  $^3J_{\text{HH}} = 5.4$ , Xy-CH), 7.51-7.43 (4H, m, Xy-CH and DIPP-*p*-CH), 7.35 (4H, bd,  $^3J_{\text{HH}} = 7.7$ , DIPP-*m*-CH), 5.41 (4H, bs,  $\text{CH}_2$ ), 3.00 (4H, bs,  $\text{CH}(\text{CH}_3)_2$ ), 1.30 (12H, d,  $^3J_{\text{HH}} = 6.7$ ,  $\text{CH}(\text{CH}_3)_2$ ), 1.16 (12H, d,  $^3J_{\text{HH}} = 6.7$ ,  $\text{CH}(\text{CH}_3)_2$ );  $^{13}\text{C}$  NMR ( $\text{CD}_3\text{CN}$ , 100 MHz, rt):  $\delta$  157.7 (s, NCHN), 145.8 (s, Ar-C), 139.9 (s, Ar-C), 134.9 (s, Ar-C), 131.7 (s, Ar-CH), 131.1 (s, Ar-CH),

130.2 (s, Ar-CH), 126.1 (s, Ar-CH), 57.9 (s, NCH<sub>2</sub>), 29.6 (s, CH(CH<sub>3</sub>)<sub>2</sub>), 24.9 (s, CH(CH<sub>3</sub>)<sub>2</sub>), 24.6 (CH(CH<sub>3</sub>)<sub>2</sub>). MS (ES): *m/z* 467.3420 ([M – Br]<sup>+</sup>; C<sub>33</sub>H<sub>43</sub>N<sub>2</sub> requires 467.3426).

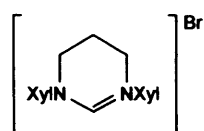
**1,3-Bis-(2,4,6-trimethylphenyl)-3,4,5,6-tetrahydro-pyrimidin-1-ium bromide.<sup>1c</sup>**



The reaction was performed on a 20.0 mmol scale of N,N'-di(mesityl)formamidine (5.60 g), 1.40 g of K<sub>2</sub>CO<sub>3</sub> (10.0 mmol) and 4.24 g of 1,3-dibromopropane (20.0 mmol) in 250 ml of acetonitrile.

The solution was heated under reflux for 17 hours to yield 6.55 g (16 mmol, 82%) of white, crystalline material.

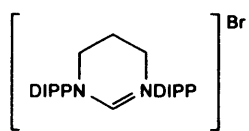
**1,3-Bis-(2,6-dimethylphenyl)-3,4,5,6-tetrahydro-pyrimidin-1-ium bromide.**



The reaction was performed on a 4.7 mmol scale of N,N'-di(xylyl)formamidine (1.13 g), 0.6 ml of 1,3-dibromopropane (1.19 g, 5.9 mmol) and 0.32 g of K<sub>2</sub>CO<sub>3</sub> (2.3 mmol) in 50 ml of acetonitrile. The

solution was heated under reflux for 17 hours to yield 1.17 g (3.24 mmol, 69%) of white, crystalline material. <sup>1</sup>H NMR (CDCl<sub>3</sub>, 400 MHz, rt): δ 7.68 (1H, s, NCHN), 7.23 (2H, d, <sup>3</sup>J<sub>HH</sub> = 7.1, <sup>3</sup>J<sub>HH</sub> = 8.1, *p*-CH), 7.12 (4H, bd, <sup>3</sup>J<sub>HH</sub> = 7.6, *m*-CH), 4.21 (4H, t, <sup>3</sup>J<sub>HH</sub> = 5.6, NCH<sub>2</sub>), 2.61 (2H, p, <sup>3</sup>J<sub>HH</sub> = 5.6, NCH<sub>2</sub>CH<sub>2</sub>), 2.38 (12H, s, CH<sub>3</sub>); <sup>13</sup>C NMR (CDCl<sub>3</sub>, 100 MHz, rt): δ 153.3 (s, NCHN), 138.6 (s, Ar-C), 134.7 (s, Ar-C), 130.3 (s, Ar-CH), 129.4 (s, Ar-CH), 46.7 (s, NCH<sub>2</sub>), 19.4 (s, NCH<sub>2</sub>CH<sub>2</sub>), 18.0 (s, CH<sub>3</sub>); MS (ES): *m/z* 293.2014 ([M – Br]<sup>+</sup>; C<sub>20</sub>H<sub>25</sub>N<sub>2</sub> requires 293.2018).

**1,3-Bis-(2,6-diisopropylphenyl)-3,4,5,6-tetrahydro-pyrimidin-1-ium bromide.**

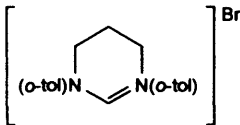


The reaction was performed on a 6.9 mmol scale of N,N'-bis(diisopropylphenyl)formamidine (2.51 g), 520 mg of K<sub>2</sub>CO<sub>3</sub> (3.8 mmol) and 1.1 ml of 1,3-dibromopropane (2.19 g, 10.9 mmol) in 100

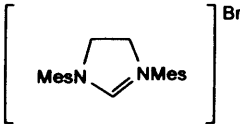
ml of acetonitrile. The solution was heated under reflux for 4 days to yield 2.395 g (4.9 mmol, 71%) of white, crystalline material. <sup>1</sup>H NMR (CDCl<sub>3</sub>, 400 MHz, rt): δ 7.55 (1H, s, NCHN), 7.41 (2H, t, <sup>3</sup>J<sub>HH</sub> = 7.7, *p*-CH), 7.23 (4H, d, <sup>3</sup>J<sub>HH</sub> = 7.7, *m*-CH), 4.21 (4H, t, <sup>3</sup>J<sub>HH</sub> = 5.5, NCH<sub>2</sub>), 3.00 (4H, sept., <sup>3</sup>J<sub>HH</sub> = 6.75, CH(CH<sub>3</sub>)<sub>2</sub>), 2.74 (2H, p, <sup>3</sup>J<sub>HH</sub> = 5.5, NCH<sub>2</sub>CH<sub>2</sub>), 1.35 (d, <sup>3</sup>J<sub>HH</sub> = 6.75, 12H, CH(CH<sub>3</sub>)<sub>2</sub>), 1.20 (d, <sup>3</sup>J<sub>HH</sub> = 6.75, 12H, CH(CH<sub>3</sub>)<sub>2</sub>); <sup>13</sup>C NMR (CDCl<sub>3</sub>, 100 MHz, rt): δ 152.8 (s, NCHN), 145.5 (s, Ar-C), 135.6 (s, Ar-C), 131.2 (s, Ar-

CH), 125.1 (s, Ar-CH), 48.8 (s, NCH<sub>2</sub>), 28.8 (s, CH(CH<sub>3</sub>)<sub>2</sub>), 24.8 (s, CH(CH<sub>3</sub>)<sub>2</sub>), 24.7 (s, CH(CH<sub>3</sub>)<sub>2</sub>), 19.3 (s, NCH<sub>2</sub>CH<sub>2</sub>); MS (ES): *m/z* 405.3265 ([M – Br]<sup>+</sup>; C<sub>28</sub>H<sub>41</sub>N<sub>2</sub> requires 405.3270).

### 1,3-Bis-(2-methylphenyl)-3,4,5,6-tetrahydro-pyrimidin-1-ium bromide.

 The reaction was performed on a 5.0 mmol scale of N,N'-di(*o*-tolyl)formamidine (1.12 g), 0.35 g. K<sub>2</sub>CO<sub>3</sub> (2.5 mmol) and 1.21 g. 1,4-diiodobutane (5.1 mmol) in 20 mL acetonitrile. The solution was heated under reflux overnight to yield 1.00 g (2.9 mmol, 58%) of white, crystalline material. <sup>1</sup>H NMR (CDCl<sub>3</sub>, 400 MHz, rt): δ 8.13 (d, <sup>3</sup>J<sub>HH</sub> = 6.9, 2H, *o*-CH), 7.72 (s, 1H, NCHN), 7.37-7.26 (m, 6H, *m,p*-CH), 4.25 (bs, 4H, N-CH<sub>2</sub>), 2.58 (bs, 2H, N-CH<sub>2</sub>-CH<sub>2</sub>), 2.39 (s, 6H, CH<sub>3</sub>); <sup>13</sup>C NMR (CDCl<sub>3</sub>, 100 MHz, rt): δ 153.7 (s, NCHN), 140.5 (s, ipsoC), 133.4 (s, C<sub>*o*-tol</sub>CH<sub>3</sub>), 131.8 (s, CH<sub>*o*-tol</sub>), 130.6 (s, CH<sub>*o*-tol</sub>), 128.8 (s, C<sub>*o*-tol</sub>CH<sub>3</sub>), 128.6 (s, CH<sub>*o*-tol</sub>), 47.9 (s, N-CH<sub>2</sub>) 20.2 (s, NCH<sub>2</sub>CH<sub>2</sub>), 18.0 (s, CH<sub>3</sub>); MS (ES): *m/z* 265.1717 ([M – I]<sup>+</sup>; C<sub>18</sub>H<sub>21</sub>N<sub>2</sub> requires 265.1705).

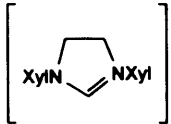
### 1,3-Bis-(2,4,6-trimethylphenyl)-4,5-dihydro-3H-imidazol-1-ium bromide.<sup>20</sup>

 The reaction was performed on a 35.7 mmol scale of N,N'-di(mesityl)formamidine (10 g), 2.59 g of K<sub>2</sub>CO<sub>3</sub> (17.8 mmol) and 5.41 mL of 1,2-dibromoethane (7.38 g, 39.3 mmol) in 500 mL of acetonitrile. The solution was heated under reflux for 3 days to yield 10.46 g of white, crystalline material (27.1 mmol, 76%). <sup>1</sup>H NMR (CDCl<sub>3</sub>, 400 MHz, rt): δ 8.92 (1H, s, NCHN), 6.94 (4H, s, *m*-CH), 4.62 (4H, s, NCH<sub>2</sub>), 2.39 (12H, s, *o*-CH<sub>3</sub>), 2.28 (6H, s, *p*-CH<sub>3</sub>); <sup>13</sup>C NMR (CDCl<sub>3</sub>, 100 MHz, 298 K): δ 159.0 (s, NCHN), 140.6 (s, Ar-C), 134.9 (s, Ar-C), 130.0 (s, Ar-CH), 52.2 (s, NCH<sub>2</sub>), 21.0 (s, *p*-CH<sub>3</sub>), 18.1 (s, *o*-CH<sub>3</sub>) (one aromatic carbon obscured by CDCl<sub>3</sub> solvent); <sup>1</sup>H NMR (DMSO-*d*<sub>6</sub>, 400 MHz, rt): δ 8.99 (1H, s, NCHN), 7.09 (4H, s, Ar-*m*-CH), 4.44 (4H, s, NCH<sub>2</sub>), 2.34 (12H, s, *o*-CH<sub>3</sub>), 2.29 (6H, s, *p*-CH<sub>3</sub>); <sup>13</sup>C NMR (DMSO-*d*<sub>6</sub>, 100 MHz, 298 K): δ 160.2 (s, NCHN), 139.6 (s, Ar-C), 135.4

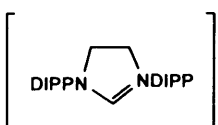
<sup>20</sup> This salt was prepared by Tracy Hamilton, Ph.D. student in our group. The chloride salt has been previously reported: Arduengo, Anthony J., III.; Goerlich, Jens R.; Marshall, William J. *J. Am. Chem. Soc.* **1995**, *117*, 11027.

(s, Ar-C), 130.8 (s, Ar-C), 129.3 (s, Ar-CH), 50.8 (s, NCH<sub>2</sub>), 20.6 (s, *p*-CH<sub>3</sub>), 17.2 (s, *o*-CH<sub>3</sub>); MS (ES): *m/z* 307.2162 ([M – Br]<sup>+</sup>; C<sub>21</sub>H<sub>27</sub>N<sub>2</sub> requires 307.2174).

**1,3-Bis-(2,6-dimethylphenyl)-4,5-dihydro-3H-imidazol-1-ium bromide.<sup>21</sup>**

 <sup>Br</sup> The reaction was performed on a 10.3 mmol scale of N,N'-di(xylyl)formamidine (2.60 g), 0.72 g of K<sub>2</sub>CO<sub>3</sub> (5.2 mmol) and 2.0 mL of 1,2-dibromoethane (4.4 g, 23.2 mmol) in 80 mL of acetonitrile. The solution was heated under reflux for 10 days. The product is less soluble in dichloromethane than the other halide salts. Yield 2.75 g (7.1 mmol, 69%) of light yellow, crystalline material. <sup>1</sup>H NMR (CDCl<sub>3</sub>, 400 MHz, rt): δ 9.20 (s, 1H, NCHN), 7.21 (2H, dd, <sup>3</sup>J<sub>HH</sub> = 7.2, <sup>3</sup>J<sub>HH</sub> = 7.9, *p*-CH), 7.10 (4H, d, <sup>3</sup>J<sub>HH</sub> = 7.6, *m*-CH), 4.60 (4H, s, NCH<sub>2</sub>), 2.41 (12H, s, CH<sub>3</sub>); <sup>13</sup>C NMR (CDCl<sub>3</sub>, 100 MHz, rt): δ 159.0 (s, NCHN), 135.4 (s, Ar-C), 132.6 (s, Ar-C), 130.4 (s, Ar-CH), 129.3 (s, Ar-CH), 52.0 (s, NCH<sub>2</sub>), 18.3 (s, CH<sub>3</sub>); <sup>1</sup>H NMR (DMSO-d<sub>6</sub>, 400 MHz, rt): δ 9.07 (1H, s, NCHN), 7.36 (2H, dd, <sup>3</sup>J<sub>HH</sub> = 6.5, <sup>3</sup>J<sub>HH</sub> = 8.5, *p*-CH), 7.29 (4H, bd, <sup>3</sup>J<sub>HH</sub> = 7.6, *m*-CH), 4.51 (4H, s, NCH<sub>2</sub>), 2.41 (12H, s, CH<sub>3</sub>); <sup>13</sup>C NMR (DMSO-d<sub>6</sub>, 100 MHz, rt): δ 160.1 (s, NCHN), 135.8 (s, Ar-C), 133.3 (s, Ar-C), 130.0 (s, Ar-CH), 128.9 (s, Ar-CH), 50.8 (s, NCH<sub>2</sub>), 17.3 (s, CH<sub>3</sub>); MS (ES): *m/z* 279.1848 ([M – Br]<sup>+</sup>; C<sub>19</sub>H<sub>23</sub>N<sub>2</sub> requires 279.1861).

**1,3-Bis-(2,6-diisopropylphenyl)-4,5-dihydro-3H-imidazol-1-ium bromide.<sup>22</sup>**

 <sup>Br</sup> The reaction was performed on a 7.75 mmol scale of N,N'-bis(diisopropyl)formamidine (2.824 g), 0.56 g of K<sub>2</sub>CO<sub>3</sub> (4.0 mmol) and 2.0 ml of 1,2-dibromoethane (4.4 g, 23.2 mmol) in 80 ml of acetonitrile. The solution was heated under reflux for 10 days. The product is less soluble in dichloromethane than the other halide salts. Crude yield 3.44 g (7.3 mmol, 94%) of white, microcrystalline material, which was converted to the BF<sub>4</sub>-salt without further purification. <sup>1</sup>H NMR (CDCl<sub>3</sub>, 400 MHz, rt): δ 8.10 (1H, s, NCHN), 7.49 (2H, t, <sup>3</sup>J<sub>HH</sub> = 7.8 Hz, *p*-CH), 7.29 (4H, d, <sup>3</sup>J<sub>HH</sub> = 7.8, *m*-CH), 4.91 (4H, s, CH<sub>2</sub>), 3.06 (4H, h, <sup>3</sup>J<sub>HH</sub> = 6.8,

<sup>21</sup> The chloride salt has been previously reported: Hintermann, Lukas *Adv. Synth. Catal.* **2002**, *344*, 749.

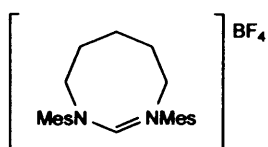
<sup>22</sup> Arduengo, Anthony J., III; Krafczyk, Roland; Schmutzler, Reinhard; Craig, Hugh A.; Goerlich, Jens R.; Marshall, William J.; Unverzagt, Markus *Tetrahedron* **1999**, *55*, 14523.



$\text{CH}(\text{CH}_3)_2$ , 1.42 (12 H, d,  $^3J_{\text{HH}} = 6.8$ ,  $\text{CH}(\text{CH}_3)_2$ ), 1.26 (12 H, d,  $^3J_{\text{HH}} = 6.8$ ,  $\text{CH}(\text{CH}_3)_2$ ).  $^{13}\text{C}$  NMR ( $\text{CDCl}_3$ , 100 MHz, rt):  $\delta$  158.0 (s, NCHN), 146.6 (s, Ar-C), 132.1 (s, Ar-C), 129.5 (s, Ar-CH), 125.5 (s, Ar-CH), 55.9 (s, NCH<sub>2</sub>), 29.6 (s,  $\text{CH}(\text{CH}_3)_2$ ), 25.9 (s,  $\text{CH}(\text{CH}_3)_2$ ), 24.3 (s,  $\text{CH}(\text{CH}_3)_2$ );  $^1\text{H}$  NMR ( $\text{DMSO-d}_6$ , 400 MHz, rt):  $\delta$  9.49 (1H, s, NCHN), 7.55 (2H, t,  $^3J_{\text{HH}} = 7.7$ , *p*-CH), 7.42 (4H, d,  $^3J_{\text{HH}} = 7.7$ , *m*-CH), 4.55 (4H, s, NCH<sub>2</sub>), 3.08 (4H, h,  $^3J_{\text{HH}} = 6.7$ ,  $\text{CH}(\text{CH}_3)_2$ ), 1.35 (d,  $^3J_{\text{HH}} = 6.7$ , 12H,  $\text{CH}(\text{CH}_3)_2$ ), 1.19 (d,  $^3J_{\text{HH}} = 6.7$ , 12H,  $\text{CH}(\text{CH}_3)_2$ );  $^{13}\text{C}$  NMR ( $\text{DMSO-d}_6$ , 100 MHz, rt):  $\delta$  160.0 (1C, s, NCHN), 146.1 (s, Ar-C), 131.1 (s, Ar-C), 129.8 (s, Ar-CH), 124.8 (s, Ar-C), 53.7 (s, NCH<sub>2</sub>), 28.3 (s,  $\text{CH}(\text{CH}_3)_2$ ), 25.0 (s,  $\text{CH}(\text{CH}_3)_2$ ), 23.3 (s,  $\text{CH}(\text{CH}_3)_2$ ); MS (ES):  $m/z$  391.3112 ( $[\text{M} - \text{Br}]^+$ ;  $\text{C}_{27}\text{H}_{39}\text{N}_2$  requires 391.3113).

**General protocol for the anion exchanges.** The halide salt is dissolved in acetone or acetonitrile, and a solution of  $\text{NaBF}_4$  in water is added. After stirring the solution for 5 minutes the organic solvent is removed *in vacuo* which results in the precipitation of the product. The product is collected on a frit and thoroughly washed with water. The solid material is dissolved in dichloromethane, water is separated off, and the solution subsequently dried over  $\text{MgSO}_4$ , filtered and ether is added to the solution until the product starts crystallizing.

**1,3-Bis-(2,4,6-trimethylphenyl)-3,4,5,6,7,8-hexahydro-1,3-diazocin-1-ium tetrafluoroborate.**

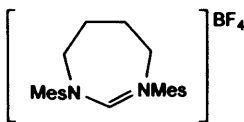


The reaction was performed on a scale of, 0.86 g of the 1,3-dimesityl-1,3-diazocane (2.0 mmol) predissolved in 20 ml of acetone. 0.27 g of sodium tetrafluoroborate (2.5 mmol) was predissolved in 10 ml of distilled water. Both solutions were stirred

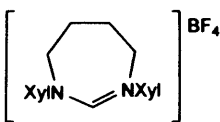
for 10 minutes at rt there after the acetone was removed *in vacuo* and the resulting salt extracted from 100 ml of DCM. The DCM solution containing product was then removed under reduced pressure to yield the final product. A 96% yield of a pale orange, crystalline material was recovered (0.84 g, 1.92 mmol).  $^1\text{H}$  NMR ( $\text{CDCl}_3$ , 400 MHz, rt):  $\delta$  7.32 (1H, s, NCHN), 6.87 (4H, s, Ar-CH), 4.4 (m, 4H, NCH<sub>2</sub>), 2.31 (12H, s, Ar-CH<sub>3</sub>), 2.25 (6H, s, Ar-*p*-CH<sub>3</sub>), 2.21 (4H, m, NCH<sub>2</sub>CH<sub>2</sub>), 1.7 (2H, m, NCH<sub>2</sub>CH<sub>2</sub>CH<sub>2</sub>).  $^{13}\text{C}$  NMR ( $\text{CDCl}_3$ , 250 MHz, rt):  $\delta$  157 (s, NCHN), 141.8 (s, Ar-C), 139.9 (s, Ar-C), 133.5 (s, Ar-C), 130.2 (s, Ar-

CH), 54.1 (s, NCH<sub>2</sub>), 29.0 (s, NCH<sub>2</sub>CH<sub>2</sub>), 21.2 (m, Ar-*p*-CH<sub>3</sub> and NCH<sub>2</sub>CH<sub>2</sub>CH<sub>2</sub>), 19.2 (Ar-*o*-CH<sub>3</sub>). LRMS calculated for C<sub>24</sub>H<sub>33</sub>N<sub>2</sub>: 349.50, found 349.37.

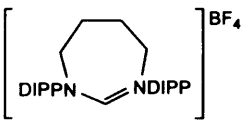
**1,3-Bis-(2,4,6-trimethylphenyl)-4,5,6,7-tetrahydro-3H-[1,3]diazepin-1-ium tetrafluoroborate.**

 The reaction was performed on a 5.4 mmol scale of halide salt (2.51 g) in 25 ml of acetone and 0.935 g of NaBF<sub>4</sub> (8.5 mmol) in water. Yield 2.05 g (4.9 mmol, 89%) of white, crystalline material. <sup>1</sup>H NMR (CDCl<sub>3</sub>, 400 MHz, rt): δ 7.21 (1H, s, NCHN), 6.95 (4H, s, Ar-CH), 4.32 (4H, t, <sup>3</sup>J<sub>HH</sub> = 5.6, NCH<sub>2</sub>), 2.52 (4H, p, <sup>3</sup>J<sub>HH</sub> = 5.6, NCH<sub>2</sub>CH<sub>2</sub>), 2.37 (12H, s, *o*-CH<sub>3</sub>), 2.27 (6H, s, *p*-CH<sub>3</sub>); <sup>13</sup>C NMR (CDCl<sub>3</sub>, 100 MHz, rt): δ 158.2 (s, NCHN), 140.3 (s, Ar-C), 139.2 (s, Ar-C), 133.5 (s, Ar-C), 130.2 (s, Ar-CH), 54.6 (s, NCH<sub>2</sub>) 25.1 (s, NCH<sub>2</sub>CH<sub>2</sub>), 20.8 (s, *p*-CH<sub>3</sub>), 17.9 (s, *o*-CH<sub>3</sub>); MS (ES): *m/z* 335.2498 ([M - BF<sub>4</sub>]<sup>+</sup>; C<sub>23</sub>H<sub>31</sub>N<sub>2</sub> requires 335.2487).

**1,3-Bis-(2,6-dimethylphenyl)-4,5,6,7-tetrahydro-3H-[1,3]diazepin-1-ium tetrafluoroborate.**

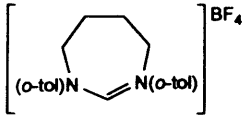
 The reaction was performed on a 11.6 mmol scale of halide salt (5.02 g) in 25 mL of acetone and 1.73 g of NaBF<sub>4</sub> (15.8 mmol) in 25 ml of H<sub>2</sub>O. Yield 3.96 g (10.1 mmol, 87%) of white, crystalline material. <sup>1</sup>H NMR (CDCl<sub>3</sub>, 400 MHz, rt): δ 7.28 (1H, s, NCHN), 7.23 (2H, dd, <sup>3</sup>J<sub>HH</sub> = 6.8, <sup>3</sup>J<sub>HH</sub> = 8.3, *p*-CH), 7.14 (4H, d, <sup>3</sup>J<sub>HH</sub> = 7.6, *m*-CH), 4.37 (4H, t, <sup>3</sup>J<sub>HH</sub> = 5.4, NCH<sub>2</sub>), 2.54 (4H, p, <sup>3</sup>J<sub>HH</sub> = 5.4, NCH<sub>2</sub>CH<sub>2</sub>), 2.42 (12H, s, CH<sub>3</sub>); <sup>13</sup>C NMR (CDCl<sub>3</sub>, 100 MHz, rt): δ 158.0 (s, NCHN), 141.4 (s, Ar-C), 133.9 (s, Ar-C), 130.1 (s, Ar-CH), 129.7 (s, Ar-CH), 54.6 (s, NCH<sub>2</sub>), 25.1 (s, NCH<sub>2</sub>CH<sub>2</sub>), 18.0 (s, CH<sub>3</sub>); MS (ES): *m/z* 307.2168 ([M - BF<sub>4</sub>]<sup>+</sup>; C<sub>21</sub>H<sub>27</sub>N<sub>2</sub> requires 307.2174).

**1,3-Bis-(2,6-diisopropylphenyl)-4,5,6,7-tetrahydro-3H-[1,3]diazepin-1-ium tetrafluoroborate.**

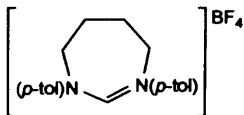
 The reaction was performed on a 4.6 mmol scale of halide salt (2.51 g) in 25 mL of acetone and 0.89 g of NaBF<sub>4</sub> (8.1 mmol) in 25 ml of water. Yield 2.22 g (4.4 mmol, 95%) of white, crystalline material. <sup>1</sup>H NMR (CDCl<sub>3</sub>, 400 MHz, rt): δ 7.41 (2H, t, <sup>3</sup>J<sub>HH</sub> = 7.8, *p*-CH), 7.29 (1H, s, NCHN), 7.24 (4H, d, <sup>3</sup>J<sub>HH</sub> = 7.8, *m*-CH), 4.42 (4H, bs, NCH<sub>2</sub>), 3.15 (4H, sept., <sup>3</sup>J<sub>HH</sub> = 6.7, CH(CH<sub>3</sub>)<sub>2</sub>),

2.56 (4H, bs, NCH<sub>2</sub>CH<sub>2</sub>), 1.38 (12H, d, <sup>3</sup>J<sub>HH</sub> = 6.7, CH(CH<sub>3</sub>)<sub>2</sub>), 1.24 (12H, d, <sup>3</sup>J<sub>HH</sub> = 6.7, CH(CH<sub>3</sub>)<sub>2</sub>); <sup>13</sup>C NMR (CDCl<sub>3</sub>, 100 MHz, rt): δ 157.3 (s, NCHN), 144.7 (s, Ar-C), 138.7 (s, Ar-C), 131.0 (s, Ar-CH), 125.3 (s, Ar-CH), 55.9 (s, NCH<sub>2</sub>), 28.9 (s, CH(CH<sub>3</sub>)<sub>2</sub>), 24.9 (s, CH(CH<sub>3</sub>)<sub>2</sub>), 24.7 (s, NCH<sub>2</sub>CH<sub>2</sub>), 24.5 (s, CH(CH<sub>3</sub>)<sub>2</sub>); MS (ES): *m/z* 419.3426 ([M – BF<sub>4</sub>]<sup>+</sup>; C<sub>29</sub>H<sub>43</sub>N<sub>2</sub> requires 419.3445).

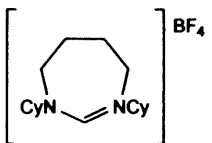
**1,3-Bis-(2-methylphenyl)-4,5,6,7-tetrahydro-3H-[1,3]diazepin-1-ium tetrafluoroborate.**

 The reaction was performed on a 9.8 mmol scale of halide salt (4.00 g) in 140 ml acetone and 10.0 mmol NaBF<sub>4</sub> (1.40 g) in water. Yield 2.95 g (8.1 mmol, 82%) of white, crystalline material. <sup>1</sup>H NMR (CDCl<sub>3</sub>, 400 MHz, rt): δ 7.71 (bs, 2H, *o*-CH), 7.36 (s, 1H, NCHN), 7.28-7.22 (m, 6H, *m,p*-CH), 4.34 (bs, 4H, N-CH<sub>2</sub>), 2.40 (bs, 4H, N-CH<sub>2</sub>-CH<sub>2</sub>), 2.36 (s, 6H, CH<sub>3</sub>); <sup>13</sup>C NMR (CDCl<sub>3</sub>, 100 MHz, rt): δ 156.5 (s, NCHN), 141.8 (s, ipsoC<sub>*o*-tol</sub>), 131.7 (s, C<sub>*o*-tol</sub>CH<sub>3</sub>), 130.7 (s, CH<sub>*o*-tol</sub>), 129.1 (s, CH<sub>*o*-tol</sub>), 127.4 (s, CH<sub>*o*-tol</sub>), 126.5 (s, C<sub>*o*-tol</sub>CH<sub>3</sub>), 54.3 (s, N-CH<sub>2</sub>), 24.4 (s, NCH<sub>2</sub>CH<sub>2</sub>), 16.8 (s, CH<sub>3</sub>); MS (ES): *m/z* 279.1853 ([M – BF<sub>4</sub>]<sup>+</sup>; C<sub>19</sub>H<sub>23</sub>N<sub>2</sub> requires 279.1861).

**1,3-Bis-(4-methylphenyl)-4,5,6,7-tetrahydro-3H-[1,3]diazepin-1-ium tetrafluoroborate.**

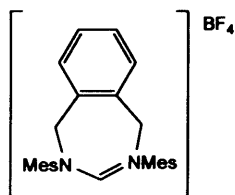
 The reaction was performed on a 4.9 mmol scale of halide salt (2.00 g) in 80 ml acetone and 5.0 mmol NaBF<sub>4</sub> (0.55 g) in water. Yield 1.72 g (4.68 mmol, 95%) of white, crystalline material. <sup>1</sup>H NMR (CDCl<sub>3</sub>, 400 MHz, rt): δ 7.50 (s, 1H, NCHN), 7.29 (d, <sup>3</sup>J<sub>HH</sub> = 8.8, 4H, *o*-CH), 7.17 (d, <sup>3</sup>J<sub>HH</sub> = 8.8, 4H, *m*-CH), 4.31 (t, <sup>3</sup>J<sub>HH</sub> = 5.6, 4H, N-CH<sub>2</sub>), 2.27 (bs, 10H, N-CH<sub>2</sub>-CH<sub>2</sub>+CH<sub>3</sub>); <sup>13</sup>C NMR (CDCl<sub>3</sub>, 100 MHz, rt): δ 155.1 (s, NCHN), 140.3 (s, ipsoC<sub>*p*-tol</sub>), 138.6 (s, C<sub>*p*-tol</sub>CH<sub>3</sub>), 129.7 (s, CH<sub>*p*-tol</sub>), 123.3 (s, CH<sub>*p*-tol</sub>), 53.5 (s, N-CH<sub>2</sub>), 23.8 (s, NCH<sub>2</sub>CH<sub>2</sub>), 20.0 (s, CH<sub>3</sub>); MS (ES): *m/z* 279.1852 ([M – BF<sub>4</sub>]<sup>+</sup>; C<sub>19</sub>H<sub>23</sub>N<sub>2</sub> requires 279.1861).

**1,3-dicyclohexyl-1,3-diazepan-2-ylidenium tetrafluoroborate.**

 The reaction was performed on a 10.0 mmol scale of halide salt (3.52 g) in 100 ml acetone and 10.0 mmol NaBF<sub>4</sub> (2.84 g) in water. Yield 2.70 g (7.7 mmol, 77%) of white, crystalline material. <sup>1</sup>H NMR (250 MHz, CDCl<sub>3</sub>): δ 8.1 (1H, s, NCHN), 3.64 (6H, m, NCH<sub>2</sub>), 3.41 (2H, m, Cy-CH), 2.02 (4H, m, CH<sub>2</sub>), 1.86 (4H, m, CH<sub>2</sub>), 1.77 (4H, m, CH<sub>2</sub>), 1.58 (2H, m, CH<sub>2</sub>), 1.39 (8H, m, CH<sub>2</sub>), 1.04

(2H, m, CH<sub>2</sub>); <sup>13</sup>C NMR (400 MHz, CDCl<sub>3</sub>): δ 155.2 (s, NCN), 60.1 (s, Cy-CH), 42.7 (s, NCH<sub>2</sub>), 31.2 (s, CH<sub>2</sub>), 27.4 (s, CH<sub>2</sub>), 24.3 (s, CH<sub>2</sub>), 22.2 (s, CH<sub>2</sub>); MS (ES): *m/z* 263.2482 ([M-PF<sub>6</sub>]<sup>+</sup>; C<sub>17</sub>H<sub>31</sub>N<sub>2</sub> requires 263.2487).

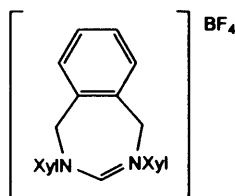
**2,4-Bis-(2,4,6-trimethylphenyl)-4,5-dihydro-1H-benzo[e][1,3]diazepin-2-ium tetrafluoroborate.**



The reaction was performed on a 10.8 mmol scale of halide salt (5.01 g) in 50 mL acetone and 1.33 g of NaBF<sub>4</sub> (12.1 mmol) in 25 mL water. Batchwise crystallization by dissolving the crude material in DCM, adding ether until saturation, and cooling to -30°C afforded 4.02 g (8.5 mmol, 79%) of a beige, crystalline material.

<sup>1</sup>H NMR (CDCl<sub>3</sub>, 400 MHz, rt): δ 7.49-7.43 (2H, m, Xy-CH), 7.33-7.27 (2H, m, Xy-CH), 7.11 (1H, s, NCHN), 6.94 (4H, s, *m*-CH), 5.38 (4H, bs; Δ*v*<sub>1/2</sub> ~ 150 Hz, NCH<sub>2</sub>), 2.27 (18H, s, *o*-CH<sub>3</sub> and *p*-CH<sub>3</sub>); <sup>13</sup>C NMR (CDCl<sub>3</sub>, 100 MHz, rt): δ 156.1 (s, NCHN), 140.4 (s, Ar-C), 140.1 (s, Ar-C), 134.2 (s, Ar-C), 133.9 (s, Ar-C), 130.3 (s, Ar-CH), 130.1 (s, Ar-CH), 129.2 (s, Ar-CH), 56.3 (s, NCH<sub>2</sub>), 20.9 (s, *p*-CH<sub>3</sub>), 18.1 (s, *o*-CH<sub>3</sub>). <sup>1</sup>H NMR (CD<sub>3</sub>CN, 400 MHz, rt): δ 7.56 (1H, s, NCHN), 7.56-7.51 (2H, m, Xy-CH), 7.50-7.45 (2H, m, Xy-CH), 7.05 (4H, s, Ar-CH), 5.28 (4H, bs; Δ*v*<sub>1/2</sub> ~ 15 Hz, NCH<sub>2</sub>), 2.30 (6H, s, *p*-CH<sub>3</sub>), 2.23 (12H, s, *o*-CH<sub>3</sub>); <sup>13</sup>C NMR (CDCl<sub>3</sub>, 100 MHz, rt): δ 158.4 (s, NCHN), 141.0 (s, Ar-C), 135.4 (s, Ar-C), 135.2 (s, Ar-C), 131.2 (s, Ar-CH), 130.6 (s, Ar-CH), 130.2 (s, Ar-CH), 56.3 (s, NCH<sub>2</sub>), 20.9 (s, *p*-CH<sub>3</sub>), 18.3 (s, *o*-CH<sub>3</sub>); MS (ES): *m/z* 383.2469 ([M - BF<sub>4</sub>]<sup>+</sup>; C<sub>27</sub>H<sub>31</sub>N<sub>2</sub> requires 383.2487).

**2,4-Bis-(2,6-dimethylphenyl)-4,5-dihydro-1H-benzo[e][1,3]diazepin-2-ium tetrafluoroborate.**

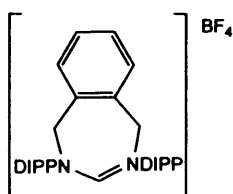


The reaction was performed on a 2.3 mmol scale of halide salt (0.99 g) in 30 ml acetonitrile and 0.34 g NaBF<sub>4</sub> (3.1 mmol) in 10 ml water. Yield 807 mg (1.8 mmol, 79%) of white, crystalline material.

<sup>1</sup>H NMR (CDCl<sub>3</sub>, 400 MHz, rt): δ 7.48 (2H, dd, <sup>3</sup>*J*<sub>HH</sub> = 3.3, <sup>3</sup>*J*<sub>HH</sub> = 5.5, Xy-CH), 7.33 (2H, dd, <sup>3</sup>*J*<sub>HH</sub> = 3.3, <sup>3</sup>*J*<sub>HH</sub> = 5.5, Xy-CH), 7.25 (2H, dd, <sup>3</sup>*J*<sub>HH</sub> = 7.2, <sup>3</sup>*J*<sub>HH</sub> = 7.9, *p*-Ar-CH), 7.17 (1H, s, NCHN), 7.15 (4H, d, <sup>3</sup>*J*<sub>HH</sub> = 7.5 Hz, *m*-Ar-CH), 5.38 (4H, bs, Δ*v*<sub>1/2</sub> ~ 400 Hz, NCH<sub>2</sub>), 2.33 (12H, s, CH<sub>3</sub>); <sup>13</sup>C NMR (CDCl<sub>3</sub>, 100 MHz, rt): δ 156.0 (s, NCHN), 142.4 (s, Ar-C), 134.4 (s, Ar-C), 134.2 (s, Ar-C), 130.4 (s, Ar-CH), 130.3 (s, Ar-CH),

129.6 (s, Ar-CH), 129.3 (s, Ar-CH), 56.3 (s, N-CH<sub>2</sub>), 18.3 (s, CH<sub>3</sub>); <sup>1</sup>H NMR (CD<sub>3</sub>CN, 400 MHz, rt): δ 7.61 (1H, s, NCHN), 7.58-7.52 (2H, m, Xy-CH), 7.51-7.46 (2H, m, Xy-CH), 7.25 (2H, dd, <sup>3</sup>J<sub>HH</sub> = 6.7, <sup>3</sup>J<sub>HH</sub> = 8.3, *p*-Ar-CH), 7.23 (4H, d, <sup>3</sup>J<sub>HH</sub> = 7.5, *m*-Ar-CH), 5.32 (4H, bs, Δν<sub>1/2</sub> ~ 30 Hz, NCH<sub>2</sub>), 2.28 (12H, s, CH<sub>3</sub>). <sup>13</sup>C NMR (CD<sub>3</sub>CN, 100 MHz, rt): δ 158.3 (s, NCHN), 143.2 (s, Ar-C), 135.5 (s, Ar-C), 135.3 (s, Ar-C), 131.3 (s, Ar-CH), 130.9 (2C, s, Ar-CH), 130.2 (2C, s, Ar-CH), 130.1 (2C, s, Ar-CH), 56.2 (2C, s, N-CH<sub>2</sub>), 18.4 (s, CH<sub>3</sub>); MS (ES): *m/z* 355.2162 ([M - BF<sub>4</sub>]<sup>+</sup>; C<sub>25</sub>H<sub>27</sub>N<sub>2</sub> requires 355.2174).

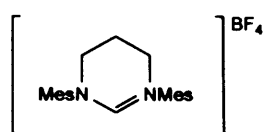
**2,4-Bis-(2,6-diisopropylphenyl)-4,5-dihydro-1H-benzo[e][1,3]diazepin-2-ium tetrafluoroborate.**



The reaction was performed on a 3.6 mmol scale of halide salt (2.00 g) in 50 mL acetonitrile and 0.56 g NaBF<sub>4</sub> (5.1 mmol) in 10 mL water. Yield 1.66 g (3.0 mmol, 82%) of white, crystalline material.

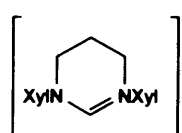
<sup>1</sup>H NMR (CDCl<sub>3</sub>, 400 MHz, rt): δ 7.51-7.46 (2H, m, Xy-CH), 7.42 (2H, t, <sup>3</sup>J<sub>HH</sub> = 7.8, *p*-Ar-CH), 7.33-7.27 (2H, m, Xy-CH), 7.25 (4H, d, <sup>3</sup>J<sub>HH</sub> = 7.8, *m*-Ar-CH), 7.23 (1H, s, NCHN), 3.09 (4H, bs, Δν<sub>1/2</sub> = 120 Hz, CH(CH<sub>3</sub>)<sub>2</sub>), 1.34 (12H, bd, <sup>3</sup>J<sub>HH</sub> ~ 4.5, CH(CH<sub>3</sub>)<sub>2</sub>), 1.17 (12H, bd, <sup>3</sup>J<sub>HH</sub> ~ 4.5 Hz, CH(CH<sub>3</sub>)<sub>2</sub>) (NCH<sub>2</sub> not observed in CDCl<sub>3</sub> at RT); <sup>13</sup>C NMR (CDCl<sub>3</sub>, 100 MHz, rt): δ 155.2 (s, NCHN), 139.3 (s, Ar-C), 133.9 (s, Ar-C), 131.0 (s, Ar-CH), 130.2 (s, Ar-CH), 129.2 (s, Ar-CH), 125.4 (s, Ar-CH), 57.7 (s, NCH<sub>2</sub>), 28.7 (s, CH(CH<sub>3</sub>)<sub>2</sub>), 25.1 (s, CH(CH<sub>3</sub>)<sub>2</sub>), 24.6 (s, CH(CH<sub>3</sub>)<sub>2</sub>) (One Ar-C not observed in CDCl<sub>3</sub>); <sup>1</sup>H NMR (CD<sub>3</sub>CN, 100 MHz, rt): δ 7.88 (1H, s, NCHN), 7.59-7.54 (2H, m, Ar), 7.52-7.44 (4H, m, *p*-Ar-CH and Xy-CH), 7.36 (4H, d, <sup>3</sup>J<sub>HH</sub> = 7.7, *m*-CH), 5.36 (4H, bs, Δν<sub>1/2</sub> = 70 Hz, NCH<sub>2</sub>), 2.98 (4H, bs, Δν<sub>1/2</sub> = 30 Hz, CH(CH<sub>3</sub>)<sub>2</sub>), 1.31 (12H, d, <sup>3</sup>J<sub>HH</sub> = 6.7, CH(CH<sub>3</sub>)<sub>2</sub>), 1.16 (12H, d, <sup>3</sup>J<sub>HH</sub> = 6.7, CH(CH<sub>3</sub>)<sub>2</sub>); <sup>13</sup>C NMR (CD<sub>3</sub>CN, 100 MHz, rt): δ 157.7 (s, NCHN), 145.8 (s, Ar-C), 139.9 (s, Ar-C), 134.8 (s, Ar-C), 131.7 (s, Ar-CH), 131.2 (s, Ar-CH), 130.2 (s, Ar-CH), 126.0 (s, Ar-CH), 57.7 (s, NCH<sub>2</sub>), 29.6 (s, CH(CH<sub>3</sub>)<sub>2</sub>), 24.8 (s, CH(CH<sub>3</sub>)<sub>2</sub>), 24.6 (s, CH(CH<sub>3</sub>)<sub>2</sub>). MS (ES): *m/z* 467.3414 ([M - BF<sub>4</sub>]<sup>+</sup>; C<sub>33</sub>H<sub>43</sub>N<sub>2</sub> requires 467.3426).

**1,3-Bis-(2,4,6-trimethylphenyl)-3,4,5,6-tetrahydro-pyrimidin-1-ium tetrafluoroborate.**<sup>1c</sup>



The reaction was performed on a 5.0 mmol scale of halide salt, (2.00 g) in 30 mL of acetone and 0.59 g of NaBF<sub>4</sub> (5.4 mmol) in 10 mL of water. Yield 1.75 g (4.3 mmol, 86%) of white, crystalline material.

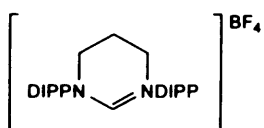
**1,3-Bis-(2,6-dimethylphenyl)-3,4,5,6-tetrahydro-pyrimidin-1-ium tetrafluoroborate.**



The reaction was performed on a 2.9 mmol scale of halide salt (1.07 g) in 20 ml of acetonitrile and 565 mg of NaBF<sub>4</sub> (5.2 mmol) in 10 ml of water. Yield 0.86 g (2.27 mmol, 79%) of white, crystalline material. <sup>1</sup>H

NMR (CDCl<sub>3</sub>, 400 MHz, rt): δ 7.83 (1H, s, NCHN), 7.18 (2H, dd, <sup>3</sup>J<sub>HH</sub> = 7.0, <sup>3</sup>J<sub>HH</sub> = 8.2, *p*-Ar-CH), 7.08 (4H, d, <sup>3</sup>J<sub>HH</sub> = 7.08, *m*-Ar-CH), 3.82 (4H, t, <sup>3</sup>J<sub>HH</sub> = 5.7, NCH<sub>2</sub>), 2.49 (2H, p, <sup>3</sup>J<sub>HH</sub> = 5.7, NCH<sub>2</sub>CH<sub>2</sub>), 2.26 (12H, s, CH<sub>3</sub>); <sup>13</sup>C NMR (CDCl<sub>3</sub>, 100 MHz, rt): δ 154.3 (s, NCHN), 138.4 (s, Ar-C), 134.4 (s, Ar-C), 130.1 (s, Ar-CH), 129.3 (s, Ar-CH), 45.9 (s, NCH<sub>2</sub>), 19.0 (s, NCH<sub>2</sub>CH<sub>2</sub>), 17.3 (s, CH<sub>3</sub>); MS (ES): *m/z* 293.2014 ([M – BF<sub>4</sub>]<sup>+</sup>; C<sub>20</sub>H<sub>25</sub>N<sub>2</sub> requires 293.2018).

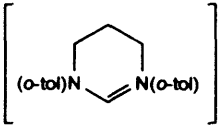
**1,3-Bis-(2,6-diisopropylphenyl)-3,4,5,6-tetrahydro-pyrimidin-1-ium tetrafluoroborate.**



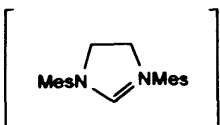
The reaction was performed on a 3.4 mmol scale of halide salt (1.67 g) in 50 mL of acetonitrile and 0.74 g of NaBF<sub>4</sub> (2.69 mmol) in 40 ml of water. Yield 1.32 g (2.7 mmol, 78%) of white, crystalline

material. <sup>1</sup>H NMR (CDCl<sub>3</sub>, 400 MHz, rt): δ 7.57 (1H, s, NCHN), 7.46 (2H, t, <sup>3</sup>J<sub>HH</sub> = 7.6, *p*-Ar-CH), 7.27 (4H, d, <sup>3</sup>J<sub>HH</sub> = 7.6, *m*-Ar-CH), 4.01 (4H, t, <sup>3</sup>J<sub>HH</sub> = 5.6, NCH<sub>2</sub>), 2.99 (4H, sept., <sup>3</sup>J<sub>HH</sub> = 6.7, CH(CH<sub>3</sub>)<sub>2</sub>), 2.67 (2H, p, <sup>3</sup>J<sub>HH</sub> = 5.6, NCH<sub>2</sub>), 1.38 (12H, d, <sup>3</sup>J<sub>HH</sub> = 6.7, CH(CH<sub>3</sub>)<sub>2</sub>), 1.25 (12H, d, <sup>3</sup>J<sub>HH</sub> = 6.7, CH(CH<sub>3</sub>)<sub>2</sub>); <sup>13</sup>C NMR (CDCl<sub>3</sub>, 100 MHz, rt): δ 153.1 (s, NCHN), 145.5 (s, Ar-C), 135.6 (s, Ar-C), 131.2 (s, *m*-Ar-CH), 125.1 (s, *p*-Ar-CH), 48.4 (s, NCH<sub>2</sub>), 30.8 (s, CH(CH<sub>3</sub>)<sub>2</sub>), 28.8 (s, CH(CH<sub>3</sub>)<sub>2</sub>), 24.6 (s, CH(CH<sub>3</sub>)<sub>2</sub>), 19.0 (s, NCH<sub>2</sub>CH<sub>2</sub>); MS (ES): *m/z* 405.3257 ([M – BF<sub>4</sub>]<sup>+</sup>; C<sub>28</sub>H<sub>41</sub>N<sub>2</sub> requires 405.3270).

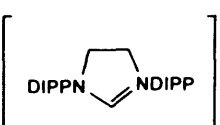
**1,3-Bis-(2-methylphenyl)-3,4,5,6-tetrahydro-pyrimidin-1-ium tetrafluoroborate.**


 $\text{BF}_4$  The reaction was performed on a 2.9 mmol scale of halide salt (1.00 g) in 100 ml acetone and 3.0 mmol  $\text{NaBF}_4$  (0.32 g) in water. Yield 0.99 g (2.8 mmol, 97%) of white, crystalline material.  $^1\text{H}$  NMR ( $\text{CDCl}_3$ , 400 MHz, rt):  $\delta$  7.61 (2H, d,  $^3J_{\text{HH}} = 8.0$ , *o*-CH), 7.55 (1H, s, NCHN), 7.30-7.16 (6H, m, *m,p*-CH), 3.71 (4H, bs,  $\text{NCH}_2$ ), 2.45 (2H, bs,  $\text{NCH}_2\text{CH}_2$ ), 2.30 (6H, s,  $\text{CH}_3$ );  $^{13}\text{C}$  NMR ( $\text{CDCl}_3$ , 100 MHz, rt):  $\delta$  153.7 (s, NCHN), 140.4 (s, ipsoC), 133.7 (s,  $\text{C}_{\text{o-tol}}\text{CH}_3$ ), 132.0 (s,  $\text{CH}_{\text{o-tol}}$ ), 130.7 (s,  $\text{CH}_{\text{o-tol}}$ ), 128.7 (s,  $\text{CH}_{\text{o-tol}}$ ), 127.9 (s,  $\text{CH}_{\text{o-tol}}$ ), 47.4 (s,  $\text{NCH}_2$ ), 19.8 (s,  $\text{NCH}_2\text{CH}_2$ ), 17.8 (s,  $\text{CH}_3$ ); MS (ES):  $m/z$  265.1699 ( $[\text{M} - \text{BF}_4]^+$ ;  $\text{C}_{18}\text{H}_{21}\text{N}_2$  requires 265.1705).

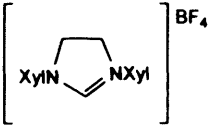
**1,3-Bis-(2,4,6-trimethylphenyl)-4,5-dihydro-3H-imidazol-1-ium tetrafluoroborate.<sup>23</sup>**


 $\text{BF}_4$  The reaction was performed on a 10.8 mmol scale of halide salt (4.18 g) in 50 ml of acetone and 1.18 g of  $\text{NaBF}_4$  (10.8 mmol) in 25 ml water. Yield 3.78 g (9.6 mmol, 89%) of white, crystalline material.

**1,3-Bis-(2,6-diisopropylphenyl)-4,5-dihydro-3H-imidazol-1-ium tetrafluoroborate.<sup>23</sup>**


 $\text{BF}_4$  The reaction was performed on a 5.2 mmol scale of halide salt (2.47 g) in 100 mL of acetone and 0.99 g of  $\text{NaBF}_4$  (9.0 mmol) in 50 ml of water. Yield 1.62 g (3.4 mmol, 65%) of white, crystalline material.

**1,3-Bis-(2,6-dimethylphenyl)-4,5-dihydro-3H-imidazol-1-ium tetrafluoroborate.**

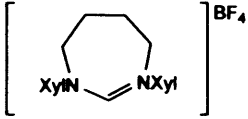

 $\text{BF}_4$  The reaction was performed on a 6.3 mmol scale of halide salt (2.28 g) in 100 ml of acetone and 1.01 g of  $\text{NaBF}_4$  (9.2 mmol) in 50 ml of water. Yield 1.84 g (5.0 mmol, 79%) of white, crystalline material.

**General protocol for the one-pot synthesis of tetrafluoroborate salts.** A suspension of 25.0 mmol amidine, 1-2 eq. of the dihalide, and 12.5 mmol  $\text{K}_2\text{CO}_3$  (0.5 eq.) in 150 mL of acetonitrile was refluxed until the ring closure was finished (by  $^1\text{H}$  NMR). At the end of

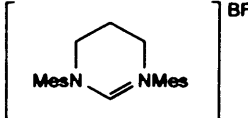
<sup>23</sup> Herrmann, W. A.; Schneider, S. K.; Öfele, K.; Sakamoto, M.; Herdtweck, E. *J. Organomet. Chem.* **2004**, *41*, 2441.

the reaction the reaction mixture was allowed to cool down to RT and a solution of 40 mmol of sodium tetrafluoroborate in 25 ml of water was added. The reaction mixture was stirred for 10 minutes, and the acetonitrile was subsequently evaporated on a rotary evaporator, resulting in the product to precipitate in the remaining water. The product was isolated by filtration, washed thoroughly with water, and dissolved in dichloromethane. The residual water was separated, and the dichloromethane solution dried over MgSO<sub>4</sub>. The solution was filtered, concentrated, and ether was slowly added to the solution to crystallize the product. The product was isolated by filtration.

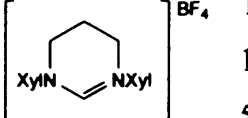
**1,3-Bis-(2,6-dimethylphenyl)-4,5,6,7-tetrahydro-3H-[1,3]diazepin-1-ium tetrafluoroborate .**

 The reaction was performed on a 9.3 mmol scale of amidine (2.34 g), 0.62 g of K<sub>2</sub>CO<sub>3</sub> (4.5 mmol), 2.5 mL (5.87 g, 19.0 mmol) of 1,4-diodobutane in 100 ml of acetonitrile. The reaction was refluxed for 17 hours. After cooling to rt, 2.44 g of NaBF<sub>4</sub> (22.2 mmol) in 100 ml of water was added. Yield 2.94 g (7.5 mmol, 79%) of white, microcrystalline material. Spectroscopically identical to the product obtained above.

**1,3-Bis-(2,4,6-trimethylphenyl)-3,4,5,6-tetrahydro-pyrimidin-1-ium tetrafluoroborate.**

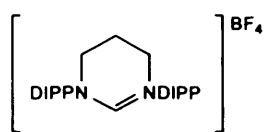
 The reaction was performed on a 35.7 mmol scale of amidine (10.01 g), 2.5 g of K<sub>2</sub>CO<sub>3</sub>, (18.1 mmol) 8.0 ml of 1,3-dibromobutane (39.6 mmol, 15.9 g) in 200 ml of acetonitrile. The reaction was refluxed for 48 hours. After cooling to rt, 7.2 g of NaBF<sub>4</sub> (65.6 mmol) in 25 ml of water was added. Yield 7.46 g (18.3 mmol, 51%) of white, crystalline material. Spectroscopically identical to the product obtained above.

**1,3-Bis-(2,6-dimethylphenyl)-3,4,5,6-tetrahydro-pyrimidin-1-ium tetrafluoroborate .**

 The reaction was performed on a 21.7 mmol scale of amidine (5.477 g), 1.53 g of K<sub>2</sub>CO<sub>3</sub> (11.1 mmol), and 6.0 ml of 1,3-dibromobutane (11.90 g, 59.1 mmol) in 150 ml of acetonitrile. The reaction was refluxed for 18 hours. After cooling to rt, 4.94 g of NaBF<sub>4</sub> (45.0 mmol) in 100 ml of water was added. Yield 5.61 g (14.7 mmol, 68%) of white, crystalline material. Spectroscopically identical to the product obtained above.



**1,3-Bis-(2,6-diisopropylphenyl)-3,4,5,6-tetrahydro-pyrimidin-1-ium tetrafluoroborate.**

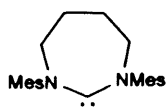


The reaction was performed on a 24.7 mmol scale of amidine (9.01 g), 14.5 mmol (2.0 g) of  $K_2CO_3$ , and 8.0 mL (15.9 g, 78.8 mmol) of 1,3-dibromobutane in 150 mL of acetonitrile. The reaction was refluxed for 48 hours. After cooling to rt, 4.20 g of  $NaBF_4$  (38.3 mmol) in 25 ml of water was added. Yield 6.29 g (12.8 mmol, 52%) of white, crystalline material. Spectroscopically identical to the product obtained above.

**General protocol for the isolation of free carbenes.** To a suspension of 1.0 mmol of the tetrafluoroborate salt in 10 ml of THF was added 1.2 mmol of  $KN(SiMe_3)_2$ . The resulting suspension was stirred for 30 min, after which the volatiles were evaporated. The residue was dissolved in 20 ml  $Et_2O$ , and filtered. The solid residue after filtration was washed with 5 ml of  $Et_2O$  and filtered. The combined organic fractions were concentrated until product started to precipitate and the solution cooled to  $-30^\circ C$ , upon which the product crystallized. The solid was isolated by filtration and dried *in vacuo*.

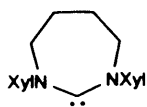
2.3.3. Isolation of free carbenes.

**7-Mes.**



**7-Mes**· $HBf_4$  (0.63 g, 1.5 mmol) in 20 ml of THF was reacted with  $KN(SiMe_3)_2$  (0.30 g, 1.5 mmol). Yield 0.28 g (1.7 mmol, 57%) of a white microcrystalline solid.  $^1H$  NMR ( $C_6D_6$ , 400 MHz, rt):  $\delta$  6.96 (4H, s, Ar-CH), 3.40 (4H, m,  $NCH_2$ ), 2.43 (12H, s, *o*- $CH_3$ ), 2.30 (6H, s, *p*- $CH_3$ ), 1.81 (4H, bs,  $NCH_2CH_2$ ).  $^{13}C$  NMR ( $C_6D_6$ , 100 MHz, rt):  $\delta$  257.3 (s, NCHN), 148.1 (s, Ar-C), 135.3 (s, Ar-C), 134.5 (s, Ar-C), 129.6 (s, Ar-CH), 51.6 (s,  $NCH_2$ ), 26.9 (s,  $NCH_2CH_2$ ), 21.0 (s, *p*-Me), 18.9 (4C, s, *o*-Me).

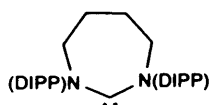
**7-Xyl.**



**7-Xyl**· $HBf_4$  (0.39 g, 1.0 mmol) in 15 mL of THF was reacted with  $KN(SiMe_3)_2$  (0.20 g, 1.0 mmol). Yield 0.20 g (0.67 mmol, 67%) of a white microcrystalline solid.  $^1H$  NMR ( $C_6D_6$ , 400 MHz, rt):  $\delta$  7.03 (6H, m, *m*-Ar-CH and *p*-Ar-CH), 3.26 (4H, t,  $^3J_{HH} = 5.7$ ,  $NCH_2$ ), 2.31 (12H, s,  $CH_3$ ), 1.68 (4H, p,  $^3J_{HH} = 5.7$ ,  $NCH_2CH_2$ ).  $^{13}C$  NMR ( $C_6D_6$ , 100 MHz, rt):  $\delta$  258.8 (s, NCHN), 150.5 (s, Ar-C), 135.0

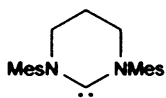
(s, Ar-C), 128.8 (s, Ar-CH), 126.2 (s, Ar-CH), 51.3 (s, NCH<sub>2</sub>), 27.0 (s, NCH<sub>2</sub>CH<sub>2</sub>), 18.9 (s, CH<sub>3</sub>).

### 7-DIPP.



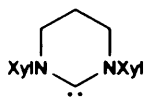
**7-DIPP**·HBF<sub>4</sub> (0.50 g, 1.0 mmol) in 20 mL of THF was reacted with KN(SiMe<sub>3</sub>)<sub>2</sub> (0.20 g, 1.0 mmol). Yield 0.25 g (0.6 mmol, 60%) of a white microcrystalline solid. <sup>1</sup>H NMR (C<sub>6</sub>D<sub>6</sub>, 400 MHz, rt): δ 7.22 (2H, dd, <sup>3</sup>J<sub>HH</sub> = 6.6, <sup>3</sup>J<sub>HH</sub> = 8.5, *p*-Ar-CH), 7.13 (4H, m, <sup>3</sup>J<sub>HH</sub> = 1.2, *m*-Ar-CH), 3.56 (4H, h, <sup>3</sup>J<sub>HH</sub> = 6.9, CH(CH<sub>3</sub>)<sub>2</sub>), 3.48 (4H, bt, <sup>3</sup>J<sub>HH</sub> = 5.4, NCH<sub>2</sub>), 1.80 (4H, p, <sup>3</sup>J<sub>HH</sub> = 5.4, NCH<sub>2</sub>CH<sub>2</sub>), 1.29 (12H, d, <sup>3</sup>J<sub>HH</sub> = 6.9, CH(CH<sub>3</sub>)<sub>2</sub>), 1.24 (12H, d, <sup>3</sup>J<sub>HH</sub> = 6.9, CH(CH<sub>3</sub>)<sub>2</sub>). <sup>13</sup>C NMR (C<sub>6</sub>D<sub>6</sub>, 100 MHz, rt): δ 260.2 (s, NCHN), 148.1 (s, Ar-C), 145.4 (s, Ar-C), 127.0 (s, *m*-Ar-CH), 124.1 (s, *p*-Ar-CH), 53.2 (s, NCH<sub>2</sub>), 28.7 (s, CH(CH<sub>3</sub>)<sub>2</sub>), 26.5 (s, NCH<sub>2</sub>CH<sub>2</sub>), 24.8 (s, CH(CH<sub>3</sub>)<sub>2</sub>), 24.6 (s, CH(CH<sub>3</sub>)<sub>2</sub>).

### 6-Mes.



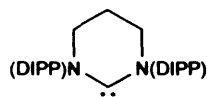
**6-Mes**·HBF<sub>4</sub> (1.16 g, 2.8 mmol) in 25 ml of THF was reacted with KN(SiMe<sub>3</sub>)<sub>2</sub> (0.57 g, 2.8 mmol). Yield 0.48 g (1.5 mmol, 73%) of a colorless, crystalline solid. <sup>1</sup>H NMR (C<sub>6</sub>D<sub>6</sub>, 400 MHz, rt): δ 6.84 (4H, s, Ar-CH), 2.73 (4H, t, <sup>3</sup>J<sub>HH</sub> = 6.0, NCH<sub>2</sub>), 2.30 (12H, s, *o*-CH<sub>3</sub>), 2.17 (6H, s, *p*-CH<sub>3</sub>), 1.66 (2H, p, <sup>3</sup>J<sub>HH</sub> = 6.0, NCH<sub>2</sub>CH<sub>2</sub>). <sup>13</sup>C NMR (C<sub>6</sub>D<sub>6</sub>, 100 MHz, rt): δ 244.9 (s, NCHN), 145.7 (s, Ar-C), 135.5 (s, Ar-C), 135.2 (s, Ar-C), 129.3 (s, Ar-CH), 42.1 (s, NCH<sub>2</sub>), 21.8 (s, NCH<sub>2</sub>CH<sub>2</sub>), 20.7 (s, *p*-CH<sub>3</sub>), 17.9 (s, *o*-CH<sub>3</sub>).

### 6-Xyl.



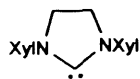
**6-Xyl**·HBF<sub>4</sub> (1.80 g, 4.74 mmol) in 50 mL of THF was reacted with KN(SiMe<sub>3</sub>)<sub>2</sub> (0.95 g, 4.7 mmol). Yield 0.37 g (1.3 mmol, 27%) of a white microcrystalline solid. <sup>1</sup>H NMR (C<sub>6</sub>D<sub>6</sub>, 400 MHz, rt): δ 6.04 (6H, m, *m*-Ar-CH and *p*-Ar-CH), 2.67 (4H, t, <sup>3</sup>J<sub>HH</sub> = 6.0 Hz, NCH<sub>2</sub>), 2.28 (12H, s, CH<sub>3</sub>), 1.60 (2H, p, <sup>3</sup>J<sub>HH</sub> = 6.0, NCH<sub>2</sub>CH<sub>2</sub>). <sup>13</sup>C NMR (C<sub>6</sub>D<sub>6</sub>, 100 MHz, rt): δ 244.5 (s, NCHN), 147.9 (s, Ar-C), 135.6 (s, Ar-C), 128.7 (s, *m*-Ar-CH), 126.6 (s, *p*-Ar-CH), 41.8 (s, NCH<sub>2</sub>), 22.1 (s, NCH<sub>2</sub>CH<sub>2</sub>), 18.3 (s, CH<sub>3</sub>).

### 6-DIPP



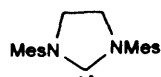
Reaction performed on a 2.1 mmol scale (1.03 g) of the salt in 20 ml of THF and 2.1 mmol of  $\text{KN}(\text{SiMe}_3)_2$  (0.41 g). Yield 0.38 g (0.9 mmol, 46%) of a colourless, crystalline solid.  $^1\text{H}$  NMR ( $\text{C}_6\text{D}_6$ , 400 MHz, rt):  $\delta$  7.22 (t,  $^3J_{\text{HH}} = 7.6$ , 2H, p-CH), 7.12 (d,  $^3J_{\text{HH}} = 7.6$ , 4H, m-CH), 3.37 (h,  $^3J_{\text{HH}} = 6.8$ , 4H,  $\text{CHMe}_2$ ), 2.82 (t,  $^3J_{\text{HH}} = 5.9$ , 4H,  $\text{NCH}_2$ ), 1.69 (p,  $^3J_{\text{HH}} = 5.7$ , 2H,  $\text{NCH}_2\text{CH}_2$ ), 1.28 & 1.27 (d,  $^3J_{\text{HH}} = 6.8$ , 12H each,  $\text{CHMe}_2$ ).  $^{13}\text{C}$  NMR ( $\text{C}_6\text{D}_6$ , 100 MHz, rt):  $\delta$  245.1 (s, NCN), 149.8 (s, Ar-C), 146.1 (s, Ar-C), 145.5 (s, Ar-CH), 124.0 (s, Ar-CH), 44.3 (s,  $\text{NCH}_2$ ), 28.6 (s,  $\text{CHMe}_2$ ), 25.1 (s,  $\text{CHMe}_2$ ), 24.5 (s,  $\text{CHMe}_2$ ), 22.0 (s,  $\text{NCH}_2\text{CH}_2$ ).

### 5-Xyl.



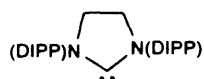
Reaction performed on a 0.94 mmol scale (0.34 g) of the salt in 15 mL of THF and 0.94 mmol of  $\text{KN}(\text{SiMe}_3)_2$  (0.19 g). Yield 0.12 g of a white microcrystalline solid (0.42 mmol, 45%).  $^1\text{H}$  NMR ( $\text{C}_6\text{D}_6$ , 400 MHz, rt):  $\delta$  7.02 (6H, bs, m-Ar-CH and p-Ar-CH), 3.17 (4H, s,  $\text{NCH}_2$ ), 2.26 (12H, s, o- $\text{CH}_3$ ).  $^{13}\text{C}$  NMR ( $\text{C}_6\text{D}_6$ , 100 MHz, rt):  $\delta$  242.0 (s, NCHN), 141.7 (s, Ar-C), 136.6 (s, Ar-C), 128.8 (s, Ar-CH), 127.4 (s, Ar-CH), 50.5 (s,  $\text{NCH}_2$ ), 18.3 (s,  $\text{CH}_3$ ).

### 5-Mes.<sup>24</sup>



Reaction performed on a 2.6 mmol scale (1.03 g) of the salt in 20 ml of THF and 2.6 mmol of  $\text{KN}(\text{SiMe}_3)_2$  (0.41 g). Yield 0.38 g (1.2 mmol, 46%) of a colorless, crystalline solid.

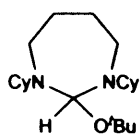
### 5-DIPP<sup>24</sup>



Reaction performed on a 2.1 mmol scale (1.026 g) of the salt in 40 ml of diethyl ether and 2.1 mmol of  $\text{KN}(\text{SiMe}_3)_2$  (0.41 g). Yield 0.38 g (46%) of a colorless, crystalline solid.

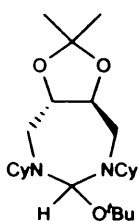
<sup>24</sup> Arduengo, Anthony J., III; Krafczyk, Roland; Schmutzler, Reinhard; Craig, Hugh A.; Goerlich, Jens R.; Marshall, William J.; Unverzagt, Markus *Tetrahedron* **1999**, *55*, 14523.

### 7-Cy·HO<sup>t</sup>Bu.



In a glovebox 7-Cy·HPF<sub>6</sub> (20 mg, 0.05 mmol), KO<sup>t</sup>Bu (6 mg, 0.06 mmol), and benzene-*d*<sub>6</sub> (0.6 ml) were placed in a Young NMR tube. The mixture was left to react for 2 h, and subsequently NMR spectra were recorded. <sup>1</sup>H NMR (400 MHz, CDCl<sub>3</sub>, rt): δ 5.08 (s, 1H, NCHN), 3.34 (2H, m, NCH), 2.75 (4H, m, NCH<sub>2</sub>), 2.15 (2H, m, CH<sub>2</sub>), 2.00 (2H, m, CH<sub>2</sub>), 1.62-1.88 (12H, m, CH<sub>2</sub>), 1.34 (9H, s, C(CH<sub>3</sub>)<sub>3</sub>), 1.32 (4H, m, CH<sub>2</sub>), 1.10 (4H, m, CH<sub>2</sub>).

### 4·HO<sup>t</sup>Bu.



In a glovebox **DIOC-Cy·HBr** (19 mg, 0.05 mmol), KO<sup>t</sup>Bu (6 mg, 0.06 mmol), and benzene-*d*<sub>6</sub> (0.6 ml) were placed in a Young NMR tube. The mixture was left to react for 2 h, and subsequently NMR spectra were recorded, confirming quantitative conversion of 4·HBr to the title compound. <sup>1</sup>H NMR (400 MHz, C<sub>6</sub>D<sub>6</sub>, rt): δ 4.95 (1H, s, NCHN), 4.76 (1H, ddd, <sup>3</sup>J<sub>HH</sub> ≈ <sup>3</sup>J<sub>HH</sub> = 9.0, <sup>3</sup>J<sub>HH</sub> = 6.5, OCH), 4.25 (1H, ddd, <sup>3</sup>J<sub>HH</sub> ≈ <sup>3</sup>J<sub>HH</sub> = 9.0, <sup>3</sup>J<sub>HH</sub> = 4.52, OCH), 3.57 (1H, dd, <sup>2</sup>J<sub>HH</sub> = 10.5, <sup>3</sup>J<sub>HH</sub> = 6.5, NCH<sub>2</sub>), 3.25 (2H, m, NCH<sub>2</sub>), 3.00 (1H, dd, <sup>3</sup>J<sub>HH</sub> ≈ <sup>2</sup>J<sub>HH</sub> = 9.0, NCH<sub>2</sub>), 2.61 (2H, m, NCH), 2.07 (2H, dd, <sup>3</sup>J<sub>HH</sub> ≈ <sup>3</sup>J<sub>HH</sub> = 14.6, CH<sub>2</sub>), 1.96 (1H, d, <sup>3</sup>J<sub>HH</sub> = 12.1, CH<sub>2</sub>), 1.89 (1H, d, <sup>3</sup>J<sub>HH</sub> = 12.1, CH<sub>2</sub>), 1.79 (4H, m, CH<sub>2</sub>), 1.67 (3H, s, OCCH<sub>3</sub>), 1.64 (3H, s, OCCH<sub>3</sub>), 1.61 (2H, d, <sup>3</sup>J<sub>HH</sub> = 14.6, CH<sub>2</sub>), 1.30 (17H, m, C(CH<sub>3</sub>)<sub>3</sub>, CH<sub>2</sub>), 1.05 (2H, m, <sup>3</sup>J<sub>HH</sub> = 3.5, CH<sub>2</sub>). <sup>13</sup>C NMR (100 MHz, C<sub>6</sub>D<sub>6</sub>, rt): δ 109.8 (s, CMe<sub>2</sub>), 100.4 (s, C(CH<sub>3</sub>)<sub>3</sub>), 81.0 (s, CHO), 80.1 (s, CHO), 73.6 (s, NCHN), 63.3 (s, NCH), 62.5 (s, NCH), 46.0 (s, NCH<sub>2</sub>), 43.8 (s, NCH<sub>2</sub>), 38.1 (s), 33.0 (s), 32.4 (s), 32.3 (s), 31.5 (s), 29.3 (s, C(CH<sub>3</sub>)<sub>3</sub>), 28.3 (s), 28.0 (s), 27.3 (s), 27.1 (s), 27.0 (s), 26.8 (s), 26.8 (s).

Chapter 3, Synthesis and structure of silver (I) carbenes

# Chapter

# 3

## Synthesis and structure of silver (I) carbenes

The use of AgCl as a source of basic silver, first reported by Liu and co-workers,<sup>1</sup> is nowadays the most widely used method for the synthesis of silver (I) carbenes.

<b>3.1. Introduction</b> .....	<b>88</b>
<b>3.2. Results and Discussion</b> .....	<b>91</b>
3.2.1. Synthesis of silver (I) carbenes.....	91
3.2.2. Solid-state structure of silver (I) carbenes.....	93
3.2.2.1. Changes upon coordination.....	93
3.2.2.2. Comparison between 5-, 6-, and 7-membered silver (I) carbenes.....	95
3.2.2.3. Effects of the substitution on the backbone in the solid-state structure of silver (I) carbenes.....	98
3.2.3. Behaviour of silver (I) carbenes in solution.....	100
3.2.4. Expanded carbenes as transfer agents.....	103
<b>3.3. Experimental</b> .....	<b>104</b>

Wang, Y.; Liu, J.; Jin, G.-X. *Organometallics* 2004, 23, 6792.  
Wang, H.; Ni, J.; Liu, J.; Jin, G.-X. *Organometallics* 1998, 17, 972.  
Yao, G.; Gorman, J.C.; Garman, R.J.; Tenkov, C.A.; Youngs, W.J. *J. Organomet. Chem.* 1993, 475, 1-9.  
Kakumoto-Nobuyuki, A.; Palmer, M.J.; Garman, R.C.; Tenkov, C.A.; Youngs, W.J. *Organometallics* 1994, 13, 1928-1930.  
Garman, R.C.; Tenkov, C.A.; Garman, J.C.; Palmer, M.J.; Tenkov, C.A.; Youngs, W.J. *Organometallics* 1994, 13, 444.

## Chapter 3. Synthesis and structure of silver (I) carbenes.

### 3.1. Introduction.

Since the isolation of the first silver (I) carbene complexes employing a silver base,<sup>1</sup> their use as carbene transfer agents have become a convenient and sometimes essential route for the synthesis of carbene complexes. Many carbene complexes can be obtained *via* the free carbene, which is generated by deprotonation of an azolium salt. However, this method might fail due to the presence of other acidic protons in the azolium salt, leading this to the impossibility of a clean deprotonation, or the instability of the free carbene.<sup>2</sup> Silver carbenes have proved to be a good system for the generation and storage of “free carbenes” as well as an efficient ligand transfer agent for most imidazolium salts.

The use of Ag<sub>2</sub>O as a source of basic silver, first reported by Lin and co-worker,<sup>3</sup> is, nowadays, the most widely used method for the synthesis of silver (I) carbene complexes. The complexation can be accomplished under aerobic condition in a wide range of solvents, including water.<sup>4</sup> The successful use of ambient conditions and, what is even more surprising, water as solvent indicates that the deprotonation of the azolium salt and

---

<sup>1</sup> a) Jafarpour, L.; Nolan, S. P. *J. Organomet. Chem.* **2001**, *17*, 617. b) Arduengo, A. J., III; Dias, H. V. R.; Calabrese, J. C.; Davidson, F. *Organometallics* **1993**, *12*, 3405. c) Guerret, O.; Solé, S.; Gornitzka, H.; Teichert, M.; Trinquier, G.; Bertrand, G. *J. Am. Chem. Soc.* **1997**, *119*, 6668.

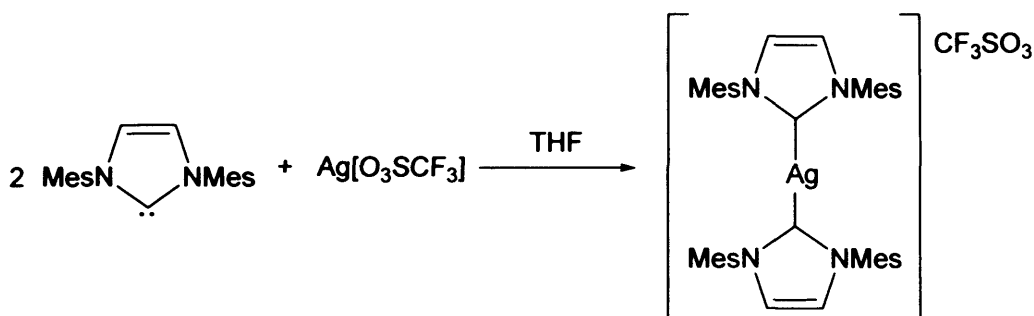
<sup>2</sup> a) Guerret, O.; Solé, S.; Gornitzka, H.; Trinquier, G.; Bertrand, G. *J. Organomet. Chem.* **2000**, *600*, 112. b) Caballero, A.; Díez-Barra, E.; Jalón, F. A.; Merino, S.; Tejada, J. *J. Organomet. Chem.* **2001**, *395*, 617. c) Caballero, A.; Díez-Barra, E.; Jalón, F. A.; Merino, S.; Rodríguez, A. M.; Tejada, J. *J. Organomet. Chem.* **2001**, *627*, 263. d) McGuinness, D. S.; Cavell, K. J. *Organometallics* **2000**, *19*, 741. e) César, V.; Bellemin-Lapponnaz, S.; Gade, L. H. *Organometallics* **2002**, *21*, 5204. f) Chen, W.; Wu, B.; Matsumoto, K. *J. Organomet. Chem.* **2002**, *654*, 233. g) Wang, X.; Liu, S.; Jin, G.-X. *Organometallics* **2004**, *23*, 6002.

<sup>3</sup> Wang, H.M.J.; Lin, I.J.B. *Organometallics* **1998**, *17*, 972.

<sup>4</sup> a) Garrison, J.C.; Simons, R.S.; Tessier, C.A.; Youngs, W.J. *J. Organomet. Chem.* **2003**, *673*, 1. b) Kascatan-Nebioglu, A.; Panzner, M.J.; Garrison, J.C.; Tessier, C.A.; Youngs, W.J. *Organometallics* **2004**, *23*, 1928. c) Quezada, C.A.; Garrison, J.C.; Panzner, M.J.; Tessier, C.A.; Youngs, W.J. *Organometallics* **2004**, *23*, 4846.

coordination to the metal centre must be a concerted process since formation of the free carbene in presence of water would result in its immediate decomposition.

Although the use of a silver base is the most commonly used method for the synthesis of  $\text{Ag}^{\text{I}}\text{NHCs}$ , the first silver carbene complex, isolated by Arduengo in 1993,<sup>5</sup> was prepared by reaction of silver (I) triflate with 2 equivalents of free carbene (scheme 3.1).



**Scheme 3.1.** Preparation of the first silver (I) carbene.

The nature of the silver-carbene bond was suggested to be mainly ionic by Frenking.<sup>6</sup> Ziegler and Rauk energy decomposition schemes agreed with this theory,<sup>7</sup> establishing that the less important orbital contribution had a 30% of  $\pi$ -back-bonding interaction, which is significantly higher than the usually observed for other carbene metal complexes.<sup>8</sup>

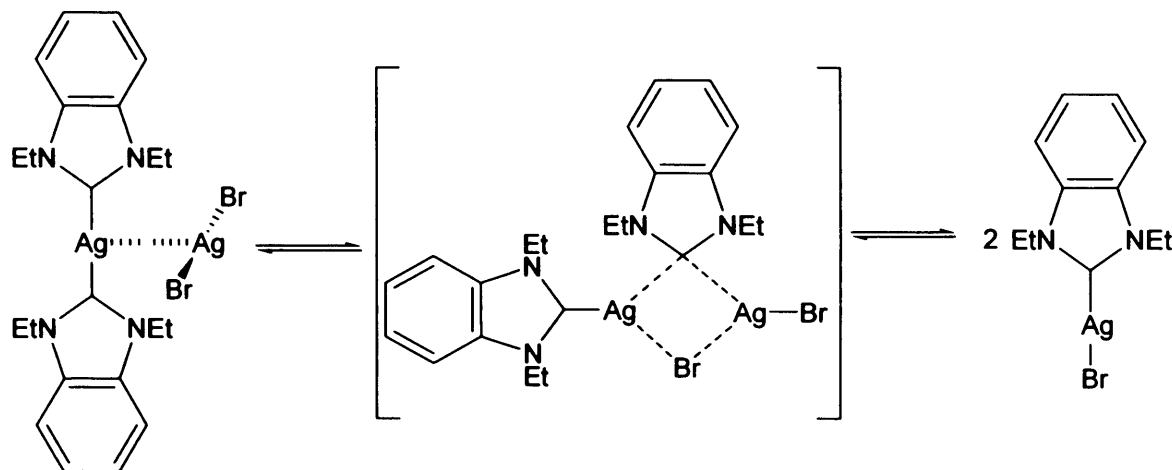
The carbene-metal bond for silver complexes, the weakest of the group 11, was suggested by Lin and co-workers to be labile in solution, leading this to an exchange of the carbene ligands between different silver atoms. This idea was based on the absence of the expected silver carbene carbon coupling in  $^{13}\text{C}$  NMR. The fluxional process proposed by Lin and co-worker is shown in scheme 3.2.

<sup>5</sup> Arduengo, A. J., III; Dias, H. V. R.; Calabrese, J. C.; Davidson, F. *Organometallics* **1993**, *12*, 3405.

<sup>6</sup> Nemcsok, D.; Wichmann, K.; Frenking, G. *Organometallics* **2004**, *23*, 3640.

<sup>7</sup> (a) Ziegler, T.; Rauk, A. *Theor. Chim. Acta* **1977**, *46*, 1; (b) Ziegler, T.; Rauk, A. *Inorg. Chem.* **1979**, *18*, 1558; (c) Ziegler, T.; Rauk, A. *Inorg. Chem.* **1979**, *18*, 1755.

<sup>8</sup> Hu, X.; Castro-Rodriguez, I.; Olsen, K.; Meyer, K. *Organometallics* **2004**, *23*, 755.



**Scheme 3.2.** Interconversion between mono-carbene and bis-carbene proposed by Lin and co-workers.

Despite the fact that most silver carbenes are only synthesised in order to function as ligand transfer agents, recently there has been a wealth of publications regarding the pharmaceutical applications of  $\text{Ag}^{\text{I}}\text{NHCs}$ .<sup>9, 4b</sup> Their activity as antimicrobials is one of the most important uses of these complexes in medicine. The slow release of silver at the wound seems to be an important factor for the efficiency of the healing process and the persistence of the antimicrobial effect.<sup>10</sup> The rate at which the silver ions are released is controlled by the stability of the complex, therefore the relatively strong  $\text{Ag}(\text{I})$ -carbene bond offers more stable silver complexes. The main problem associated with the use of carbene complexes for pharmaceutical applications is the toxicity of their decomposition products. The most likely decomposition pathway of silver (I) carbenes leads to formation of silver halide and the consequent azolium salt. Therefore, the use of non-toxic azolium salts is required. This can be achieved making use of biologically relevant molecules as

<sup>9</sup> a) Melaiye, A.; Simons, R.S.; Milsted, A.; Pingitore, F.; Wesdemiotis, C.; Tessier, C.A.; W.J.; Youngs *J. Med. Chem.* **2004**, *47*, 973. b) Herrmann, W.A.; Kocher, C.; Gossen, L.; *US Patent* 6, 025, 496 (2000). c) Andrews, J.M. *J. Antimicrob. Chemother* **2001**, *48*, 5. d) Kascatan-Nebioglu, A.; Melaiye, A.; Hindi, K.; Durmus, S.; Panzner, M.; Milsted, A.; Ely, D.; Tessier, C.A.; Hogue, L.A.; Mallett, R.J.; Hovis, C.E.; Coughenour, M.; Crosby, S.D.; Cannon, C.L.; Youngs, W.J. *J. Med. Chem.* **2006**, *49*, 6811. e) ; Garrison, Jered C.; Tessier, Claire A.; Youngs, W. J.; *J. Organomet. Chem.* **2005**, *690*, 6008.

<sup>10</sup> Kascatan-Nebioglu, A.; Panzner, Matthew J.; Tessier, Claire A.; Cannonb, Carolyn L.; Youngs, W. J. *Coord. Chem. Rev.* **2007**, *251*, 884.



carbene precursors. For example the caffeine derivative shown in Figure 3.1, published by Youngs *et al.*, shows very low toxicity in preliminary studies.<sup>4b</sup>

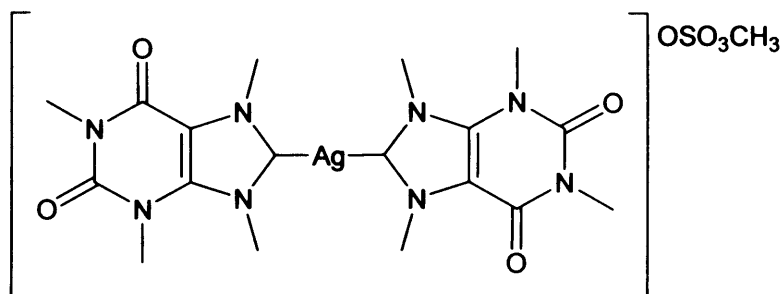


**Figure 3.1.** Silver carbene derived from the xanthine commonly known as caffeine.

The activity of silver carbenes in catalytic processes is virtually unexplored. Although there are several examples in the literature on silver catalysed processes not many of them use carbenes as ancillary ligands.<sup>11</sup>

In this chapter the synthesis and reactivity of Ag(I) complexes of 5-, 6- and 7-membered carbenes, some of them with backbone substitution will be discussed. Moreover, the solid state (crystal structures), behaviour in solution and in the gas phase (NMR and MS) were studied with the intention of shedding some light on the capabilities of expanded carbenes as ligands for transition metal complexes.

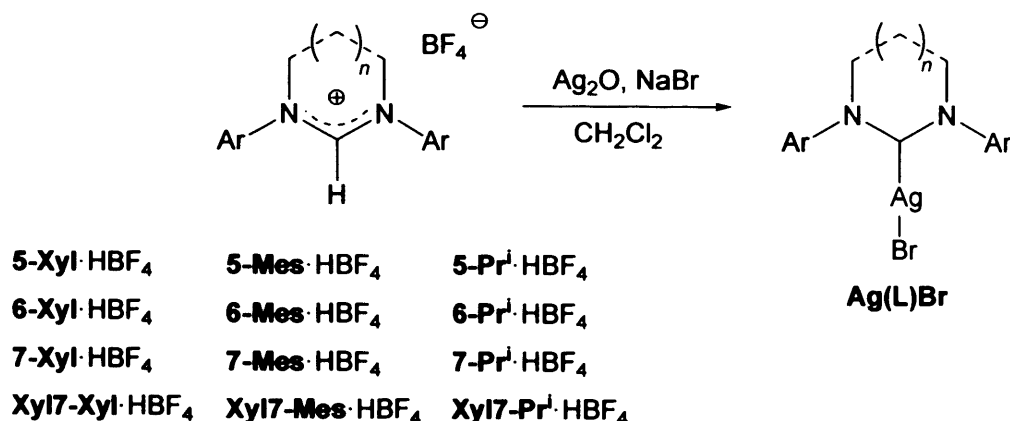
## 3.2. Results and Discussion.

### 3.2.1. Synthesis of silver (I) carbenes.

Reaction of the amidinium bromide salts with 1 equivalent of Ag<sub>2</sub>O generally gave the corresponding silver complexes in good yields, whilst results with the iodide salts were variable. Best yields however, were obtained from the reaction of amidinium-BF<sub>4</sub><sup>-</sup> salts with an excess of Ag<sub>2</sub>O in the presence of NaBr, forming the corresponding silver-bromide complexes shown in Scheme 3.4.

---

<sup>11</sup> Ramírez, J.; Corberán, R.; Sanaú, M.; Peris, E.; Fernandez, E. *Chem. Commun.* **2005**, 3056.

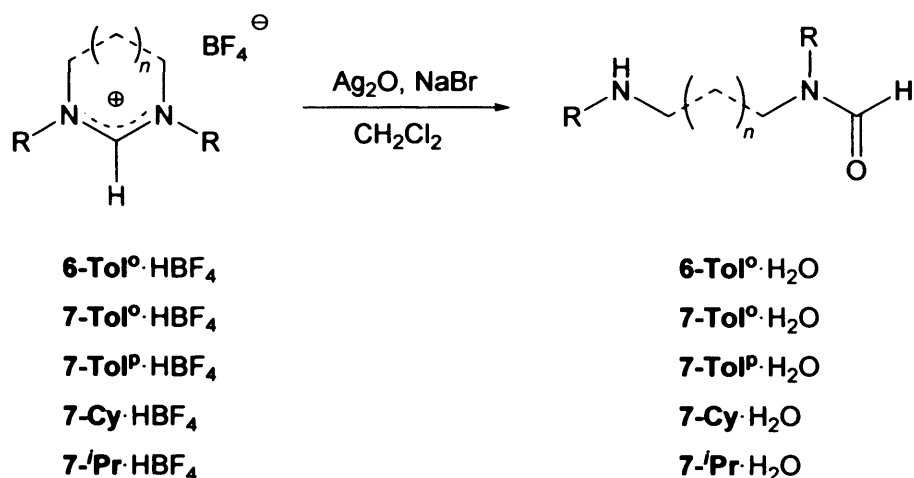


**Scheme 3.4.** Synthesis of 5, 6 and 7-membered saturated NHC silver complexes.

These reactions were performed in aerobic conditions, stirring at ambient temperature a dichloromethane suspension of 2 equivalents of silver (I) oxide and the corresponding amidinium salt in presence of a large excess of sodium bromide (5 to 10 equivalents) in the dark. The reaction times range from 1 to 7 days. The formation of the silver compounds was monitored by the disappearance of the peak that corresponds to the amidinium proton in <sup>1</sup>H NMR. Additionally, a <sup>1</sup>H NMR shift to high field (0.5-1 ppm) is observed upon coordination for the NCH<sub>2</sub> groups. In the case of the xylene derivatives the benzylic protons become visible in CDCl<sub>3</sub>, occurring as a broad singlet at approximately 5 ppm. A definitive proof of the formation of a silver complex is the emergence of the signal that belongs to the carbene carbon in <sup>13</sup>C NMR in the region of 200-220 ppm in the case of saturated carbenes. This resonance occurs as two doublets due to the coupling of the carbene carbon with the two NMR active isotopes of silver (<sup>107</sup>Ag and <sup>109</sup>Ag), both of them with spin ½.

After completion of the reaction, the mixture was filtered and the remaining solution concentrated under reduced pressure. Slow addition of ether to a dichloromethane solution of the crude mixture affords the silver carbene as a crystalline white solid.

Attempts to prepare silver (I) complexes of expanded carbenes with alkyl (cyclohexyl and isopropyl) or tolyl substituents on the nitrogens led always to hydrolysis of the free carbene (Scheme 3.5). It is not clear whether this result is a consequence of the instability of the silver carbene under ambient conditions or a change in the concerted mechanism of deprotonation and subsequent coordination.



**Scheme 3.5.** Failed synthesis of silver (I) carbene complexes.

### 3.2.2. Solid-state structure of silver (I) carbenes.

The solid state structures of representative AgX (where X represents a halide) carbene complexes of the six- and seven-membered carbenes were determined with the hope of attaining a better understanding of the coordination properties of expanded carbenes. All complexes form monomeric structures of the type LAgX, with no Ag-Ag interactions observed in the crystal lattice. The C(1)-Ag-X bond angles show small deviations from linearity, within the range of 174.26(18)° to 178.65(11)°, independent on the ring size.

#### 3.2.2.1. Changes upon coordination.

Previously, somewhat shorter C<sub>NHC</sub>-N bonds have been observed in the Ag carbenes when compared to the free ligand. This has been attributed to an increased  $\pi$ -donation of the nitrogen atoms to the empty carbene p-orbital upon complexation, caused by donation of electron density from the carbene to the metal.<sup>12</sup> The C<sub>NHC</sub>-N bond distance, 1.3464(12) Å, in **6-Mes** is somewhat longer than in the corresponding AgCl complex at 1.334(4) Å.<sup>13</sup> Interestingly, the same bond shortening is not observed when comparing the C<sub>NHC</sub>-N bond lengths of the free ligand, **7-Mes**, and its corresponding AgBr complex (Figure 3.2), at  $r_{av}$  = 1.347(5) and 1.346(8) Å, respectively.

<sup>12</sup> Garisson, J. C.; Youngs, W. J. *Chem. Rev.* **2005**, *105*, 3978.

<sup>13</sup> Herrmann, Wolfgang A.; Schneider, Sabine K.; Öfele, Karl; Sakamoto, Masato; Herdtweck, Eberhardt *J. Organomet. Chem.* **2004**, *689*, 2441.

**Table 3.1.** Selected bond lengths (Å) and angles (°) of the free carbenes and corresponding silver complexes.

	7-Mes	Ag(7-Mes)Br	6-Mes <sup>a</sup>	Ag(6-Mes)Cl <sup>b</sup>
Ag-C <sub>NCN</sub>	-	2.097(6)	-	2.095(3)
Ag-X	-	2.3792(11)	-	2.3213(10)
N(1)-C <sub>NCN</sub>	1.349(5)	1.346(8)	1.3464(12)	1.338(4)
N(2)-C <sub>NCN</sub>	1.346(5)	1.347(8)	-	1.329(4)
N(1)-C(2)	1.483(5)	1.497(7)	1.4809(14)	
C(5)-N(2)	1.502(6)	1.493(8)	-	
N(1)-C <sub>Ar</sub>	1.444(5)	1.444(7)	1.4381(15)	
N(2)-C <sub>Ar</sub>	1.438(5)	1.464(8)	-	
N(1)-C <sub>NCN</sub> -N(2)	116.6(4)	118.8(6)	114.65(13)	118.3(3)
C(1)-Ag-X	-	174.56(16)	-	
C <sub>NCN</sub> -N(1)-C(2)	126.9(4)	129.4(5)	126.28(10)	
C <sub>NCN</sub> -N(1)-C <sub>Ar</sub>	115.5(3)	117.0(5)	117.08(9)	119.4(2)
C <sub>Ar</sub> -N(1)-C(2)	115.5(3)	116.8(5)	116.52(9)	
C <sub>NCN</sub> -N(2)-C(5)	130.6(4)	124.2(5)	-	
C <sub>NCN</sub> -N(2)-C <sub>Ar</sub>	115.0(4)	117.3(5)	-	118.5(2)
C(5)-N(2)-C <sub>Ar</sub>	114.0(3)	116.8(5)	-	
N(1)-C(2)-C(3)	113.5(4)	112.0(5)	108.88(10)	
C(2)-C(3)-C(4)	111.4(4)	112.4(6)	108.37(14)	
C(3)-C(4)-C(5)	112.7(4)	110.6(5)	-	
C(4)-C(5)-N(2)	112.6(4)	112.8(5)	-	
C <sub>Ar</sub> -N...N-C <sub>Ar</sub> ( $\alpha$ )	13.6	30.3	0	5.1

<sup>a</sup> **6-Xyl** C<sub>2</sub> symmetric.<sup>14</sup>

<sup>b</sup> selected data included for comparison only, previously reported by Herrmann *et al.*<sup>13</sup>

<sup>14</sup> Compound crystallised in the group by Dirk Beetsma.

An increase in the N-C-N angle is observed when comparing the free carbene with the corresponding silver complex. The **7-Mes** angle changes from 116.6(4) to 118.8(6) in the complex, and for **6-Mes** the angle changes from 114.65(13)° to 118.3(3)°.

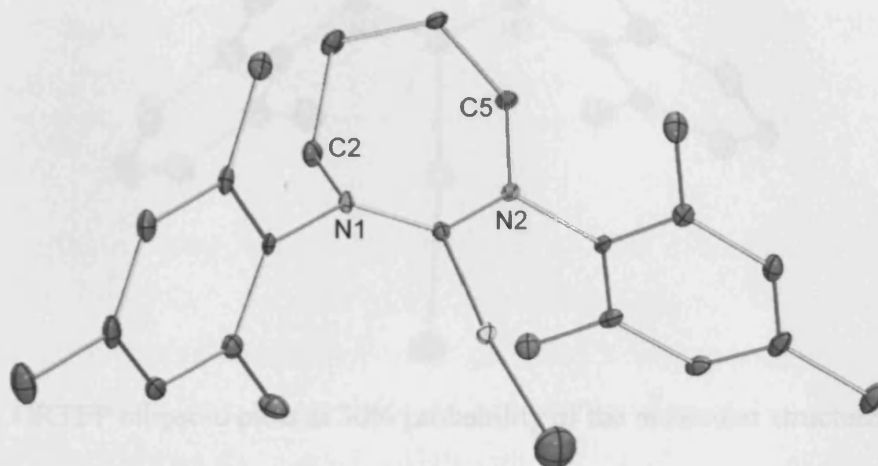


**Figure 3.2.** ORTEP ellipsoid plots at 30% probability of the molecular structure of Ag(**7-Mes**)Br.

Another point of interest is the torsional angle  $\alpha$  (Figure 3.3) between the planes, defined by the  $C_{Ar}-N \cdots N-C_{Ar}$  atoms, which is a measure of this spatial twist and the relative position of the aromatic substituents, which point directly into the metal's coordination sphere. The torsional angle  $\alpha$  in **7-Xyl** is 28.7° whereas in Ag(**7-Xyl**)I (Figure 3.2) is 23.1° (compared with  $\alpha = 0^\circ$  for **6-Mes** and  $\alpha = 5.1^\circ$  for Ag(**6-Mes**)Cl).

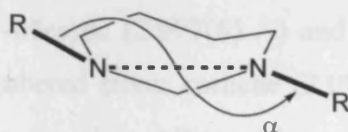


**Figure 3.3.** Depiction of the torsion angle  $\alpha$ .

### 3.2.2.2. Comparison between 5-, 6-, and 7-membered silver (I) carbenes.

A comparison between the seven-membered silver complexes Ag(**7-Xyl**)I (Figure 3.4), Ag(**7-Mes**)Br (Figure 3.2) and the six-membered Ag(**6-Mes**)Br (previously reported by Herrmann *et al.*<sup>13</sup>) shows the differences caused by the transition from six-membered to seven-membered ring geometry (Table 3.1 and 3.2).



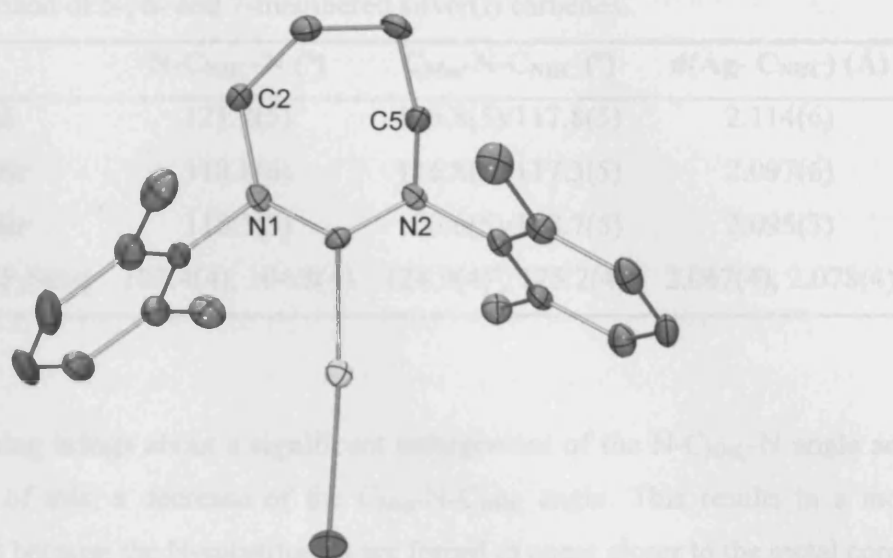


**Figure 3.4.** ORTEP ellipsoid plots at 30% probability of the molecular structures of Ag(7-Xyl)I.

The  $N-C_{NHC}-N$  and  $C_{Mes}-N-C_{NHC}$  angles remain virtually the same (table 3.2). As a consequence of the little steric relief that Ag(7-Mes)Br obtains from the enlargement of the NCN angle in comparison to Ag(6-Mes)Br, the torsion angle ( $\alpha$ ) is expanded from  $5.1^\circ$  to  $30.5^\circ$  in the seven-membered carbene in order to accommodate the steric tension arising from the expansion of the ring, as it was observed for the amidinium salts and free carbenes. Despite this twisting of the ring, the two nitrogen atoms of the 7-membered carbenes maintain a near planar geometry as evidenced by the close to  $360^\circ$  sum of the C-N-C angles (Figure 3.5).

The  $C_{NHC}-Ag$  distance in Ag(7-Mes)Br ( $2.097(6)$  Å) and the one reported by Herrmann and co-workers for the six-membered silver carbene ( $2.095(3)$  Å) are virtually identical, presumably due to the similar  $\sigma$ -donating ability and steric hindrance at the carbene core between the six- and the seven membered carbenes.

When these expanded carbenes are compared against the five-membered silver carbene ( $[Ag(5-Mes)_2][CF_3SO_3]$ ) synthesised by Arduengo in 1993<sup>1b</sup> noticeable differences emerge (Table 3.2).

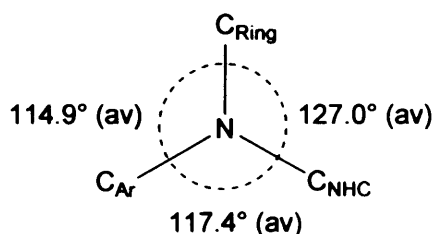
**Table 3.2.** Comparison of 5-, 6- and 7-membered silver(I) carbenes.

	N-C <sub>NHC</sub> -N (°)	C <sub>Mes</sub> -N-C <sub>NHC</sub> (°)	d(Ag- C <sub>NHC</sub> ) (Å)
Ag(7-Xyl)I	121.2(5)	116.8(5)/117.8(5)	2.114(6)
Ag(7-Mes)Br	118.8(6)	116.8(5)/117.3(5)	2.097(6)
Ag(6-Mes)Br	118.3(3)	120.6(5)/118.7(5)	2.095(3)
[Ag(5-Mes) <sub>2</sub> ][CF <sub>3</sub> SO <sub>3</sub> ]	103.4(4), 104.8(4)	124.9(4) <sup>a</sup> , 125.2(4) <sup>a</sup>	2.067(4), 2.078(4)

<sup>a</sup>Average values.

Expansion of the ring brings about a significant enlargement of the N-C<sub>NHC</sub>-N angle and, as a consequence of this, a decrease of the C<sub>Mes</sub>-N-C<sub>NHC</sub> angle. This results in a more encumbered ligand because the N-substituents are forced to come closer to the metal core. The shorter C<sub>NHC</sub>-Ag distance observed for the five-membered silver (I) carbene suggests a steric interaction between the mesityl substituents and the silver atom that pushes the carbene away from the metal centre.

Typically, the C<sub>NHC</sub>-N-C<sub>Ring</sub> angle in 7-membered silver (I) carbenes is the largest of the three, with an average value of 127.0°. Average values for the C<sub>NHC</sub>-N-C<sub>Ar</sub> and C<sub>Ar</sub>-N-C<sub>Ring</sub> angles are 117.4° and 114.9°, respectively (Scheme 3.5). The average 117.4° value for C<sub>NHC</sub>-N-C<sub>Ar</sub> in the silver complexes, is close to the one for the Ag(6-Mes)Cl complex (av. 119.0°) but significantly smaller than the typical value of 124° for 5-membered carbenes.<sup>15</sup>



**Scheme 3.5.** Newman representation of the C-N-C angles.

<sup>15</sup> a) Paas, M.; Wibbeling, B.; Frohlich, R.; Hahn, F.E.; *Eur. J. Inorg. Chem.* **2006**, 158; b) de Fremont, P.; Scott, N. M.; Stevens, E. D.; Ramnial, T.; Lightbody, O.C.; Macdonald, C.L.B.; Clyburne, J.A.C.; Abernethy, C.D.; Nolan, S.P. *Organometallics* **2005**, *24*, 6301.

### 3.2.2.3. Effects of the substitution on the backbone in the solid-state structure of silver (I) carbenes.

The aromatic substitution on the backbone does not provide the amidinium salt with larger N-C<sub>NHC</sub>-N angles (127.5° for **Xyl7-Mes**·HBr and 127.4° for **7-Cy**·HPF<sub>6</sub>). However, upon coordination the N-C<sub>NHC</sub>-N angle in Ag(**Xyl7-Mes**)Br (Figure 3.6) is wider than in the case of its unsubstituted analogue (Ag(**7-Mes**)Br), 121.6(3)° and 118.8(6)° respectively.

The expansion of the N-C<sub>NHC</sub>-N angle results in a slight enlargement of the C<sub>NHC</sub>-N-C<sub>Mes</sub> angle from average 117.1(5) in the unsubstituted to average 117.7(3) in **Xyl7-Mes**·HBr and a longer Ag-C<sub>NHC</sub> distance observed for Ag(**Xyl7-Mes**)Br (2.122(3) Å compared to 2.097(6) Å in Ag(**7-Mes**)Br).

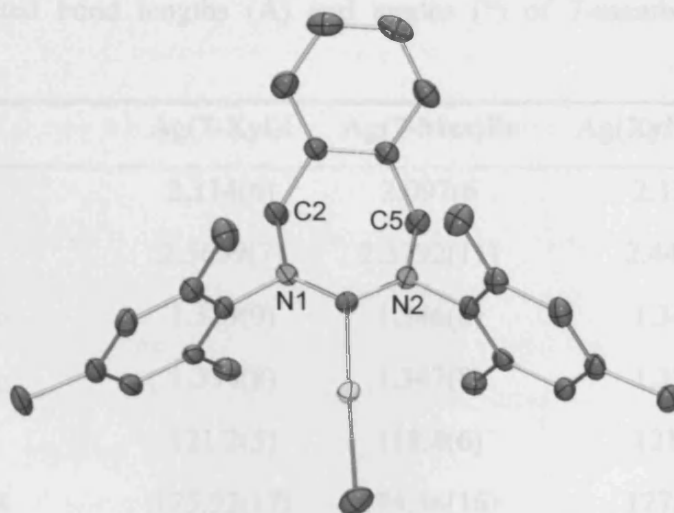


**Figure 3.6.** ORTEP ellipsoid plots at 30% probability of the molecular structures of Ag(**Xyl7-Xyl**)Br.

Similarly as was explained in *Chapter 2* **DIOC-Cy**·HBr, the enlargement of the N-C<sub>NHC</sub>-N angle can be explained as a consequence of the rigidity of the ring, arisen from the backbone substitution, which prevents the ring from releasing its annular tension by torsion ( $\beta = 5.4^\circ$  in Ag(**Xyl7-Mes**)Br and  $30.5^\circ$  in Ag(**7-Mes**)Br) (Figure 3.7). Another important structural adjustment derived from the backbone substitution is the  $sp^2$  deviation of the ring carbon atoms fused with the aromatic ring, values of  $118.3(3)^\circ$  and  $117.6(3)^\circ$  are observed for C3 and C4, as well as a small deviation from zero ( $2.5^\circ$ ) of the torsion angle C2-C3-C4-C5.



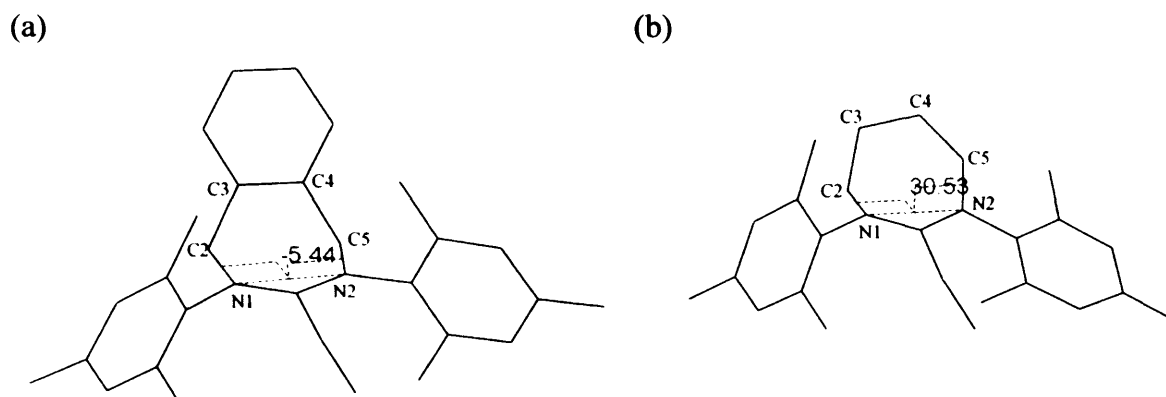


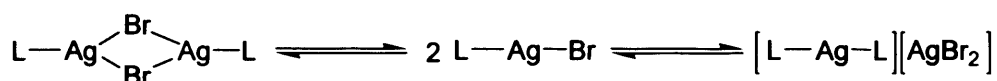
**Figure 3.7.** Mercury representation of the  $C_{ring}N1\cdots N2C_{ring}$  torsional angle ( $\beta$ ) in the silver (I) complexes  $Ag(Xyl7-Mes)Br$  (Figure 3.7.a) and  $Ag(7-Mes)Br$  (Figure 3.7.b). Hydrogen atoms are omitted for clarity.

**Table 3.3.** Selected bond lengths (Å) and angles ( $^\circ$ ) of 7-membered silver carbene complexes.

	Ag(7-Xyl)I	Ag(7-Mes)Br	Ag(Xyl7-Mes)Br
Ag-C <sub>NHC</sub>	2.114(6)	2.097(6)	2.122(3)
Ag-X	2.5659(7)	2.3792(11)	2.4475(7)
N(1)-C <sub>NHC</sub>	1.329(9)	1.346(8)	1.342(4)
N(2)-C <sub>NHC</sub>	1.334(8)	1.347(8)	1.328(4)
N-C(1)-N	121.2(5)	118.8(6)	121.6(3)
C(1)-Ag-X	175.92(17)	174.56(16)	177.42(9)
C <sub>NHC</sub> -N(1)-C(2)	128.8(5)	129.4(5)	128.6(3)
C <sub>NHC</sub> -N(1)-C <sub>Ar</sub>	116.8(5)	117.0(5)	117.9(3)
C <sub>Ar</sub> -N(1)-C(2)	114.0(6)	113.5(5)	113.5(3)
C <sub>NHC</sub> -N(2)-C(5)	123.7(5)	124.2(5)	127.5(3)
C <sub>NHC</sub> -N(2)-C <sub>Ar</sub>	117.8(5)	117.3(5)	117.5(3)
C(5)-N(2)-C <sub>Ar</sub>	117.5(5)	116.8(5)	115.0(3)
C <sub>Ar</sub> -N $\cdots$ N-C <sub>Ar</sub> ( $\alpha$ )	23.1	30.5	3.8

### 3.2.3. Behaviour of silver (I) carbenes in solution.

Silver (I) halide complexes of NHCs with 1:1 stoichiometry have been reported in the literature<sup>16</sup> to afford a variety of bonding motifs in the solid state, forming either neutral or ionic species. The ultimate arrangement adopted by the silver complex depends on a large number of factors, such as the particular halide, sterics and flexibility of the ligand, argentophilic interactions, silver-halide interactions, or solvent interactions. This causes difficulties in establishing the structure of the species present in solution. However, the steric hindrance of the ligand probably limits the possibility of Ag<sup>I</sup>-Ag<sup>I</sup> interactions and, consequently the formation of intricate patterns. Considering this assertion true, the possible structures are restricted to the ones shown in Scheme 3.6.



**Scheme 3.6.** behaviour of silver (I) carbenes in solution.

Assignment of the linear L-Ag-Br structure to the Ag<sup>I</sup>-NHC complexes reported here (Scheme 3.4) was made according to their solid state structures. However, after inspection of their <sup>1</sup>H and <sup>13</sup>C NMR data (Table 3.4) it became evident that the neutral Ag(NHC)Br complex was not always present in solution and that it existed in equilibrium with the ionic [Ag(NHC)<sub>2</sub>][AgBr<sub>2</sub>] species.

Two observations assisted us in the assignment of the silver complexes formed in solution; first it was noted that the  $J(^{109/107}\text{Ag}-^{13}\text{C})$  of the neutral complexes was ca. 55-60 Hz greater than the corresponding ionic complexes, and secondly that higher field <sup>1</sup>H NMR shifts were observed for the [Ag(NHC)<sub>2</sub>]<sup>+</sup> species. The latter observation was particularly useful in the case of NHCs with mesityl and xylyl aromatic substituents, where a significant high-field shift was observed for the *ortho*-methyl aromatic substituents from ~2.3 ppm in the neutral complex, to ~1.8 ppm in the ionic complex. Accordingly, 5- and 6-membered carbenes with mesityl substituents afforded the cationic [Ag(5/6-Mes)<sub>2</sub>][AgBr<sub>2</sub>] complexes as the major product, whereas the 7-membered carbenes, 7-Mes and Xyl7-Mes, formed the neutral Ag(L)Br complexes. The carbene ligands bearing xylyl substituents gave close to 1:1 mixtures of Ag(L)Br complexes and the corresponding

<sup>16</sup> Wang, Harrison M. J.; Lin, Ivan J. B. *Organometallics* 1998, 17, 972.

disproportionation products,  $[\text{Ag}(\text{L})_2][\text{AgBr}_2]$ . In the case of the complexes with xylyl substituents,  $\text{Ag}(7\text{-Xyl})\text{Br}$  and  $\text{Ag}(\text{Xyl}7\text{-Xyl})\text{Br}$ , the monomer-dimer isomers were formed in higher ratios, ca. 3/2, that persisted after recrystallisation.

The electrospray ionization mass spectrometry data agree with the observations in solution, where for all the  $\text{Ag}(\text{L})\text{Br}$  complexes the  $[\text{Ag}(\text{carbene})(\text{CH}_3\text{CN})]^+$  fragment was observed ( $\text{CH}_3\text{CN}$  is used as the carrier solvent). Whereas  $\text{Ag}(7\text{-Xyl})\text{Br}$ ,  $\text{Ag}(\text{Xyl}7\text{-Xyl})\text{Br}$  and  $[\text{Ag}(5/6\text{-Mes})_2][\text{AgBr}_2]$ , for which mixtures of neutral and ionic complexes were observed in solution, only the  $[\text{Ag}(\text{carbene})_2]^+$  fragment was observed in ES-MS. Negative ES-MS mode showed the  $[\text{AgBr}_2]^-$  fragment in the of  $[\text{Ag}(7\text{-Xyl}/\text{Xyl}7\text{-Xyl})_2]^+$ . This can be explained as a consequence of the disproportionation to ionic complex in gas phase or, possibly, as a rearrangement due to the solution in acetonitrile, that drives the equilibrium to formation of the cationic compound.

As mentioned in the introduction of this chapter, Lin and co-worker attributed the absence of resonance for the carbene carbon in  $^{13}\text{C}$  NMR to the fast interconversion in NMR time scale between the mono-carbene and the bis-carbene (Scheme 3.2). However, according to the results obtained during this work, the absence of  $\text{C}_{\text{NHC}}$  resonance can be only attributed to the low solubility of certain silver complexes.

**Table 3.4.**  $^1\text{H}$  and  $^{13}\text{C}$  NMR data of  $\text{Ag}^{\text{I}}$  complexes in  $\text{CDCl}_3$  except for: (a) in  $\text{CD}_2\text{Cl}_2$ , (b) in  $d^8$ -thf.

	$\text{C}_{\text{NHC}}$	$^1J_{\text{AgC}}$	$^1\text{H}$ notable shifts
Ag(7-Mes)Br	218.4	226/261	2.25 (12H, Me), 2.18 (6H, Me)
Ag(Xyl7-Mes)Br	214.3	225/261	2.27 (6H, Me), 2.23 (12H, Me)
Ag(6-Mes)Br	-	-	2.33 (18H, Me)
Ag(6-Mes)Cl <sup>13</sup> (b)	205.9	228/260	2.30 (12H, Me), 2.27 (6H, Me)
[Ag(6-Mes) <sub>2</sub> ][AgBr <sub>2</sub> ]	204.5	174/201	2.27 (6H, Me), 1.69 (12H, Me)
[Ag(6-Mes) <sub>2</sub> ][Pd <sub>2</sub> Cl <sub>6</sub> ] <sub>1/2</sub> <sup>13</sup> (b)	205.8	174/201	2.33 (12H, Me), 1.76 (6H, Me)
[Ag(6-Mes) <sub>2</sub> ][Rh <sub>2</sub> (COD)(CF <sub>3</sub> CO <sub>2</sub> ) <sub>3</sub> ] <sup>17</sup> (b)	206.3	173/199	2.32 (6H, Me), 1.81 (12H, Me)
Ag(5-Mes)Br	-	-	2.23 (18 H, Me)
Ag(5-Mes)Cl <sup>18</sup> (a)	207.5	222/256	2.30 (12H, Me), 2.28 (6H, Me)
[Ag(5-Mes) <sub>2</sub> ][AgBr <sub>2</sub> ]	207.0	167/193	2.30 (6H, Me), 1.78 (12H, Me)
[Ag(Im-Mes) <sub>2</sub> ][CF <sub>3</sub> SO <sub>3</sub> ] <sup>5</sup> (b)	183.6	209/188	2.43 (6H, Me), 1.75 (12H, Me)
Ag(7-Xyl)Br	218.2	228/259	2.32 (12H, Me)
[Ag(7-Xyl) <sub>2</sub> ][AgBr <sub>2</sub> ]	-	-	1.64 (12H, Me)
Ag(Xyl7-Xyl)Br	214.5	226/259	2.22 (12H, Me)
[Ag(Xyl7-Xyl) <sub>2</sub> ][AgBr <sub>2</sub> ]	210.07	179/206	1.68 (12H, Me)
Ag(6-Xyl)Br	206.4	224/259	2.32 (12H, Me)
Ag(5-Xyl)Br	-	-	2.29 (12H, Me)
[Ag(5-Xyl) <sub>2</sub> ][AgBr <sub>2</sub> ]	-	-	1.84 (12H, Me)
Ag(7-DIPP)Br	-	-	-
Ag(Xyl7-DIPP)Br	214.1	260/225	-
Ag(5-DIPP)Br	-	-	-

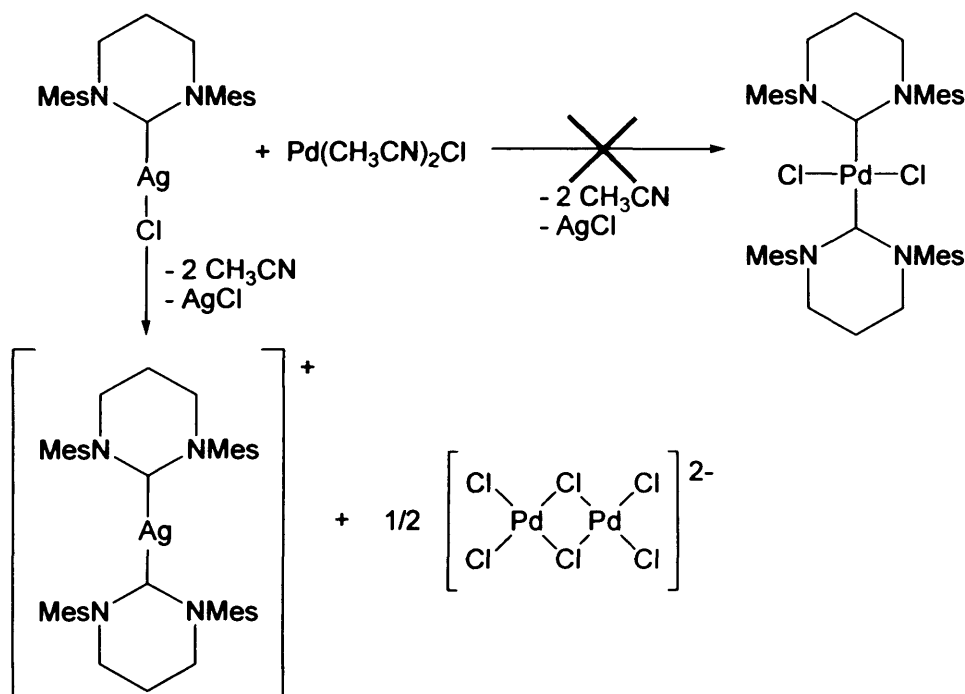
<sup>17</sup> Imlinger, N.; Mayr, M.; Wang, D.; Wurst, K.; Buchmeiser, M. R. *Adv. Synth. Catal.* **2004**, *346*, 1836.

<sup>18</sup> Viciu, Mihai S.; Navarro, Oscar; Germaneau, Romain F.; Kelly, Roy A., III; Sommer, William; Marion, Nicolas; Stevens, Edwin D.; Cavallo, Luigi; Nolan, S. P. *Organometallics* **2004**, *23*, 1629.

### 3.2.4. Expanded carbenes as transfer agents.

The preparation of silver (I) carbenes was, on paper, a good approach for the synthesis of more valuable carbene metal complexes *via* transmetalation reactions. However, all the attempts to use the six- and seven-membered Ag(I)-carbene complexes as transfer agents on Pd(II), Rh(I) and Ir(I) failed.

Despite the short number of articles regarding expanded silver carbenes in the literature, several examples of their inactivity towards transmetalation have been previously described.<sup>13, 19</sup> Herrmann reported that when a solution of  $\text{Pd}(\text{CH}_3\text{CN})_2\text{Cl}_2$  in dichloromethane is treated with silver carbene  $\text{Ag}(\mathbf{6}\text{-Mes})\text{Cl}$ , the corresponding cationic silver biscarbene,  $[\text{Ag}(\mathbf{6}\text{-Mes})_2]_2[\text{Pd}_2\text{Cl}_6]$ , is formed (Scheme 3.7). In contrast to the known examples of imidazol-2-ylidene compounds, the silver (I) monocarbene does not transfer the ligand to palladium but to silver, resulting in the formation of the biscarbene silver (I) complex  $[\text{Ag}(\mathbf{6}\text{-Mes})_2]_2[\text{Pd}_2\text{Cl}_6]$ . Moreover, in this publication Herrmann *et al.* also refute the formation of the biscarbene palladium (II) complex  $[\text{PdL}_2]_2[\text{Ag}_2\text{Br}_2\text{Cl}_6]$  ( $\text{L}$ =dimesityltetrahydropyrimid-2-ylidene) claimed by Buchmeiser *et al.*<sup>20</sup>



**Scheme 3.7.** Failed carbene transfer to  $\text{Pd}(\text{CH}_3\text{CN})_2\text{Cl}_2$ .

<sup>19</sup> Scarborough, C. C.; Popp, B. V.; Guzei, I. A.; Stahl, S. S. *J. Organomet. Chem.*, **2005**, *690*, 6143.

<sup>20</sup> Mayr, M.; Wurst, K.; Ongania, K.-H.; Buchmeiser, M. R., *Chem. Eur. J.*, **2004**, *10*, 1256

It has been reported that the transfer of the carbene ligand is mainly affected by its steric hindrance and basicity, with the more bulky and basic carbenes being less likely to undergo transfer reactions.<sup>13, 21</sup> Accordingly, expanded carbenes are unlikely to be transferred from silver to other metals. This leaves the free carbene as the only viable route for the synthesis of transition metal complexes. Results *via* this synthetic route are discussed in *Chapters 4* and *5*.

### 3.3. Experimental.

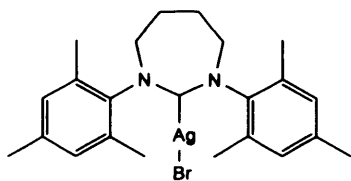
#### General remarks.

The solvents (dichloromethane, acetonitrile, diethylether, chloroform) were used as purchased. All other reagents were used as received. <sup>1</sup>H and <sup>13</sup>C NMR spectra were obtained on Bruker Avance AMX 400, 500 or Jeol Eclipse 300 spectrometers. The chemical shifts are given as dimensionless  $\delta$  values and are frequency referenced relative to TMS. Coupling constants *J* are given in Hertz (Hz) as positive values regardless of their real individual signs. Mass spectra and high-resolution mass spectra were obtained in electrospray (ES) mode unless otherwise reported, on a Waters Q-TOF micromass spectrometer.

#### General protocol for the synthesis of the silver complexes.

A suspension of 1 mmol amidinium of the BF<sub>4</sub>-salt, 0.5 – 1 mmol of Ag<sub>2</sub>O and 5 mmol of NaBr in 25 mL dichloromethane is stirred for 3 days. The resulting suspension was filtered and ether was added to the solution until the product crystallized. The product was isolated by filtration, washed with diethylether and dried *in vacuo*.

#### Ag(7-Mes)Br.



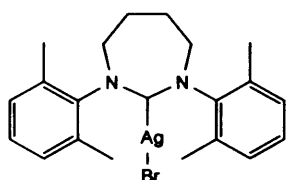
7-Mes·HBF<sub>4</sub> (1.249 g, 3.0 mmol), Ag<sub>2</sub>O (0.530 g, 2.3 mmol) and NaBr (1.702 g, 16.5 mmol) were suspended in 50 mL of DCM. The suspension was stirred for 3 days to yield 1.198 g (2.3 mmol, 78%) of the product as a white microcrystalline

---

<sup>21</sup> Roland, S.; Audouin, M.; Mangeney, P. *Organometallics* **2004**, *23*, 3075. b) Lee, H. M.; Chiu, P. L.; Hu, C.-H.; Lai, C.-L.; Chou, Y.-C. *J.Organomet. Chem.* **2005**, *690*, 403.

material. Crystals suitable for X-ray diffraction were obtained by layering a chloroform solution of the compound with diethyl ether.  $^1\text{H}$  NMR ( $\text{CDCl}_3$ , 400 MHz, rt):  $\delta$  6.84 (4H, s, Ar-CH), 3.85 (4H, t,  $^3J_{\text{HH}} = 5.4$ ,  $\text{NCH}_2$ ), 2.25 (12H, s, *o*- $\text{CH}_3$ ), 2.23 (4H, p,  $^3J_{\text{HH}} = 5.4$ ,  $\text{NCH}_2$ ), 2.18 (6H, s, *p*- $\text{CH}_3$ ).  $^{13}\text{C}$  NMR ( $\text{CDCl}_3$ , 100 MHz, rt):  $\delta$  218.6 (dd,  $^1J_{\text{C}^{107}\text{Ag}} = 226$ ,  $^1J_{\text{C}^{109}\text{Ag}} = 262$ , NCHN), 145.6 (s, Ar-C), 138.3 (s, Ar-C), 134.3 (s, Ar-C), 130.4 (s, Ar-CH), 52.8 (s,  $\text{NCH}_2$ ), 25.9 (s,  $\text{NCH}_2\text{CH}_2$ ), 21.4 (s, *p*- $\text{CH}_3$ ), 18.9 (s, *o*- $\text{CH}_3$ ). HRMS (ES):  $m/z$  482.1715 [ $\text{M}-\text{Br}+\text{CH}_3\text{CN}$ ] $^+$  (5%) ( $\text{C}_{25}\text{H}_{33}\text{N}_3\text{Ag}$  requires 482.1725); 335.2397 [(7-Mes)H] $^+$  (100%).

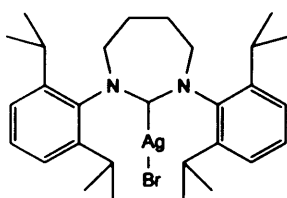
### Ag(7-Xyl)Br and [Ag(7-Xyl) $_2$ ][AgBr $_2$ ].



7-Xyl· $\text{HBF}_4$  (2.504 g, 6.4 mmol),  $\text{Ag}_2\text{O}$  (0.765 g, 3.3 mmol) and  $\text{NaBr}$  (3.265 g, 31.7 mmol) were suspended in 250 mL of DCM. The suspension was stirred for 2 days to yield 2.118 g (4.4 mmol, 70 %) of the product as a white microcrystalline material. The ratio

of the title compounds in solution was 78% and 22%, respectively.  $^1\text{H}$  NMR ( $\text{CDCl}_3$ , 400 MHz, rt):  $\delta$  Ag(7-Xyl)Br 7.16-6.93 (6H, m, Ar-CH), 3.90 (4H, t,  $^3J_{\text{HH}} = 5.6$ ,  $\text{NCH}_2$ ), 2.32 (12H, s,  $\text{CH}_3$ ), 2.28 (4H, m,  $^3J_{\text{HH}} = 2.8$ ,  $\text{NCH}_2\text{CH}_2$ ); [Ag(7-Xyl) $_2$ ][AgBr $_2$ ] 7.16-6.93 (6H, m, Ar-CH), 3.61 (4H, t,  $^3J_{\text{HH}} = 5.6$ ,  $\text{NCH}_2$ ), 2.02 (4H, p,  $^3J_{\text{HH}} = 2.8$ ,  $\text{NCH}_2\text{CH}_2$ ), 1.64 (12H, s,  $\text{CH}_3$ ).  $^{13}\text{C}$  NMR ( $\text{CDCl}_3$ , 100 MHz, rt):  $\delta$  Ag(7-Xyl)Br 147.9 (s, Ar-C), 134.9 (s, Ar-C), 129.9 (s, Ar-CH), 128.8 (s, Ar-CH) 52.8 (s,  $\text{NCH}_2$ ), 26.0 (s,  $\text{NCH}_2\text{CH}_2$ ), 19.1 (s,  $\text{CH}_3$ ); [Ag(7-Xyl) $_2$ ][AgBr $_2$ ] 210.1 (dd,  $^1J_{\text{C}^{107}\text{Ag}} = 206$ ,  $^1J_{\text{C}^{109}\text{Ag}} = 179$ ), 147.4 (s, Ar-C), 134.7 (s, Ar-C), 127.9 (s, Ar-CH), 128.6 (s, Ar-CH), 52.7 (s,  $\text{NCH}_2$ ), 25.7 (s,  $\text{NCH}_2\text{CH}_2$ ), 19.0 (s,  $\text{CH}_3$ ). HRMS (ES):  $m/z$  454.1434 ([ $\text{M}-\text{Br}+\text{CH}_3\text{CN}$ ] $^+$ ;  $\text{C}_{23}\text{H}_{29}\text{N}_3\text{Ag}$  requires 454.1412).

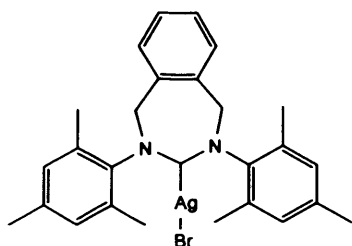
### Ag(7-DIPP)Br.



7-Pr $^i$ · $\text{HBF}_4$  (1.108 g, 2.2 mmol),  $\text{Ag}_2\text{O}$  (0.267 g, 1.2 mmol) and  $\text{NaBr}$  (1.25 g, 12.2 mmol) were suspended in 80 mL of DCM. The suspension was stirred for 7 days to yield 0.82 g (1.35 mmol, 62 %) of the product as a white microcrystalline material.  $^1\text{H}$  NMR ( $\text{CDCl}_3$ , 400 MHz, rt):  $\delta$  7.35 (2H, t,  $^3J_{\text{HH}} = 7.9$ , *p*-Ar-CH), 7.12 (4H, d,  $^3J_{\text{HH}} = 7.7$ , *m*-CH), 3.96 (4H, m,  $\text{NCH}_2$ ), 3.18 (4H, sept.,  $^3J_{\text{HH}} = 6.9$ ,  $\text{CH}(\text{CH}_3)_2$ ), 2.29 (4H, m,  $\text{NCH}_2\text{CH}_2$ ), 1.28 (d,  $^3J_{\text{HH}} = 6.9$ , 12H,  $\text{CH}(\text{CH}_3)_2$ ), 1.25 (d,  $^3J_{\text{HH}} = 6.9$ , 12H,  $\text{CH}(\text{CH}_3)_2$ ).  $^{13}\text{C}$  NMR ( $\text{CDCl}_3$ , 100 MHz, rt):  $\delta$  145.3 (s, Ar-C), 145.1 (s, Ar-C), 129.6 (s,

Ar-CH), 125.4 (s, Ar-CH), 54.2 (s, NCH<sub>2</sub>), 29.1 (s, CH(CH<sub>3</sub>)<sub>2</sub>), 25.6 (s, CH(CH<sub>3</sub>)<sub>2</sub>), 25.3 (s, NCH<sub>2</sub>CH<sub>2</sub>), 25.1 (s, CH(CH<sub>3</sub>)<sub>2</sub>). HRMS (ES): *m/z* 566.2689 [M-Br+CH<sub>3</sub>CN]<sup>+</sup> (100%) (C<sub>31</sub>H<sub>45</sub>N<sub>3</sub>Ag requires 566.2664).

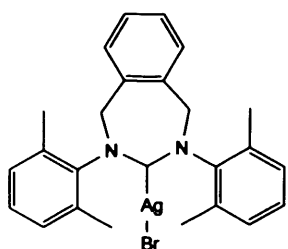
#### Ag(Xyl7-Mes)Br.



Xyl7-Mes·HBF<sub>4</sub> (1.518 g, 3.23 mmol), Ag<sub>2</sub>O (0.382 g, 1.65 mmol) and NaBr (2.045 g, 19.9 mmol) were suspended in 30 mL of DCM. The suspension was stirred for 7 days to yield 775 mg (1.36 mmol, 42%) of the product as a white microcrystalline material. Crystals suitable for X-ray diffraction were obtained by layering a dichloromethane

solution of the compound with diethyl ether. <sup>1</sup>H NMR (CDCl<sub>3</sub>, 400 MHz, rt): δ 7.39 (2H, dd, <sup>3</sup>J<sub>HH</sub> = 3.3, <sup>3</sup>J<sub>HH</sub> = 5.4, Xy-CH), 7.21 (2H, dd, <sup>3</sup>J<sub>HH</sub> = 5.4, <sup>3</sup>J<sub>HH</sub> = 3.3, Xy-CH), 6.9 (4H, s, Ar-CH), 4.99 (4H, s, NCH<sub>2</sub>), 2.27 (6H, s, *p*-CH<sub>3</sub>), 2.23 (12H, s, *o*-CH<sub>3</sub>). <sup>13</sup>C NMR (CDCl<sub>3</sub>, 100 MHz, rt): δ 146.5 (s, Ar-C), 138.1 (s, Ar-C), 135.8 (s, Ar-C), 133.6 (s, Ar-C), 130.0 (s, Ar-CH), 129.4 (s, Ar-CH), 128.1 (s, Ar-CH), 55.3 (s, NCH<sub>2</sub>), 21.0 (*p*-CH<sub>3</sub>), 18.5 (*o*-CH<sub>3</sub>). HRMS (ES): *m/z* 530.1750 [M-Br+CH<sub>3</sub>CN]<sup>+</sup> (5%) (C<sub>29</sub>H<sub>33</sub>N<sub>3</sub>Ag requires 530.1725); 383.2434 [(Xyl7-Mes)+H]<sup>+</sup> (100%).

#### Ag(Xyl7-Xyl)Br.



Xyl7-Xyl·HBF<sub>4</sub> (0.501 g, 2.2 mmol), Ag<sub>2</sub>O (0.145 g, 0.63 mmol) and NaBr (0.638 g, 6.20 mmol) were suspended in 50 mL of DCM.

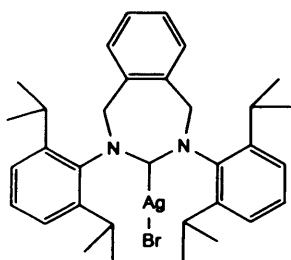
The suspension was stirred for 7 days to yield 221 mg (0.41 mmol, 36%) of the product as a white microcrystalline material. (Mixture of the two isomers (monomer:dimer = 70%:30%))

<sup>1</sup>H NMR (CDCl<sub>3</sub>, 400 MHz, rt): δ [Ag(Xy7-Xy)<sub>2</sub>][AgBr<sub>2</sub>] 7.22 (4H, m, Ar-CH), 7.11 (4H, t, <sup>3</sup>J<sub>HH</sub> = 7.5, Ar-CH), 7.01 (8H, d, <sup>3</sup>J<sub>HH</sub> = 7.5, Ar-CH), 6.96 (4H, m, Ar-CH), 4.66 (8H, br. s, Δν<sub>1/2</sub> ~ 200 Hz, NCH<sub>2</sub>), 1.69 (12H, s, CH<sub>3</sub>); Ag(Xyl7-Xyl)Br 7.34 (2H, m, Ar-CH), 7.18 (2H, m, Ar-CH), 7.04 (6H, m, Ar-CH), 4.97 (4H, br. s, Δν<sub>1/2</sub> ~ 400 Hz, NCH<sub>2</sub>), 2.22 (6H, s, CH<sub>3</sub>). <sup>13</sup>C NMR (CDCl<sub>3</sub>, 100 MHz, rt): δ [Ag(Xy7-Xy)<sub>2</sub>][AgBr<sub>2</sub>] 210.1 (dd, <sup>1</sup>J<sub>C<sup>107</sup>Ag</sub> = 179, <sup>1</sup>J<sub>C<sup>109</sup>Ag</sub> = 206, NCHN), 147.2 (s, Ar-C), 134.9 (s, Ar-C), 134.7 (s, Ar-C), 133.3 (s, Ar-C), 133.1 (s, Ar-C), 128.4 (s, Ar-CH), 127.5 (s, Ar-CH), 127.3 (s, Ar-CH), 127.3 (s, Ar-CH), 127.0 (s, Ar-CH), 54.7 (s, NCH<sub>2</sub>), 54.6 (s, NCH<sub>2</sub>), 18.0 (s, CH<sub>3</sub>), 17.8 (s, CH<sub>3</sub>); Ag(Xyl7-



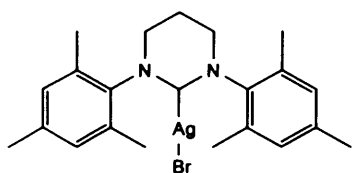
**Xyl)Br** 149.2 (s, Ar-C), 136.2 (s, Ar-C), 134.7 (s, Ar-C), 129.8 (s, Ar-CH), 129.7 (s, Ar-CH), 128.9 (s, Ar-CH), 55.9 (s, NCH<sub>2</sub>), 55.8 (s, NCH<sub>2</sub>), 19.2 (s, CH<sub>3</sub>). HRMS (ES): *m/z* 815.3235 [M+(Xyl7-Xyl)-Br]<sup>+</sup> (100%) (C<sub>50</sub>H<sub>52</sub>N<sub>4</sub>Ag requires 815.3243). MS (ES): *m/z* 264.61 [AgBr<sub>2</sub>]<sup>-</sup> (30%), 973.18 [AgC<sub>50</sub>H<sub>52</sub>N<sub>4</sub>Br<sub>2</sub>]<sup>-</sup> (100%).

**Ag(Xyl7-Pr<sup>i</sup>)Br.**



Xyl7-Pr<sup>i</sup>-HBF<sub>4</sub> (1.67 g, 3.0 mmol), Ag<sub>2</sub>O (0.695 g, 3.0 mmol) and NaBr (3.00 g, 30.0 mmol) were suspended in 50 mL of DCM. The suspension was stirred for 3 days to yield 350 mg (0.54 mmol, 18%) of the product as a white microcrystalline material. <sup>1</sup>H NMR (CDCl<sub>3</sub>, 400 MHz, rt): δ 7.42 (2H, dd, <sup>3</sup>J<sub>HH</sub> = 3.3, <sup>3</sup>J<sub>HH</sub> = 5.5, Xy-CH), 7.35 (2H, t, <sup>3</sup>J<sub>HH</sub> = 7.7, *p*-Ar-CH), 7.23 (2H, dd, <sup>3</sup>J<sub>HH</sub> = 5.5, <sup>3</sup>J<sub>HH</sub> = 3.3 Hz, Xy-CH) overlapping with 7.20 (4H, d, <sup>3</sup>J<sub>HH</sub> = 7.7, *m*-Ar-CH), 5.07 (4H, br.s., Δ*v*<sub>1/2</sub> = 16.8 Hz, NCH<sub>2</sub>), 3.12 (4H, hept., <sup>3</sup>J<sub>HH</sub> = 6.7, CH(CH<sub>3</sub>)<sub>2</sub>), 1.29 (12H, d, <sup>3</sup>J<sub>HH</sub> = 6.7, CH(CH<sub>3</sub>)<sub>2</sub>), 1.28 (12H, d, <sup>3</sup>J<sub>HH</sub> = 6.7, CH(CH<sub>3</sub>)<sub>2</sub>). <sup>13</sup>C NMR (CDCl<sub>3</sub>, 100 MHz, rt): δ 144.8 (s, Ar-C), 143.5 (s, Ar-C), 134.2 (s, Ar-C), 128.3 (s, Ar-CH), 127.2 (s, Ar-CH), 124.1 (s, Ar-CH), 55.8 (s, NCH<sub>2</sub>), 27.6 (s, CH(CH<sub>3</sub>)<sub>2</sub>), 24.0 (s, CH(CH<sub>3</sub>)<sub>2</sub>), 23.9 (s, CH(CH<sub>3</sub>)<sub>2</sub>). HRMS (ES): *m/z* 614.2650 [M-Br+CH<sub>3</sub>CN]<sup>+</sup> (100%) (C<sub>35</sub>H<sub>45</sub>N<sub>3</sub>Ag requires 614.2664).

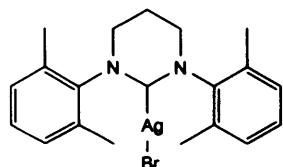
**Ag(6-Mes)Br and [Ag(6-Mes)<sub>2</sub>][AgBr<sub>2</sub>].<sup>13</sup>**



Reaction performed on a 4.29 mmol scale (1.72 g) of 6-Mes·HBr and 0.500 g (2.16 mmol) of Ag<sub>2</sub>O in 20 mL of DCM. The suspension is stirred for 7 days to yield 1.072 g (2.11 mmol, 49%) of white microcrystalline material (95% mono-carbene complex). <sup>1</sup>H NMR (CDCl<sub>3</sub>, 400 MHz, rt): δ [Ag(6-Mes)<sub>2</sub>][AgBr<sub>2</sub>] 6.83 (8H, s, Ar-CH), 3.10 (8H, m, *J*<sub>HH</sub> = 5.8, NCH<sub>2</sub>), 2.27 (12H, s, *o*-CH<sub>3</sub>), 2.09 (8H, p., *J*<sub>HH</sub> = 5.4, NCH<sub>2</sub>CH<sub>2</sub>), 1.69 (s, 24H, *p*-CH<sub>3</sub>); Ag(6-Mes)Br 7.20 (4H, m, Ar-CH), 3.45 (4H, m, NCH<sub>2</sub>), 2.38 (2H, m, NCH<sub>2</sub>CH<sub>2</sub>), 2.33 (18H, s, *o/p*-CH<sub>3</sub>). <sup>13</sup>C NMR (CDCl<sub>3</sub>, 100 MHz, 298 K): δ [Ag(6-Mes)<sub>2</sub>][AgBr<sub>2</sub>] 218.6 (dd, <sup>1</sup>J<sub>C<sup>107</sup>Ag</sub> = 174, <sup>1</sup>J<sub>C<sup>109</sup>Ag</sub> = 201, NCHN), 141.3 (s, Ar-C), 137.1 (s, Ar-C), 133.6 (s, Ar-C), 128.6 (s, Ar-CH), 42.6 (s, NCH<sub>2</sub>), 20.0 (s, *p*-CH<sub>3</sub>), 19.5 (s, NCH<sub>2</sub>CH<sub>2</sub>), 16.6 (s, *o*-CH<sub>3</sub>); Ag(6-Mes)Br 141.7 (s, Ar-C), 137.1 (s, Ar-C), 133.3 (s, Ar-C), 128.9 (s, Ar-CH), 43.1 (s, NCH<sub>2</sub>), 19.8 (s, *p*-CH<sub>3</sub>), 19.5 (s, NCH<sub>2</sub>CH<sub>2</sub>), 17.0 (s,

*o*-CH<sub>3</sub>); HRMS (ES): *m/z* 747.3592 [M+(6-Mes)-Br]<sup>+</sup> (100%) (C<sub>44</sub>H<sub>56</sub>N<sub>4</sub>Ag requires 747.3556).

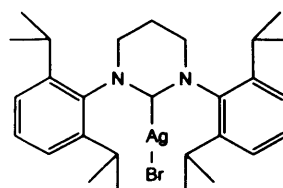
#### Ag(6-Xyl)Br.



6-Xyl·HBF<sub>4</sub> (1.13 g, 3.0 mmol), Ag<sub>2</sub>O (0.695 g, 3.0 mmol) and NaBr (3.00 g, 30.0 mmol) were suspended in 25 mL of DCM. The suspension was stirred overnight to yield 1.05 g (2.16 mmol, 72 %) of the product as a white microcrystalline material.

<sup>1</sup>H NMR (CDCl<sub>3</sub>, 400 MHz, rt): δ 7.22-7.13 (6H, m, Ar-CH), 3.45 (4H, t, <sup>3</sup>J<sub>HH</sub> = 5.9, NCH<sub>2</sub>), 2.38 (2H, m, <sup>3</sup>J<sub>HH</sub> = 5.5, NCH<sub>2</sub>CH<sub>2</sub>), 2.32 (12H, s, CH<sub>3</sub>). <sup>13</sup>C NMR (CDCl<sub>3</sub>, 100 MHz, rt): δ 206.4 (dd, <sup>1</sup>J<sub>C<sup>107</sup>Ag</sub> = 224, <sup>1</sup>J<sub>C<sup>109</sup>Ag</sub> = 259, NCHN), 145.4 (s, Ar-C), 135.1 (s, Ar-C), 129.7 (s, Ar-CH), 129.1 (s, Ar-CH), 44.3 (s, NCH<sub>2</sub>), 21.1 (s, NCH<sub>2</sub>CH<sub>2</sub>), 18.4 (s, CH<sub>3</sub>). HRMS (ES): *m/z* 478.0163 [M]<sup>+</sup> (100%) (C<sub>20</sub>H<sub>24</sub>N<sub>2</sub>AgBr requires 478.0174).

#### Ag(6-Pr<sup>i</sup>)Br.



6-Pr<sup>i</sup>·HBr (1.268 g, 3.16 mmol) and Ag<sub>2</sub>O (0.308 g, 1.33 mmol) were suspended in 20 mL of DCM. The suspension was stirred for 7 days to yield 1.191 g (2.34 mmol, 74 %) of the product as a white microcrystalline material.

<sup>1</sup>H NMR (CDCl<sub>3</sub>, 400 MHz, rt): δ 7.37 (2H, t, <sup>3</sup>J<sub>HH</sub> = 7.8, *p*-Ar-CH), 7.21 (4H, d, <sup>3</sup>J<sub>HH</sub> = 7.8, *o*-Ar-CH), 3.47 (4H, t, <sup>3</sup>J<sub>HH</sub> = 5.7, NCH<sub>2</sub>), 3.05 (4H, hept., <sup>3</sup>J<sub>HH</sub> = 6.9, CH(CH<sub>3</sub>)<sub>2</sub>), 2.39 (2H, p., <sup>3</sup>J<sub>HH</sub> = 5.7, NCH<sub>2</sub>CH<sub>2</sub>), 1.34 (d, <sup>3</sup>J<sub>HH</sub> = 6.9, 12H, CH(CH<sub>3</sub>)<sub>2</sub>), 1.31 (d, <sup>3</sup>J<sub>HH</sub> = 6.9, 12H, CH(CH<sub>3</sub>)<sub>2</sub>). <sup>13</sup>C NMR (CDCl<sub>3</sub>, 100 MHz, rt): δ 145.3 (s, Ar-C), 129.5 (s, Ar-CH), 124.9 (s, Ar-CH), 46.0 (s, NCH<sub>2</sub>), 28.6 (s, CH(CH<sub>3</sub>)<sub>2</sub>), 25.0 (s, CH(CH<sub>3</sub>)<sub>2</sub>), 24.7 (s, CH(CH<sub>3</sub>)<sub>2</sub>), 20.4 (s, NCH<sub>2</sub>CH<sub>2</sub>). HRMS (ES): *m/z* 554.2528 [M-Br+CH<sub>3</sub>CN]<sup>+</sup> (100%) (C<sub>30</sub>H<sub>43</sub>N<sub>3</sub>Ag requires 554.2505).

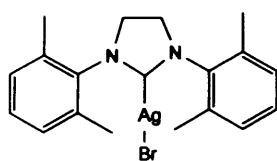
#### Ag(5-Mes)Br and [Ag(5-Mes)<sub>2</sub>][AgBr<sub>2</sub>].



Reaction performed on a 2 mmol scale (0.78 g) of the amidinium salt, 463 mg (2 mmol) of Ag<sub>2</sub>O and 2.0 g (20 mmol) of NaBr in 20 mL of DCM. The suspension was stirred overnight to yield 830 mg (1.68 mmol, 84%) of white microcrystalline material. <sup>1</sup>H NMR (CDCl<sub>3</sub>, 400 MHz, rt): δ [Ag(5-Mes)<sub>2</sub>][AgBr<sub>2</sub>] 6.80 (4H, s, Ar-CH), 3.82 (4H, m, NCH<sub>2</sub>), 2.30 (6H, s, *p*-CH<sub>3</sub>), 1.78 (12H, s, *o*-CH<sub>3</sub>); Ag(5-

**Mes)Br** 6.88 (4H, s, Ar-CH), 3.93 (4H, m, NCH<sub>2</sub>), 2.23 (18H, s, *o/p*-CH<sub>3</sub>). <sup>13</sup>C NMR (CDCl<sub>3</sub>, 100 MHz, rt):  $\delta$  [**Ag(5-Mes)<sub>2</sub>][AgBr<sub>2</sub>]** 207.0 (dd, <sup>1</sup>J<sub>C<sup>107</sup>Ag</sub> = 167, <sup>1</sup>J<sub>C<sup>109</sup>Ag</sub> = 193, NCHN), 138.7 (s, Ar-C), 135.8 (s, Ar-C), 129.7 (s, Ar-CH), 50.5 (s, NCH<sub>2</sub>), 21.5 (s, *p*-CH<sub>3</sub>), 17.7 (s, *o*-CH<sub>3</sub>); **Ag(5-Mes)Br** 139.1 (s, Ar-C), 135.2 (s, Ar-C), 130.1 (s, Ar-CH), 50.6 (s, NCH<sub>2</sub>), 21.4 (s, *p*-CH<sub>3</sub>), 18.3 (s, *o*-CH<sub>3</sub>); HRMS (ES): *m/z* 538.2368 [M+(5-Mes)-Br]<sup>+</sup> (100%) (C<sub>29</sub>H<sub>41</sub>N<sub>3</sub>Ag requires 538.2351).

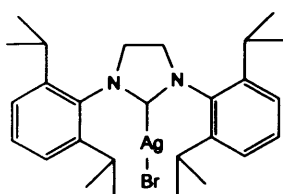
### Ag(5-Xyl)Br.



Reaction performed on a 1 mmol scale (364 mg) of the amidinium salt, 262 mg (1 mmol) of Ag<sub>2</sub>O and 1 g (10 mmol) of NaBr in 15 mL of DCM. The suspension is stirred for 3 days to yield 268 mg (0.57 mmol, 57%) of white microcrystalline material. (Mixture of

the two isomers (i1:i2 =70:30)) <sup>1</sup>H NMR (CD<sub>2</sub>Cl<sub>2</sub>, 400 MHz, rt):  $\delta$  [**Ag(5-Xyl)<sub>2</sub>][AgBr<sub>2</sub>]** 7.18 (4H, t, <sup>3</sup>J<sub>HH</sub> = 7.0, Ar-CH), 6.81 (8H, d, <sup>3</sup>J<sub>HH</sub> = 7.0, Ar-CH), 3.82 (8H, m, NCH<sub>2</sub>) 1.84 (24H, s, CH<sub>3</sub>); **Ag(5-Xyl)Br** 7.18 (2H, t, <sup>3</sup>J<sub>HH</sub> = 7.6, Ar-CH), 6.81 (4H, d, <sup>3</sup>J<sub>HH</sub> = 7.6, Ar-CH), 3.99 (4H, m, NCH<sub>2</sub>), 2.29 (12H, s, CH<sub>3</sub>). <sup>13</sup>C NMR (CD<sub>2</sub>Cl<sub>2</sub>, 100 MHz, rt):  $\delta$  [**Ag(5-Xyl)<sub>2</sub>][AgBr<sub>2</sub>]** 138.0 (s, Ar-C), 136.6 (s, Ar-CH), 129.7 (s, Ar-CH), 51.8 (s, NCH<sub>2</sub>), 19.2 (s, CH<sub>3</sub>). **Ag(5-Xyl)Br** 138.6 (s, Ar-C), 137.0 (s, Ar-CH), 129.8 (s, Ar-CH, i1), 51.9 (s, NCH<sub>2</sub>), 19.7 (s, CH<sub>3</sub>). HRMS (ES): *m/z* 663.2624 [M+(5-Xyl)-Br]<sup>+</sup> (70%) (C<sub>38</sub>H<sub>44</sub>N<sub>4</sub>Ag requires 663.2617), 426.12 [M+CH<sub>3</sub>CN-Br]<sup>+</sup> (100%).

### Ag(5-Pr<sup>i</sup>)Br.



Reaction performed on a 0.38 mmol scale (150 mg) of the amidinium salt, 49 mg (0.19 mmol) of Ag<sub>2</sub>O in 5 mL of DCM. The suspension was stirred for 7 days to yield 160 mg (0.32 mmol, 84%) of white microcrystalline material. <sup>1</sup>H NMR (DMSO-*d*<sub>6</sub>, 400

MHz, rt):  $\delta$  7.41 (2H, t, <sup>3</sup>J<sub>HH</sub> = 7.8, *p*-Ar-CH), 7.25 (4H, d, <sup>3</sup>J<sub>HH</sub> = 7.7, *m*-Ar-CH), 4.07 (4H, s, NCH<sub>2</sub>), 3.05 (4H, hept., <sup>3</sup>J<sub>HH</sub> = 6.9, CH(CH<sub>3</sub>)<sub>2</sub>), 1.35 (12H, d, <sup>3</sup>J<sub>HH</sub> = 1.6, CH(CH<sub>3</sub>)<sub>2</sub>), 1.33 (12H, d, <sup>3</sup>J<sub>HH</sub> = 1.6, CH(CH<sub>3</sub>)<sub>2</sub>). <sup>13</sup>C NMR (DMSO-*d*<sub>6</sub>, 100 MHz, rt):  $\delta$  146.5 (s, Ar-C), 134.4 (s, Ar-CH), 130.1 (Ar-C), 124.7 (Ar-CH), 53.9 (NCH<sub>2</sub>), 28.9 (s, CH(CH<sub>3</sub>)<sub>2</sub>), 25.5 (s, CH(CH<sub>3</sub>)<sub>2</sub>), 24.0 (s, CH(CH<sub>3</sub>)<sub>2</sub>). HRMS (ES): *m/z* 538.2368 [M-Br+CH<sub>3</sub>CN]<sup>+</sup> (100%) (C<sub>29</sub>H<sub>41</sub>N<sub>3</sub>Ag requires 538.2351).

## Chapter 4. Synthesis of complexes with expanded-ring N-heterocyclic carbenes as ligands

## Chapter

## 4

**Complexes of expanded-ring N-heterocyclic carbenes**

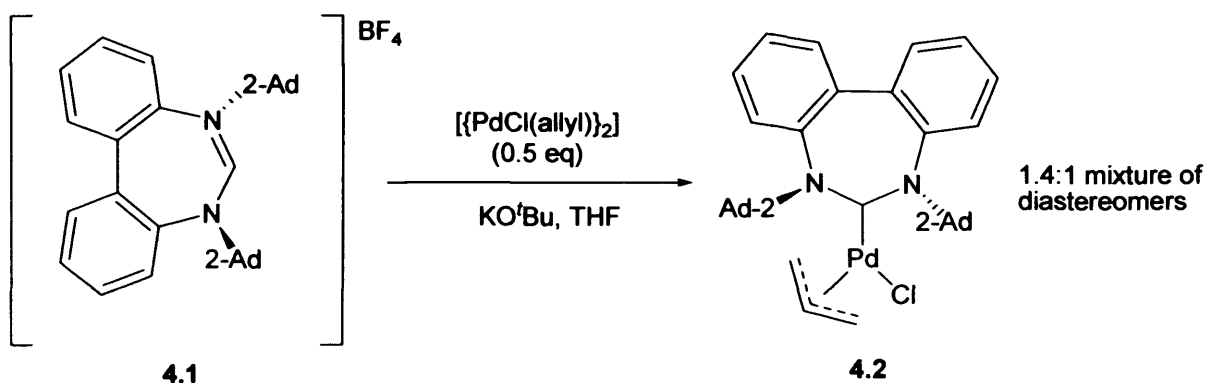
<b>4.1. Introduction</b> .....	<b>111</b>
<b>4.2. Results and discussion</b> .....	<b>114</b>
4.2.1. <i>Complexation of cyclohexyl derivatives</i> .....	114
4.2.1.1. <i>Synthesis of the [Pt(7-Cy)(nbe)<sub>2</sub>] complex</i> .....	114
4.2.1.2 <i>Solid state structure of the [Pt(7-Cy)(nbe)<sub>2</sub>] complex</i> .....	115
4.2.1.3. <i>Rhodium(I) and Iridium(I) COD complexes</i> .....	117
4.2.1.4. <i>Solid state structures of Rh(I) and Ir(I) COD complexes</i> .....	120
4.2.1.5. <i>Rhodium(I) and Iridium(I) biscarbonyl complexes</i> .....	124
4.2.1.6. <i>Solid state structure of Rh(I) and Ir(I) biscarbonyl complexes</i> .....	126
4.2.1.7. <i>Solution NMR studies</i> .....	127
4.2.2. <i>Complexation of aromatic derivatives</i> .....	129
4.2.2.1. <i>Rh(I)COD complexes</i> .....	129
4.2.2.2. <i>Rhodium(I) carbonyl complexes</i> .....	134
<b>4.3. Experimental</b> .....	<b>137</b>

## Chapter 4. Synthesis of complexes with expanded-ring N-heterocyclic carbenes as ligands.

### 4.1. Introduction.

The structure and electronic properties of expanded carbenes and their effect on the catalytic performance is virtually unexplored in comparison with their saturated and unsaturated 5-membered analogues.

Hitherto, the only seven-membered carbene complexes that have been published, with the exception of the work herein, have been the palladium(II) complexes prepared by Stahl and co-workers.<sup>1</sup> These Pd(II) complexes were synthesised by *in situ* deprotonation of the BF<sub>4</sub> salt with potassium *tert*-butoxide in presence of the metal precursor (Scheme 4.1). However, attempts of isolation of the free carbene led to formation of the alcohol adduct, which does not react with the metal precursor. This suggests that the metal precursor reacts with the free carbene before this reacts with the *tert*-butanol generated as a byproduct of the *in situ* by deprotonation of 4.1 with potassium *tert*-butoxide.



**Scheme 4.1.** Synthesis of Stahl's Pd(II) carbene complex.

The most distinctive feature of these complexes in comparison with 5-membered and even 6-membered carbenes is the torsional twist, which Stahl defines by two parameters: The

<sup>1</sup> Scarborough, C. C.; Grady, M. J. W.; Guzei, I. A.; Gandhi, B. A.; Bunel, E. E.; Stahl, S. S. *Angew. Chem., Int. Ed.* **2005**, *44*, 5269; (b) Scarborough, C. C.; Popp, B. V.; Guzei, I. A.; Stahl, S. S. *J. Organomet. Chem.* **2005**, *690*, 6143.

dihedral angle between the two aryl rings of the biphenyl backbone and the torsional angle between the two N $\cdots$ N–C<sub>ring</sub> planes of the carbene ring (C<sub>ring</sub>–N $\cdots$ N–C<sub>ring</sub>), previously defined in *Chapter 2* as  $\beta$ . The torsion of the ring, defined by these two parameters, dictates the spatial disposition of the substituents into the coordination sphere. Interestingly, the flexibility of the ligand allows the repositioning of the substituents, by a modification of the dihedral angle between the two aryl rings of the biphenyl backbone and  $\beta$ , depending on the steric requirements of the ligands present in the metal coordination sphere.

An enantiomerically pure and less flexible analogue of this ligand would be highly interesting in asymmetric catalysis, because a more rigid disposition of the N-substituents in the coordination sphere would make possible a more efficient transfer of the chiral information into the substrate. However, the preparation of enantiomerically resolved analogues of these compounds has not yet been reported.

A greater number of 6-membered carbenes complexes have been published and compared against their 5-membered analogues in terms of electronic and steric properties, as well as their coordination chemistry and catalytic performance.<sup>12,2</sup> Analysis of their crystal structures shows the opening of the N–C–N angle and the corollary decrease of the C<sub>NHC</sub>–N–C<sub>subst</sub> as main feature. This results in an increase of the steric hindrance around the metal core.

The donor capabilities of carbene ligands have been mainly studied by comparison of the C–O stretching frequencies of different carbonyl NHC-complexes. The carbonyl stretching frequency detected by an infrared spectrometer is a widespread method to estimate the electron density on the metal centre, and therefore the donating capabilities of the ligand.

With the intention of attaining a better understanding of the information obtained from the infrared spectra, the nature of the carbonyl-metal bond is reviewed below.

The carbonyl ligand binds to the metal by  $\sigma$ -donation from the non-bonding electron pair at the carbon and, simultaneously, the metal back-donates electron density from the  $d_{\pi}$

---

<sup>2</sup> For examples see: (a) Bortenschlager, M.; Mayr, M.; Nuyken, O.; Buchmeiser, Michael R. *J. Molec. Cat. A: Chem.* **2005**, *233*, 67. (b) Yun, Jaesook; Marinez, Eric R.; Grubbs, Robert H. *Organometallics* **2004**, *23*, 4172. (c) Kremzow, Doris; Seidel, Günter; Lehmann, Christian W.; Fürstner, A. *Chem. Eur. J.* **2005**, *11*, 1833. (d) Imlinger, N.; Mayr, M.; Wang, D.; Wurst, K.; Buchmeiser, Michael R. *Adv. Synth. Catal.* **2004**, *346*, 1836. (e) Wang, D.; Yang, L.; Decker, U.; Findeisen, M.; Buchmeiser, Michael R. *Macromol. Rapid Commun.* **2005**, *26*, 1757.

orbitals into the  $\pi$ -anti-bonding orbitals at the carbon atom (Figure 4.1). Consequently, an electron rich metal centre back-donates more electron density into the  $\pi^*$  orbital of the CO ligand, weakening the C-O bond. This results in a reduction of the carbonyl stretching frequency. Therefore, assuming that the nature of the M-Carbene interaction is not only electrostatic,<sup>3</sup> the IR carbonyl frequencies obtained for corresponding metal complexes with different carbene ligands does not only account for the basicity or the  $\sigma$ -donating ability, but for the overall electron density donated by the carbene.

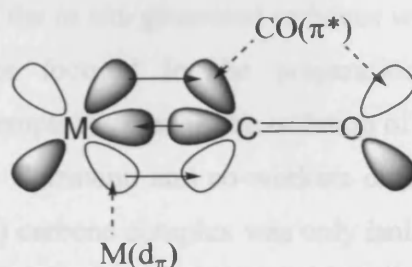


**Figure 4.1.** Molecular orbital picture of the M-CO fragment.

The basicity and steric hindrance of the ligand system influencing the catalytic activity of the metal complex are important characteristics. For example, the higher catalytic activity of saturated 5-membered carbenes in alkene metathesis has been attributed to its greater basicity.<sup>4</sup> However, the 6-membered carbene ruthenium complex reported by Grubbs *et al.* shows a lower activity in RCM and ROMP despite its higher basicity.<sup>5</sup> This was explained by the author as a consequence of the larger steric environment around the metal atom, which disfavours the olefin binding or the formation of the metallacyclobutane.

This chapter is focused on the coordination chemistry of expanded carbenes. Rhodium, iridium and platinum complexes are presented. Additionally, the crystal structure data of analogous 5-, 6- and 7-membered rhodium carbene complexes are presented and compared in order to study the effects of the expansion of the ring on square planar complexes. Rhodium bis-carbonyl complexes were also synthesised to assess the donor ability of expanded carbenes.

<sup>3</sup> Díez-González, Silvia; Nolan, Steven P. *Coord. Chem.Rev.* **2007**, *251*, 874.

<sup>4</sup> Scholl, M.; Trnka, T.M.; Morgan, J.P.; Grubbs, R.H. *Tetrahedron Lett.* **1999**, *40*, 2247.

<sup>5</sup> Yun, Jaesook; Marinez, Eric R.; Grubbs, Robert H. *Organometallics* **2004**, *23*, 4172.

## 4.2. Results and discussion.

### 4.2.1. Complexation of cyclohexyl derivatives.

As previously mentioned in *Chapter 3*, attempts to isolate a silver(I) complex from the reaction of the amidinium salt **7-Cy**·HX (X = <sup>-</sup>Br, <sup>-</sup>PF<sub>6</sub>) with Ag<sub>2</sub>O, which could be subsequently used for transmetalation reactions, did not afford a silver complex. Therefore, the preferred method for the synthesis of transition metal complexes with **7-Cy** and **DIOC-Cy** was the direct reaction of the *in situ* generated carbenes with suitable metal salts.

Initial complexation studies focused in the preparation of Pd(II) complexes but unfortunately none of the attempts resulted in the isolation of a stable complex. This agrees with the results obtained by Herrmann and co-workers on six-membered ring carbenes.<sup>6</sup> According to them, the Pd(II) carbene complex was only isolated by reaction of carbene **6-DIPP** with [Pd(PPh<sub>3</sub>)<sub>2</sub>Cl<sub>2</sub>], whilst reaction with [Pd(OAc)<sub>2</sub>] or [Pd(CH<sub>3</sub>CN)<sub>2</sub>Cl<sub>2</sub>] failed to afford the desired complex. Herrmann attributes the different behaviour of six-membered ring carbenes compared to their unsaturated five-membered analogues to the higher basicity and greater reducing capability arising from the expansion of the ring.

When **7-Mes** was reacted with [Pd(PPh<sub>3</sub>)<sub>2</sub>Cl<sub>2</sub>] according to Herrmann's method no Pd(II) complex was isolated, instead a suspension of palladium black was obtained.

#### 4.2.1.1. Synthesis of the [Pt(**7-Cy**)(nbe)<sub>2</sub>] complex.

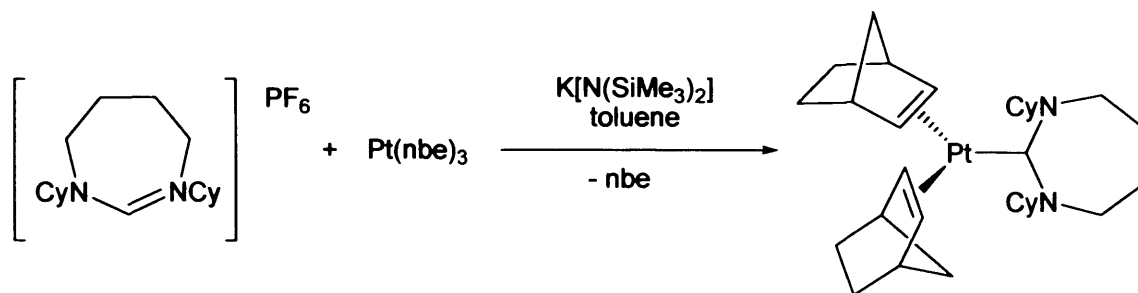
The difficult synthesis and/or isolation of a Pd(II) complex led to the use of a different metal in the search for a stable complex.

Reaction of the free diazepanylidene carbene **7-Cy** with platinum(0)-tris-norbornene forms readily the corresponding monocarbene complex [Pt(**7-Cy**)(nbe)<sub>2</sub>] (Scheme 4.2). The platinum complex is air sensitive, both in the solid state and in solution, but stable under anaerobic condition. The complex was characterised in solution by <sup>1</sup>H and <sup>13</sup>C NMR and in the solid state by single-crystal X-ray diffraction.

---

<sup>6</sup> Schneider, Sabine K.; Herrmann, Wolfgang A.; Herdtweck, Eberhardt *J. Molec. Cat. A: Chem* **2006**, *245*, 248.





**Scheme 4.2.** Synthesis of the  $[\text{Pt}(7\text{-Cy})(\text{nbe})_2]$  complex.

$^1\text{H}$  and  $^{13}\text{C}$  NMR spectra of  $[\text{Pt}(7\text{-Cy})(\text{nbe})_2]$  in  $d^6$ -benzene show broad resonances for the coordinated carbene ligand but sharp signals for the coordinated norbornenes at room temperature, consistent with a slow rotation of 7-Cy about the Pt-C bond or a fluxional behaviour of the backbone.

#### 4.2.1.2 Solid state structure of the $[\text{Pt}(7\text{-Cy})(\text{nbe})_2]$ complex.

Crystals suitable for X-Ray diffraction were obtained after standing a hexane solution of  $[\text{Pt}(7\text{-Cy})(\text{nbe})_2]$  at  $0^\circ\text{C}$ . The crystal structure of the  $[\text{Pt}(7\text{-Cy})(\text{nbe})_2]$  complex shows the metal occupying the centre of a trigonal planar arrangement with both olefinic carbons of the alkenes in the coordination plane (Figure 4.2), a characteristic coordination mode for  $\text{Pt}(0)(\text{alkene})_2$  complexes. This trigonal planar conformation around the platinum centre provides a better overlap of the Pt d-orbitals and the olefinic  $\pi^*$  systems. A  $C_2$  crystallographic axis passes through the Pt-C(1) bond and bisects the C(3)-C(3') bond of the carbene ligand, with the carbene ring adopting a chair conformation. Comparison of the Pt-C(1) distance at  $2.077(4)\text{ \AA}$  with other  $\text{Pt}(0)(\text{alkene})_2(\text{carbene})$  complexes reveals a small variation from the average value of  $2.05\text{ \AA}$ .<sup>7, 8</sup> The NCN angle of the platinum complex of 7-Cy is much smaller,  $115.5(3)^\circ$ , than the corresponding angle in the Rh(I) and Ir(I) complexes, which remains close to  $120^\circ$  for all three structures (Rh and Ir complexes will be discussed in section 4.2.1.3 and 4.2.1.4). The carbene tilt angle  $\theta$  from the coordination plane is  $84.5^\circ$ . Markó and co-workers have observed that the greater the deviation of the carbene ligand from a perpendicular arrangement the greater the strain on

<sup>7</sup> Berthon-Gelloz, G.; Buisine, O.; Brière, J.-F.; Michaud, G.; Stérin, S.; Mignani, G.; Tinant, B.; Declercq, J.-P.; Chapon, D.; Markó, I. E. *J. Organomet. Chem.* **2005**, *690*, 6156.

<sup>8</sup> De Bo, G.; Berthon-Gelloz, G.; Tinant, B.; Markó, I. E. *Organometallics* **2006**, *25*, 1881.

the remaining ligands. In the  $[\text{Pt}(\mathbf{7-Cy})(\text{nbe})_2]$  complex an  $8.5^\circ$  tilt of the norbornene C=C bonds from the coordination plane is observed. The C=C bond length of the coordinated olefins is a good indicator of the extent of  $\pi$ -back bonding from the metal. In the presence of strong  $\sigma$  donors, such as NHCs, long olefinic bonds are expected as a consequence of the stronger  $\pi$  back-donation from the electron rich metal centre into the  $\pi^*$  orbitals of the olefine. In the  $[\text{Pt}(\mathbf{7-Cy})(\text{nbe})_2]$  complex the C=C bond length of the norbornene ligands is  $1.436(4)$  Å; this value is within the range for NHCs<sup>9</sup> and slightly longer than  $\text{Pt}(0)(\text{alkene})_2\text{L}$  complexes, where L = phosphine ligand, with values between  $1.409$  and  $1.422$  Å.<sup>10</sup>

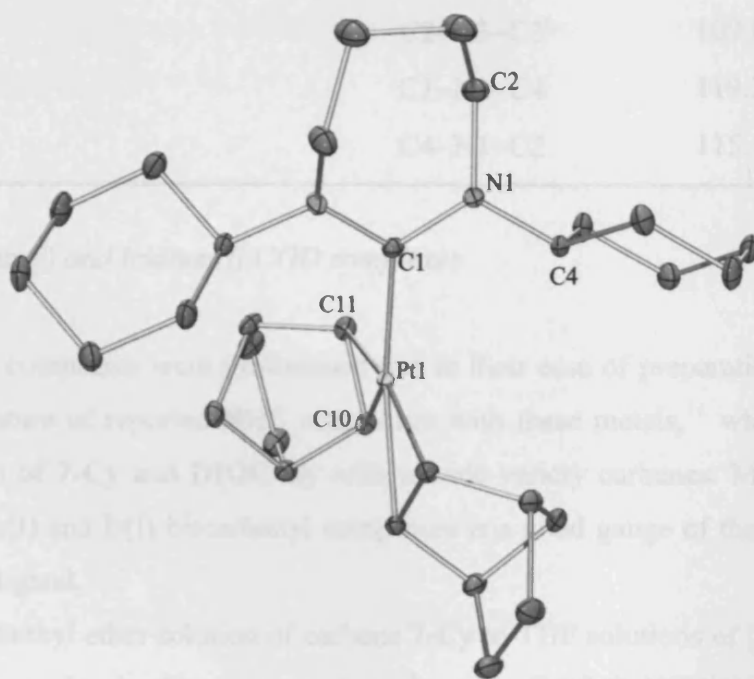


**Figure 4.2.** ORTEP ellipsoid plot at 30% probability of the molecular structure of  $[\text{Pt}(\mathbf{7-Cy})(\text{nbe})_2]$ . Solvent molecules and hydrogen atoms have been omitted for clarity.

<sup>9</sup> Schumann H.; Cielusek, G.; Pickardt, J.; Bruncks, N. *J. Organomet. Chem.* **1979**, *172*, 359.

<sup>10</sup> (a) Chandra, G.; Lo, P. Y.; Hitchcock, P. B.; Lappert, M. F. *Organometallics* **1987**, *6*, 191. (b) Hitchcock, P. B.; Lappert, M. F.; MacBeath, C.; Scott, F. P. E.; Warhurst, N. J. W. *J. Organomet. Chem.* **1997**, *534*, 139. (c) Hitchcock, P. B.; Lappert, M. F.; Mac Beath, C.; Scott, F. P. E.; Warhurst, N. J. W. *J. Organomet. Chem.* **1997**, *528*, 185.

**Table 4.1.** Selected bond lengths (Å) and angles (°) in the [Pt(7-Cy)(nbe)<sub>2</sub>] complex.

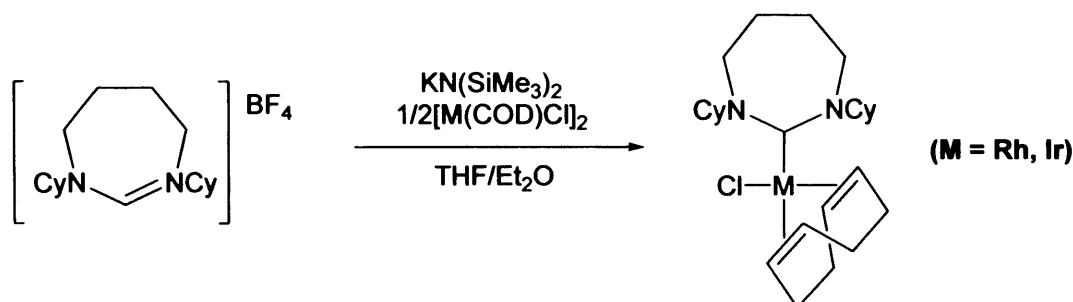
Bond lengths (Å)		Angles (°)	
C1–Pt1	2.077(4)	C1–Pt1–C11	97.57(8)
C10–Pt1	2.104(3)	C10–Pt1–C10 <sup>i</sup>	86.96(16)
C11–Pt1	2.140(3)	C1–Pt1–C10	136.52(8)
C10–C11	1.436(4)	C10–Pt1–C11	39.52(11)
C(1)–N(1)	1.353(3)	N1 <sup>i</sup> –C1–N1	115.5(3)
C(2)–N(1)	1.487(4)	C1–N1–C2	120.9(3)
C(4)–N(1)	1.475(4)	N1–C2–C3	115.8(3)
		C2–C3–C3 <sup>i</sup>	109.6(3)
		C1–N1–C4	119.2(2)
		C4–N1–C2	115.1(2)

#### 4.2.1.3. Rhodium(I) and Iridium(I) COD complexes.

Rh(I) and Ir(I) complexes were synthesised due to their ease of preparation, handling and extensive literature of reported NHC complexes with these metals,<sup>11</sup> which would allow the comparison of 7-Cy and DIOC-Cy with a wide variety carbenes. Moreover, the CO vibration of Rh(I) and Ir(I) biscarbonyl complexes is a good gauge of the donating ability of the carbene ligand.

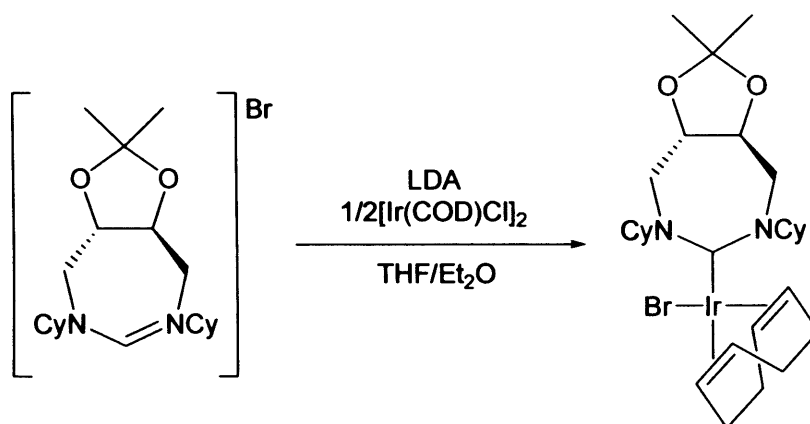
Addition of a diethyl ether solution of carbene 7-Cy to THF solutions of [M(COD)Cl]<sub>2</sub>, M = Rh or Ir, forms cleanly the corresponding air-stable [M(7-Cy)(COD)Cl] complexes as yellow solids in good to high yields (Scheme 4.3).

<sup>11</sup> (a) Lee, H. M.; Jiang, T.; Stevens, E. D.; Nolan, S. P. *Organometallics* **2001**, *20*, 1255; (b) Chianese, A. R.; Li, Xingwei; Janzen, M. C.; Faller, J. W.; Crabtree, R. H. *Organometallics* **2003**, *22*, 1663; (c) Hanasaka, F.; Fujita, K.; Yamaguchi, R. *Organometallics* **2005**, *24*, 3422; (d) Imlinger, N.; Mayr, M.; Wang, D.; Wurst, K.; Buchmeiser, M. R. *Adv. Synth. Catal.* **2004**, *346*, 1836; (e) Zhang, Y.; Wang, D.; Wurst, K.; Buchmeiser, M. R.; *J. Organomet. Chem.*; **2005**, *690*, 5728.



**Scheme 4.3.** Preparation of Rh and Ir COD complexes with ligand 7-Cy.

Due to the instability of free carbene **DIOC-Cy** complex  $[\text{Ir}(\text{DIOC-Cy})(\text{COD})\text{Br}]$  was synthesised by in situ reaction in toluene of **DIOC-Cy-HBr** with LDA, followed by addition of  $[\text{Ir}(\text{COD})\text{Cl}]_2$  and a halogen exchange between the metal chloride and LiBr present in solution (Scheme 4.4).



**Scheme 4.4.** Preparation of Rh and Ir COD complexes with ligand **DIOC-Cy**.

Table 4.2 shows characteristic NMR chemical shifts for the rhodium and iridium **7-Cy** and **DIOC-Cy** complexes. Upon complexation of carbene **7-Cy** the most characteristic chemical shift in the  $^1\text{H}$  NMR is that for the  $\alpha$  protons of the *N*-cyclohexyl substituents, which changes from 3.50 ppm in **7-Cy** to 6.18 ppm in  $[\text{Rh}(\text{7-Cy})(\text{COD})\text{Cl}]$  and 5.74 ppm in  $[\text{Ir}(\text{7-Cy})(\text{COD})\text{Cl}]$ . This large change in the  $\delta_{\text{H}}$  is attributed to the close proximity of the methine protons to the electron rich metal centres. The  $^1\text{H}$  NMR spectrum of  $[\text{Ir}(\text{DIOC-Cy})(\text{COD})\text{Cl}]$  shows, in addition to two signals of diastereotopic methylene groups, two resonances for the  $\alpha$  *N*-cyclohexyl protons and four resonances for the olefinic protons of the coordinated 1,5-cyclooctadiene. In this case, due to the asymmetric carbene

ligand, there is no plane of symmetry in the molecule as with the [Rh/Ir(7-Cy)(COD)Cl] analogues.

In  $^{13}\text{C}$  NMR the most notable chemical shift is that of the carbene carbon, which changes from a singlet at 251.2 ppm in  $\text{C}_6\text{D}_6$  for the free carbene, 7-Cy, to a doublet at 215.3 ( $^1J_{\text{RhC}} = 43.7$  Hz) and an singlet at 208.3 ppm in  $\text{CDCl}_3$  for the rhodium and iridium complexes, respectively. The carbene carbon chemical shift of [Ir(DIOC-Cy)(COD)Cl] appears at 223.6 ppm in  $\text{C}_6\text{D}_6$ . These values are higher than the ones reported for the corresponding complexes of carbenes 4.3 – 4.5, with the exception of the acyclic carbene 4.6, which shows a shift of 225.6 ppm for its rhodium complex<sup>12, 13, 14</sup> (Figure 4.3).

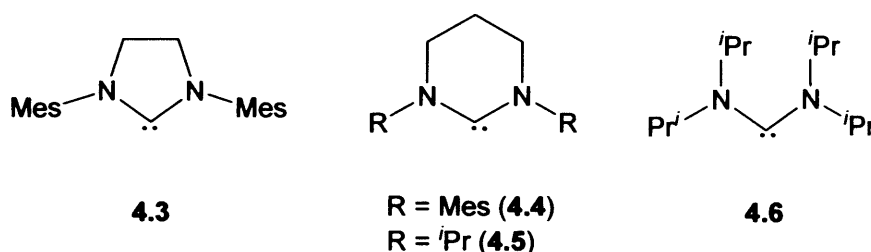


**Figure 4.3.** Previously reported saturated carbenes.

**Table 4.2.** Characteristic NMR shifts for carbenes 7-Cy, DIOC-Cy and their complexes.

	$\text{H}_{\text{Cy}}(\delta_{\text{H}})$	$\text{C}_{\text{NHC}}(\delta_{\text{C}})$
7-Cy <sup>b</sup>	3.50	251.2
[Rh(7-Cy)(COD)Cl]	6.18	215.3 ( $^1J_{\text{Rh}} = 43.7$ )
[Ir(7-Cy)(COD)Cl]	5.74	208.3
[Ir(DIOC-Cy)(COD)Br]	6.36, 6.09	223.6
DIOC-Cy <sup>b</sup>	3.40	-

<sup>a</sup>measured in  $\text{CDCl}_3$ , unless otherwise noted;  $\text{H}_{\text{Cy}}$ : cyclohexyl methinic proton,  $\text{C}_{\text{NHC}}$ : carbene carbon.; <sup>b</sup>measured in  $\text{C}_6\text{D}_6$ .

<sup>12</sup> Mayr, M.; Wurst, K.; Ongania, K.-H.; Buchmeiser, M. R. *Chem. Eur. J.* **2004**, *10*, 1256.

<sup>13</sup> Denk, K.; Sirsch, P.; Herrmann, W. A. *J. Organomet. Chem.* **2002**, *649*, 219.

<sup>14</sup> Doyle, M. J.; Lappert, M. F. *J. Chem. Soc., Chem. Commun.* **1974**, 679.

#### 4.2.1.4. Solid state structures of Rh(I) and Ir(I) COD complexes.

Single-crystal X-ray diffraction studies confirmed the identities of [Rh(7-Cy)(COD)Cl], [Ir(7-Cy)(COD)Cl] and [Ir(DIOP-Cy)(COD)Br] (Figure 4.4). Upon coordination of the diazepane carbene 7-Cy to Rh or Ir the NCN angle changes from 127.35(15)° in 7-Cy·HPF<sub>6</sub> to close to 120°. The corresponding value for the [Ir(DIOP-Cy)(COD)Br] complex is 123° (135.90(10)° in DIOP-Cy·HPF<sub>6</sub>). These NCN angles are larger than those observed in complexes of 5-membered carbenes, which fall in the 103 – 107° range, and even 6-membered NHCs, 115 – 118°. <sup>11d,e</sup> Although there are no reported 7-membered NHC iridium or rhodium complexes, the corresponding values for palladium complexes of **4.2** range from 113 to 117°. The larger NCN angles in the 7-membered carbene series and their salts may reflect an increase in the ring strain, which in the case of carbene **4.2** is partially relieved by the torsional twist of the biaryl backbone.

The Rh-C(1) bond distance for [Rh(COD)(7-Cy)Cl] is 2.056(2) Å. For comparison, the imidazole-based analogue values range from 2.016 – 2.056 Å, and for saturated imidazo-2-ylidenes between 1.994 – 2.032 Å. The same bond distances with the acyclic carbene **4.6** is 2.041(2) Å, and the Rh-C(1) distances for the bromide complexes of tetrahydropyrimidines **4.4** and **4.5** are 2.0896(18) and 2.047(3) Å, respectively. From the above it is difficult to reach any conclusions with regards to the donor ability of 7-Cy as it seems that other factors, such as the greater NCN angles in larger ring carbenes and the steric/electronic constraints of the N-substituents play a significant role in the M-C<sub>NHC</sub> bond distances. In both complexes the carbene ligand adopts the usual perpendicular arrangement with respect to the coordination plane; the tilt angle ( $\theta$ ), defined by the coordination and N1-C1-N2 planes is 89.3° for the rhodium and 89.5° for the iridium complex, respectively.

The tetrahedral deviation of the ring carbon atoms shows that in the amidinium salt 7-Cy·HPF<sub>6</sub> the C2-C5 carbon ring angles ranged from 111.5 to 113.3° and in DIOP-Cy·HPF<sub>6</sub> an even more strained ring was observed as indicated from the corresponding angle range, 112.6 - 116.0°. Complexation of the corresponding free carbenes offers little relief to the ring strain; the corresponding ring angles in [Ir(7-Cy)(COD)Cl] and [Ir(DIOP-Cy)(COD)Br] range from 110.4 to 114.2° and 112.0° to 114.9° respectively. However, as it was mentioned before in this section, the NCN angle decreases upon coordination, adopting a geometry closer to that expected for an sp<sup>2</sup> hybridisation, especially in the case of [Ir(DIOP-Cy)(COD)Br].



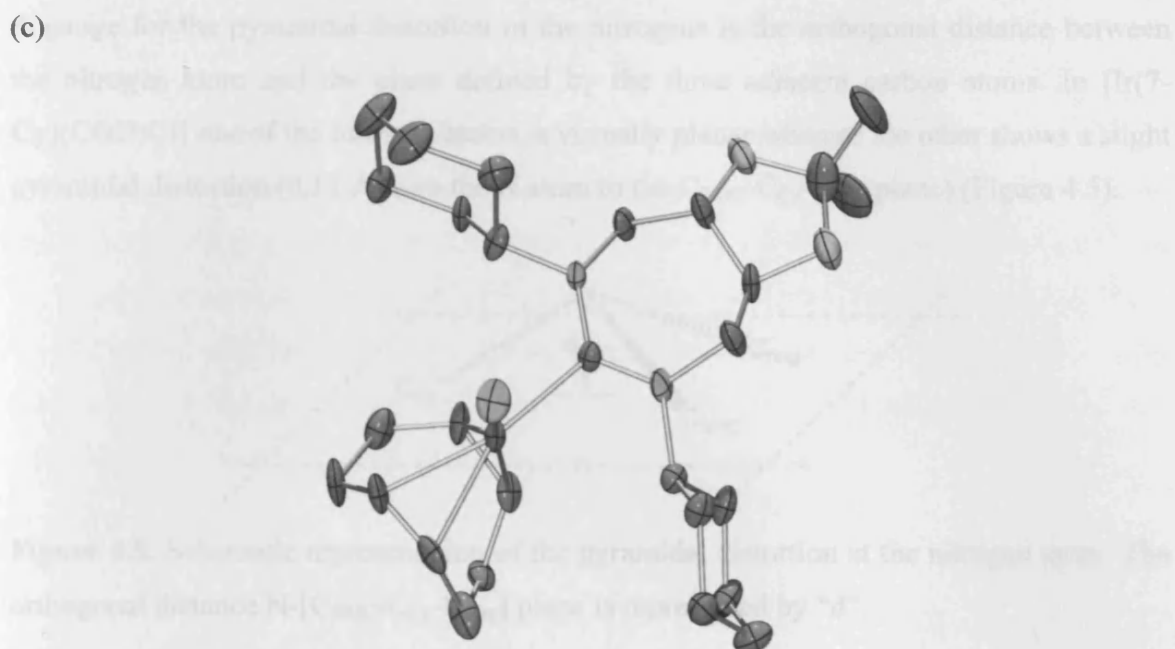


**Figure 4.5.** ORTEP ellipsoid plot at 30% probability of the molecular structures of (a) [Rh(7-Cy)(COD)Cl], (b) [Ir(7-Cy)(COD)Cl] and (c) [Ir(DIOP-7-Cy)(COD)Br]. Hydrogen atoms are omitted for clarity.

The spatial orientation of the cyclohexyl substituents which point directly into the metal's coordination sphere, defined by dihedral angle  $\alpha$  between the planes defined by the  $C_{Cy}-N\cdots N$  atoms previously described in section 2.2.3.1, is  $23.33^\circ$  and  $3.26^\circ$  in the amidinium salts **7-Cy**·HPF<sub>6</sub> and **DIOP-Cy**·HPF<sub>6</sub>, respectively. A small increase is observed upon coordination to iridium in the [Ir(7-Cy)(COD)Cl] complex to  $28.31^\circ$ , while in [Ir(DIOP-Cy)(COD)Br] a more significant increase is observed, from  $3.26^\circ$  to an average value of  $28.7^\circ$ . For comparison, the torsional angle in the biaryl amidinium salt **4.1** is  $56.2(5)^\circ$  increasing to  $72.3(8)^\circ$  in the palladium complex **4.2**.

The torsion angle ( $\beta$ ) increases slightly from  $23.3^\circ$  in **7-Cy**·HPF<sub>6</sub> to  $25.2^\circ$  in [Ir(7-Cy)(COD)Cl] to minimise the bond opposition strain and transannular interactions. Yet, the tartrate derivative shows a more prominent increase of  $\beta$  upon coordination, from  $9.92^\circ$  in **DIOP-Cy**·HPF<sub>6</sub> to an average value of  $40.68^\circ$  in the iridium complex. This effect, together with the decrease of the NCN angle, might account for the pyramidal distortion observed in the nitrogen atoms, instead of the expected planar geometry, causing the cyclohexyl substituent to be out of the N-C-N plane.



A gauge for the pyramidal distortion in the nitrogens is the orthogonal distance between the nitrogen atom and the plane defined by the three adjacent carbon atoms. In [Ir(7-Cy)(COD)Cl] one of the nitrogen atoms is virtually planar whereas the other shows a slight pyramidal distortion (0.11 Å from the N atom to the C<sub>NHC</sub>-C<sub>Cy</sub>-C<sub>ring</sub> plane) (Figure 4.5).

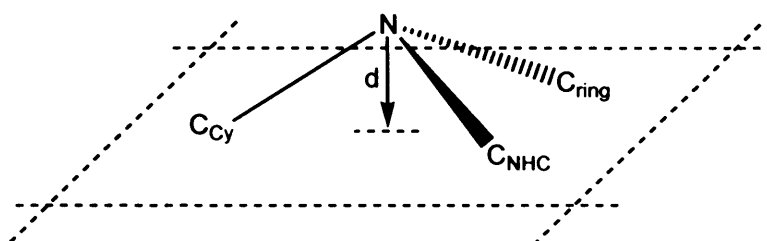


**Figure 4.5.** Schematic representation of the pyramidal distortion at the nitrogen atom. The orthogonal distance N-[C<sub>NHC</sub>-C<sub>Cy</sub>-C<sub>ring</sub>] plane is represented by “d”.

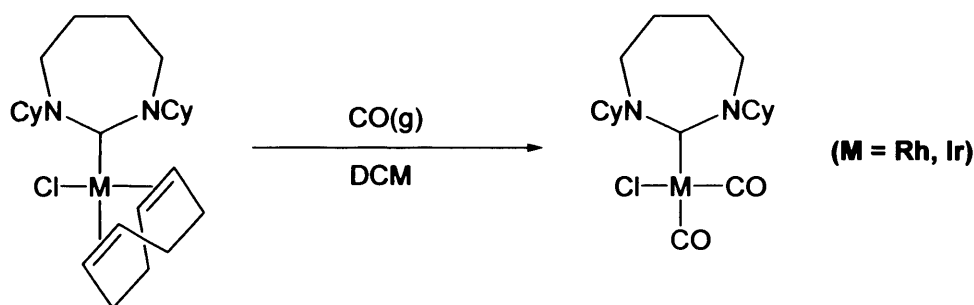
**Table 4.3.** Selected bond lengths (Å) and angles (°) in the [Rh(7-Cy)(COD)Cl], [Ir(7-Cy)(COD)Cl] and [Ir(DIOP-7-Cy)(COD)Br] complexes.

	[Rh(7-Cy)(COD)Cl]	[Ir(7-Cy)(COD)Cl]	[Ir(COD)(DIOP-7-Cy)Br] <sup>b</sup>
M-C <sub>NHC</sub>	2.056(2)	2.072(3)	2.088(12)
M-X	2.3935(8)	2.3747(6)	2.4929(19)
M(1)-C <sub>C=trans-X</sub>	2.113(2)	2.106(2)	2.146(12)
M(1)-C <sub>C=trans-X</sub>	2.126(2)	2.120(2)	2.150(12)
M(1)-C <sub>C=trans-NHC</sub>	2.188(3)	2.163(3)	2.164(12)
M(1)-C <sub>C=trans-NHC</sub>	2.219(3)	2.188(3)	2.174(11)
C=C <sub>trans-X</sub>	1.401(3)	1.422(4)	1.428(19)
C=C <sub>trans-NHC</sub>	1.365(4)	1.387(5)	1.366(17)
C <sub>NHC</sub> -M-X	88.86(7)	89.36(7)	88.88(4)
N-C <sub>NHC</sub> -N	120.4(2)	120.4(2)	122.2(11)
C <sub>NHC</sub> -N(1)-C <sub>Cy</sub>	117.8(2)	118.2(2)	117.2(10)
C <sub>Cy</sub> -N(1)-C	114.3(2)	114.7(2)	112.9(9)
C <sub>NHC</sub> -N(1)-C	127.9(2)	127.1(2)	127.9(10)
tilt angle (θ)	89.3	89.5	88.7

<sup>a</sup> Abbreviations: C<sub>NHC</sub>, carbene carbon; C=C<sub>trans-X</sub>, double bond *trans* to halide; C=C<sub>trans-NHC</sub>, double bond *trans* to carbene; C<sub>Cy</sub>, cyclohexyl tertiary carbon.<sup>b</sup> Reported values are the average from the four molecules in the unit cell.

## 4.2.1.5. Rhodium(I) and Iridium(I) biscarbonyl complexes.

The infrared carbonyl stretching frequencies of the rhodium and iridium carbonyl complexes, *cis*-[M(L)(CO)<sub>2</sub>Cl], are well documented to be a good measure of the donor ability of ligand L; the more basic the ligand the lower the observed  $\nu(\text{CO})$  values.<sup>15</sup> The corresponding air-stable carbonyl complexes with the diazepanylidene carbene, *cis*-[Rh(7-Cy)(CO)<sub>2</sub>Cl] and *cis*-[Ir(7-Cy)(CO)<sub>2</sub>Cl], were obtained in quantitative yields after treatment of a dichloromethane solution of the corresponding 1,5-cyclooctadiene complex with carbon monoxide (1 atm) for twenty minutes, Scheme 4.5.



**Scheme 4.5.** Synthesis of carbonyl complexes.

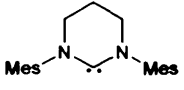
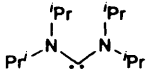
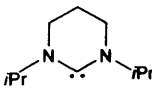
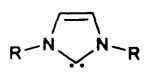
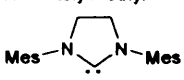
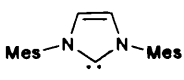
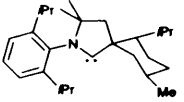
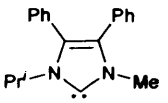
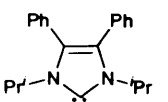
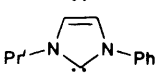
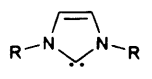
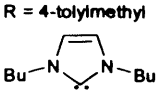
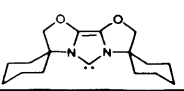
The <sup>1</sup>H NMR spectra of both complexes show a notable downfield shift of the methinic cyclohexyl protons when compared to the parent COD complexes (from 6.18 in [Rh(7-Cy)(COD)Cl] and 5.74 in [Ir(7-Cy)(COD)Cl] to 5.34 in [Rh(7-Cy)(CO)<sub>2</sub>Cl] and 5.11 ppm in [Ir(7-Cy)(CO)<sub>2</sub>Cl]), attributed to the stronger donor ability of the carbonyl ligands compared to COD (Table 4.2).

In Table 4.4 the carbonyl stretching frequencies of *cis*-[Rh(7-Cy)(CO)<sub>2</sub>Cl] and *cis*-[Ir(7-Cy)(CO)<sub>2</sub>Cl] are listed and compared to analogous complexes. The average carbonyl stretching frequency for the rhodium complex, *cis*-[Rh(7-Cy)(CO)<sub>2</sub>Cl], is 2031 cm<sup>-1</sup> indicating a donor ability of 7-Cy higher than that of electron-rich alkyl phosphines but lower than the tetrahydropyrimidine and acyclic carbenes 4.3, 4.4 and 4.5. Similarly the Ir carbonyl complex has an  $\nu_{\text{av}}(\text{CO})$  value at 2016 cm<sup>-1</sup> which suggests that the donor ability of 7-Cy is higher than that of unsaturated NHC ( $\nu_{\text{av}}(\text{CO}) = 2017 - 2024 \text{ cm}^{-1}$ ).<sup>15</sup> Although,

<sup>15</sup> Chianese, A. R.; Kovacevic, A.; Zeglis, B. M.; Faller, J. W.; Crabtree, R. H. *Organometallics* **2004**, *23*, 2461, and references therein.

Bertrand's and co-workers alkyl-aminocarbenes show an even lower  $\nu_{\text{av}}(\text{CO})$  stretch at  $2013 \text{ cm}^{-1}$ .<sup>16</sup>

**Table 4.4.** IR  $\nu(\text{CO})$  for  $\text{Rh}(\text{CO})_2(\text{L})\text{Cl}$  and  $\text{Ir}(\text{CO})_2(\text{L})\text{Cl}$  complexes recorded in  $\text{CH}_2\text{Cl}_2$ .

$\text{Rh}(\text{CO})_2(\text{L})\text{Cl}$ L=	$\nu(\text{CO}) (\text{cm}^{-1})$	$\nu_{\text{av}}(\text{CO}) (\text{cm}^{-1})$	Ref.
7-Cy	2071, 1990	2031	-
	2062, 1976	2019	11
	2057, 1984	2021	13
	2063, 1982	2023	11
 R = 4-tolylmethyl	2076, 1995	2036	10b
	2081, 1996	2039	12
	2076, 2006	2041	12
<hr/>			
$\text{Ir}(\text{CO})_2(\text{L})\text{Cl}$ L=	$\nu(\text{CO}) (\text{cm}^{-1})$	$\nu_{\text{av}}(\text{CO}) (\text{cm}^{-1})$	Ref.
7-Cy	2058, 1973	2016	
	2055, 1971	2013	16
	2059, 1974	2017	15
	2061, 1972	2017	15
	2061, 1976	2019	15
 R = 4-tolylmethyl	2063, 1976	2020	10b
	2062, 1978	2020	10b
	2065, 1982	2024	17

<sup>16</sup> Lavallo, V.; Canac, Y.; Präsang, C.; Donnadiou, B.; Bertrand, G. *Angew. Chem. Int. Ed.* **2005**, *44*, 5705.

<sup>17</sup> Altenhoff, G.; Goddard, R.; Lehmann, C. W.; Glorius F. *J. Am. Chem. Soc.* **2004**, *126*, 15195.

4.2.1.6. Solid state structure of Rh(I) and Ir(I) biscarbonyl complexes.

Crystal data for the iridium complex *cis*-[Ir(7-Cy)(CO)<sub>2</sub>Cl] were collected and an ORTEP representation is shown in Figure 4.6. Selected bond lengths and angles are summarised in Table 4.5. The tilt angle  $\theta$ , defined by the coordination (Ir-C1-Cl) and N1-C1-N2 planes shows a small deviation from the right angles at 85.1°.

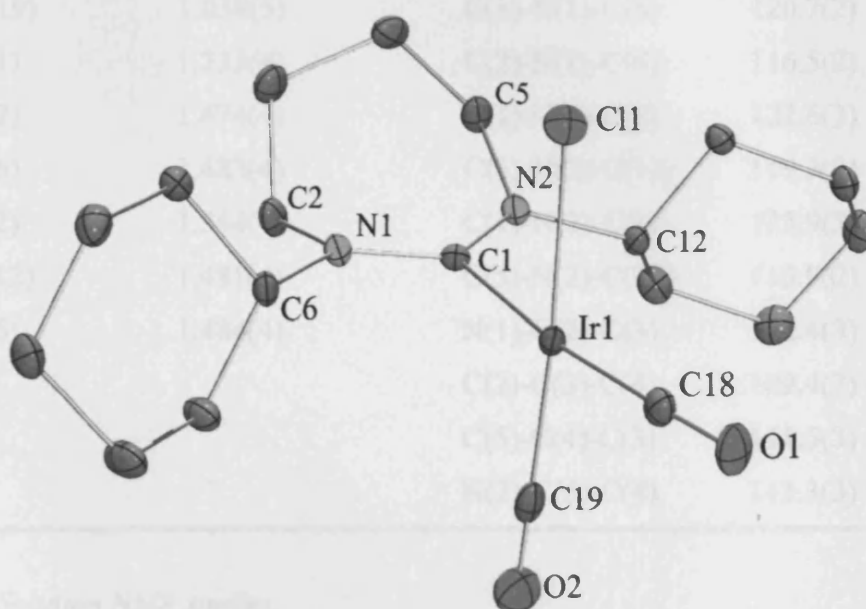


**Figure 4.6.** ORTEP ellipsoid plot at 30% probability of the molecular structure of *cis*-[Ir(7-Cy)(CO)<sub>2</sub>Cl]. Solvent molecules have been omitted for clarity.

A longer M-C<sub>NHC</sub> bond is observed upon substitution of the cyclooctadiene with two carbonyl ligands, from 2.072(3) to 2.115(3) Å, respectively. The two M-CO bonds are virtually identical at 1.893(4-5) Å. Of note is that the M-CO bond lengths are almost the same, despite having different *trans* substituents. The C-O bond *trans* to the carbene is longer than the one *trans* to the chloride ligand by ca. 0.1 Å, in line with the higher *trans* influence of the carbene ligand. A similar trend can also be observed in the crystal structures of other *cis*-[Ir(NHC)(CO)<sub>2</sub>Cl].<sup>18</sup>

<sup>18</sup> Schumann H.; Cielusek, G.; Pickardt, J.; Bruncks, N. *J. Organomet. Chem.* **1979**, *172*, 359.

**Table 4.5.** Selected bond lengths (Å) and angles (°) for Ir(CO)<sub>2</sub>(3)Cl.

Lengths (Å)		Angles (°)	
Ir(1)-C(1)	2.115(3)	C(19)-Ir(1)-C(18)	92.22(14)
Ir(1)-Cl(1)	2.365(1)	C(19)-Ir(1)-C(1)	91.91(13)
Ir(1)-C(18)	1.893(4)	C(18)-Ir(1)-Cl(1)	91.61(11)
Ir(1)-C(19)	1.893(5)	C(1)-M(1)-Cl(1)	84.50(8)
O(1)-C(18)	1.132(4)	N(1)-C(1)-N(2)	120.8(3)
O(2)-C(19)	1.038(5)	C(1)-N(1)-C(6)	120.7(2)
N(1)-C(1)	1.333(4)	C(2)-N(1)-C(6)	116.5(2)
N(1)-C(2)	1.474(4)	C(1)-N(1)-C(2)	122.6(3)
N(1)-C(6)	1.483(4)	C(1)-N(2)-C(12)	119.3(2)
C(1)-N(2)	1.344(4)	C(1)-N(2)-C(5)	125.9(3)
N(2)-C(12)	1.481(4)	C(5)-N(2)-C(12)	113.9(2)
N(2)-C(5)	1.484(4)	N(1)-C(2)-C(3)	112.4(3)
		C(2)-C(3)-C(4)	109.4(3)
		C(5)-C(4)-C(3)	111.5(3)
		N(2)-C(5)-C(4)	113.3(3)

#### 4.2.1.7. Solution NMR studies.

At room temperature, the rhodium and iridium complexes, M(COD)(7-Cy)Cl, show a sharp AB pattern for the diastereotopic NCH<sub>2</sub> ring protons in the <sup>1</sup>H NMR spectrum, which indicates that there is slow rotation about the metal-carbene bond. Variable temperature <sup>1</sup>H NMR experiments up to 100° C in toluene-*d*<sub>8</sub> show no line broadening for the rhodium and iridium complexes of 7-Cy. This is consistent with a free energy rotation barrier greater than 74 kJ.mol<sup>-1</sup>. In contrast, in the <sup>1</sup>H NMR room temperature spectrum of the carbonyl complexes *cis*-[Rh(7-Cy)(CO)<sub>2</sub>Cl] and *cis*-[Ir(7-Cy)(CO)<sub>2</sub>Cl] the NCH<sub>2</sub> protons are equivalent, thus indicating rapid rotation about the M-C<sub>NHC</sub> bond at that temperature. Variable-temperature <sup>1</sup>H NMR spectra in the range of +20 to -90 °C in dichloromethane-*d*<sub>2</sub> confirms a fluxional behaviour for the *cis*-[Ir(7-Cy)(CO)<sub>2</sub>Cl] complex (Figure 4.7). At -90 °C two relatively sharp signals are observed for the NCH<sub>2</sub> protons in a 1:1 ratio. As the

temperature is increased the signals coalesce at about  $-65\text{ }^{\circ}\text{C}$ . Line shape analysis of the NMR data affords a value of  $50.9 \pm 3.1\text{ kJ mol}^{-1}$  for the enthalpy of activation ( $\Delta H^{\ddagger}$ ).<sup>19</sup>

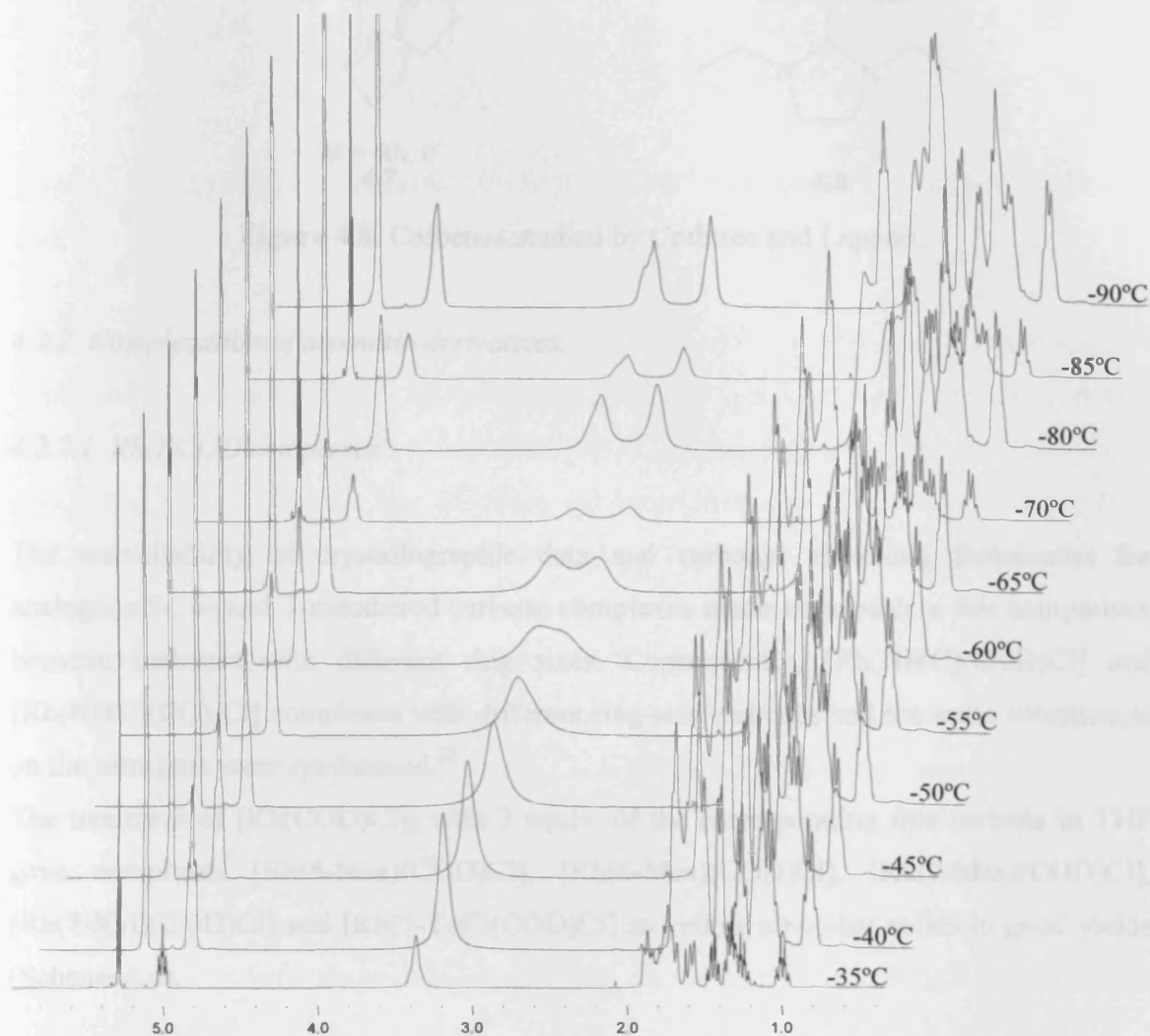


**Figure 4.7** Variable temperature  $^1\text{H}$  NMR of *cis*-[Ir(7-Cy)(CO)<sub>2</sub>Cl].

These results agree with those of Crabtree<sup>11b</sup> and Lappert,<sup>14</sup> where high rotation metal-carbene barriers were observed for the complexes **4.7** and **4.8**, respectively (Figure 4.8). Previous studies with metal-carbene complexes have shown that no electronic rotation barrier exists for the M-C<sub>NHC</sub> bonds, thus suggesting a steric origin of the rotation barrier.<sup>21, 20, 21</sup>

<sup>19</sup> Berger, S.; Braun, S. *200 and more NMR experiments*; Wiley-VCH: New York, 2004.

<sup>20</sup> Enders, D.; Gielen, H. *J. Organomet. Chem.* **2001**, *617*, 70.

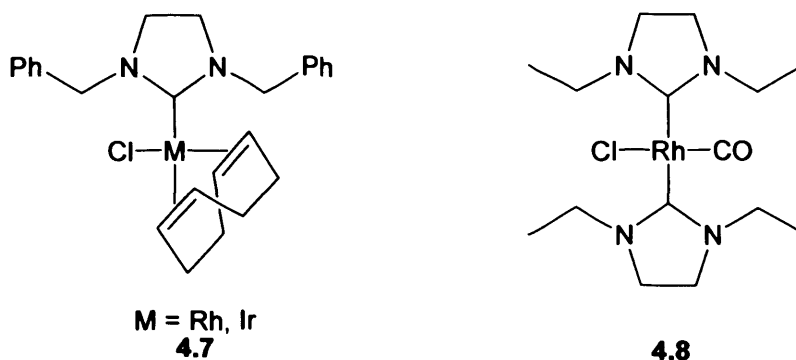


**Figure 4.8.** Carbenes studied by Crabtree and Lappert.

#### 4.2.2. Complexation of aromatic derivatives.

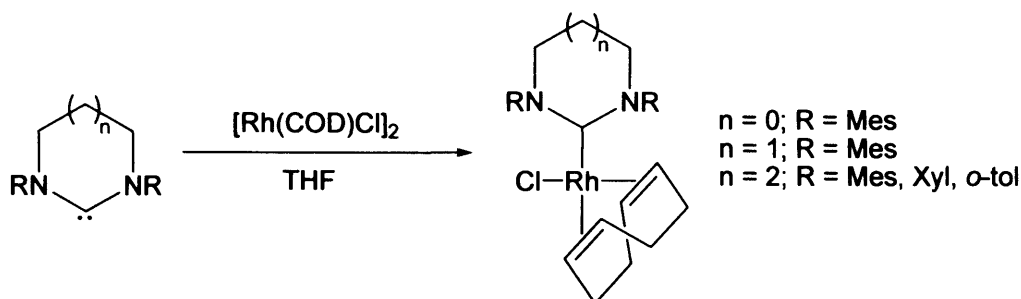
##### 4.2.2.1. Rh(I)COD complexes.

The unavailability of crystallographic data and carbonyl stretching frequencies for analogous 5-, 6- and 7-membered carbene complexes made impossible a fair comparison between carbenes with different ring sizes. Consequently, [Rh(NHC)(COD)Cl] and [Rh(NHC)(CO)<sub>2</sub>Cl] complexes with different ring-size carbenes and the same substituents on the nitrogens were synthesised.<sup>22</sup>

The treatment of [Rh(COD)Cl]<sub>2</sub> with 2 equiv. of the corresponding free carbene in THF gave complexes [Rh(**5-Mes**)(COD)Cl], [Rh(**6-Mes**)(COD)Cl], [Rh(**7-Mes**)(COD)Cl], [Rh(**7-Xyl**)(COD)Cl] and [Rh(**7-Tol**<sup>o</sup>)(COD)Cl] as yellow air-stable solids in good yields (Scheme 4.6).

<sup>21</sup> Burling, S.; Douglas, S.; Mahon, M. F.; Nama, D.; Pregosin, P. S.; Whittlesey, M. K. *Organometallics* **2006**, *25*, 2642.

<sup>22</sup> Complexes [Rh(**5-Mes**)(COD)Cl] and [Rh(**5-Mes**)(CO)<sub>2</sub>Cl] were first reported by Herrmann et al.: Denk, K.; Sirsch, P.; Herrmann, W. A. *J. Organomet. Chem.* **2002**, *649*, 219. The crystal structure of [Rh(**5-Mes**)(COD)Cl] has been recently reported by Grubbs and co-workers: Blum, Angela P.; Ritter, Tobias; Grubbs, Robert H. *Organometallics* **2007**, *26*, 2122. Complexes [Rh(**6-Mes**)(COD)Cl] and [Rh(**6-Mes**)(CO)<sub>2</sub>Cl] were published by Buchmeiser et al. but without a crystal structure, see ref 11.



**Scheme 4.6.** Synthesis of  $[\text{Rh}(\text{NHC})(\text{COD})\text{Cl}]$  (NHC = **5-Mes**, **6-Mes**, **7-Mes**, **7-Xyl**, **Tol<sup>o</sup>**).

Free carbenes, **5-Mes**, **6-Mes**, **7-Mes** and **7-Xyl**, were obtained according to the procedure described in *Chapter 2*. **7-Tol<sup>o</sup>** was generated *in situ* by deprotonation of the corresponding salt with  $\text{K}[\text{HMDS}]$  and reacted with  $[\text{Rh}(\text{COD})\text{Cl}]_2$ . Assuming there is not free rotation about the  $\text{M}-\text{C}_{\text{NHC}}$  bond, four different conformations can be envisaged for  $[\text{Rh}(\text{7-Tol}^{\text{o}})(\text{COD})\text{Cl}]$  depending on the orientation of the methyl groups of the *o*-tolyl rings, two *syn* and two *anti*. The  $^1\text{H}$  and  $^{13}\text{C}$  NMR show only one resonance for the two methyl groups, which confirms formation of one of the *syn* isomers. However, it is not clear whether the methyl groups are positioned on the face of the chloride or the COD ligand. A more thorough examination of the  $^1\text{H}$  and  $^{13}\text{C}$  NMR spectra shows that the second *syn* and the *anti* isomers are also formed in traces.

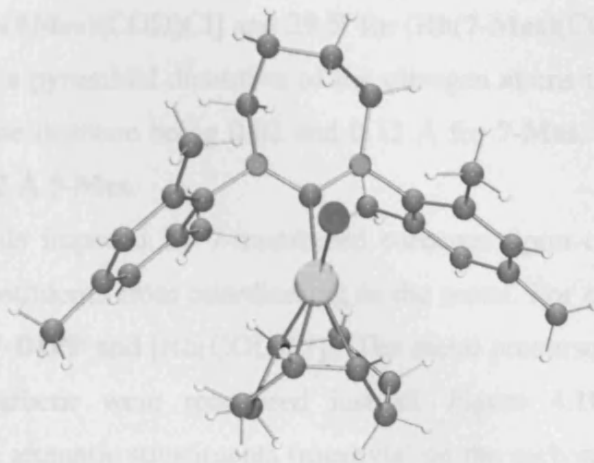
Crystals of  $[\text{Rh}(\text{5-}, \text{6-}, \text{7-Mes})(\text{COD})\text{Cl}]$  suitable for X-ray diffraction were obtained by layering a dichloromethane solution of the corresponding complex with hexane. The crystal structures are shown in Figure 4.9 and selected bond lengths and angles can be found in Table 4.6.

It is clear from the crystallographic data that expansion of the NHC-ring leads to wide  $\text{N}-\text{C}_{\text{NHC}}-\text{N}$  angles. A significant increase of this angle is observed between the five-membered ring  $[\text{Rh}(\text{5-Mes})(\text{COD})\text{Cl}]$  ( $106.8(3)^\circ$ ) and the expanded ring carbenes  $[\text{Rh}(\text{6-Mes})(\text{COD})\text{Cl}]$  and  $[\text{Rh}(\text{7-Mes})(\text{COD})\text{Cl}]$  ( $117.5(4)^\circ$  and  $118.0^\circ$ , respectively). This leads to dramatic changes in the  $\text{C}_{\text{Mes}}-\text{N}-\text{C}_{\text{NHC}}$  angles that are again compressed from an average of  $126.7^\circ$  in  $[\text{Rh}(\text{5-Mes})(\text{COD})\text{Cl}]$  to  $120.3^\circ$  in  $[\text{Rh}(\text{6-Mes})(\text{COD})\text{Cl}]$  and  $118.1^\circ$   $[\text{Rh}(\text{7-Mes})(\text{COD})\text{Cl}]$ . As a result of this, the mesityl substituents on the nitrogens come closer to the metal centre in the expanded carbenes, virtually blocking the two faces of the metal coordination sphere. Therefore, the  $\text{Rh}-\text{C}_{\text{Carbene}}$  distances for expanded ring carbenes  $[\text{Rh}(\text{7-Mes})(\text{COD})\text{Cl}]$  and  $[\text{Rh}(\text{6-Mes})(\text{COD})\text{Cl}]$  ( $2.085 \text{ \AA}$  and  $2.075(10) \text{ \AA}$  respectively)

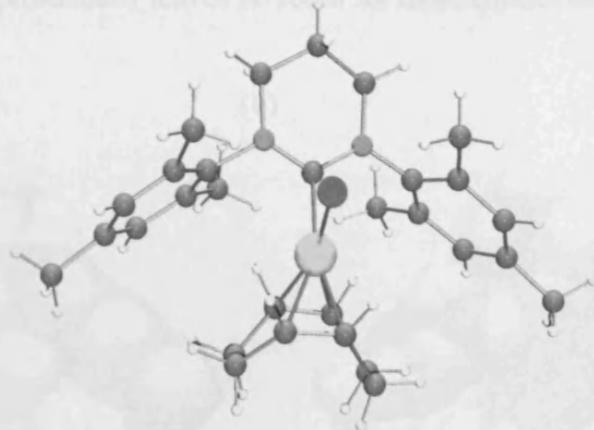


are significantly longer than the one found for five-membered ring [Rh(5-Mes)(COD)Cl] (2.069(3) Å) (Table 4.6).

(a)



(b)



(c)

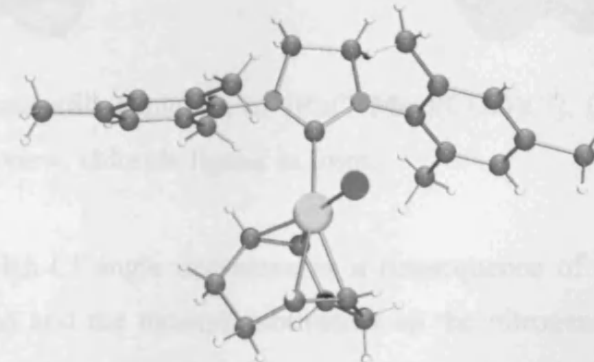


**Figure 4.9.** Solid state molecular structures of [Rh(7-Mes)(COD)Cl] (a), [Rh(6-Mes)(COD)Cl] (b), [Rh(5-Mes)(COD)Cl] (c).

As previously described for silver complexes in *Chapters 2 and 3* for 6- and 7-membered carbene ligands, the extra tension originated by the expansion of the ring does not result in a significant increase of the NCN angle, but in an enlargement of the torsion angle  $\beta$  ( $C_{\text{ring}}-N\cdots N-C_{\text{ring}}$ ), 4.9° for  $[\text{Rh}(\mathbf{6}\text{Mes})(\text{COD})\text{Cl}]$  and 29.5° for  $[\text{Rh}(\mathbf{7}\text{-Mes})(\text{COD})\text{Cl}]$ .

For all three complexes a pyramidal distortion of the nitrogen atoms is observed, with the  $N-[C_{\text{ring}}-C_{\text{NHC}}-C_{\text{Mes}}]$  plane distance being 0.02 and 0.12 Å for **7-Mes**, 0.05 and 0.07 Å for **6-Mes** and 0.15 and 0.02 Å **5-Mes**.

The great steric demands imposed by 7-membered carbenes upon coordination prevent NHC's with bulkier substituents from coordinating to the metal. For example, no reaction was observed between **7-DIPP** and  $[\text{Rh}(\text{COD})\text{Cl}]_2$ . The metal precursor and the hydrolysis product of the free carbene were recovered instead. Figure 4.10 shows the steric interactions between the aromatic substituents (mesityls) on the carbene with the COD and chloride ligands, which presumably leaves no room for more encumbered N-substituents.

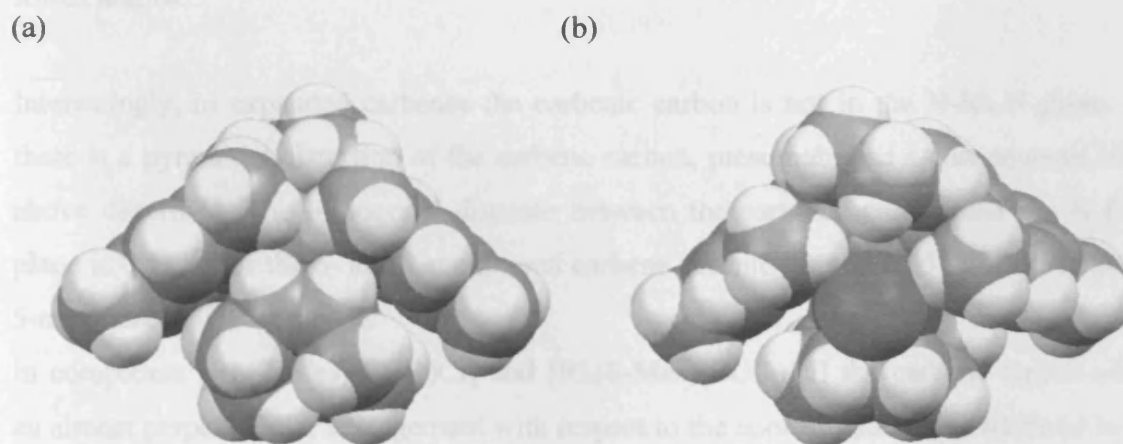


**Figure 4.10.** Mercury spacefill depiction of  $[\text{Rh}(\mathbf{7}\text{-Mes})(\text{COD})\text{Cl}]$ . (a) Side-view, COD ligand in front; (b) Side-view, chloride ligand in front.

Additionally, the  $C_{\text{NHC}}-\text{Rh}-\text{Cl}$  angle decreases as a consequence of the steric repulsion between the COD ligand and the mesityl substituents on the nitrogens, 85.3, 86.7(3) and 93.72(8)° for the 7-, 6- and 5-membered carbene complexes, respectively (Figure 4.10).

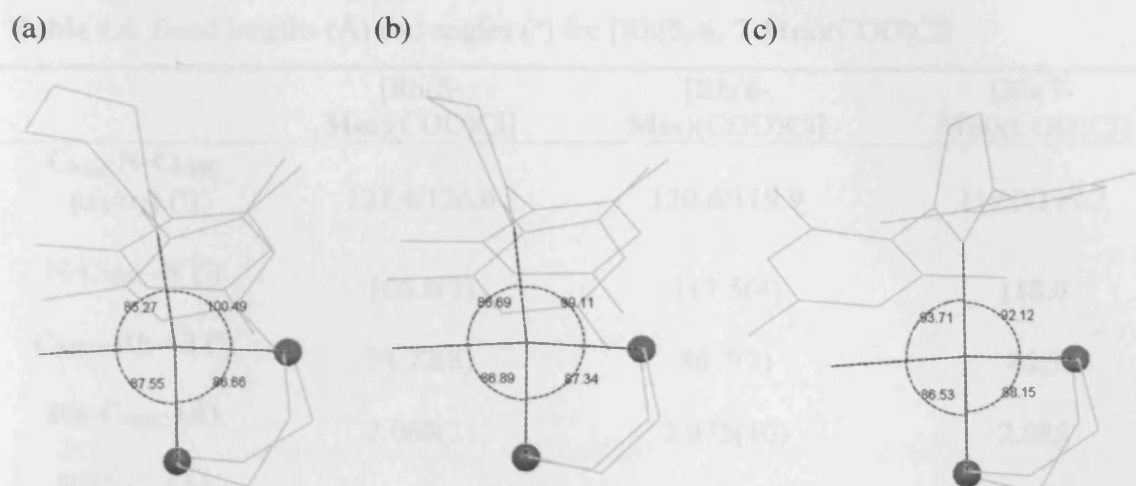


**Figure 4.10.** Mercury plots of the molecular structures of (a)  $[\text{Rh}(\text{7-Mes})(\text{COD})\text{Cl}]$ , (b)  $[\text{Rh}(\text{6-Mes})(\text{COD})\text{Cl}]$  and (c)  $[\text{Rh}(\text{5-Mes})(\text{COD})\text{Cl}]$ . Hydrogen atoms are omitted for clarity. The blue and red dots represent the centroids defined by the  $\text{C}=\text{C}_{\text{COD}}$  atoms and are used for the measurement of the  $\text{C}=\text{C}_{\text{COD}}\text{-Rh-C}_{\text{NHC}}$ ,  $\text{C}=\text{C}_{\text{COD}}\text{-Rh-C}'=\text{C}'_{\text{COD}}$  and  $\text{C}=\text{C}_{\text{COD}}\text{-Rh-Cl}$  angles.

Interestingly, in expanded carbenes the carbenic carbon is not in the N-Rh-N plane, i.e., there is a pyramidal distortion of the carbene carbon, presumably as a consequence of the above described. The orthogonal distance between the carbenic carbon and the N-Rh-N plane is 0.11 Å for the 6- and 7-membered carbene complexes and 0.05 Å in the saturated 5-membered NHC complex.

In complexes  $[\text{Rh}(\text{7-Mes})(\text{COD})\text{Cl}]$  and  $[\text{Rh}(\text{6-Mes})(\text{COD})\text{Cl}]$  the carbene ligand adopts an almost perpendicular arrangement with respect to the coordination plane (defined by the Rh-Cl atoms); the tilt angle  $\theta$  (defined by the coordination and N-C-N planes) is 83.6° for  $[\text{Rh}(\text{6-Mes})(\text{COD})\text{Cl}]$  and 80.4° for  $[\text{Rh}(\text{7-Mes})(\text{COD})\text{Cl}]$  complexes. However, the tilt angle  $\theta$  is only 63.0° for  $[\text{Rh}(\text{5-Mes})(\text{COD})\text{Cl}]$ .

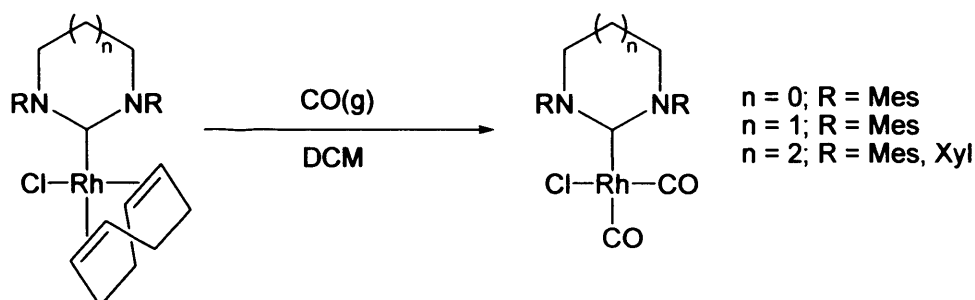
**Table 4.6.** Bond lengths (Å) and angles (°) for [Rh(**5**, **6**, **7-Mes**)(COD)Cl]

	[Rh( <b>5</b> - <b>Mes</b> )(COD)Cl]	[Rh( <b>6</b> - <b>Mes</b> )(COD)Cl]	[Rh( <b>7</b> - <b>Mes</b> )(COD)Cl]
$C_{\text{Mes}}\text{-N-C}_{\text{NHC}}$ ( $\alpha_1/\alpha_2$ ) (°)	127.4/126.0	120.6/119.9	119.0/117.2
N-C <sub>NHC</sub> -N (°)	106.8(3)	117.5(4)	118.0
C <sub>NHC</sub> -Rh-Cl (°)	93.72(8)	86.7(3)	85.3
Rh-C <sub>NHC</sub> (Å)	2.068(3)	2.075(10)	2.085
N-C <sub>NHC</sub> (Å) ( $\alpha_1$ -site/ $\alpha_2$ -site)	1.354/1.354	1.365/1.466	1.360/1.352
$\beta$ (C <sub>ring</sub> -N...N-C <sub>ring</sub> )	7.4	4.9	29.5

The <sup>1</sup>H NMR and <sup>13</sup>C NMR show three different resonances for the methyl groups at the mesityls for [Rh(**5-Mes**)(COD)Cl], [Rh(**6-Mes**)(COD)Cl] and [Rh(**7-Mes**)(COD)Cl], indicating that in solution the carbene keeps the perpendicular orientation to the coordination plane observed in the solid state. The same behaviour is observed for [Rh(**6-Mes**)(CO)<sub>2</sub>Cl] and [Rh(**7-Mes**)(CO)<sub>2</sub>Cl] despite the fact that the steric hindrance of the carbonyl ligands is significantly lower than that of cyclooctadiene. Interestingly, as previously explained in section 4.2.1.5 the carbene ligand in complex [Rh(**7-Cy**)(CO)<sub>2</sub>Cl] rotates at ambient temperature, whereas **7-Mes** does not, indicating that the aromatic N-substitution affords a more encumbered ligand. However, in the case of the biscarbonyl complex [Rh(**5-Mes**)(CO)<sub>2</sub>Cl] the <sup>1</sup>H NMR and <sup>13</sup>C NMR show only two resonances, i.e., the two *ortho* methyls are magnetically equivalent. This implies free rotation of the carbene ligand about the Rh-C<sub>NHC</sub> bond as a consequence of the reduced steric demand of **5-Mes** in comparison with **6-Mes** and **7-Mes**.

#### 4.2.2.2. Rhodium(I) carbonyl complexes.

The carbonyl complexes [Rh(NHC)(CO)<sub>2</sub>Cl] (NHC = **5-Mes**, **6-Mes**, **7-Mes** and **7-Xyl**) were obtained in good yields after treatment of a dichloromethane solution of the corresponding 1,5-cyclooctadiene complex with carbon monoxide (1 atm) for twenty minutes, Scheme 4.7.



Scheme 4.7. Synthesis of carbonyl complexes.

In Table 4.7 the carbonyl stretching frequencies of *cis*-[Rh(**5-Mes**)(CO)<sub>2</sub>Cl], *cis*-[Rh(**6-Mes**)(CO)<sub>2</sub>Cl], *cis*-[Rh(**7-Mes**)(CO)<sub>2</sub>Cl] and *cis*-[Rh(**7-Xyl**)(CO)<sub>2</sub>Cl] are listed and compared to bibliographic values.

Table 4.7. Infrared  $\nu(\text{CO})$  for Rh(CO)<sub>2</sub>(L)Cl complexes recorded in CH<sub>2</sub>Cl<sub>2</sub>.

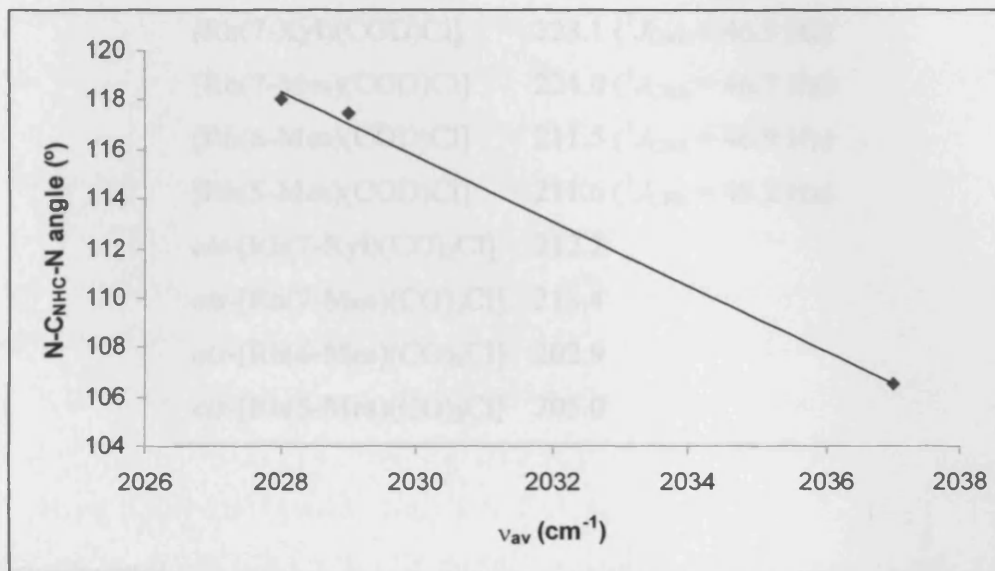
Complex	$\nu_{\text{as}} (\text{cm}^{-1})$	$\nu_{\text{av}} (\text{cm}^{-1})$	$\nu_{\text{av}} (\text{cm}^{-1})$ (bibliography)
<i>cis</i> -[Rh( <b>5-Mes</b> )(CO) <sub>2</sub> Cl]	1995, 2080	2037	2038 <sup>22</sup>
<i>cis</i> -[Rh( <b>6-Mes</b> )(CO) <sub>2</sub> Cl]	1987, 2071	2029	2019 <sup>22</sup>
<i>cis</i> -[Rh( <b>7-Mes</b> )(CO) <sub>2</sub> Cl]	1987, 2069	2028	-
<i>cis</i> -[Rh( <b>7-Xyl</b> )(CO) <sub>2</sub> Cl]	1986, 2071	2028	-

The average carbonyl stretching frequencies for the rhodium complexes shows an almost linear increase of the electron density on the metal with the NCN angle (plot 4.1), which agrees with recent theoretical calculations.<sup>23</sup> According to them, in the absence of other influences (such as electron-withdrawing/donating groups), it is the NCN angle that has the strongest influence on basicity.

It is worth noting that the difference in electron density on the metal centre, indicated by the carbonyl stretching frequencies, is virtually non-existent between the 6- and the 7-membered carbene complexes, but is significant between the 5- and the 6-membered. On the other hand, <sup>13</sup>C NMR shows a shift to high field of the carbene carbon for *cis*-[Rh(**7-Mes**)(COD)Cl] and *cis*-[Rh(**7-Mes**)(CO)<sub>2</sub>Cl] respect to *cis*-[Rh(**5-**, **6-Mes**)(COD)Cl] and *cis*-[Rh(**5**, **6-Mes**)(CO)<sub>2</sub>Cl] (Table 4.8). This suggests that **7-Mes** has, either a higher electron density at the carbene carbon than **6-Mes** or a greater contribution of the triplet

<sup>23</sup> Magill, A. M.; Cavell, K. J.; Yates, B.F. *J. Am. Chem. Soc.* **2004**, *126*, 8717.

state. A similar behaviour was observed for the free carbenes in *Chapter 2* and silver complexes in *Chapter 3*.



**Plot 4.1.** Relationship between the N-C<sub>NHC</sub>-N angle and the average carbonyl frequency.

In the light of the similar values obtained for the steric parameters (Table 4.6) and the carbonyl stretching frequencies (Table 4.7) of [Rh(**6-Mes**)(COD)Cl] and [Rh(**7-Mes**)(COD)Cl], the longer M-C bond observed in the case of [Rh(**7-Mes**)(COD)Cl] in relation to its 6-membered analogue can not be explained considering carbenes as pure  $\sigma$ -donors, as the average carbonyl frequencies are virtually the same, 2028 and 2029  $\text{cm}^{-1}$ , respectively. The carbonyl vibration is a measurement of the overall electron density on the metal centre. This electron density is the outcome of the electron density donated by the carbene ligand from its  $\sigma$ -orbital to the metal and the electron density back-donated from the metal to the empty  $p$  orbital on the carbene. Therefore, a better  $\sigma$  donor ability and an enhanced behaviour as  $\pi$ -acceptor in the case of the 6-membered carbene would explain its shorter M-C bond and the similar carbonyl stretching frequencies observed for the 6- and 7-membered NHC's.

**Table 4.8.**  $^{13}\text{C}$  NMR shifts and coupling constants for the carbene carbon.

Complex	$^{13}\text{C}$ NMR $\delta$ (ppm)
[Rh(7-Tol <sup>o</sup> )(COD)Cl]	222.8 ( $^1J_{\text{CRh}} = 45.0$ Hz)
[Rh(7-Xyl)(COD)Cl]	223.1 ( $^1J_{\text{CRh}} = 46.3$ Hz)
[Rh(7-Mes)(COD)Cl]	224.0 ( $^1J_{\text{CRh}} = 46.7$ Hz)
[Rh(6-Mes)(COD)Cl]	211.5 ( $^1J_{\text{CRh}} = 46.9$ Hz)
[Rh(5-Mes)(COD)Cl]	211.6 ( $^1J_{\text{CRh}} = 48.2$ Hz)
<i>cis</i> -[Rh(7-Xyl)(CO) <sub>2</sub> Cl]	212.2
<i>cis</i> -[Rh(7-Mes)(CO) <sub>2</sub> Cl]	213.4
<i>cis</i> -[Rh(6-Mes)(CO) <sub>2</sub> Cl]	202.9
<i>cis</i> -[Rh(5-Mes)(CO) <sub>2</sub> Cl]	205.0

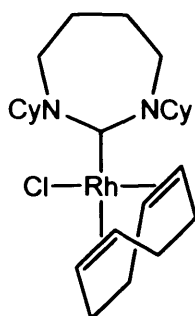
### 4.3. Experimental

#### General remarks:

In an MBraun glove box, the solids were combined together in a Schlenk under a nitrogen atmosphere, removed from the glove box and transferred to a Schlenk line where the solvents were added by syringe. Diethyl ether, tetrahydrofurane and hexane were distilled from sodium and benzophenone under  $\text{N}_2$  atmosphere. Dichloromethane was distilled from calcium hydride under  $\text{N}_2$  atmosphere.  $[\text{Rh}(\text{COD})\text{Cl}]_2$ ,  $[\text{Rh}(\text{COD})\text{Cl}]_2$  and  $[\text{Pt}(\text{nbe})_3]$  was synthesised according to literature methods.<sup>24</sup>  $^1\text{H}$  and  $^{13}\text{C}$  spectra were recorded using a Bruker Advance DPX<sub>400</sub> spectrometer. Chemical shifts ( $\delta$ ) were expressed in ppm downfield from tetramethylsilane using the residual proton as an internal standard ( $\text{CDCl}_3$ ,  $^1\text{H}$  7.26 ppm and  $^{13}\text{C}$  77.0 ppm; benzene- $\text{d}_6$   $^1\text{H}$  7.15 ppm and  $^{13}\text{C}$  128.0 ppm). Coupling constants are expressed in Hertz. HRMS were obtained on a Waters LCT Premier XE instrument and are reported as  $m/z$  (relative intensity). Infrared spectra were recorded using a JASCO FT/IR-660 *Plus* spectrometer and analysed in solution (dichloromethane).

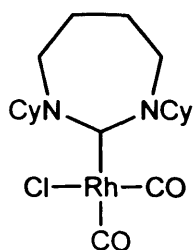
#### [Rh(7-Cy)(COD)Cl]

<sup>24</sup> (a) Crascall, Louise E.; Spencer, John L. *Inorganic Syntheses* 1990, 28 (Reagents Transition Met. Complex Organomet. Synth.), 126. (b) Giordano, G.; Crabtree, R. H. *Inorganic Syntheses* 1990, 28 (Reagents Transition Met. Complex Organomet. Synth.), 88.



KNSi(Me<sub>3</sub>)<sub>2</sub> (140 mg, 0.7 mmol) and 7-Cy·HPF<sub>6</sub> (285 mg, 0.7 mmol) were placed into a Schlenk tube followed by the addition of diethyl ether (10 mL). The solution was stirred for 30 min and subsequently filtered into another Schlenk tube containing a 10 mL thf solution of [Rh(COD)Cl]<sub>2</sub> (0.35 mmol). An immediate color change was observed from light to dark yellow. After the reaction was stirred at room temperature for 1 h, the volatiles were removed *in vacuo*. The yellow solid obtained was washed with hexane (2 x 20 mL) and dried. Crystals suitable for X-ray diffraction were obtained by layering a dichloromethane solution of the compound with hexane. Yield: [200 mg] 66%. <sup>1</sup>H NMR (CDCl<sub>3</sub>, 500 MHz, rt): δ 6.18 (2H, dddd, <sup>3</sup>J<sub>HH</sub> ≅ <sup>3</sup>J<sub>HH</sub> = 11.5, <sup>3</sup>J<sub>HH</sub> ≅ <sup>3</sup>J<sub>HH</sub> = 3.2, NCH), 4.78 (2H, m, CH<sub>COD</sub>), 3.34 (2H, m, <sup>2</sup>J<sub>HH</sub> =, <sup>3</sup>J<sub>HH</sub> =, NCH<sub>2</sub>), 3.21 (2H, ddd, <sup>2</sup>J<sub>HH</sub> =, <sup>3</sup>J<sub>HH</sub> =, NCH<sub>2</sub>), 3.17 (2H, m, CH<sub>COD</sub>), 2.29 (6H, m, CH<sub>2</sub>), 1.87 (2H, m, CH<sub>2</sub>), 1.79 (10H, m, CH<sub>2</sub>), 1.69 (4H, m, CH<sub>2</sub>), 1.52 (6H, m, CH<sub>2</sub>), 1.26 (2H, dddd, <sup>2</sup>J<sub>HH</sub> ≅ <sup>3</sup>J<sub>HH</sub> = 12.0, <sup>3</sup>J<sub>HH</sub> ≅ <sup>3</sup>J<sub>HH</sub> = 3.7, CH<sub>2</sub>), 1.08 (2H, ddddd, <sup>2</sup>J<sub>HH</sub> ≅ <sup>3</sup>J<sub>HH</sub> = 13.0, <sup>3</sup>J<sub>HH</sub> ≅ <sup>3</sup>J<sub>HH</sub> ≅ <sup>3</sup>J<sub>HH</sub> = 3.8, CH<sub>2</sub>); <sup>13</sup>C NMR (CDCl<sub>3</sub>, 100 MHz, rt): δ 215.3 (d, <sup>1</sup>J<sub>Rh</sub> = 43.7, NCN), 93.9 (d, <sup>1</sup>J<sub>Rh</sub> = 6.8, C<sub>C=C</sub>), 66.8 (d, <sup>1</sup>J<sub>Rh</sub> = 5.4, C<sub>C=C</sub>), 65.8 (s, NCH), 42.7 (s, NCH<sub>2</sub>), 31.8 (s, CH<sub>2</sub>), 31.2 (s, CH<sub>2</sub>), 30.3 (s, CH<sub>2</sub>), 27.9 (s, CH<sub>2</sub>), 25.6 (s, CH<sub>2</sub>), 25.3 (s, CH<sub>2</sub>), 24.9 (s, CH<sub>2</sub>); Anal. Found (Calcd) for C<sub>25</sub>H<sub>42</sub>ClRhN<sub>2</sub>: C, 58.87 (58.99); H, 8.37 (8.32). *m/z* (ES, CH<sub>3</sub>CN) 473.2382 (M-Cl<sup>+</sup>. C<sub>25</sub>H<sub>42</sub>N<sub>2</sub>Rh requires 473.2403), 514.2619 (M+MeCN-Cl<sup>+</sup>).

### *Cis*-[Rh(7-Cy)(CO)<sub>2</sub>Cl]

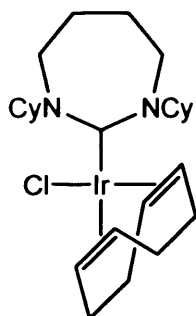


Carbon monoxide was slowly bubbled for 30 min through a solution of Rh(COD)(3)Cl (100 mg, 0.075 mmol) in dichloromethane (10 mL). A color change from yellow to pale yellow was observed during the reaction. The volatiles were removed under reduced pressure, and the obtained solid was washed with cold hexane (2 x 30 mL) and dried. Yield: 84% (0.065 g). <sup>1</sup>H NMR (toluene-*d*<sup>8</sup>, 500 MHz, rt): δ 5.34 (2H, dddd, <sup>3</sup>J<sub>HH</sub> ≅ <sup>3</sup>J<sub>HH</sub> = 11.9, <sup>3</sup>J<sub>HH</sub> ≅ <sup>3</sup>J<sub>HH</sub> = 3.4, NCH), 2.91 (4H, m, NCH<sub>2</sub>), 2.30 (2H, m, CH<sub>2</sub>), 1.68 (6H, m, CH<sub>2</sub>), 1.55 (4H, m, CH<sub>2</sub>), 1.40 (6H, m, CH<sub>2</sub>), 1.16 (2H, dddd, <sup>2</sup>J<sub>HH</sub> ≅ <sup>3</sup>J<sub>HH</sub> = 12.2, <sup>3</sup>J<sub>HH</sub> ≅ <sup>3</sup>J<sub>HH</sub> = 3.5, CH<sub>2</sub>), 1.08 (2H, dddd, <sup>2</sup>J<sub>HH</sub> ≅ <sup>3</sup>J<sub>HH</sub> = 12.1, <sup>3</sup>J<sub>HH</sub> ≅ <sup>3</sup>J<sub>HH</sub> = 3.7, CH<sub>2</sub>), 0.91 (2H, ddddd, <sup>2</sup>J<sub>HH</sub> ≅ <sup>3</sup>J<sub>HH</sub> = 13.1, <sup>3</sup>J<sub>HH</sub> ≅ <sup>3</sup>J<sub>HH</sub> ≅ <sup>3</sup>J<sub>HH</sub> = 3.6, CH<sub>2</sub>); <sup>13</sup>C NMR (toluene-*d*<sup>8</sup>, 125 MHz, rt): δ 206.2 (d, <sup>1</sup>J<sub>Rh</sub> = 38, NCN), 188.2 (d, <sup>1</sup>J<sub>Rh</sub> = 54, CO), 184.9 (d, <sup>1</sup>J<sub>Rh</sub> = 76, CO), 67.6 (s, NCH),



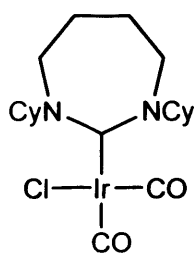
44.1 (s, NCH<sub>2</sub>), 30.8 (s, CH<sub>2</sub>), 30.1 (s, CH<sub>2</sub>), 26.1 (s, CH<sub>2</sub>), 25.8 (s, CH<sub>2</sub>), 25.7 (s, CH<sub>2</sub>); Anal. Found (Calcd) for C<sub>19</sub>H<sub>30</sub>ClRhN<sub>2</sub>O<sub>2</sub>: C, 50.06 (49.96); H, 6.61 (6.62). MS (ES, CH<sub>3</sub>CN): *m/z* 462.1648 (M-Cl<sup>+</sup>; C<sub>19</sub>H<sub>30</sub>N<sub>2</sub>O<sub>2</sub>Rh requires 462.1628).

### [Ir(7-Cy)(COD)Cl]



KNSi(Me<sub>3</sub>)<sub>2</sub> (0.200 g, 1.0 mmol) and 7-Cy·HPF<sub>6</sub> (0.408 g, 1.0 mmol) were placed into a Schlenk tube followed by the addition of diethyl ether (10 mL). The solution was stirred for 30 min and subsequently filtered into a Schlenk tube containing a 10 mL thf solution of [Ir(COD)Cl]<sub>2</sub> (0.336 g, 0.5 mmol); an immediate color change was observed from light to dark yellow. After the reaction mixture was stirred at room temperature for 1 h, the solvent was removed *in vacuo*. The precipitate was washed with hexane and dried under vacuum to afford 450 mg of a brown solid. The product was purified by chromatography on silica gel with dichloromethane as the mobile phase. The product was eluted as a yellow band in the first fraction (R<sub>f</sub> = 0.6). The product fractions were pooled and evaporated to dryness to yield a yellow solid. Crystals suitable for X-ray diffraction were obtained by layering hexane on a dichloromethane solution of the compound. Yield: 62% (370 mg). <sup>1</sup>H NMR (CDCl<sub>3</sub>, 500 MHz, rt): δ 5.74 (2H, dddd, <sup>3</sup>J<sub>HH</sub> ≈ <sup>3</sup>J<sub>HH} = 11.4, <sup>3</sup>J<sub>HH} ≈ <sup>3</sup>J<sub>HH} = 3.1, NCH), 4.33 (2H, m, CH<sub>COD</sub>), 3.39 (2H, m, NCH<sub>2</sub>), 3.26 (2H, m, NCH<sub>2</sub>), 2.86 (2H, m, CH<sub>COD</sub>), 2.11 (6H, m, CH<sub>2</sub>), 1.3 – 1.9 (20H, m, CH<sub>2</sub>), 1.27 (4H, m, CH<sub>2</sub>), 1.03 (2H, m, CH<sub>2</sub>); <sup>13</sup>C NMR (CDCl<sub>3</sub>, 100 MHz, rt): δ 208.3 (s, NCN), 78.4 (s, C<sub>C=C</sub>), 65.3 (s, C<sub>C=C</sub>), 50.6 (s, NCH), 43.4 (s, NCH<sub>2</sub>), 32.5 (s, CH<sub>2</sub>), 31.3 (s, CH<sub>2</sub>), 30.2 (s, CH<sub>2</sub>), 28.5 (s, CH<sub>2</sub>), 25.5 (s, CH<sub>2</sub>), 25.1 (s, CH<sub>2</sub>), 24.8 (s, CH<sub>2</sub>); Anal. Found (Calcd) for C<sub>25</sub>H<sub>42</sub>ClIrN<sub>2</sub>: C, 49.91 (50.19); H, 7.01 (7.08). *m/z* (ES, CH<sub>3</sub>CN) 488.1728 ([M-Cl]<sup>+</sup> C<sub>25</sub>H<sub>42</sub>N<sub>2</sub>Ir requires 488.1701).</sub></sub></sub>

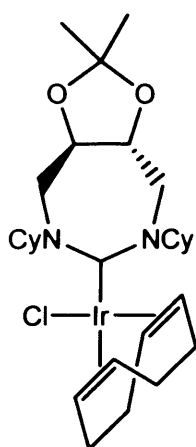
### Cis-[Ir(7-Cy)(CO)<sub>2</sub>Cl]



Ir(COD)(7-Cy)Cl (100 mg, 0.17 mmol) was placed in a round-bottom flask, and subsequently, 10 mL of dichloromethane was added. Into the yellow solution carbon monoxide was bubbled for 30 min, after which the color changed to light yellow, the volatiles were subsequently removed under reduced pressure, and the crude solid was washed with cold hexane. Yield: 82% (78 mg). <sup>1</sup>H NMR (CDCl<sub>3</sub>, 500MHz, rt): δ 5.11 (2H, m, NCH), 3.39 (4H, m, NCH<sub>2</sub>),

1.99 (2H, m, CH<sub>2</sub>), 1.89 (2H, m, CH<sub>2</sub>), 1.76 (6H, m, CH<sub>2</sub>), 1.69 (2H, m, CH<sub>2</sub>), 1.59 (2H, m, CH<sub>2</sub>), 1.34 (8H, m, CH<sub>2</sub>), 1.02 (2H, m, CH<sub>2</sub>); <sup>1</sup>H NMR (toluene-*d*<sup>8</sup>, 500 MHz, rt): δ 5.18 (2H, dddd, <sup>3</sup>J<sub>HH</sub> ≈ <sup>3</sup>J<sub>HH</sub> = 11.6, <sup>3</sup>J<sub>HH</sub> ≈ <sup>3</sup>J<sub>HH</sub> = 3.5, NCH), 2.63 (4H, m, NCH<sub>2</sub>), 1.96 (2H, m, CH<sub>2</sub>), 1.53 (2H, m, CH<sub>2</sub>), 1.44 (4H, m, CH<sub>2</sub>), 1.39 (4H, m, CH<sub>2</sub>), 1.14 (6H, m, CH<sub>2</sub>), 0.93 (2H, m, CH<sub>2</sub>), 0.89 (2H, m, CH<sub>2</sub>), 0.65 (2H, m, CH<sub>2</sub>); <sup>13</sup>C NMR (CDCl<sub>3</sub>, 125 MHz, rt): δ 199.8 (s, NCN), 180.2 (s, CO), 168.2 (s, CO), 66.1 (s, NCH), 44.0 (s, NCH<sub>2</sub>), 30.6 (s, CH<sub>2</sub>), 29.8 (s, CH<sub>2</sub>), 29.0 (s, CH<sub>2</sub>), 24.7 (s, CH<sub>2</sub>), 24.5 (s, CH<sub>2</sub>), 24.4 (s, CH<sub>2</sub>); <sup>13</sup>C NMR (toluene-*d*<sup>8</sup>, 125 MHz, rt): δ 200.5 (s, NCN), 180.8 (s, CO), 169.2 (s, CO), 65.9 (s, NCH), 43.4 (s, NCH<sub>2</sub>), 29.6 (s, CH<sub>2</sub>), 28.8 (s, CH<sub>2</sub>), 24.6 (s, CH<sub>2</sub>), 24.4 (s, CH<sub>2</sub>), 24.3 (s, CH<sub>2</sub>), 24.2 (s, CH<sub>2</sub>); Anal. Found (Calcd) for C<sub>17</sub>H<sub>30</sub>ClN<sub>2</sub>O<sub>2</sub>Ir: C, 41.62 (41.79); H, 5.46 (5.54). MS (ES, CH<sub>3</sub>CN): *m/z* 488.1728 (M - 2CO<sup>+</sup>; C<sub>17</sub>H<sub>30</sub>N<sub>2</sub>ClIr requires 488.1704).

### [Ir(DIOC-Cy)(COD)Cl]

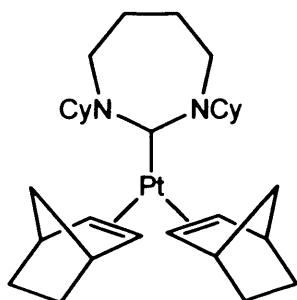


LiN(iPr)<sub>2</sub> (6 mg, 0.05 mmol) and **DIOC-7-Cy·HBr** (19 mg, 0.05 mmol) were placed into a Schlenk tube followed by the addition of diethyl ether (10 mL). The solution was stirred for 30 min and subsequently filtered into another Schlenk tube containing a 10 mL THF solution of [Ir(COD)Cl]<sub>2</sub> (17 mg, 0.025 mmol). After the reaction was stirred at room temperature for 1 h, the volatiles were removed in vacuo. The yellow solid obtained was washed with hexane (2 x 20 mL) and dried. Crystals suitable for X-ray diffraction were obtained by layering a dichloromethane solution of the complex with hexane. <sup>1</sup>H NMR (400

MHz, C<sub>6</sub>D<sub>6</sub>, rt): δ 6.37 (1H, dddd, <sup>3</sup>J<sub>HH</sub> ≈ <sup>3</sup>J<sub>HH</sub> = 12.1, <sup>3</sup>J<sub>HH</sub> ≈ <sup>3</sup>J<sub>HH</sub> = 3.1, NCH), 6.09 (1H, dddd, <sup>3</sup>J<sub>HH</sub> ≈ <sup>3</sup>J<sub>HH</sub> = 11.5, <sup>3</sup>J<sub>HH</sub> ≈ <sup>3</sup>J<sub>HH</sub> = 3.5, NCH), 5.16 (1H, ddd, <sup>3</sup>J<sub>HH</sub> ≈ <sup>3</sup>J<sub>HH</sub> = 8.0, <sup>3</sup>J<sub>HH</sub> = 3.0, OCH), 5.01 (1H, ddd, <sup>3</sup>J<sub>HH</sub> ≈ <sup>3</sup>J<sub>HH</sub> = 8.0, <sup>3</sup>J<sub>HH</sub> = 5.1, OCH), 3.58 (2H, ddd, <sup>3</sup>J<sub>HH</sub> = 13.1, <sup>3</sup>J<sub>HH</sub> = 6.0, <sup>3</sup>J<sub>HH</sub> = 3.5), 3.39 (1H, ddd, <sup>3</sup>J<sub>HH</sub> = 11.0, <sup>3</sup>J<sub>HH</sub> = 8.5, <sup>3</sup>J<sub>HH</sub> = 3.0), 3.27 (1H, ddd, <sup>3</sup>J<sub>HH</sub> = 11.0, <sup>3</sup>J<sub>HH</sub> = 8.5, <sup>3</sup>J<sub>HH</sub> = 3.0), 3.17 (1H, ddd, <sup>3</sup>J<sub>HH</sub> ≈ <sup>3</sup>J<sub>HH</sub> = 7.0, <sup>3</sup>J<sub>HH</sub> = 2.0), 3.07 (1H, m), 3.00 (1H, m), 2.53 (1H, m), 2.37 (2H, m), 2.30 - 1.30 (33H, m). <sup>13</sup>C NMR (100 MHz, C<sub>6</sub>D<sub>6</sub>, rt): δ 223.6 (s, NCHN), 113.6 (s, CMe<sub>2</sub>), 82.1 (s, C=C), 81.1 (s, C=C), 80.6 (s, C=C), 79.9 (s, C=C), 66.3 (s, OCH), 68.2 (s, OCH), 54.3 (s), 50.8 (s), 47.9 (s), 46.9 (s), 46.7 (s), 35.3 (s), 33.4 (s), 33.0 (s), 32.1 (s), 31.7 (s), 30.0 (s), 29.1 (s), 27.4 (s), 27.3 (s),

27.0 (s), 26.8 (s), 26.5 (s), 26.2 (s), 26.1 (s). MS (ES, CH<sub>3</sub>CN): *m/z* 676.3452 (M+ CH<sub>3</sub>CN-Br<sup>+</sup>; C<sub>30</sub>H<sub>49</sub>N<sub>3</sub>O<sub>2</sub>Ir requires 676.3454).

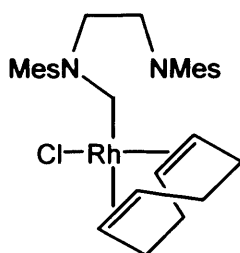
### [Pt(7-Cy)(nbe)<sub>2</sub>Cl]



KNSi(Me<sub>3</sub>)<sub>2</sub> (10 mg, 0.05 mmol) and 3-HPF<sub>6</sub> (20 mg, 0.05 mmol) were placed into a flamed Schlenk tube followed by addition of diethyl ether (5 mL). The solution was stirred for 30 min and subsequently filtered into another Schlenk tube containing a 4 mL THF solution of platinum tris(norbornene) (23 mg, 0.05 mmol). After the reaction mixture was stirred at room temperature for 1 h,

the volatiles were removed in vacuo. The residue was dissolved in dry hexane and filtered through a cannula, fitted with a glass filter paper, to another Schlenk tube. Crystals of the title compound were grown after the hexane solution was allowed to stand in the fridge for 2 days. Yield: 82% (32 mg). <sup>1</sup>H NMR (C<sub>6</sub>D<sub>6</sub>, 400 MHz, rt): δ 4.43 (2H, br, NCH), 3.05 (2H, br, nbe), 2.93 (4H, br, NCH<sub>2</sub>), 2.70 (2H, br, nbe), 2.25 (2H, br, nbe), 2.0 - 1.0 (30H, br), 0.80 (4H, br, nbe), 0.32 (2H, br, nbe), 0.15 (2H, br, nbe). <sup>13</sup>C NMR (C<sub>6</sub>D<sub>6</sub>, 100 MHz, rt): δ 64.2 (br), 55.2 (br), 45.2 (br), 43.9 (br), 30.6-33.5 (br), 26.2 (br).

### [Rh(5-Mes)(COD)Cl]

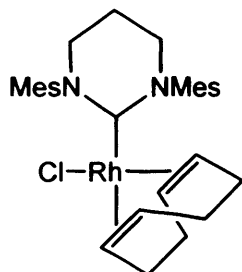


A solution of 5-Mes (67 mg, 0.22 mmol) in dry THF (10 mL) was added to a solution of [Rh(COD)Cl]<sub>2</sub> (50 mg, 0.10 mmol) in dry THF (10 mL) and stirred at ambient temperature for 1 h under argon atmosphere. The solvent was then removed *in vacuo* to give a dark yellow solid which was subsequently triturated with hexanes to give 63 mg (0.11 mmol) of 1 as a bright yellow powder (57% yield).

Crystals suitable for X-ray analysis were obtained by layering diethyl ether on a dichloromethane solution of the complex. <sup>1</sup>H-NMR (400 MHz, CDCl<sub>3</sub>, rt): δ 6.96 (2H, s, CH<sub>Mes</sub>), 6.91 (2H, s, CH<sub>Mes</sub>), 4.40 (2H, m, CH<sub>COD</sub>), 3.75-3.82 (4H, m, NCH<sub>2</sub>), 3.30 (2H, m, CH<sub>COD</sub>), 2.53 (6H, s, CH<sub>3</sub>), 2.27 (6H, s, CH<sub>3</sub>), 2.25 (6H, s, CH<sub>3</sub>), 1.70-1.72 (4H, m, CH<sub>2</sub> COD), 1.43-1.47 (4H, m, CH<sub>2</sub> COD). <sup>13</sup>C NMR (100 MHz, CDCl<sub>3</sub>, rt): δ 211.6 (d, <sup>1</sup>J<sub>CRh</sub> = 48.2, C<sub>Carbene</sub>), 137.4 (s, C<sub>Mes</sub>), 136.8 (s, C<sub>Mes</sub>), 135.2 (s, C<sub>Mes</sub>), 134.2 (s, C<sub>Mes</sub>), 128.9 (s, CH<sub>Mes</sub>), 127.3 (s, CH<sub>Mes</sub>), 96.1 (s, d, <sup>1</sup>J<sub>RhC</sub> = 7.1, CH<sub>COD</sub>), 66.5 (s, d, <sup>1</sup>J<sub>RhC</sub> = 7.5 Hz, CH<sub>COD</sub>), 50.3 (s, NCH<sub>2</sub>), 31.6 (s, CH<sub>2</sub> COD), 27.1 (s, CH<sub>2</sub> COD), 20.1 (s, CH<sub>3</sub>), 18.9 (s, CH<sub>3</sub>),

17.3 (s, CH<sub>3</sub>); MS (ES, CH<sub>3</sub>CN): *m/z* 558.2354 (M-Cl+CH<sub>3</sub>CN<sup>+</sup>; C<sub>31</sub>H<sub>41</sub>N<sub>3</sub>Rh requires 558.2356).

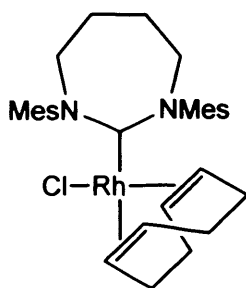
### [Rh(6-Mes)(COD)Cl]



A solution of **6-Mes** (74 mg, 0.22 mmol) in dry THF (10 mL) was added to a solution of [Rh(COD)Cl]<sub>2</sub> (50 mg, 0.10 mmol) in dry THF (10 mL) and stirred at ambient temperature for 1h under argon atmosphere. The solvent was then removed *in vacuo* to give a dark yellow solid which was subsequently triturated with hexanes to give 71 mg (0.12 mmol) of **3** as a bright yellow powder (62% yield).

Crystals suitable for X-ray analysis were obtained by layering diethyl ether on a dichloromethane solution of the complex. <sup>1</sup>H NMR (400 MHz, CDCl<sub>3</sub>, rt): 6.98 (2H, bs, CH<sub>Mes</sub>), 6.88 (2H, bs, CH<sub>Mes</sub>), 4.16 (2H, m, CH<sub>COD</sub>), 3.27 (4H, m, NCH<sub>2</sub>), 3.13 (2H, m, CH<sub>COD</sub>), 2.52 (6H, s, CH<sub>3</sub>), 2.28 (6H, s, CH<sub>3</sub>), 2.20 (6H, s, CH<sub>3</sub>), 2.08 (2H, bs, CH<sub>2</sub>), 1.39 (4H, m, CH<sub>2</sub> COD), 1.19 (4H, m, CH<sub>2</sub> COD). <sup>13</sup>C NMR (100 MHz, CDCl<sub>3</sub>, rt): δ 211.5 (d, <sup>1</sup>J<sub>CRh</sub> = 46.9, C<sub>Carbene</sub>), 142.3 (s, C<sub>Mes</sub>), 137.8 (s, C<sub>Mes</sub>), 130.6 (s, CH<sub>Mes</sub>), 128.5 (s, CH<sub>Mes</sub>), 94.3 (d, <sup>1</sup>J<sub>CRh</sub> = 7.4, CH<sub>COD</sub>), 67.3 (d, <sup>1</sup>J<sub>CRh</sub> = 14.7, CH<sub>COD</sub>), 48.0 (s, NCH<sub>2</sub>), 32.7 (s, CH<sub>2</sub> COD), 32.0 (s, CH<sub>2</sub> COD), 21.6 (s, NCH<sub>2</sub>CH<sub>2</sub>), 21.4 (s, CH<sub>3</sub>), 20.6 (s, CH<sub>3</sub>), 19.4 (s, CH<sub>3</sub>). MS (ES): *m/z* 531.2221 (M-Cl<sup>+</sup>; C<sub>30</sub>H<sub>40</sub>N<sub>2</sub>Rh requires 531.2247).

### [Rh(7-Mes)(COD)Cl]

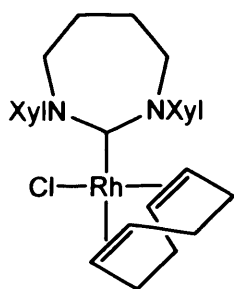


A solution of **7-Mes** (71 mg, 0.22 mmol) in dry THF (10 mL) was added to a solution of [Rh(COD)Cl]<sub>2</sub> (50 mg, 0.10 mmol) in dry THF (10 mL) and stirred at ambient temperature for 1h under argon atmosphere. The solvent was then removed *en vacuo* to give a dark yellow solid which was subsequently triturated with hexanes to give 73 mg (0.12 mmol) of **5** as a bright yellow powder (63 % yield).

Crystals suitable for X-ray analysis were obtained by layering diethyl ether on a tetrahydrofuran solution of the complex. <sup>1</sup>H NMR (400 MHz, C<sub>6</sub>D<sub>6</sub>, rt): 7.06 (2H, s, CH<sub>Mes</sub>), 6.96 (2H, s, CH<sub>Mes</sub>), 5.00 (2H, m, CH<sub>COD</sub>), 3.70 (2H, m, NCH<sub>2</sub>), 3.18 (2H, m, CH<sub>COD</sub>), 3.10 (6H, s, CH<sub>3</sub>), 2.93 (2H, m, NCH<sub>2</sub>), 2.39 (2H, m, NCH<sub>2</sub>CH<sub>2</sub>), 2.32 (6H, s, CH<sub>3</sub>), 2.19 (6H, s, CH<sub>3</sub>), 1.70 (2H, m, CH<sub>2</sub> COD), 1.42-1.58(4H, m, CH<sub>2</sub> COD), 1.32 (2H, m, NCH<sub>2</sub>CH<sub>2</sub>). <sup>13</sup>C NMR (100 MHz, C<sub>6</sub>D<sub>6</sub>, rt): δ 224.0 (d, <sup>1</sup>J<sub>CRh</sub> = 46.7, C<sub>NHC</sub>), 143.2 (s,

$C_{Mes}$ ), 136.5 (s,  $C_{Mes}$ ), 135.4 (s,  $C_{Mes}$ ), 133.5 (s,  $C_{Mes}$ ), 129.6 (s,  $CH_{Mes}$ ), 127.0 (s,  $CH_{Mes}$ ), 93.2 (d,  $^1J_{CRh} = 6.8$ ,  $CH_{COD}$ ), 65.9 (d,  $^1J_{CRh} = 14.6$ ,  $CH_{COD}$ ), 53.6 (s,  $NCH_2$ ), 31.5 (s,  $CH_2$  COD), 26.5 (s,  $CH_2$  COD), 23.5 (s,  $NCH_2CH_2$ ), 20.4 (s,  $CH_3$ ), 19.5 (s,  $CH_3$ ), 18.5 (s,  $CH_3$ ). MS (ES,  $CH_3CN$ ):  $m/z$  545.2379 ( $M-Cl^+$ ;  $C_{31}H_{42}N_2Rh$  requires 545.2403).

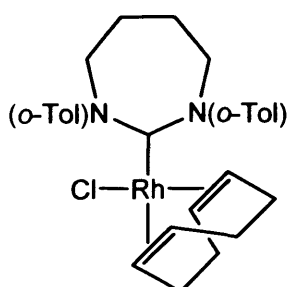
### [Rh(7-Xyl)(COD)Cl]



A solution of 7-Xyl (67 mg, 0.22 mmol) in dry THF (10 mL) was added to a solution of  $[Rh(COD)Cl]_2$  (50 mg, 0.10 mmol) in dry THF (10 mL) and stirred at ambient temperature for 1h under argon atmosphere. The solvent was then removed *in vacuo* to give a dark yellow solid which was subsequently triturated with hexanes to give 78 mg (0.14 mmol) of **3** as a bright yellow powder (70 % yield).

Crystals suitable for X-Ray analysis were obtained by layering hexanes on a dichloromethane solution of the complex.  $^1H$  NMR (400 MHz,  $C_6D_6$ , rt): 7.06 (2H, t,  $^3J_{HH} = 7.4$ ,  $CH_{Xyl}$ ), 7.05 (4H, d,  $^3J_{HH} = 7.1$ ,  $CH_{Xyl}$ ), 5.00 (2H, m,  $CH_{COD}$ ), 3.66 (2H, m,  $NCH_2$ ), 3.10 (2H, m,  $CH_{COD}$ ), 3.10 (6H, s,  $CH_3$ ), 2.85 (2H, m,  $NCH_2$ ), 2.33 (2H, m,  $NCH_2CH_2$ ), 2.16 (6H, s,  $CH_3$ ), 1.70 (2H, m,  $CH_2$  COD), 1.42-1.53 (4H, m,  $CH_2$  COD), 1.23 (2H, m,  $NCH_2CH_2$ ).  $^{13}C$  NMR (100 MHz,  $C_6D_6$ , rt):  $\delta$  145.5 (s,  $C_{Xyl}$ ), 137.0 (s,  $C_{Xyl}$ ), 133.8 (s,  $C_{Xyl}$ ), 129.1 (s,  $CH_{Xyl}$ ), 127.0 (s,  $CH_{Xyl}$ ), 93.5 (d,  $^1J_{RhC} = 14.8$ ,  $CH_{COD}$ ), 66.3 (d,  $^1J_{RhC} = 6.8$ ,  $CH_{COD}$ ), 53.5 (s,  $NCH_2$ ), 31.4 (s,  $CH_2$  COD), 26.6 (s,  $CH_2$  COD), 23.5 (s,  $NCH_2CH_2$ ), 20.5 (s,  $CH_3$ ), 18.6 (s,  $CH_3$ ).  $^{13}C$  NMR (100 MHz,  $CDCl_3$ , rt):  $\delta$  223.1 (d,  $^1J_{CRh} = 46.3$ ,  $C_{NHC}$ ), 145.2 (s,  $C_{Xyl}$ ), 136.6 (bs,  $C_{Xyl}$ ), 134.2 (bs,  $C_{Xyl}$ ), 128.8 (bs,  $CH_{Xyl}$ ), 126.6 (bs,  $CH_{Xyl}$ ), 126.5 (s,  $CH_{Xyl}$ ), 93.8 (d,  $^1J_{RhC} = 7.1$ ,  $CH_{COD}$ ), 66.3 (d,  $^1J_{RhC} = 14.9$ ,  $CH_{COD}$ ), 54.6 (s,  $NCH_2$ ), 54.4 (s,  $NCH_2$ ), 31.2 (s,  $CH_2$  COD), 26.3 (s,  $CH_2$  COD), 24.0 (s,  $NCH_2CH_2$ ), 19.1 (s,  $CH_3$ ), 17.5 (s,  $CH_3$ ). MS (ES,  $CH_3CN$ ):  $m/z$  517.2110 ( $M-Cl^+$ ;  $C_{29}H_{38}N_2Rh$  requires 517.2090).

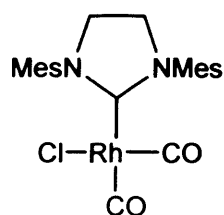
### [Rh(7-Tol<sup>o</sup>)(COD)Cl]



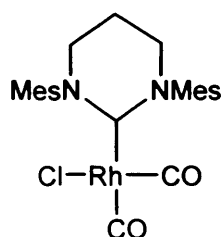
$KNSi(Me_3)_2$  (0.200 g, 1.0 mmol) and 7-Tol<sup>o</sup>· $HBf_4$  (0.361 g, 1.0 mmol) were placed into a Schlenk tube followed by the addition of diethyl ether (10 mL). The solution was stirred for 30 min and subsequently filtered into a Schlenk tube containing a 10 ml THF solution of  $[Ir(COD)Cl]_2$  (0.336 g, 0.5 mmol); an immediate color

change was observed from light to dark yellow. After the reaction mixture was stirred at room temperature for 1 h, the solvent was removed *in vacuo*. The precipitate was washed with hexane and dried under vacuum to afford a brown solid. The product was dissolved in 5 ml of DCM and precipitated with diethyl ether to yield 140 mg of a yellow microcrystalline solid (0.25 mmol, 25%).  $^1\text{H}$  NMR (500 MHz,  $\text{CDCl}_3$ , rt): 8.50 (2H, d,  $^3J_{\text{HH}} = 7.9$ ,  $\text{CH}_{\text{Ar}}$ ), 7.32 (2H, d,  $^3J_{\text{HH}} = 7.8$ ,  $\text{CH}_{\text{Ar}}$ ), 7.22 (4H, m,  $\text{CH}_{\text{Ar}}$ ), 4.39 (2H, m,  $\text{CH}_{\text{COD}}$ ), 4.19 (2H, t,  $^3J_{\text{HH}} = 12.6$ ,  $\text{NCH}_2$ ), 3.42 (2H, d,  $^3J_{\text{HH}} = 13.3$ ,  $\text{NCH}_2$ ), 2.46 (2H, m,  $\text{NCH}_2\text{CH}_2$ ), 2.04 (2H, m,  $\text{CH}_{\text{COD}}$ ), 2.21 (6H, s,  $\text{CH}_3$ ), 1.77 (2H, d,  $^3J_{\text{HH}} = 7.7$ ,  $\text{NCH}_2\text{CH}_2$ ), 1.42 (2H, m,  $\text{CH}_2\text{COD}$ ), 1.23 (2H, m,  $\text{CH}_2\text{COD}$ ), 1.19 (2H, m,  $\text{CH}_2\text{COD}$ ), 1.04 (2H, m,  $\text{CH}_2\text{COD}$ ).  $^{13}\text{C}$  NMR (125 MHz,  $\text{CDCl}_3$ , rt):  $\delta$  222.8 (d,  $^1J_{\text{CRh}} = 45.0$ ,  $\text{C}_{\text{NHC}}$ ), 146.8 (s, ipso- $\text{C}_{\text{Ar}}$ ), 133.5 (s,  $\text{C}_{\text{Ar}}$ ), 133.0 (s,  $\text{C}_{\text{Ar}}$ ), 130.0 (s,  $\text{C}_{\text{Ar}}$ ), 127.4 (s,  $\text{C}_{\text{Ar}}$ ), 126.6 (s,  $\text{C}_{\text{Ar}}$ ), 95.3 (d,  $^1J_{\text{RhC}} = 19.8$ ,  $\text{CH}_{\text{COD}}$ ), 66.8 (d,  $^1J_{\text{RhC}} = 15.1$ ,  $\text{CH}_{\text{COD}}$ ), 53.3 (s,  $\text{NCH}_2$ ), 31.6 (s,  $\text{CH}_2\text{COD}$ ), 27.4 (s,  $\text{CH}_2\text{COD}$ ), 24.0 (s,  $\text{NCH}_2\text{CH}_2$ ), 18.4 (s,  $\text{CH}_3$ ). MS (ES,  $\text{CH}_3\text{CN}$ ):  $m/z$  489.1776 ( $\text{M}-\text{Cl}^+$ ;  $\text{C}_{29}\text{H}_{38}\text{N}_2\text{Rh}$  requires 489.1790).

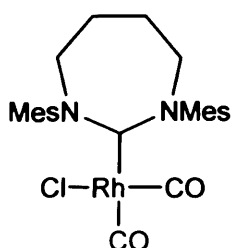
#### *Cis*-[Rh(5-Mes)(CO)<sub>2</sub>Cl]



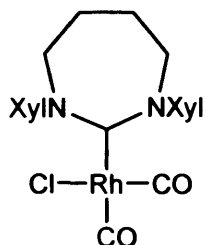
Complex [Rh(5-Mes)(COD)Cl] (50 mg, 0.090 mmol) was dissolved in dichloromethane (10 mL) and stirred under an atmosphere of carbon monoxide for 30 min. The solvent was then removed *in vacuo* and the resulting solid was washed with cold hexanes to remove residual 1,5-cyclooctadiene. The resulting solid was dried *in vacuo* to afford 38 mg (0.076 mmol) of a pale yellow solid (83% yield).  $^1\text{H}$  NMR (400 MHz,  $\text{CDCl}_3$ , rt):  $\delta$  6.88 (4H, s,  $\text{CH}_{\text{Mes}}$ ), 3.92 (4H, s,  $\text{NCH}_2$ ), 2.35 (12H, s,  $\text{CH}_3$ ), 2.23 (6H, s,  $\text{CH}_3$ ).  $^{13}\text{C}$ -NMR (100 MHz,  $\text{CDCl}_3$ , rt):  $\delta$  205.0 (d,  $^1J_{\text{RhC}} = 40.8$ ,  $\text{C}_{\text{NHC}}$ ), 184.2 (d,  $^1J_{\text{RhC}} = 57.3$ , CO), 181.9 (d,  $^1J_{\text{RhC}} = 74.4$ , CO), 135.1 (bs,  $\text{C}_{\text{Mes}}$ ), 137.6 (s,  $\text{C}_{\text{Mes}}$ ), 133.9 (s,  $\text{C}_{\text{Mes}}$ ), 128.5 (s,  $\text{CH}_{\text{Mes}}$ ), 50.5 (s,  $\text{NCH}_2$ ), 20.1 (s,  $\text{CH}_3$ ), 17.6 (s,  $\text{CH}_3$ ). IR ( $\text{cm}^{-1}$ ): 1995, 2080 ( $\text{CH}_2\text{Cl}_2$ ).

**Cis-[Rh(6-Mes)(CO)<sub>2</sub>Cl]**

Complex [Rh(6-Mes)(COD)Cl] (50 mg, 0.088 mmol) was dissolved in dichloromethane (10 mL) and stirred under an atmosphere of carbon monoxide for 30 min. The solvent was then removed *in vacuo* and the resulting solid was washed with cold hexanes to remove residual 1,5-cyclooctadiene. The resulting solid was dried *in vacuo* to afford 40 mg (0.078 mmol) of a pale yellow solid (88% yield). <sup>1</sup>H NMR (400 MHz, CDCl<sub>3</sub>, rt): δ 6.87 (4H, s, CH<sub>Mes</sub>), 3.37 (4H, m, NCH<sub>2</sub>), 2.35 (6H, s, CH<sub>3</sub>), 2.31 (6H, s, CH<sub>3</sub>), 2.29 (2H, m, NCH<sub>2</sub>CH<sub>2</sub>), 2.25 (6H, s, CH<sub>3</sub>). <sup>13</sup>C NMR (100 MHz, CDCl<sub>3</sub>, rt): δ 202.9 (d, <sup>1</sup>J<sub>RhC</sub> = 40.8, C<sub>NHC</sub>), 186.1 (d, <sup>1</sup>J<sub>RhC</sub> = 52.5, CO), 183.7 (d, <sup>1</sup>J<sub>RhC</sub> = 67.6, CO), 141.7 (s, C<sub>Mes</sub>), 138.4 (s, C<sub>Mes</sub>), 136.7 (s, C<sub>Mes</sub>), 134.5 (s, C<sub>Mes</sub>), 130.4 (s, CH<sub>Mes</sub>), 129.3 (s, CH<sub>Mes</sub>), 47.2 (s, NCH<sub>2</sub>), 21.5 (s, CH<sub>3</sub>), 21.1 (s, NCH<sub>2</sub>CH<sub>2</sub>), 19.9 (s, CH<sub>3</sub>), 18.6 (s, CH<sub>3</sub>). IR (cm<sup>-1</sup>): 1987, 2071 (CH<sub>2</sub>Cl<sub>2</sub>).

**Cis-[Rh(7-Mes)(CO)<sub>2</sub>Cl]**

Complex [Rh(7-Mes)(COD)Cl] (50 mg, 0.082 mmol) was dissolved in dichloromethane (10 mL) and stirred under an atmosphere of carbon monoxide for 30 min. The solvent was then removed *in vacuo* and the resulting solid was washed with cold hexanes to remove residual 1,5-cyclooctadiene. The resulting solid was dried *in vacuo* to afford 40 mg (0.077 mmol) of a pale yellow solid (94 % yield). <sup>1</sup>H NMR (400 MHz, CDCl<sub>3</sub>, rt): δ 6.89 (4H, s, CH<sub>Mes</sub>), 4.00 (2H, m, NCH<sub>2</sub>), 3.71 (2H, m, NCH<sub>2</sub>), 2.43 (6H, s, CH<sub>3</sub>), 2.36 (6H, s, CH<sub>3</sub>), 2.34 (2H, m, NCH<sub>2</sub>CH<sub>2</sub>), 2.23 (6H, s, CH<sub>3</sub>), 2.11 (2H, m, NCH<sub>2</sub>CH<sub>2</sub>). <sup>13</sup>C NMR (100 MHz, CDCl<sub>3</sub>, rt): δ 213.4 (d, <sup>1</sup>J<sub>RhC</sub> = 40.8, C<sub>NHC</sub>), 187.1 (d, <sup>1</sup>J<sub>RhC</sub> = 52.5, CO), 184.5 (d, <sup>1</sup>J<sub>RhC</sub> = 77.7, CO), 143.6 (s, C<sub>Mes</sub>), 138.2 (s, C<sub>Mes</sub>), 136.6 (s, C<sub>Mes</sub>), 134.3 (s, C<sub>Mes</sub>), 130.5 (s, CH<sub>Mes</sub>), 129.4 (s, CH<sub>Mes</sub>), 55.2 (s, NCH<sub>2</sub>), 25.4 (s, NCH<sub>2</sub>CH<sub>2</sub>), 21.4 (s, CH<sub>3</sub>), 20.5 (s, CH<sub>3</sub>), 19.3 (s, CH<sub>3</sub>). IR (cm<sup>-1</sup>): 1987, 2069 (CH<sub>2</sub>Cl<sub>2</sub>). MS (ES, CH<sub>3</sub>CN): *m/z* 506.1682 ([M-Cl-CO+CH<sub>3</sub>CN]<sup>+</sup>; C<sub>26</sub>H<sub>33</sub>N<sub>3</sub>ORh requires 506.1679).

**Cis-[Rh(7-Xyl)(CO)<sub>2</sub>Cl]**

Complex [Rh(7-Xyl)(COD)Cl] (50 mg, 0.090 mmol) was dissolved in dichloromethane (10 mL) and stirred under an atmosphere of carbon monoxide for 30 min. The solvent was then removed *in vacuo* and the resulting solid was washed with cold hexanes to remove residual 1,5-cyclooctadiene. The resulting solid was dried *in vacuo* to afford 35 mg (0.070 mmol) of a pale yellow solid (78% yield). <sup>1</sup>H NMR (400 MHz, CDCl<sub>3</sub>, rt): δ 7.12 (2H, t, <sup>3</sup>J<sub>HH</sub> = 7.0, CH<sub>Xyl</sub>), 7.05 (4H, d, <sup>3</sup>J<sub>HH</sub> = 7.5, CH<sub>Xyl</sub>), 4.04 (4H, m, NCH<sub>2</sub>), 3.76 (4H, m, NCH<sub>2</sub>CH<sub>2</sub>), 2.48 (6H, s, CH<sub>3</sub>), 2.41 (6H, s, CH<sub>3</sub>), 2.34 (4H, m, CH<sub>2</sub> COD), 2.15 (4H, m, CH<sub>2</sub> COD). <sup>13</sup>C NMR (100 MHz, CDCl<sub>3</sub>, rt): δ 212.2 (d, <sup>1</sup>J<sub>RhC</sub> = 40.8, C<sub>NHC</sub>), 184.5 (d, <sup>1</sup>J<sub>RhC</sub> = 52.5, CO), 182.6 (d, <sup>1</sup>J<sub>RhC</sub> = 77.3, CO), 144.5 (s, C<sub>Xyl</sub>), 135.6 (s, C<sub>Xyl</sub>), 133.3 (s, C<sub>Xyl</sub>), 128.4 (s, CH<sub>Xyl</sub>), 127.4 (s, CH<sub>Xyl</sub>), 127.1 (s, CH<sub>Xyl</sub>), 53.7 (s, NCH<sub>2</sub>), 24.1 (s, NCH<sub>2</sub>CH<sub>2</sub>), 18.0 (s, CH<sub>3</sub>), 13.1 (s, CH<sub>3</sub>). IR (cm<sup>-1</sup>): 1986, 2071 (CH<sub>2</sub>Cl<sub>2</sub>). MS (ES, CH<sub>3</sub>CN): *m/z* 478.1377 (M-Cl-CO+CH<sub>3</sub>CN<sup>+</sup>; C<sub>24</sub>H<sub>29</sub>N<sub>3</sub>ORh requires 478.1366).



# Chapter

# 5

## Functionalisation of the carbene backbone

<b>5.1. Introduction</b> .....	<b>148</b>
<b>5.2. Results and discussion</b> .....	<b>151</b>
<b>5.2.1. Synthesis and deprotonation experiments of 1,3-Bis-(2,4,6-trimethylphenyl)-4,7-dihydro-3H-[1,3]diazepin-1-ium tetrafluoroborate (5.7) and 1,3-Bis-(2,6-diisopropylphenyl)-4,7-dihydro-3H-[1,3]diazepin-1-ium tetrafluoroborate (5.8)</b> .....	<b>151</b>
<b>5.2.2. Reactivity of the alkenic backbone</b> .....	<b>154</b>
<b>5.2.2.1. Attempts of epoxidation</b> .....	<b>155</b>
<b>5.2.2.2. Reactivity towards Diels-Alder cycloaddition</b> .....	<b>159</b>
<b>5.2.3. Coordination chemistry of the functionalised amidinium salts 5.11 and 5.12</b> .....	<b>163</b>
<b>5.2.3.2. Synthesis of silver complexes</b> .....	<b>163</b>
<b>5.2.3.2. Synthesis of rhodium complexes</b> .....	<b>163</b>
<b>5.2.3. Self-catalytic-hydrogenation of complex 5.15</b> .....	<b>171</b>
<b>5.3. Experimental</b> .....	<b>173</b>

## Chapter 5. Functionalisation of the carbene backbone.

### 5.1. Introduction.

N-Heterocyclic carbenes complexes are known to be extremely successful in homogeneous catalysis.<sup>1</sup> However, a practically useful heterogeneous catalyst, which would allow the use of carbene catalysts in industrial reactors, has not yet been developed.<sup>2</sup> The anchoring of the carbene ligand shows potential as a method to recover the catalyst, which makes possible its recycling and a straightforward purification of the reaction products. For the past 10 years, interest has grown towards tethered versions of this type of ligands onto a variety of supports including polymers, silica and nanoparticles.<sup>4</sup>

Hitherto, the immobilisation of carbene catalysts has been most widely studied for ruthenium and palladium systems. However, several examples of supported rhodium complexes were published.<sup>3</sup> These metal complexes can be linked to soluble supports or insoluble supports, i.e. heterogeneous catalysis. The latter allows for easy removal of the catalysts with the possibility to use the insoluble catalysts in continuous flow reactors. However, the activity for more challenging substrates was lower than their small molecule analogues. On the other hand, the soluble supports produced more active catalysts but lacked the ease of removal that insoluble supports offer.<sup>4</sup>

Examples of catalysts anchored to support through substituted carbene backbones are scarce. The 5-membered carbene published by Blechert and co-workers represents the most successful example so far (Figure 5.1).<sup>5</sup> The authors explored the activity of this

---

<sup>1</sup> (a) Bourissou, D.; Guerret, O.; Gabbaï, F. P.; Bertrand, G. *Chem. Rev.* **2000**, *100*, 39. (b) Fürstner, A. *Angew. Chem. Int. Ed. Engl.* **2000**, *39*, 3012. (c) Herrmann, W.A. *Angew. Chem. Int. Ed.* **2002**, *41*, 1290. (d) Herrmann, W. A.; Kocher, C. *Angew. Chem. Int. Ed. Engl.* **1997**, *36*, 2162.

<sup>2</sup> Schwarz, Jürgen; Böhm, Volker P. W.; Gardiner, Michael G.; Grosche, Manja; Herrmann, W. A.; Hieringer, Wolfgang; Raudaschl-Sieber, Gabriele *Chem. Eur. J.* **2000**, *6*, 1773.

<sup>3</sup> (a) Zarka, M.T.; Bortenschlager, M.; Wurst, K.; Nuyken, O.; Weberskirch, R. *Organometallics*, **2004**, *23*, 4817. (b) Özdemir, I.; Gürbüz, N.; Seçkin, T.; Çetinkaya, B. *Appl. Organomet. Chem.* **2005**, *19*, 633.

<sup>4</sup> Sommer, William J.; Weck, M. *Coord. Chem. Rev.* **2007**, *251*, 860.

<sup>5</sup> Schürer, S.C.; Gessler, S.; Buschmann, N.; Blechert, S. *Angew. Chem. Int. Ed.* **2000**, *39*, 3898.

supported catalyst in the olefin metathesis reactions of a wide variety of reagents. They reported near quantitative conversions for all reagents, from RCM of simple diallyl malonate to the cross-metathesis of cyclohexyl acetylene with allyl trimethyl silane, demonstrating the utility of this supported catalyst. Moreover, the complex is permanently immobilised on the support, which permits easy removal of the catalyst by simple filtration methods. This improves the recovery and recycling of the supported carbene complexes compared to those previously reported by Nolan and Barret, where immobilisation was designed *via* the alkylidene (boomerang catalysts).

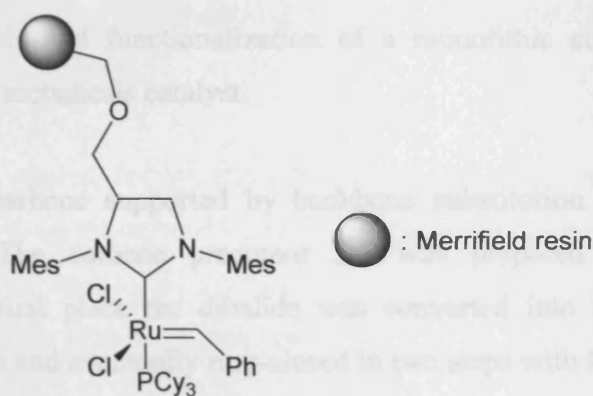
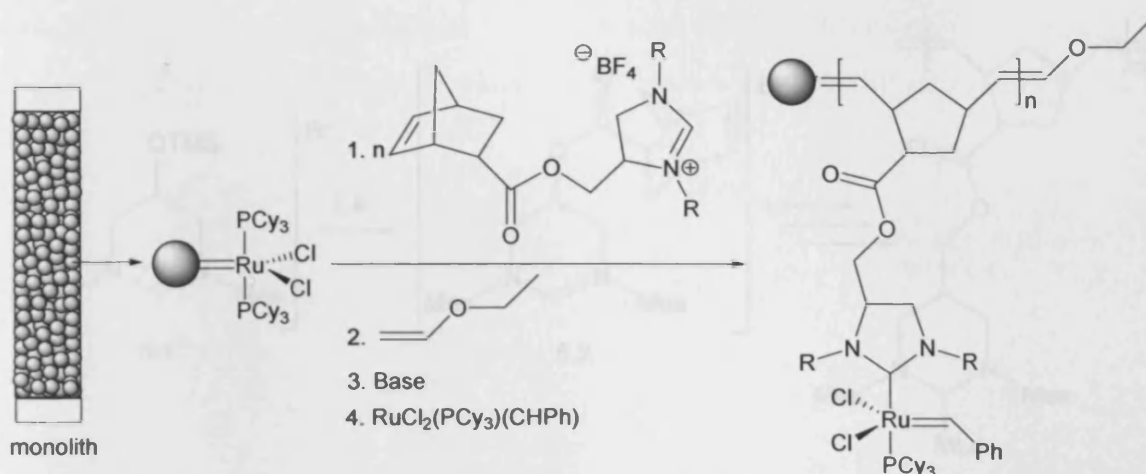


**Figure 5.1.** Blechert's supported catalyst.

Following Blechert's work, a few more examples were published by Buchmeiser and co-workers on carbenes supported through substituted backbone.<sup>6</sup>

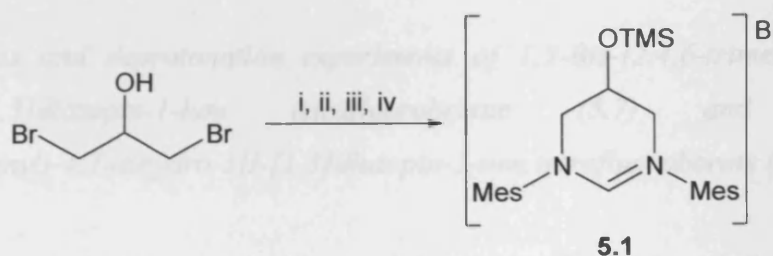
The immobilisation of Grubb's second-generation supported catalyst (Scheme 5.1) had as final goal to combine the advantages of homogeneous and heterogeneous catalysis and, simultaneously, eliminate the disadvantages typical for many heterogeneous systems, such as diffusion-controlled reactions and catalyst bleeding, among others. This was achieved by the use of a monolithic media as catalyst support. The unique structure and pore size distribution of monolithic materials in combination with a suitable interparticle porosity, resulted in a comparatively fast mass transfer between the support and liquid phase.<sup>6a</sup>

<sup>6</sup> (a) Mayr, M.; Mayr, B.; Buchmeiser, M. R. *Angew. Chem. Int. Ed.* **2001**, *40*, 3839. (b) Mayr, M.; Buchmeiser, M. R. *Macromol. Rapid Commun.* **2004**, *25*, 231.



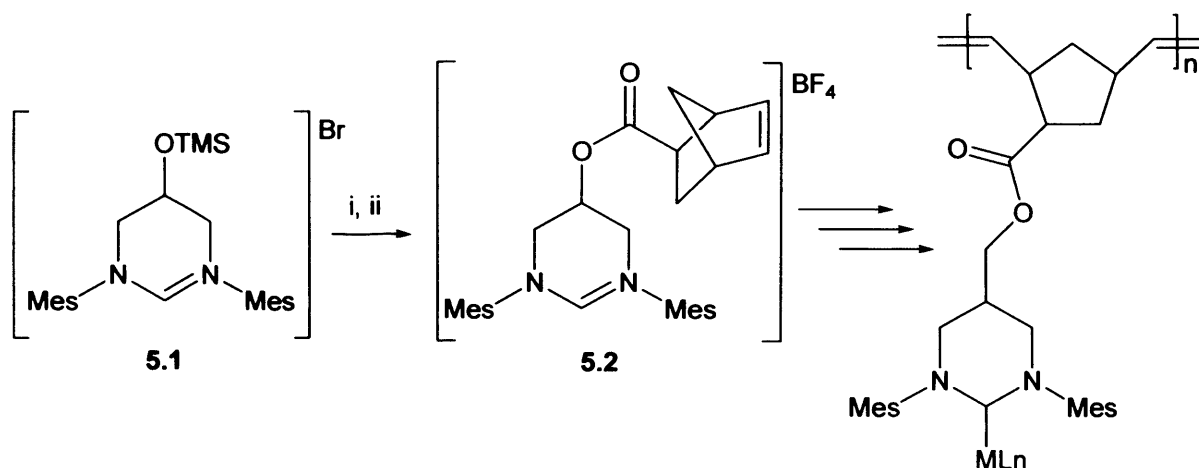
**Scheme 5.1.** Synthesis and functionalization of a monolithic support and subsequent immobilization of the metathesis catalyst.

The first expanded carbene supported by backbone substitution was also reported by Buchmeiser *et al.* The carbene precursor **5.1** was prepared from 2-hydroxy-1,3-dibromopropane. In first place the dihalide was converted into the diamine, secondly protected with TMSCl and eventually ring-closed in two steps with formaldehyde and NBS (Scheme 5.2).



**Scheme 5.2.** Synthesis of Buchmeiser's functionalised 6-membered carbene precursor. i)  $\text{MesNH}_2$ , diglyme,  $\text{NaOH}$ ; ii)  $\text{ClSi}(\text{Me}_3)_3$ ,  $\text{DCM}$ ,  $\text{NEt}_3$ ; iii)  $\text{H}_2\text{C}=\text{O}$ ,  $\text{MeOH}$ ; iv)  $\text{NBS}$ ,  $\text{DME}$ .

Deprotection of the alcohol function followed by reaction with norborn-5-ene-2-carbonyl chloride affords compound **5.2**, which can be polymerised by ROMP (Scheme 5.3).



**Scheme 5.3.** Immobilisation of compound **5.2**. i)  $\text{AgBF}_4$ , EtOH; ii) norborn-5-ene-2-carbonyl chloride,  $\text{NEt}_3$ , DCM.

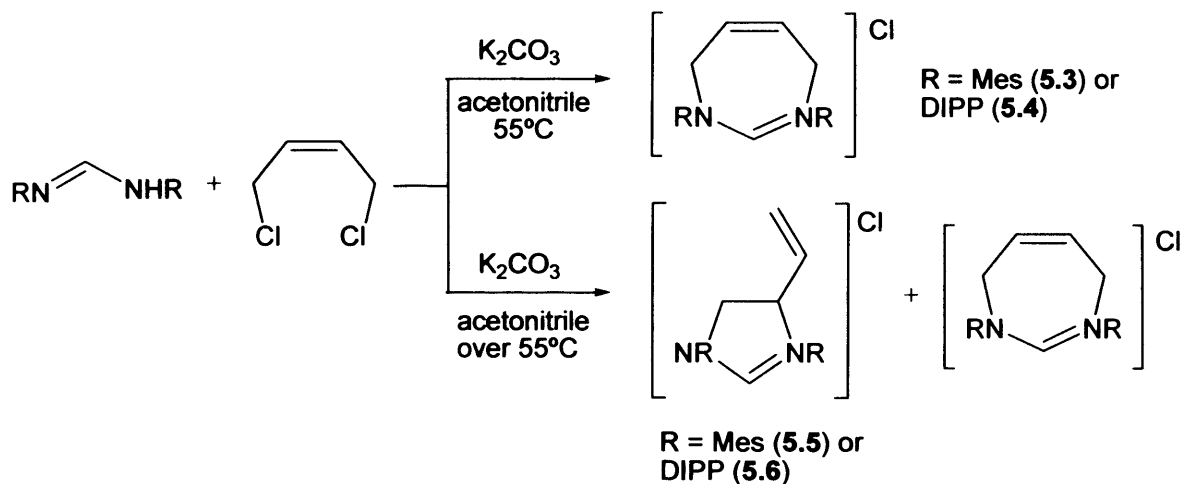
In this chapter the synthesis, coordination chemistry and reactivity of functionalised 7-membered carbenes will be described. These functionalised carbenes open a new route for the synthesis of tethered ligands, which can be covalently linked to supports by aliphatic chains, affording therefore robust anchored catalysts.

## 5.2. Results and discussion.

5.2.1. *Synthesis and deprotonation experiments of 1,3-Bis-(2,4,6-trimethylphenyl)-4,7-dihydro-3H-[1,3]diazepin-1-ium tetrafluoroborate (5.7) and 1,3-Bis-(2,6-diisopropylphenyl)-4,7-dihydro-3H-[1,3]diazepin-1-ium tetrafluoroborate (5.8).*

The carbene precursors **5.3** and **5.4** (Scheme 5.4) were synthesised according to the method described in *Chapter 2*. In this case the use of lower temperatures was required in order to prevent  $\text{S}_{\text{N}}2'$  side-reactions (Scheme 5.4). Only reaction temperatures below  $55\text{ }^\circ\text{C}$  afforded clean formation of the butene derivative. When the temperature was increased beyond this limit a loss of selectivity was observed. At temperatures above  $100\text{ }^\circ\text{C}$  the reaction proceeded without selectivity, affording mixtures of **5.3** and **5.5** or **5.4** and **5.6** in approximately 50:50 ratios. This restriction in the temperature led to long reaction times.

The product was isolated by addition of diethyl ether to a solution of the crude mixture in dichloromethane. This afforded the chloride salt as a white crystalline material in yields of nearly 50%.



**Scheme 5.4.** Synthesis of carbene precursors 5.3 and 5.4.

Crystals of **5.3** suitable for X-Ray diffraction were obtained layering ether into dichloromethane solution of the amidinium salt. The crystal structure is depicted in Figure 5.2, selected bond lengths and angles in Table 5.1.

As previously observed for the benzylic backbone, the unsaturated C(3)-C(4) bond brings about an additional rigidity in the NHC ring, which results in a decrease of the  $\text{C}_{\text{ring}}\text{N}\cdots\text{NC}_{\text{ring}}$  torsion angle and forces the alkenic carbons, C(3) and C(4), to be simultaneously above or below the  $\text{NC}_{\text{NHC}}\text{N}$  plane. Despite the increased rigidity of the NHC ring no significant augment of the  $\text{N}-\text{C}_{\text{NHC}}-\text{N}$  angle was observed with respect to the saturated 7-membered carbene, from  $127.3^\circ$  in  $7\text{-Cy}\cdot\text{HBF}_4$  to  $127.4^\circ$  in **5.3**.

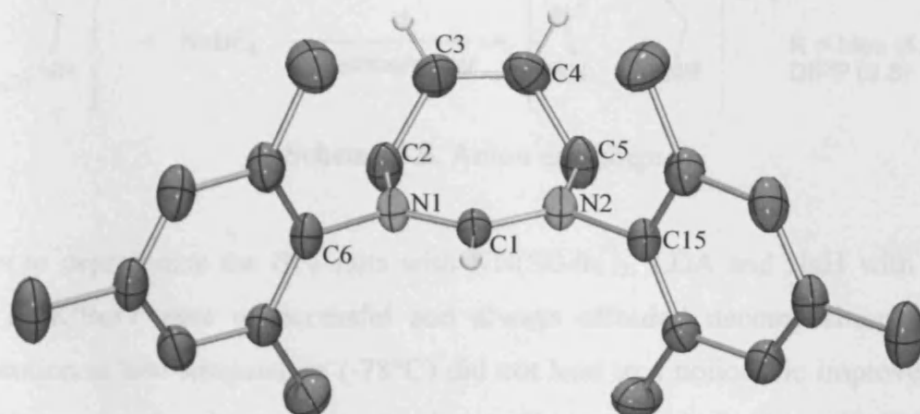
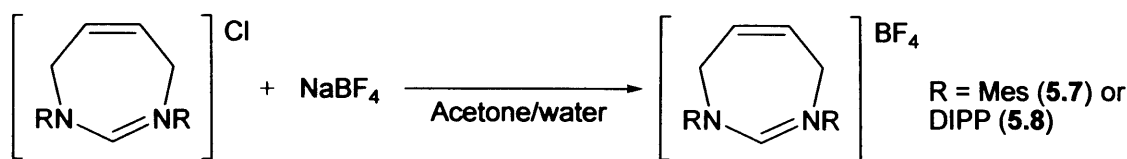


**Figure 5.2.** ORTEP ellipsoid plots at 30% probability of the amidinium salt **5.3**. The chloride counter anion, protons and solvent molecules were omitted for clarity.

**Table 5.1.** Selected bond lengths and angles for **5.3**.

Lengths (Å)		Angles (°)	
N(1)-C(1)	1.318(3)	N(1)-C(1)-C(6)	117.41(19)
N(1)-C(6)	1.456(3)	C(1)-N(1)-C(2)	125.1(2)
N(1)-C(2)	1.482(3)	C(6)-N(1)-C(2)	117.52(18)
C(1)-N(2)	1.319(3)	N(1)-C(1)-N(2)	127.4(2)
N(2)-C(15)	1.456(3)	C(1)-N(2)-C(15)	117.49(19)
N(2)-C(5)	1.485(3)	C(1)-N(2)-C(5)	116.90(18)
C(2)-C(3)	1.486(4)	N(1)-C(2)-C(3)	111.7(2)
C(3)-C(4)	1.328(4)	C(4)-C(3)-C(2)	120.8(3)
C(4)-C(5)	1.486(4)	C(3)-C(4)-C(5)	119.9(3)
		N(2)-C(5)-C(4)	112.1(2)
		C(2)N(1)⋯N(2)C(5)	1.3

The halide salts were converted into the correspondent  $\text{BF}_4$  salts adding 1 equivalent of  $\text{NaBF}_4$  in water to a solution in acetone of the chloride salt. Following the method discussed in *Chapter 2* the tetrafluoroborate salts were isolated as white crystalline solids in high yields (Scheme 5.5).



**Scheme 5.5.** Anion exchange.

Attempts to deprotonate the  $\text{BF}_4$  salts with  $\text{KN}(\text{SiMe}_3)_2$ , LDA and NaH with a catalytic amount of  $\text{K}^t\text{BuO}$  were unsuccessful and always afforded decomposition of the salt. Deprotonation at low temperature ( $-78^\circ\text{C}$ ) did not lead to a noticeable improvement. This behaviour, previously observed for the benzo-diazepanyl derivatives (**Xyl7-Mes** $\cdot\text{HBF}_4$ , **Xyl7-Xyl** $\cdot\text{HBF}_4$  and **Xyl7-DIPP** $\cdot\text{HBF}_4$ ), might be due to the presence of allylic protons adjacent to the nitrogen atoms of the NCN core. The presumably high acidity of these protons together with the steric hindrance around the NCN core probably makes the allylic protons more reactive.

### 5.2.2. Reactivity of the alkenic backbone.

The alkenic function on the backbone offers a wide range of possibilities for the functionalisation of carbene ligands. The intensively studied reactivity of alkenes is a powerful tool for the design of the desired carbene framework (Figure 5.3). Hopefully, this will help to broaden the scope of carbene chemistry, allowing the anchorage of the catalyst to diverse surfaces, synthesis of polymeric carbenes (self-supported catalysts) or even the preparation water soluble derivatives. Ultimately, the above described might enable the use of carbene complexes as catalysts in more efficient and “green” industrial processes.

The reactions attempted in this work represent just a small incursion in this chemistry, and were intended to probe the reactivity of the alkenic backbone. Nevertheless, despite the short number reactions tested, some interesting results were obtained and these will be described in the following sections.



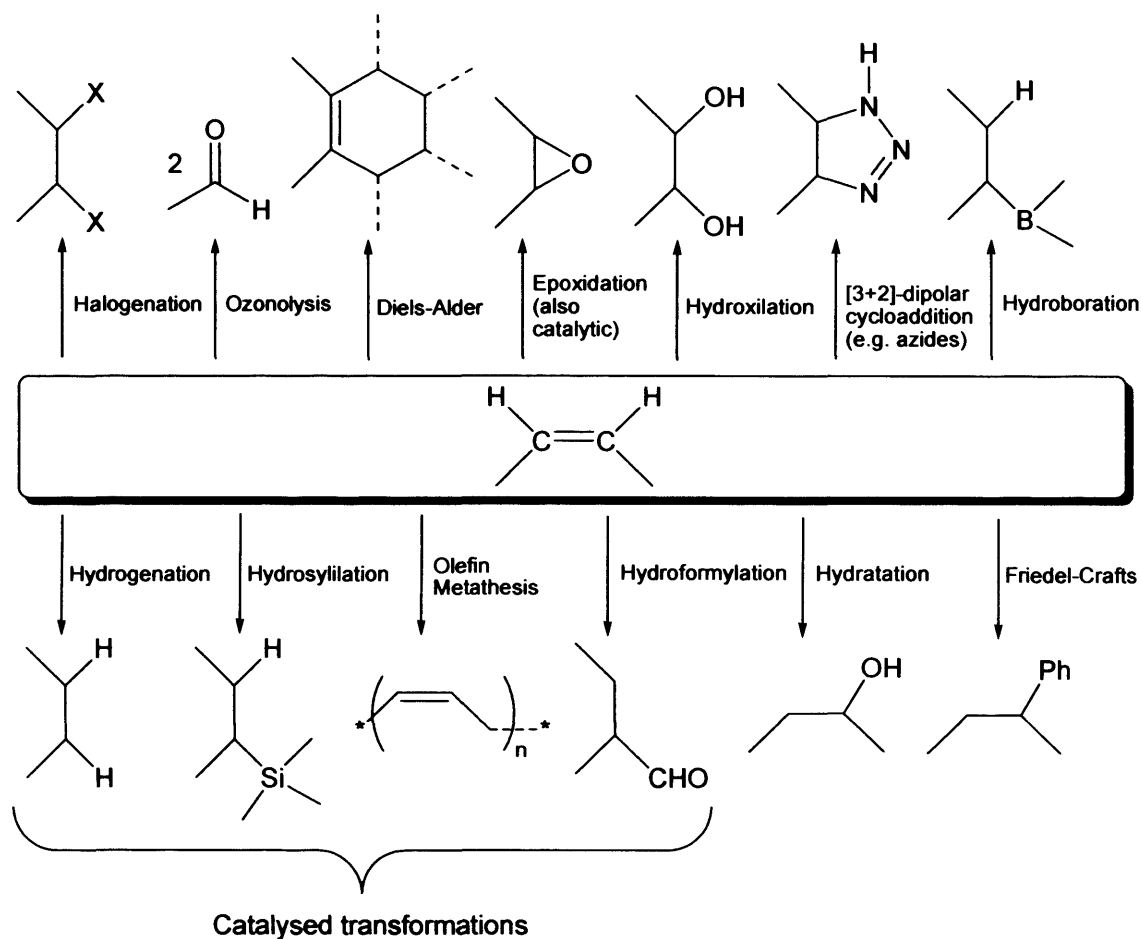
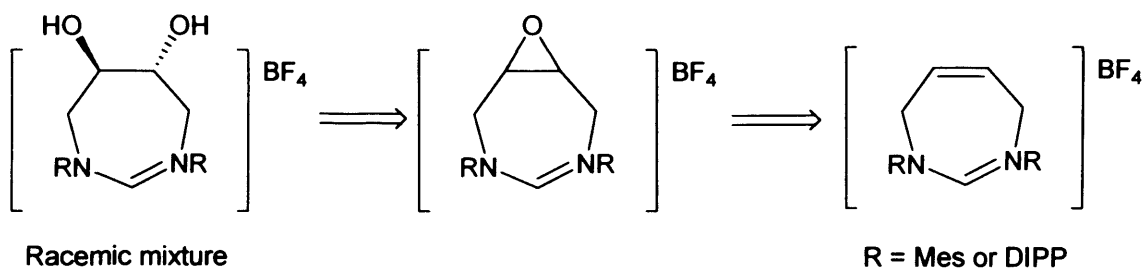


**Figure 5.3.** Summary of alkene reactivity.

#### 5.2.2.1. Attempts of epoxidation.

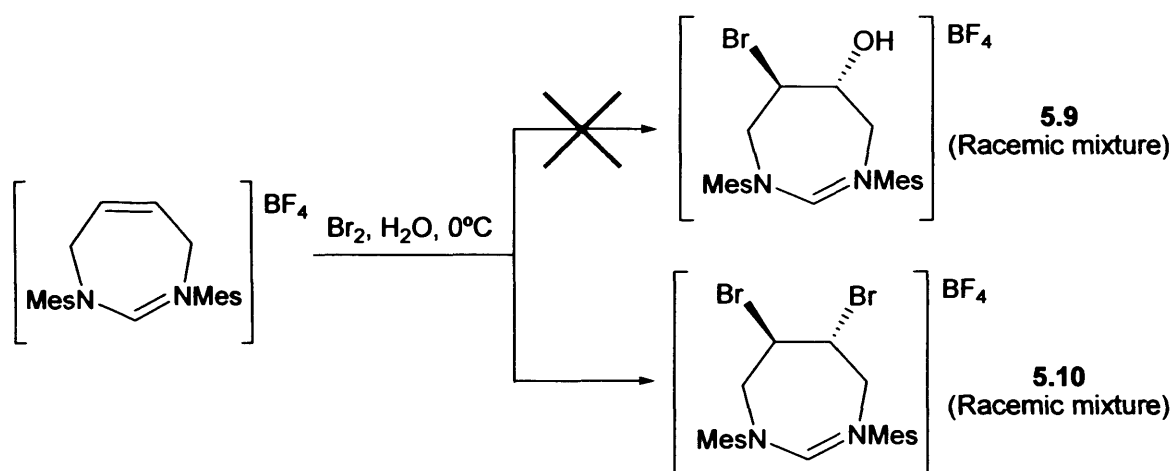
Originally, the butene derivative was prepared as a stepping stone for the synthesis of a *trans* diol or protected diol. This new approach entailed an initial epoxidation of the double bond followed by treatment with  $\text{OH}^-$  or  $\text{RO}^-$  (Scheme 5.6).



**Scheme 5.6.** Retrosynthetic analysis for the synthesis of a *trans* diol.

The epoxidation was first attempted with *m*-chloroperbenzoic acid (MCPBA) in DCM and later with hydrogen peroxide in the presence of NaOH in MeOH. However, no evolution was observed for any of the reactions.

A new attempt to synthesise the epoxide entailed the formation of bromohydrin **5.9** as a first step (Scheme 5.7). Subsequent treatment with a base such as sodium hydride would promote intramolecular S<sub>N</sub>2 reaction and, therefore, formation of the desired epoxide. The alkene was reacted with bromine in water, using acetonitrile as a co-solvent to dissolve the salt. The expected product of the reaction, the bromohydrin **5.9**, was not isolated. Instead, the dibrominated alkene **5.10** was obtained in a 30% yield (Scheme 5.7).



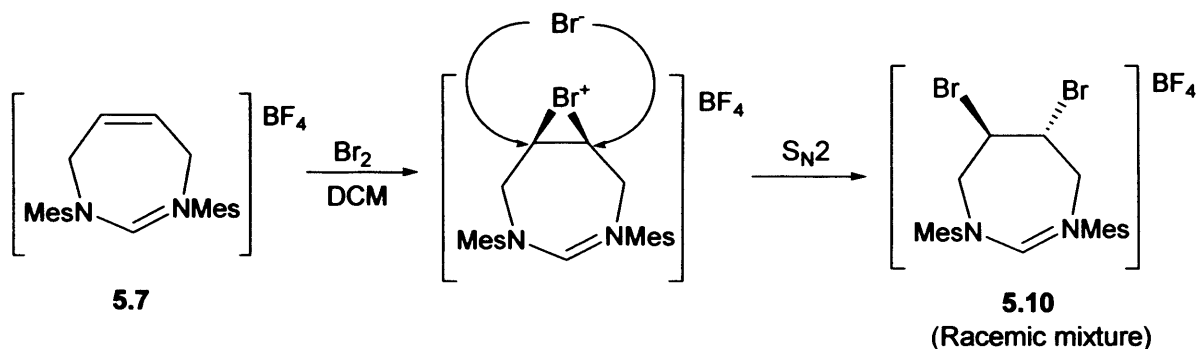
**Scheme 5.7.** Attempted synthesis of bromohydrin **5.9**.

A more efficient method for the synthesis of amidinium salt **5.10** was developed in our group by Dr Dirk Beetstra.<sup>7</sup> This method entails slow addition of 1 equivalent of bromine to a dichloromethane solution of **5.7** which is subsequently stirred for 30 minutes at ambient temperature (Scheme 5.8). The desired *trans*-dibromide salt **5.10** can be precipitated from the resulting solution by addition of diethyl ether.

The dibromination of an alkene is a diastereospecific reaction because it provides only the *trans*-dibromide, i.e., the reaction takes place *via anti*-addition of a bromine molecule. The stereochemistry of the bromination of a double bond is explained by the nucleophilic attack of the alkene's  $\pi$ -system on one of the atoms in the bromine molecule, which leads to formation of a cyclic bromonium cation and a bromide anion. The 3-membered ring

<sup>7</sup> Unpublished work.

which contains the bromonium cation can be opened by  $S_N2$  reaction of the bromide anion on any of the carbon atoms adjacent to the  $Br^+$ , affording each attack a different enantiomer. The lack of selectivity on the ring-opening leads to a 50:50 enantiomers ratio of **5.10** (racemic mixture).



**Scheme 5.8.** Bromination of **5.7**.

The formation of salt **5.10** was monitored by the disappearance of the alkene resonance at 6.44 ppm in the  $^1H$  NMR of **5.7**. The *trans* substitution on the backbone induces asymmetry on the ligand, which is reflected in the  $^1H$  and  $^{13}C$  NMR. The  $^1H$  NMR features two singlets for the *ortho* methyls and two different resonances for the methylenic protons, a broad resonance at 5.11 and a doublet 4.50 ppm. The  $^{13}C$  NMR also shows diastereotopic signals for the *ortho* methyls (two resonances) and aromatic carbons (six signals).

Crystals suitable for X-ray diffraction were obtained by layering a dichloromethane solution of **5.10** with diethyl ether. The crystal structure of one of the isomers is depicted in Figure 5.4, selected bond length and angles are given in Table 5.2.

The *trans* substitution on the backbone forces the carbene ring in **2.10** to adopt a twisted chair conformation, with both bromine atoms occupying axial positions. The steric repulsion between the two bulky bromine atoms leads to a torsion angle Br-C-C-Br of  $178.3^\circ$ , which ensures a maximum separation between them. This results in a substantial increase of the NCN angle ( $131.0(3)^\circ$ ) in comparison with its precursor **5.3** ( $117.41(19)^\circ$ ) but it is not as wide the one obtained for **DIOC-Cy**· $HPF_6$  ( $135.9(10)^\circ$ ).

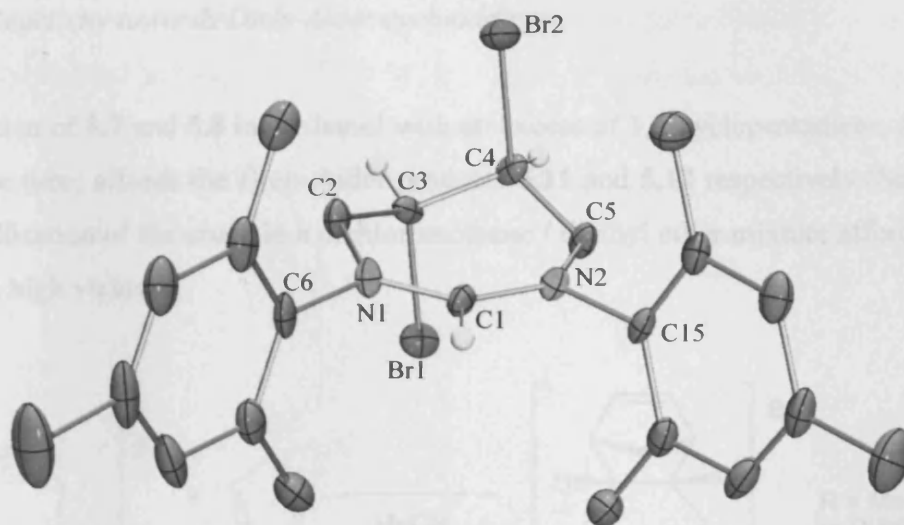


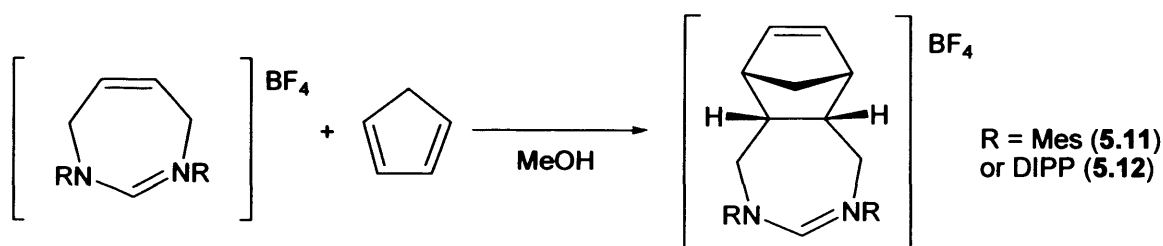
**Figure 5.4.** ORTEP ellipsoid plots at 30% probability of the amidinium salt **5.10**. The  $\text{BF}_4$  counter anion and solvent molecules were omitted for clarity.

**Table 5.2.** Selected bond lengths and angles for **5.10**.

Lengths (Å)		Angles (°)	
N(1)-C(1)	1.317(5)	N(1)-C(1)-C(6)	131.0(3)
N(1)-C(2)	1.475(5)	C(1)-N(1)-C(6)	113.0(3)
N(1)-C(6)	1.475(5)	C(2)-N(1)-C(6)	115.9(3)
C(1)-N(2)	1.304(5)	N(2)-C(1)-N(1)	133.7(4)
N(2)-C(5)	1.457(5)	C(1)-N(2)-C(5)	130.3(4)
N(2)-C(15)	1.462(5)	C(1)-N(2)-C(15)	114.1(4)
C(3)-Br(1)	1.964(6)	C(5)-N(2)-C(15)	115.4(3)
C(4)-Br(2)	1.980(6)	N(1)-C(2)-C(3)	117.4(4)
		N(1)-C(2)-C(3)	117.4(4)
		N(2)-C(5)-C(4)	117.9(4)
		C(7)-C(6)-N(1)	118.2(4)
		C(11)-C(6)-N(1)	118.0(4)
		C(2)N(1)⋯N(2)C(5)	8.7

## 5.2.2.2. Reactivity towards Diels-Alder cycloaddition.

The reaction of **5.7** and **5.8** in methanol with an excess of 1,3-cyclopentadiene, at 60 °C, in a pressure tube, affords the Diels-Alder products **5.11** and **5.12** respectively (Scheme 5.9). Recrystallisation of the crude in a dichloromethane / diethyl ether mixture affords the *endo* adduct in high yields.



**Scheme 5.9.** Synthesis of Diels-Alder products **5.11** and **5.12**.

$^1\text{H}$  NMR spectroscopy confirms the formation of only one of the two possible isomers, but it does not clarify whether the formed isomer is the result of the *endo* or *exo* addition. These terms refer to the position of the alkene's substituents relative to the diene during a Diels-Alder cycloaddition, in this case the position of the carbene ring relative to the  $\pi$ -system of the cyclopentadiene (Figure 5.5).

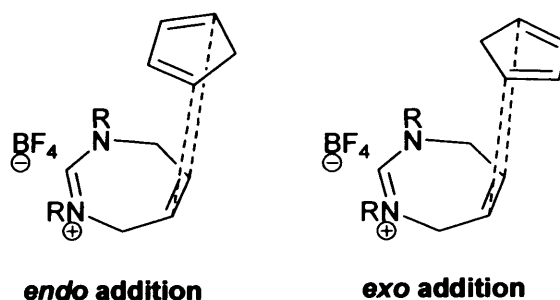
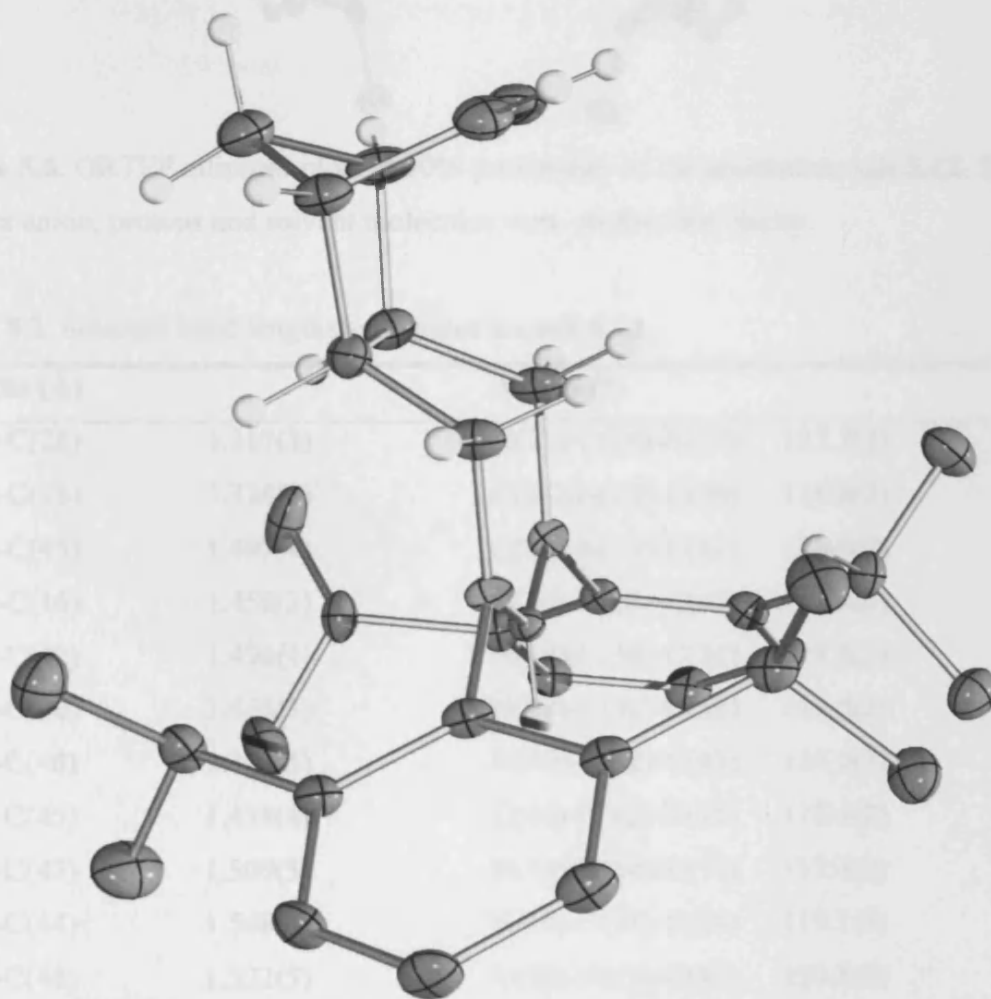


**Figure 5.5.** Possible orientations of the cyclopentadiene molecule during the cycloaddition.

The formation of the *endo* isomer is usually favoured compared with the *exo* due to secondary orbital interactions in the transition state which stabilises the *endo* transition state relative to the *exo*, this is known as the *endo* rule.

Crystals suitable for X-Ray diffraction were obtained by slow diffusion of diethyl ether into a chloroform solution of **5.12**. It is worth a note that crystallisation of these compounds led most of times to formation of long hollow needles not suitable for X-Ray diffraction. Single-crystal X-ray diffraction studies confirmed the formation of the *endo* isomer. The crystal structure is depicted in Figure 5.6, selected bond lengths and angles in Table 5.3.

(a)



(b)

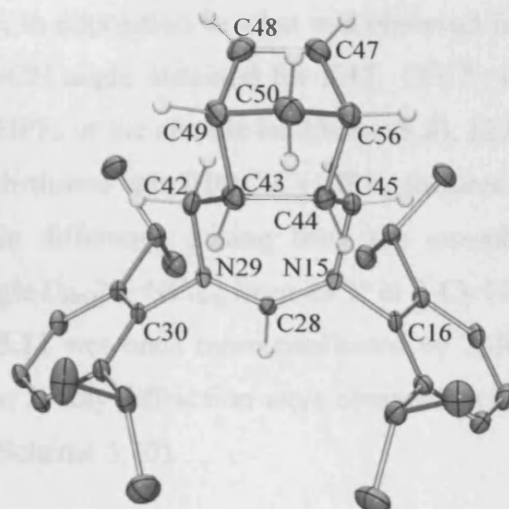


**Figure 5.6.** ORTEP ellipsoid plots at 30% probability of the amidinium salt **5.12**. The  $\text{BF}_4$  counter anion, protons and solvent molecules were omitted for clarity.

**Table 5.3.** Selected bond lengths and angles for salt **5.12**.

Lengths (Å)		Angles (°)	
N(29)-C(28)	1.317(3)	N(15)-C(28)-N(29)	127.7(2)
N(15)-C(28)	1.316(3)	C(28)-N(29)-C(30)	116.8(2)
N(15)-C(45)	1.497(4)	C(28)-N(29)-C(42)	126.0(2)
N(15)-C(16)	1.458(3)	C(30)-N(29)-C(42)	116.8(2)
N(29)-C(42)	1.496(4)	N(29)-C(30)-C(31)	118.0(2)
N(29)-C(30)	1.465(3)	N(29)-C(30)-C(38)	118.6(2)
C(47)-C(48)	1.322(5)	N(29)-C(42)-C(43)	114.0(3)
C(44)-C(45)	1.498(4)	C(44)-C(45)-N(15)	112.4(2)
C(42)-C(43)	1.509(5)	N(15)-C(16)-C(17)	117.4(3)
C(43)-C(44)	1.568(4)	N(15)-C(16)-C(24)	119.1(3)
C(47)-C(48)	1.322(5)	C(28)-N(15)-C(45)	124.8(2)
		C(16)-N(15)-C(45)	117.3(2)
		C(16)-N(15)-C(28)	117.8(2)
		C(42)-C(43)-C(44)	115.7(3)
		C(43)-C(44)-C(45)	114.7(3)
		C(42)-C(43)-C(49)	112.9(3)
		C(45)-C(44)-C(46)	112.7(3)

The *cis* substitution on the backbone in **5.12** does not lead to an important disruption in the geometry of the carbene, in opposition to what was observed for the *trans*-substituted salt, **DIOC-Cy·HPF<sub>6</sub>**. The NCN angle obtained for **5.12**, 127.7°, is virtually the same in the unsubstituted salt **7-Cy·HPF<sub>6</sub>** or the alkenic backbone (**5.3**), 127.3° and 127.4° respectively, in contrast, the *trans*-substituted salt **DIOC-Cy·HPF<sub>6</sub>** features a significantly wider NCN angle, 135.9°. The main difference arising from the *cis*-substitution is the prominent change in the torsion angle C<sub>ring</sub>N...NC<sub>ring</sub> from 23.3° in **7-Cy·HPF<sub>6</sub>** to 3.3° in **5.12**.

The *endo* geometry of **5.11** was once more confirmed by X-Ray crystallography (Figure 5.7). Crystals suitable for X-Ray diffraction were obtained as a by-product of the synthesis of silver complex **5.14** (Scheme 5.10).

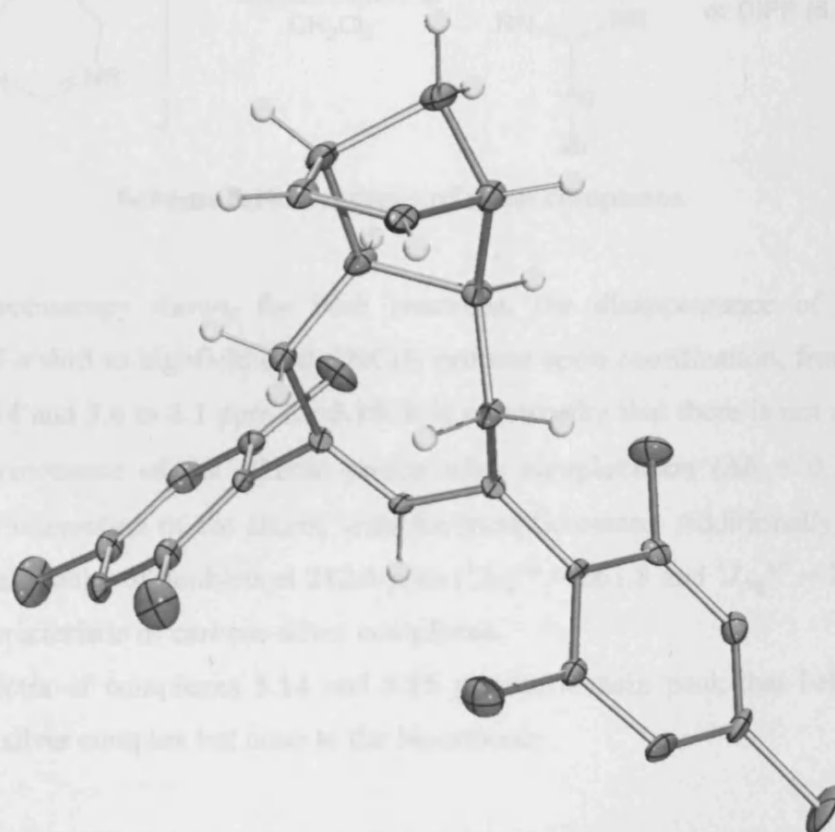


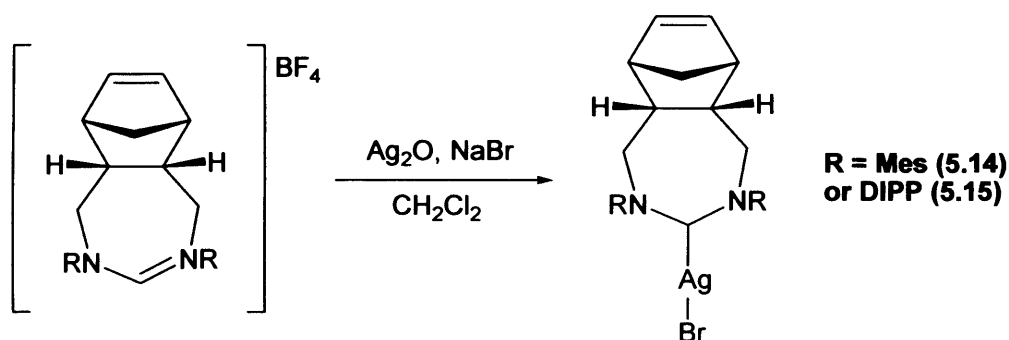
**Figure 5.7.** ORTEP ellipsoid plots at 30% probability of the amidinium salt **5.13**. The Br counter anion, protons and solvent molecules were omitted for clarity.



### 5.2.3. Coordination chemistry of the functionalised amidinium salts 5.11 and 5.12.

#### 5.2.3.1. Synthesis of silver complexes.

The silver salts **5.14** and **5.15** were synthesised according to the procedure described in *Chapter 3* (Scheme 5.10), affording complexes **5.14** and **5.15** in good yields with reaction times of approximately 2 days.



**Scheme 5.10.** Synthesis of silver complexes.

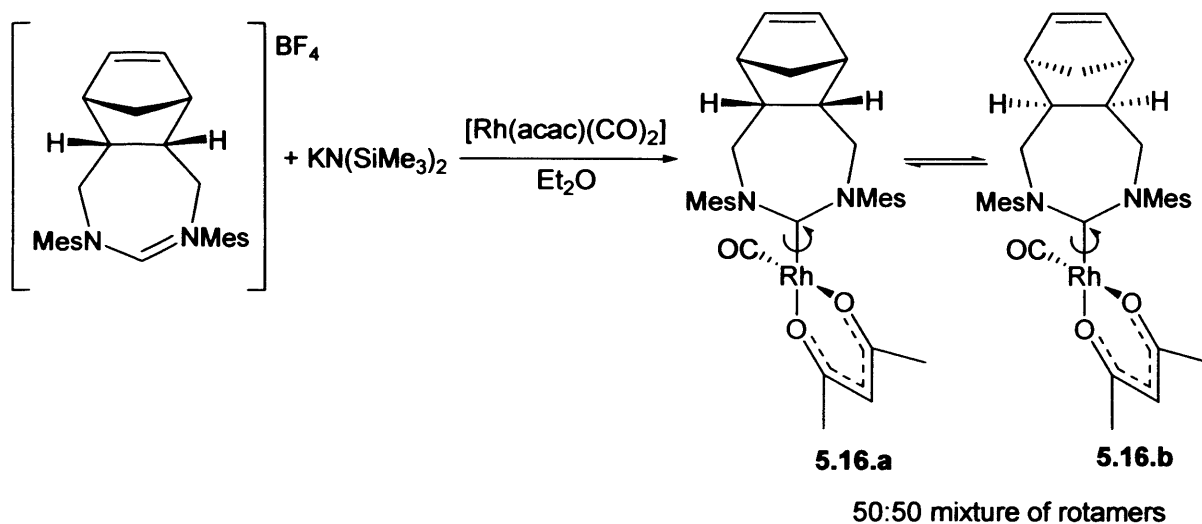
$^1\text{H}$  NMR spectroscopy shows, for both reactions, the disappearance of the  $\text{NCHN}$  resonance and a shift to highfield of the  $\text{NCH}_2$  protons upon coordination, from *ca.* 4.4 to *ca.* 3.5 for **5.14** and 3.4 to 3.1 ppm for **5.15**. It is noteworthy that there is not a significant shift on the resonance of the alkenic proton after complexation ( $\Delta\delta = 0.1\text{-}0.2$  ppm), suggesting no interaction of the alkene with the metallic centre. Additionally, compound **5.14** features a doublet of doublets at 212.6 ppm ( $^1J_{\text{Ag}}^{109} = 261.8$  and  $^1J_{\text{Ag}}^{107} = 226.9$  Hz) in  $^{13}\text{C}$  NMR, characteristic of carbene silver complexes.

The mass spectra of complexes **5.14** and **5.15** present a main peak that belongs to the monocarbene silver complex but none to the biscarbene.

#### 5.2.3.2. Synthesis of rhodium complexes.

Compound **5.16** was prepared in good yields generating the free carbene *in situ* by reaction of amidinium salt **5.11** with  $\text{KN}(\text{SiMe}_3)_2$ , in presence of the metal precursor in diethyl ether (Scheme 5.11). Compound **5.16** was isolated as a mixture of two isomers **5.16.a** and **5.16.b**.

Initial attempts to coordinate the free carbenes of **5.11** and **5.12** to  $[\text{Rh}(\text{COD})\text{Cl}]_2$  were unsuccessful, and the decomposition products were recovered instead. However, when they were reacted with  $[\text{Rh}(\text{acac})(\text{CO})_2]$  the expected compounds **5.16** and **5.17** were obtained by substitution of one of the carbonyl ligands.

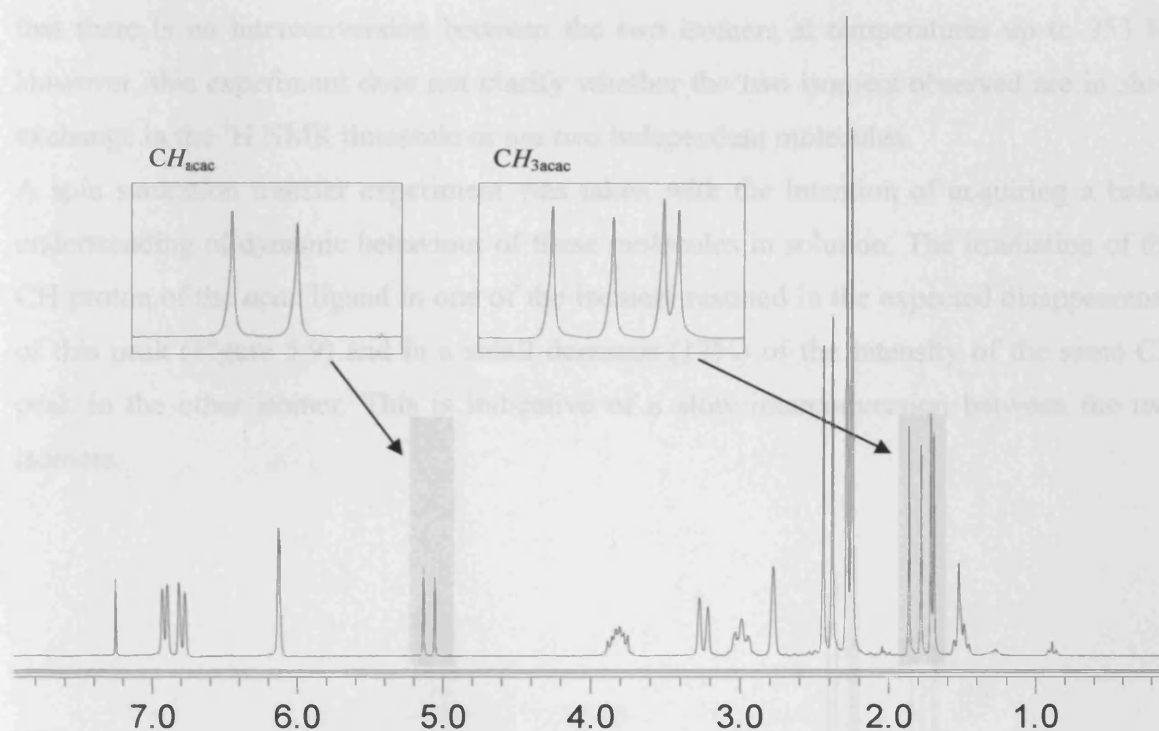


**Scheme 5.11.** Synthesis of complex **5.16**.

The IR spectrum of  $[\text{Rh}(\text{acac})(\text{CO})_2]$  shows two CO vibration modes, typical of biscarbonyl complexes, changes upon coordination of **5.11**-HX to the one expected for a monocarbonyl complex, with only one carbonyl stretching frequency at  $1942\text{ cm}^{-1}$ . This confirms the exchange of one of the two carbonyls in the metal precursor for the carbene ligand.

Unexpectedly, the  $^{13}\text{C}$  NMR spectrum of **5.16** shows two carbene carbon resonances at 206.9 ( $^1J_{\text{RhC}} = 53.6\text{ Hz}$ ) and 206.7 ( $^1J_{\text{RhC}} = 54.3\text{ Hz}$ ) ppm and two carbonyl carbon resonances at 190.5 ( $^1J_{\text{RhC}} = 49.5\text{ Hz}$ ) and 189.6 ( $^1J_{\text{RhC}} = 49.4\text{ Hz}$ ) ppm as two sets of doublets in both cases due to rhodium-carbon coupling. Likewise, two peaks of equal intensity are observed for the CH of the acac ligand in  $^1\text{H}$  NMR (Figure 5.8). The above observations suggest the formation of a 50:50 rotamers ratio, defined by the orientation of the carbene double bond with respect to the rest of the molecule. Assuming that the carbene ligand is perpendicular to the coordination plane, in one of the isomers the double bond would be pointing towards the acac ligand (**5.16.a**) and in the other towards the carbonyl ligand (**5.16.b**).

(a)



(b)

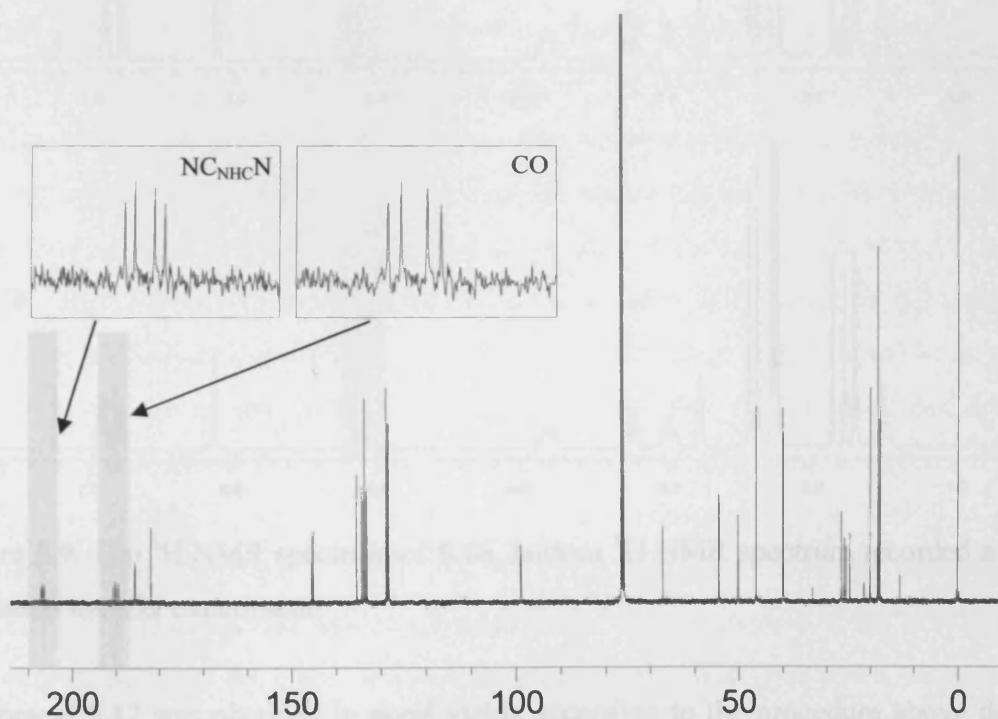


**Figure 5.8.**  $^1\text{H}$  NMR (a) and  $^{13}\text{C}$  NMR (b) of complex **5.16** show the formation of two isomers **5.16.a** and **5.16.b**.

When a  $^1\text{H}$  NMR sample of compound **5.16** was heated to  $80^\circ\text{C}$  no broadening of the peaks belonging to the CH of the *acac* ligand of the two isomers was observed, which indicates that there is no interconversion between the two isomers at temperatures up to 353 K. However, this experiment does not clarify whether the two isomers observed are in slow exchange in the  $^1\text{H}$  NMR timescale or are two independent molecules.

A spin saturation transfer experiment was taken with the intention of acquiring a better understanding of dynamic behaviour of these molecules in solution. The irradiation of the CH proton of the *acac* ligand in one of the isomers resulted in the expected disappearance of this peak (Figure 5.9) and in a small decrease (17%) of the intensity of the same CH peak in the other isomer. This is indicative of a slow interconversion between the two isomers.

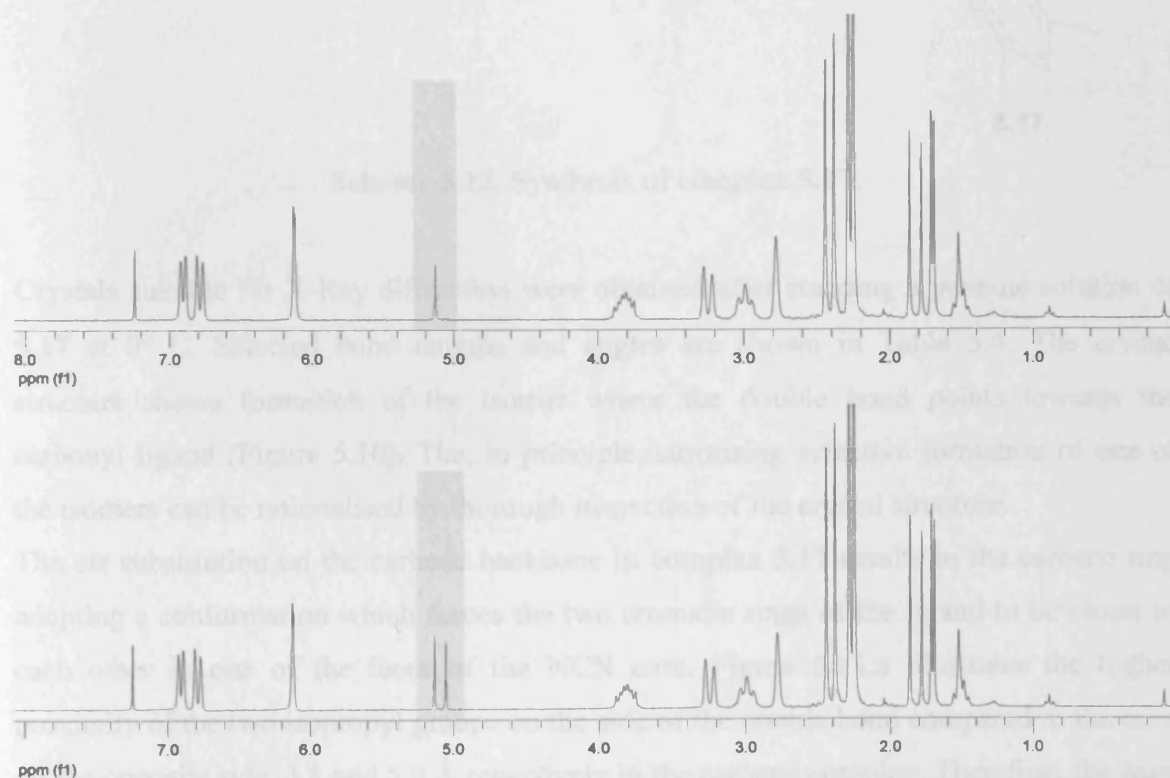
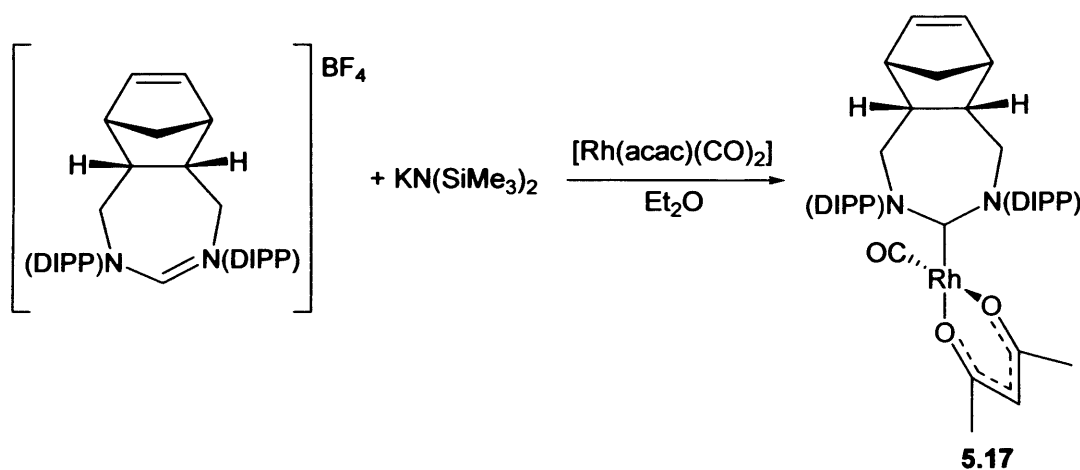


**Figure 5.9.** Top  $^1\text{H}$  NMR spectrum of **5.16**, bottom  $^1\text{H}$  NMR spectrum recorded after spin saturation transfer experiment.

Compound **5.17** was obtained in good yields according to the procedure above described for its analogous mesityl derivative (Scheme 5.12). Unexpectedly, in this case, only one of the two possible isomers is observed by  $^1\text{H}$  NMR and  $^{13}\text{C}$  NMR. The most noticeable

evidence for the formation of only one of the isomers is the appearance of only one resonance for the acac's CH at 5.18 ppm in proton NMR. Additionally, only two singlets are observed for the methyl groups at the acac ligand in  $^1\text{H}$  NMR and  $^{13}\text{C}$  NMR. The data obtained from infrared spectroscopy, where only one carbonyl vibration was observed at  $1948\text{ cm}^{-1}$ , confirms the formation of the monocarbonyl complex.



**Scheme 5.12.** Synthesis of complex **5.17**.

Crystals suitable for X-Ray diffraction were obtained after standing a pentane solution of **5.17** at  $0^\circ\text{ C}$ . Selected bond lengths and angles are shown in Table 5.4. The crystal structure shows formation of the isomer where the double bond points towards the carbonyl ligand (Figure 5.10). The, in principle, surprising selective formation of one of the isomers can be rationalised by thorough inspection of the crystal structure.

The *cis* substitution on the carbene backbone in complex **5.17** results in the carbene ring adopting a conformation which forces the two aromatic rings of the ligand to be closer to each other in one of the faces of the NCN core. Figure 5.11.a illustrates the higher proximity of the two isopropyl groups on the side of the double bond compared to the ones on the opposite side, 3.8 and 5.9 Å respectively in the carbene complex. Therefore, the least encumbered face of the ligand can tilt over the *cis* ligand. This allows the methinic protons of the *iso*-propyls to establish weak hydrogen bonds with the oxygen of the acac ligand and the methyl protons on the other face of the carbene with the oxygen of the carbonyl ligand (Figure 5.12). Interestingly, the previously described asymmetry of the aromatic substituents is not observed in salt **5.12**, where the distances between the *iso*-propyl groups on the opposite aromatic substituents are virtually the same, 4.7 and 4.5 Å (Figure 5.11.b).

This can be explained as a result of the increase of the torsion angle  $C_{Ar}-N\cdots N-C_{Ar}$  upon coordination, from  $9.7^\circ$  in **5.12** to  $14.5^\circ$  in **5.17**, due to the pyramidalisation of the nitrogen atoms in the rhodium complex relative to the salt (from 0.03 and 0.05 Å from N to the  $C_{NHC}-C_{DIPP}-C_{ring}$  plane in **5.12** to 0.07 and 0.08 Å in **5.17**).

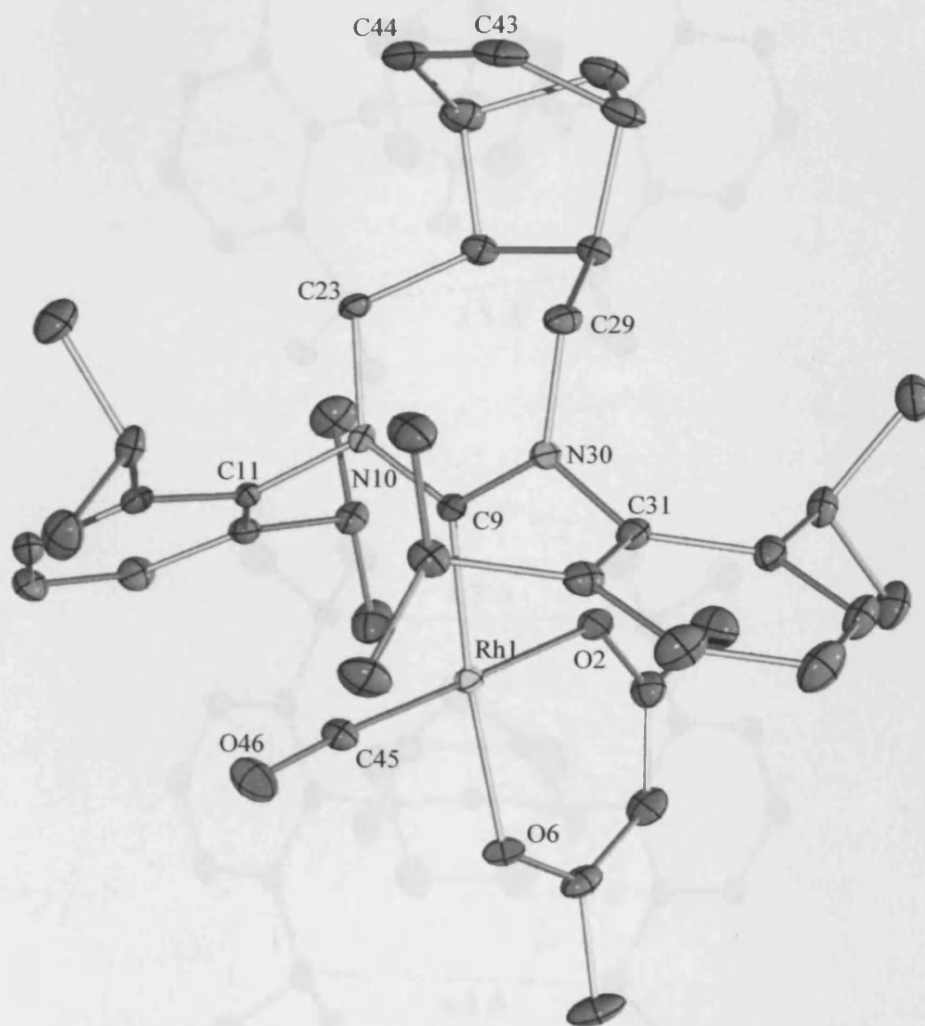
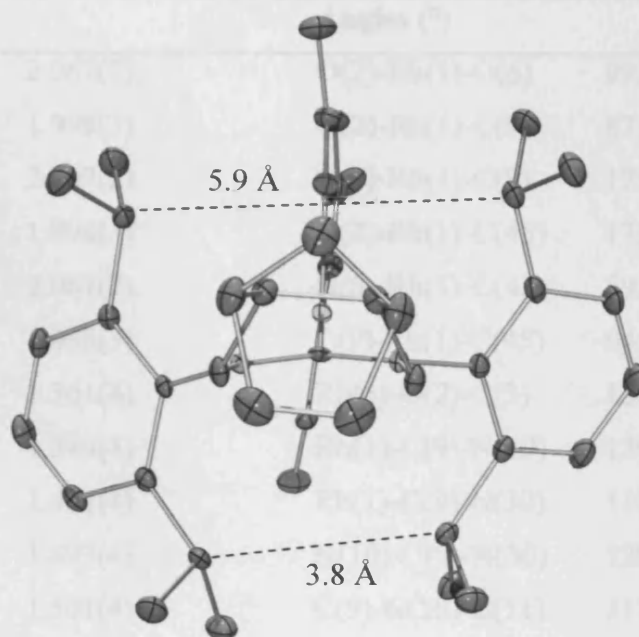


**Figure 5.10.** ORTEP ellipsoid plots at 30% probability of complex **5.17**. Protons were omitted for clarity.

(a)



(b)

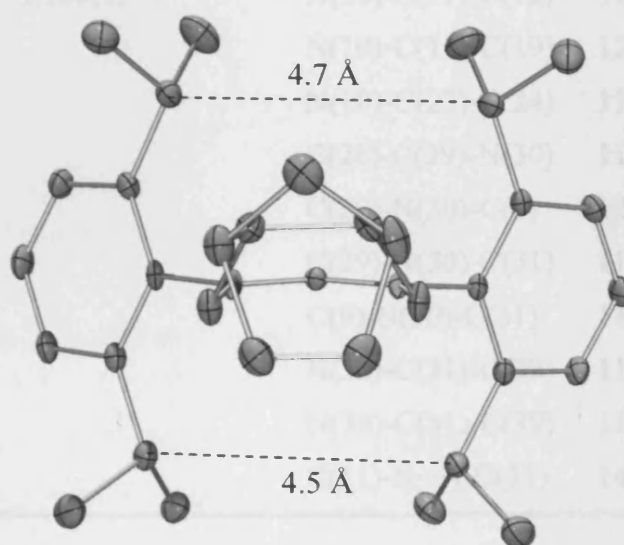


**Figure 5.11.** (a) View of complex 5.17 from the C(9)-Rh(1) bond; (b) View of salt 5.12 from the backbone.

**Table 5.4.** Selected bond lengths and angles for complex **5.17**.

Lengths (Å)		Angles (°)	
Rh(1)-O(2)	2.067(2)	O(2)-Rh(1)-O(6)	89.11(8)
Rh(1)-C(9)	1.998(3)	O(2)-Rh(1)-C(9)	87.04(10)
Rh(1)-O(2)	2.067(2)	O(6)-Rh(1)-C(9)	175.20(10)
Rh(1)-C(9)	1.998(3)	O(2)-Rh(1)-C(45)	173.34(11)
Rh(1)-O(2)	2.067(2)	O(6)-Rh(1)-C(45)	89.17(11)
Rh(1)-C(9)	1.998(3)	C(9)-Rh(1)-C(45)	94.98(12)
C(9)-N(10)	1.361(4)	Rh(1)-O(2)-C(3)	125.3(2)
C(9)-N(30)	1.349(4)	Rh(1)-C(9)-N(10)	120.6(2)
N(10)-C(11)	1.457(4)	Rh(1)-C(9)-N(30)	118.8(2)
N(10)-C(23)	1.493(4)	N(10)-C(9)-N(30)	120.0(2)
C(29)-N(30)	1.501(4)	C(9)-N(10)-C(11)	117.9(2)
N(30)-C(31)	1.462(4)	C(9)-N(10)-C(23)	129.2(2)
C(43)-C(44)	1.329(5)	C(11)-N(10)-C(23)	112.0(2)
C(45)-O(46)	1.155(4)	N(10)-C(11)-C(12)	117.9(3)
		N(10)-C(11)-C(19)	120.1(3)
		N(10)-C(23)-C(24)	114.7(2)
		C(28)-C(29)-N(30)	113.5(2)
		C(29)-N(30)-C(9)	127.0(2)
		C(29)-N(30)-C(31)	113.1(2)
		C(9)-N(30)-C(31)	119.2(2)
		N(30)-C(31)-C(32)	118.9(3)
		N(30)-C(31)-C(39)	119.5(3)
		C(11)-N...N-C(31)	14.5



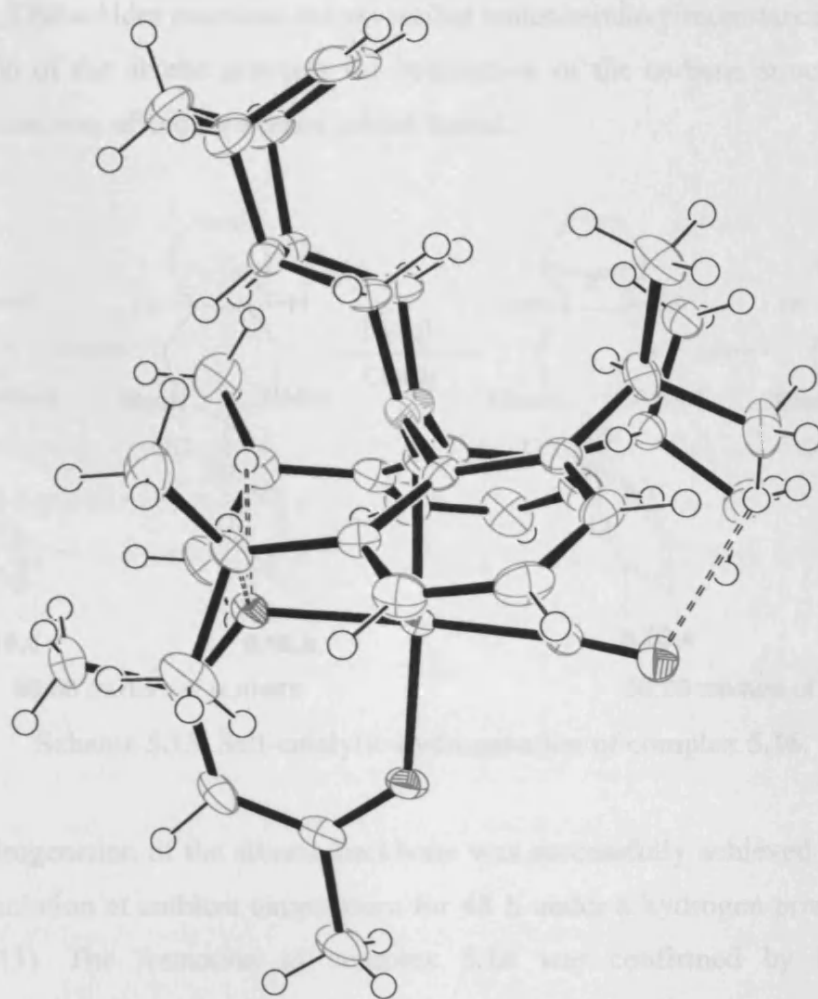


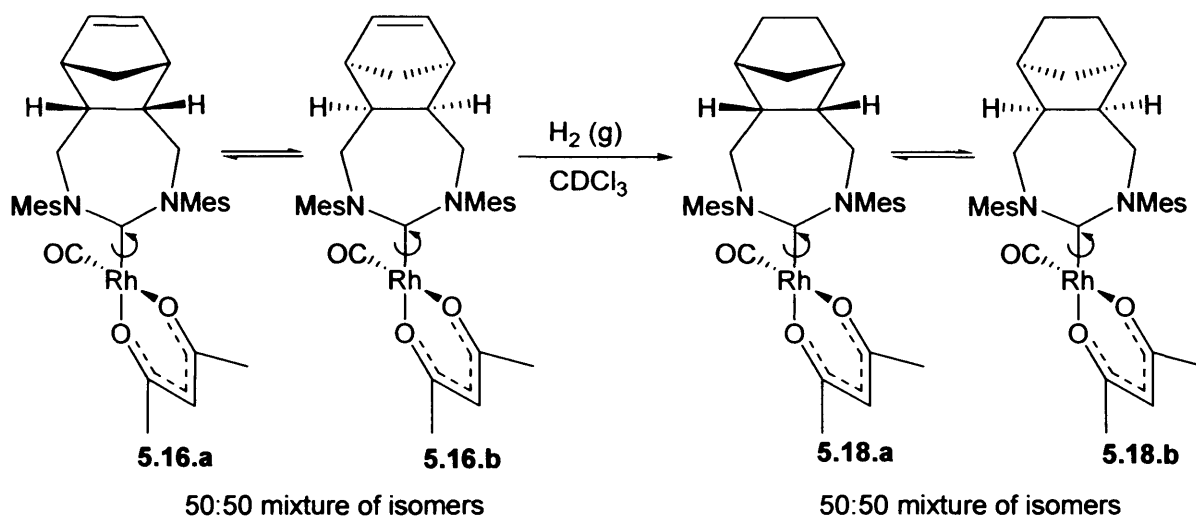
**Figure 5.12.** Ortep representation of 5.17. The hydrogen bonds are drawn as dashed lines.

### 5.2.3. Self-catalytic-hydrogenation of complex 5.16.

The self-hydrogenation of the backbone was attempted in order to test the potential reactivity of these complexes towards metal self-catalytic processes. Previous to this, other self-catalytic hydrogenation reactions have been reported. For example, Hahn and co-workers described the hydrogenation of the allyl substituents at the nitrogens by hydrogen transfer from ethanol in  $[\text{Ir}(\text{NHC})(\text{COD})\text{Br}]$  (NHC = 1,3-di(allyl)benzimidazol-2-ylidene) to afford  $[\text{Ir}(\text{NHC})(\text{COD})\text{Br}]$  (NHC = 1,3-di(propyl)benzimidazol-2-ylidene).<sup>8</sup>

<sup>8</sup> Hahn, F. Ekkehardt; Holtgrewe, Christian; Pape, Tania; Martin, Marta; Sola, Eduardo; Oro, Luis A. *Organometallics* **2005**, *24*, 2203.

Furthermore, Diels-Alder reactions are reversible under certain circumstances.<sup>9</sup> Hence, the hydrogenation of the alkene prevents the breakdown of the carbene structure *via* retro-Diels-Alder reaction, affording a more robust ligand.



**Scheme 5.13.** Self-catalytic-hydrogenation of complex **5.16**.

The self-hydrogenation of the alkenic backbone was successfully achieved after stirring a chloroform solution at ambient temperature for 48 h under a hydrogen pressure of 2 bars (Scheme 5.13). The formation of complex **5.18** was confirmed by IR and NMR spectroscopy. Infrared spectroscopy shows one band corresponding to a carbonyl vibration at  $1944\text{ cm}^{-1}$ , which confirms that the carbonyl ligand is still coordinated to the metal centre. This observation agrees with the information obtained from the  $^{13}\text{C}$  NMR, where two sets of doublets were identified for the carbene carbon (206.9 and 206.7 ppm) and for the carbonyl ligands (190.5 and 189.6 ppm), as observed for compounds **5.18.a** and **5.18.b**. The hydrogenation of the double bond is proved by the disappearance of the olefinic resonance at 6.05 ppm in  $^1\text{H}$  NMR and 135.5 in  $^{13}\text{C}$  NMR. Moreover,  $^1\text{H}$  NMR shows two peaks corresponding to the *CH* of the *acac* ligand, four for the  $\text{CH}_3$  and no hydride resonance when the spectrum is expanded until  $-40$  ppm.

The above observations seem to provide enough evidence for self-hydrogenation of the alkenic backbone of **5.16**, but no further hydrogen addition to the metal centre leading to a hydride complex was observed.

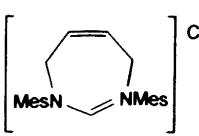
<sup>9</sup> (a) Kwart, H.; King, K. *Chem. rev.* **1968**, *68*, 415. (b) Smith, G.G.; Kelly, F.W. *Progr. Phys. Org. Chem.* **1971**, *8*, 75.

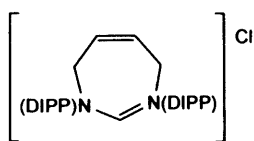
When the salt **5.11** was treated under the same conditions no hydrogenation was observed, confirming that this is a metal mediated addition.

### 5.3. Experimental.

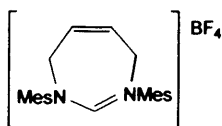
**General remarks.** All air sensitive experiments were performed under a nitrogen atmosphere in an MBraun glove box or under argon by standard Schlenk techniques. Diethyl ether, tetrahydrofuran and hexane were distilled from sodium and benzophenone under N<sub>2</sub> atmosphere. Pentane was used as purchased. Dichloromethane was distilled from calcium hydride under N<sub>2</sub> atmosphere. <sup>1</sup>H and <sup>13</sup>C spectra were recorded using a Bruker Advance DPX<sub>400</sub> spectrometer. Chemical shifts (δ) were expressed in ppm downfield from tetramethylsilane using the residual proton as an internal standard (CDCl<sub>3</sub>, <sup>1</sup>H 7.26 ppm and <sup>13</sup>C 77.0 ppm; benzene-d<sub>6</sub> <sup>1</sup>H 7.15 ppm and <sup>13</sup>C 128.0 ppm). Coupling constants are expressed in Hertz. HRMS were obtained on a Waters LCT Premier XE instrument and are reported as *m/z* (relative intensity). Infrared spectra were recorded using a JASCO FT/IR-660 *Plus* spectrometer and analysed in solution (dichloromethane).

#### 1,3-Bis-(2,4,6-trimethylphenyl)-4,7-dihydro-3*H*-[1,3]diazepin-1-ium chloride (**5.3**).

 Dimesitylamidine (8.37 g, 30 mmol), potassium carbonate (2.1 g, 15 mmol) and 1,4-dichloro-*cis*-2-butene (3.5 mL, 33 mmol) were dissolved in 250 mL of acetonitrile. The reaction was heated to 55°C for 5 days, after which time the solvent was evaporated under reduced pressure. The remaining residue was dissolved in dichloromethane and any insoluble impurities were filtered off. Addition of ether to the dichloromethane solution afforded 4.42 g (12 mmol, 40%) of white, crystalline material. <sup>1</sup>H NMR (CDCl<sub>3</sub>, 400 MHz, rt): δ 7.06 (s, 1H, NCHN), 6.88 (s, 4H, *m*-CH), 6.46 (t, <sup>3</sup>J<sub>HH</sub> = 4.4, 2H, =CH-), 5.29 (d, <sup>2</sup>J<sub>HH</sub> = 7.9, 4H, NCH<sub>2</sub>), 2.40 (s, 12H, *o*-CH<sub>3</sub>), 2.21 (s, 6H, *p*-CH<sub>3</sub>). <sup>13</sup>C NMR (CDCl<sub>3</sub>, 100 MHz, rt): δ 157.4 (s, NCN), 140.7 (s, C<sub>Mes</sub>), 140.6 (s, C<sub>Mes</sub>), 134.2 (s, C<sub>Mes</sub>), 131.6 (s, *m*-CH), 130.4 (s, =CH-), 50.8 (s, NCH<sub>2</sub>), 20.9 (s, *p*-CH<sub>3</sub>), 18.5 (s, *o*-CH<sub>3</sub>). MS (ES): *m/z* 333.2328 (M – BF<sub>4</sub><sup>+</sup>; C<sub>23</sub>H<sub>29</sub>N<sub>2</sub> requires 333.2331).

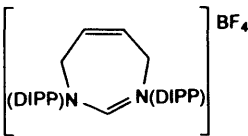
**1,3-Bis-(2,6-diisopropylphenyl)-4,7-dihydro-3*H*-[1,3]diazepin-1-ium chloride (5.4).**

Diisopropylamidine (13.57 g, 30 mmol), potassium carbonate (2.1 g, 15 mmol) and 1,4-dichloro-*cis*-2-butene (3.5 mL, 33 mmol) were dissolved in 250 mL of acetonitrile. The reaction was heated to 55°C for 8 days, after which time the solvent was evaporated under reduced pressure. The remaining residue was dissolved in dichloromethane and any insoluble impurities were filtered off. Addition of ether to the dichloromethane solution afforded 6.7 g (13.2 mmol, 44%) of white, crystalline material.  $^1\text{H}$  NMR ( $\text{CDCl}_3$ , 400 MHz, rt):  $\delta$  7.37 (2H, t,  $^3J_{\text{HH}} = 7.7$ , *p*- $\text{CH}_{\text{Ar}}$ ), 7.22 (4H, d,  $^3J_{\text{HH}} = 7.7$ , *o*- $\text{CH}_{\text{Ar}}$ ), 7.21 (1H, s, NCHN), 6.49 (2H, t,  $^3J_{\text{HH}} = 4.4$ , =CH-), 5.48 (4H, d,  $^2J_{\text{HH}} = 7.9$ , NCH<sub>2</sub>), 3.49 (4H, sept.,  $^3J_{\text{HH}} = 6.8$ , CH(CH<sub>3</sub>)<sub>2</sub>), 2.72 (4H, d,  $^3J_{\text{HH}} = 6.8$ , CH(CH<sub>3</sub>)<sub>2</sub>), 1.24 (4H, d,  $^3J_{\text{HH}} = 6.8$ , CH(CH<sub>3</sub>)<sub>2</sub>);  $^{13}\text{C}$  NMR ( $\text{CDCl}_3$ , 400 MHz, rt):  $\delta$  156.5 (s, NCN), 145.6 (s, C<sub>Ar</sub>), 140.3 (s, C<sub>Ar</sub>), 131.6 (s, CH<sub>Ar</sub>), 131.2 (s, CH<sub>Ar</sub>), 125.5 (s, CH<sub>Ar</sub>), 52.5 (s, NCH<sub>2</sub>), 29.1 (s, CH(CH<sub>3</sub>)<sub>2</sub>), 25.5 (s, CH(CH<sub>3</sub>)<sub>2</sub>), 24.6 (s, CH(CH<sub>3</sub>)<sub>2</sub>); MS (ES): *m/z* 417.3258 (M – BF<sub>4</sub><sup>+</sup>; C<sub>29</sub>H<sub>41</sub>N<sub>2</sub> requires 417.3270).

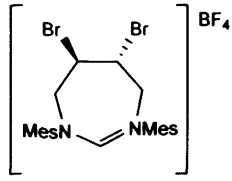
**1,3-Bis-(2,4,6-trimethylphenyl)-4,7-dihydro-3*H*-[1,3]diazepin-1-ium tetrafluoroborate (5.7).**

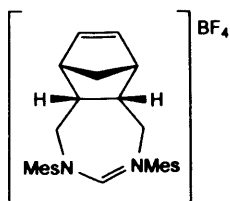
1,3-Bis-(2,4,6-trimethylphenyl)-4,5,6,7-tetrahydro-3*H*-[1,3]diazepin-1-ium chloride (7.0 g, 19 mmol) in 100 mL acetone and NaBF<sub>4</sub> (2.1 g, 19 mmol) in 25 mL water were stirred together at ambient temperature for 10 min. The acetone was evaporated under reduced pressure to afford a suspension of the BF<sub>4</sub> salt in water. After filtration the white solid obtained was recrystallised from a mixture dichloromethane/ether to yield 7.1 g (17 mmol, 89%) of white, crystalline material.  $^1\text{H}$  NMR ( $\text{CDCl}_3$ , 400 MHz, rt):  $\delta$  7.03 (1H, s, NCHN), 6.82 (4H, s, *m*-CH), 6.44 (2H, t,  $^3J_{\text{HH}} = 4.4$ , =CH-), 4.71 (4H, d,  $^3J_{\text{HH}} = 8.0$ , NCH<sub>2</sub>), 2.30 (12H, s, *o*-CH<sub>3</sub>), 2.19 (6H, s, *p*-CH<sub>3</sub>);  $^{13}\text{C}$  NMR ( $\text{CDCl}_3$ , 100 MHz, rt):  $\delta$  156.3 (s, NCN), 139.4 (s, C<sub>Ar</sub>), 139.1 (s, C<sub>Ar</sub>), 132.7 (s, C<sub>Ar</sub>), 129.8 (s, *m*-CH), 129.1 (s, =CH-), 48.6 (s, NCH<sub>2</sub>), 19.9 (s, *p*-CH<sub>3</sub>), 17.0 (s, *o*-CH<sub>3</sub>). MS (ES): *m/z* 333.2338 (M – BF<sub>4</sub><sup>+</sup>; C<sub>23</sub>H<sub>29</sub>N<sub>2</sub> requires 333.2331).

**1,3-Bis-(2,4-diisopropylphenyl)-4,7-dihydro-3*H*-[1,3]diazepin-1-ium tetrafluoroborate (5.8).**

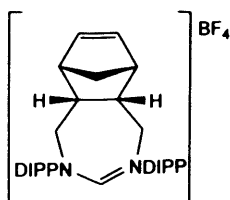

 $\text{BF}_4^-$  1,3-Bis-(2,6-diisopropylphenyl)-4,5,6,7-tetrahydro-3*H*-[1,3]diazepin-1-ium chloride (5.0 g, 11 mmol) in 100 mL acetone and  $\text{NaBF}_4$  (1.22 g, 11 mmol) in 25 mL water were stirred together at ambient temperature for 10 min. The acetone was evaporated under reduced pressure to afford a suspension of the  $\text{BF}_4$  salt in water. After filtration the white solid obtained was recrystallised in a mixture dichloromethane/ether to yield 5.2 g (10.3 mmol, 94%) of white, crystalline material.  $^1\text{H}$  NMR ( $\text{CDCl}_3$ , 400 MHz, rt):  $\delta$  7.34 (2H, t,  $^3J_{\text{HH}} = 7.8$ , *p*- $\text{CH}_{\text{Ar}}$ ), 7.17 (4H, d,  $^3J_{\text{HH}} = 7.8$ , *o*- $\text{CH}_{\text{Ar}}$ ), 7.14 (1H, s, NCHN), 6.48 (2H, t,  $^3J_{\text{HH}} = 4.4$ , =CH-), 4.88 (4H, d,  $^2J_{\text{HH}} = 8.1$ , NCH<sub>2</sub>), 3.21 (4H, sept.,  $^3J_{\text{HH}} = 6.8$ , CH(CH<sub>3</sub>)<sub>2</sub>), 1.30 (4H, d,  $^3J_{\text{HH}} = 6.8$ , CH(CH<sub>3</sub>)<sub>2</sub>), 1.18 (4H, d,  $^3J_{\text{HH}} = 6.8$ , CH(CH<sub>3</sub>)<sub>2</sub>);  $^{13}\text{C}$  NMR ( $\text{CDCl}_3$ , 400 MHz, rt):  $\delta$  155.5 (s, NCHN), 143.9 (s,  $\text{C}_{\text{Ar}}$ ), 138.5 (s,  $\text{C}_{\text{Ar}}$ ), 130.1 (s,  $\text{CH}_{\text{Ar}}$ ), 129.9 (s,  $\text{CH}_{\text{Ar}}$ ), 124.2 (s,  $\text{CH}_{\text{Ar}}$ ), 50.0 (s, NCH<sub>2</sub>), 27.8 (s, CH(CH<sub>3</sub>)<sub>2</sub>), 23.8 (s, CH(CH<sub>3</sub>)<sub>2</sub>), 23.1 (s, CH(CH<sub>3</sub>)<sub>2</sub>); MS (ES): *m/z* 417.3281 (M –  $\text{BF}_4^+$ ; C<sub>29</sub>H<sub>41</sub>N<sub>2</sub> requires 417.3270).

**Compound 5.10.**


 $\text{BF}_4^-$  1,3-Bis-(2,4,6-trimethylphenyl)-4,7-dihydro-3*H*-[1,3]diazepin-1-ium tetrafluoroborate (1.02 g, 1.76 mmol) was dissolved in 10 mL of DCM. The resulting solution was cooled to 0°C and bromine (25 ml, 1.76 mmol) was added dropwise. The resulting solution was stirred for 30 minutes. Ether was added to the solution until the solution became cloudy, and subsequently cooled to -30°C upon which the product slowly crystallised. Yield 988 mg (1.23 mmol, 70%) of slightly yellow microcrystalline material.  $^1\text{H}$  NMR ( $\text{CDCl}_3$ , 500 MHz, rt)  $\delta$  7.60 (1H, s, NCHN), 7.00 (2H, s, *m*-CH), 6.98 (2H, s, *m*-CH), 5.11 (2H, bs, NCH<sub>2</sub>), 5.05 (2H, bd,  $^3J_{\text{HH}} = 16.2$ , -CHBr), 4.50 (2H, bd,  $^3J_{\text{HH}} = 16.2$ , NCH<sub>2</sub>), 2.51 (6H, s, CH<sub>3</sub>), 2.38 (6H, s, CH<sub>3</sub>), 2.29 (6H, s, *o*-CH<sub>3</sub>);  $^{13}\text{C}$  NMR ( $\text{CDCl}_3$ , 100 MHz, rt):  $\delta$  158.8 (s, NCHN), 141.1 (s,  $\text{C}_{\text{Ar}}$ ), 138.5 (s,  $\text{C}_{\text{Ar}}$ ), 133.9 (s,  $\text{C}_{\text{Ar}}$ ), 133.1 (s,  $\text{C}_{\text{Ar}}$ ), 133.1 (s,  $\text{C}_{\text{Ar}}$ ), 130.8 (s, *m*-CH), 130.7 (s, *m*-CH), 60.1 (-CHBr), 48.9 (s, NCH<sub>2</sub>), 21.0 (s, CH<sub>3</sub>), 18.3 (s, CH<sub>3</sub>), 17.9 (s, CH<sub>3</sub>). MS (ES): *m/z* 491.0719 (M –  $\text{BF}_4^+$ ; C<sub>23</sub>H<sub>29</sub>N<sub>2</sub>Br<sub>2</sub> requires 491.0697).

**Compound 5.11.**

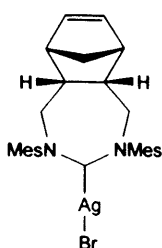
1,3-Bis-(2,4,6-trimethylphenyl)-4,7-dihydro-3*H*-[1,3]diazepin-1-ium tetrafluoroborate (2 g, 4.76 mmol) and cyclopentadiene (2 mL, 24 mmol) were dissolved in 40 mL of methanol. The reaction was heated to 60°C in a pressure tube overnight, after which time the solvent was evaporated under reduced pressure. The residue was recrystallised by addition of ether to a dichloromethane solution of the crude material to afford 2 g (3.81 mmol, 82%) of white crystals. <sup>1</sup>H NMR (CDCl<sub>3</sub>, 400 MHz, rt) δ 7.13 (1H, s, NCHN), 6.88 (4H, s, *m*-CH), 6.32 (2H, s, =CH-), 4.29 (4H, t, <sup>3</sup>J<sub>HH</sub> = 13.6, NCH<sub>2</sub>), 3.33 (2H, d, <sup>3</sup>J<sub>HH</sub> = 14.5, NCH<sub>2</sub>), 3.09 (2H, m, NCH<sub>2</sub>CH), 2.90 (2H, s, =CHCH-), 2.35 (6H, s, *p*-CH<sub>3</sub>), 2.28 (6H, s, *o*-CH<sub>3</sub>), 2.20 (6H, s, *o*-CH<sub>3</sub>), 1.53 (1H, d, <sup>3</sup>J<sub>HH</sub> = 8.7, CHCH<sub>2</sub>CH), 1.47 (1H, d, <sup>3</sup>J<sub>HH</sub> = 8.7, CHCH<sub>2</sub>CH); <sup>13</sup>C NMR (CDCl<sub>3</sub>, 100 MHz, rt): δ 156.8 (s, NCHN), 140.7 (s, C<sub>Ar</sub>), 140.4 (s, C<sub>Ar</sub>), 135.3 (s, C<sub>Ar</sub>), 134.8 (s, C<sub>Ar</sub>), 133.1 (s, =CH-), 130.9 (s, *m*-CH), 130.5 (s, *m*-CH), 55.5 (s, NCH<sub>2</sub>), 50.4 (s, CHCH<sub>2</sub>CH), 47.8 (s, =CHCH-), 41.6 (s, NCH<sub>2</sub>CH), 21.3 (s, CH<sub>3</sub>), 19.0 (s, CH<sub>3</sub>), 18.4 (s, CH<sub>3</sub>). MS (ES): *m/z* 399.2792 (M – BF<sub>4</sub><sup>+</sup>; C<sub>28</sub>H<sub>35</sub>N<sub>2</sub> requires 399.2800).

**Compound 5.12.**

1,3-Bis-(2,6-diisopropylphenyl)-4,7-dihydro-3*H*-[1,3]diazepin-1-ium tetrafluoroborate (2.4 g, 4.76 mmol) and cyclopentadiene (5 mL, 60 mmol) were dissolved in 40 mL of methanol. The reaction was heated to 65°C in a pressure tube for 2 days. The resulting solution was evaporated under reduced pressure and the residue crystallised by addition of ether to a dichloromethane solution to afford 2.36 g (4.09 mmol, 86%) of white crystals. Crystals suitable for X-Ray diffraction were obtained by slow diffusion of diethyl ether into a chloroform solution of **5.12**. <sup>1</sup>H NMR (CDCl<sub>3</sub>, 400 MHz, rt): δ 7.42 (2H, t, <sup>3</sup>J<sub>HH</sub> = 7.8, *p*-CH), 7.28 (4H, d, <sup>3</sup>J<sub>HH</sub> = 4.8, *m*-CH), 7.27 (1H, s, NCHN), 6.44 (2H, s, =CH-), 4.49 (2H, t, <sup>3</sup>J<sub>HH</sub> = 13.5, NCH<sub>2</sub>), 3.46 (2H, d, <sup>3</sup>J<sub>HH</sub> = 14.6, NCH<sub>2</sub>), 3.29-3.12 (6H, m, CH(CH<sub>3</sub>)<sub>2</sub>+NCH<sub>2</sub>CH), 2.98 (2H, s, =CHCH-), 1.65 (1H, d, <sup>3</sup>J<sub>HH</sub> = 8.8, CHCH<sub>2</sub>CH), 1.61 (1H, d, <sup>3</sup>J<sub>HH</sub> = 8.8, CHCH<sub>2</sub>CH), 1.42 (6H, d, <sup>3</sup>J<sub>HH</sub> = 7.1, CH(CH<sub>3</sub>)<sub>2</sub>), 1.40 (6H, d, <sup>3</sup>J<sub>HH</sub> = 7.1, CH(CH<sub>3</sub>)<sub>2</sub>), 1.32 (6H, d, <sup>3</sup>J<sub>HH</sub> = 6.8, CH(CH<sub>3</sub>)<sub>2</sub>), 1.22 (6H, d, <sup>3</sup>J<sub>HH</sub> = 6.8, CH(CH<sub>3</sub>)<sub>2</sub>); <sup>13</sup>C NMR (CDCl<sub>3</sub>, 100 MHz, rt): δ 155.8 (s, NCHN), 146.2 (s, C<sub>Ar</sub>), 144.2 (s, C<sub>Ar</sub>), 139.8 (s, C<sub>Ar</sub>), 135.4 (s, *m*-CH), 131.3 (s, *m*-CH), 126.1 (s, *p*-CH), 125.4 (s, =CH-), 56.8 (s,

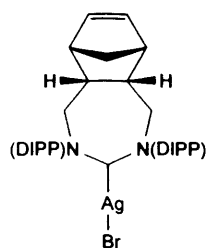
NCH<sub>2</sub>), 50.4 (s, CHCH<sub>2</sub>CH), 48.0 (s, =CHCH-), 40.9 (s, NCH<sub>2</sub>CH), 29.4 (s, CH(CH<sub>3</sub>)<sub>2</sub>), 29.2 (s, CH(CH<sub>3</sub>)<sub>2</sub>), 25.7 (s, CH(CH<sub>3</sub>)<sub>2</sub>), 25.2 (s, CH(CH<sub>3</sub>)<sub>2</sub>), 25.1 (s, CH(CH<sub>3</sub>)<sub>2</sub>), 24.7 (s, CH(CH<sub>3</sub>)<sub>2</sub>). MS (ES): *m/z* 483.3721 (M – BF<sub>4</sub><sup>+</sup>; C<sub>34</sub>H<sub>47</sub>N<sub>2</sub> requires 483.3739).

#### Compound 5.14.



A suspension of 300 mg (0.62 mmol) amidinium salt, 143 mg (2 eq, 0.62 mmol) of silver (I) oxide and 639 mg (10 eq, 6.2 mmol) of sodium bromide in 15 mL in dichloromethane is stirred for 2 days at ambient temperature. The resulting suspension was filtered and ether was added to the solution until the product crystallised. The product was isolated by filtration, washed with diethyl ether and dried *in vacuo* to afford 294 mg (0.5 mmol, 81%) of white crystals. <sup>1</sup>H NMR (CDCl<sub>3</sub>, 400 MHz, rt) δ 6.89 (2H, s, *m*-CH), 6.85 (2H, s, *m*-CH), 6.11 (2H, s, =CH-), 3.73 (4H, t, <sup>3</sup>J<sub>HH</sub> = 13.3, NCH<sub>2</sub>), 3.15 (2H, dd, <sup>3</sup>J<sub>HH</sub> = 14.1, <sup>3</sup>J<sub>HH</sub> = 1.5, NCH<sub>2</sub>), 2.95 (2H, m, NCH<sub>2</sub>CH), 2.75 (2H, s, =CHCH-), 2.34 (6H, s, *p*-CH<sub>3</sub>), 2.18 (6H, s, *o*-CH<sub>3</sub>), 2.16 (6H, s, *o*-CH<sub>3</sub>), 1.50 (1H, d, <sup>3</sup>J<sub>HH</sub> = 8.5, CHCH<sub>2</sub>CH), 1.44 (1H, d, <sup>3</sup>J<sub>HH</sub> = 8.5, CHCH<sub>2</sub>CH); <sup>13</sup>C NMR (CDCl<sub>3</sub>, 100 MHz, rt): δ 212.6 (dd, J<sub>Ag</sub><sup>109</sup> = 261.8, J<sub>Ag</sub><sup>107</sup> = 226.9, NCN), 145.6 (s, C<sub>Ar</sub>), 136.7 (s, C<sub>Ar</sub>), 133.5 (s, C<sub>Ar</sub>), 133.5 (s, C<sub>Ar</sub>), 132.6 (s, =CH-), 129.2 (s, *m*-CH), 129.1 (s, *m*-CH), 52.5 (s, NCH<sub>2</sub>), 50.0 (s, CHCH<sub>2</sub>CH), 47.4 (s, =CHCH-), 40.5 (s, NCH<sub>2</sub>CH), 20.0 (s, CH<sub>3</sub>), 18.1 (s, CH<sub>3</sub>), 17.3 (s, CH<sub>3</sub>). MS (ES): *m/z* 548.2185 ([M – Br + CH<sub>3</sub>CN]<sup>+</sup>; C<sub>30</sub>H<sub>38</sub>N<sub>3</sub>Ag requires 548.2194).

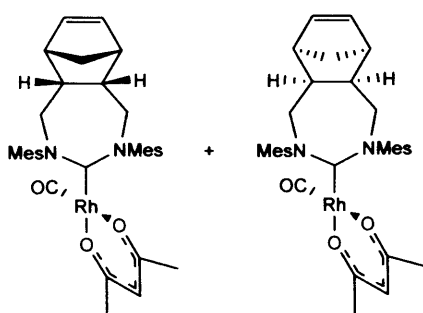
#### Compound 5.15.



A suspension of 570 mg (1 mmol) amidinium salt, 231.7 mg (2 eq, 1 mmol) of silver (I) oxide and 1.029 mg (10 eq, 10 mmol) of sodium bromide in 20 mL in dichloromethane is stirred for 2 days at ambient temperature. The resulting suspension was filtered and ether was added to the solution until the product crystallised. The product was isolated by filtration, washed with diethyl ether and dried *in vacuo* to afford 413 mg (0.66 mmol, 66%) of white crystals. <sup>1</sup>H NMR (CDCl<sub>3</sub>, 400 MHz, rt) δ 7.25 (2H, t, <sup>3</sup>J<sub>HH</sub> = 7.7, *p*-CH), 7.13 (4H, d, <sup>3</sup>J<sub>HH</sub> = 7.8, *m*-CH), 7.10 (4H, d, <sup>3</sup>J<sub>HH</sub> = 7.7, *m*-CH), 6.36 (2H, s, =CH-), 3.77 (2H, t, <sup>3</sup>J<sub>HH</sub> = 13.3, NCH<sub>2</sub>CH), 3.31 (2H, p, <sup>3</sup>J<sub>HH</sub> = 6.9, CH(CH<sub>3</sub>)<sub>2</sub>), 3.26 (2H, d, <sup>3</sup>J<sub>HH</sub> = 12.4, NCH<sub>2</sub>), 3.00 (4H, m, CH(CH<sub>3</sub>)<sub>2</sub> + NCH<sub>2</sub>), 2.76 (2H, s, =CHCH-), 1.55 (1H, d, <sup>3</sup>J<sub>HH</sub> = 8.5, CHCH<sub>2</sub>CH), 1.49 (1H, d, <sup>3</sup>J<sub>HH</sub> = 8.6, CHCH<sub>2</sub>CH), 1.32 (6H, d, <sup>3</sup>J<sub>HH</sub> = 6.8, CH(CH<sub>3</sub>)<sub>2</sub>),

1.25 (6H, d,  $^3J_{\text{HH}} = 6.9$ ,  $\text{CH}(\text{CH}_3)_2$ ), 1.23 (6H, d,  $^3J_{\text{HH}} = 6.9$ ,  $\text{CH}(\text{CH}_3)_2$ ), 1.20 (6H, d,  $^3J_{\text{HH}} = 6.8$ ,  $\text{CH}(\text{CH}_3)_2$ )  $^{13}\text{C}$  NMR ( $\text{CDCl}_3$ , 100 MHz, rt):  $\delta$  146.1 (s,  $\text{C}_{\text{Ar}}$ ), 144.5 (s,  $\text{C}_{\text{Ar}}$ ), 144.1 (s,  $\text{C}_{\text{Ar}}$ ), 134.5 (s, *m*-CH), 129.0 (s, *m*-CH), 125.1 (s, *p*-CH), 124.4 (s, =CH-), 54.9 (s,  $\text{NCH}_2$ ), 54.8 (s,  $\text{NCH}_2$ ), 53.4 (s,  $\text{CHCH}_2\text{CH}$ ), 47.4 (s, =CHCH-), 40.7 (s,  $\text{NCH}_2\text{CH}$ ), 29.5 (s,  $\text{CH}(\text{CH}_3)_2$ ), 28.9 (s,  $\text{CH}(\text{CH}_3)_2$ ), 25.3 (s,  $\text{CH}(\text{CH}_3)_2$ ), 24.9 (s,  $\text{CH}(\text{CH}_3)_2$ ), 24.8 (s,  $\text{CH}(\text{CH}_3)_2$ ), 24.6 (s,  $\text{CH}(\text{CH}_3)_2$ ). MS (ES):  $m/z$  630.2976 ( $[\text{M}-\text{Br}+\text{CH}_3\text{CN}]^+$ ;  $\text{C}_{36}\text{H}_{49}\text{N}_3\text{Ag}$  requires 630.2977).

### Compound 5.16.



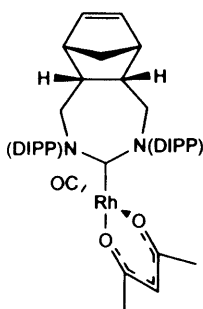
A solution of the free carbene, prepared by deprotonation of the salt (95 mg, 0.2 mmol) with  $\text{K}[\text{HMDS}]$  (40 mg, 0.2 mmol) in 5 mL of diethyl ether, was added dropwise to a stirred solution of  $\text{Rh}(\text{CO})_2(\text{acac})$  (50 mg, 0.2 mmol in 5 mL of  $\text{Et}_2\text{O}$ ). Immediately colour change was observed from light to dark yellow. After stirring the reaction at room

temperature overnight the insoluble impurities filtered off and the solvent was removed *in vacuo* to afford 85 mg (0.14 mmol, 68%) of a yellow solid. Crystals of the title compound suitable for X-ray diffraction were grown after a pentane solution was allowed to stand in the fridge for 3 days.  $^1\text{H}$  NMR ( $\text{CDCl}_3$ , 400 MHz, rt)  $\delta$  6.86 (2H, s, *m*-CH, i1), 6.82 (2H, s, *m*-CH, i1), 6.74 (2H, s, *m*-CH, i2), 6.70 (2H, s, *m*-CH, i2), 6.05 (4H, m, =CH-, i1+i2), 5.04 (1H, s,  $\text{CH}_{\text{acac}}$ , i1), 4.99 (1H, s,  $\text{CH}_{\text{acac}}$ , i2), 3.79-3.70 (4H, bq,  $^3J_{\text{HH}} = 13.0$   $\text{NCH}_2$ , i1+i2), 3.17 (4H, bd,  $^3J_{\text{HH}} = 14.2$ ,  $\text{NCH}_2\text{CH}$ , i1+i2), 2.95-2.88 (4H, m,  $\text{NCH}_2\text{CH}$ , i1+i2), 2.71 (4H, s, =CHCH-, i1+i2), 2.37 (6H, s, *p*- $\text{CH}_3$ , i1), 2.31 (6H, s, *p*- $\text{CH}_3$ , i2), 2.21 (12H, s, *o*- $\text{CH}_3$ , i1+i2), 2.18 (6H, s, *o*- $\text{CH}_3$ , i1), 2.17 (6H, s, *o*- $\text{CH}_3$ , i1), 1.79 (3H, s,  $\text{CH}_{3\text{acac}}$ , i1), 1.71 (3H, s,  $\text{CH}_{3\text{acac}}$ , i2), 1.64 (3H, s,  $\text{CH}_{3\text{acac}}$ , i1), 1.62 (3H, s,  $\text{CH}_{3\text{acac}}$ , i2), 1.47-1.39 (4H, m,  $\text{CHCH}_2\text{CH}$ , i1+i2);  $^{13}\text{C}$  NMR ( $\text{CDCl}_3$ , 100 MHz, rt):  $\delta$  206.9 (d,  $^1J_{\text{RhC}} = 53.6$ ,  $\text{NCN}$ , i1), 206.7 (d,  $^1J_{\text{RhC}} = 54.3$ ,  $\text{NCN}$ , i2), 190.5 (d,  $^1J_{\text{RhC}} = 49.5$ , CO, i1), 189.6 (d,  $^1J_{\text{RhC}} = 49.4$ , CO, i2), 185.7 (s,  $\text{CCH}_{3\text{acac}}$ , i1), 185.6 (s,  $\text{CCH}_{3\text{acac}}$ , i1), 182.0 ( $\text{CCH}_{3\text{acac}}$ , i1 and i2), 145.3 (s,  $\text{C}_{\text{Ar}}$ , i1), 144.9 (s,  $\text{C}_{\text{Ar}}$ , i1), 135.2 (s, *p*- $\text{C}_{\text{Ar}}$ , i1 and i2), 134.1 (s, *o*- $\text{C}_{\text{Ar}}$ , i1), 133.6 (s, *o*- $\text{C}_{\text{Ar}}$ , i2), 133.5 (s, =CH-, i1 and i2), 128.5 (s, *m*-CH), 128.2 (s, *m*-CH), 128.0 (s, *m*-CH), 98.6 (s,  $\text{CH}_{\text{acac}}$ , i1 and i2), 54.4 and 54.3 (s,  $\text{NCH}_2$ , i1 and i2), 50.0 (s,  $\text{CHCH}_2\text{CH}$ , i1 and i2), 46.0 (s, =CHCH-, i1 and i2), 39.9 and 39.8 (s,  $\text{NCH}_2\text{CH}$ , i1 and i2), 26.5, 25.8, 25.5

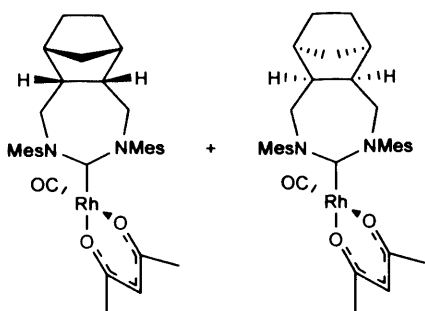


and 24.6 (s, CH<sub>3acac</sub>, i1 and i2), 20.0 (s, *p*-CH<sub>3</sub>, i1 and i2), 18.4, 17.9 and 17.7 (s, *o*-CH<sub>3</sub>, i1 and i2). IR:  $\nu(\text{CO}) = 1942.9 \text{ cm}^{-1}$ . MS (ES):  $m/z$  570.1992 (M - acac + CH<sub>3</sub>CN<sup>+</sup>; C<sub>31</sub>H<sub>37</sub>N<sub>3</sub>ORh requires 570.2009).

### Compound 5.17.



A solution of the free carbene, prepared by deprotonation of the salt (228 mg, 0.4 mmol) with K[HMDS] (40 mg, 0.2 mmol) in 10 mL of diethyl ether, was added dropwise to a stirred solution of Rh(CO)<sub>2</sub>(acac) (100 mg, 0.4 mmol in 10 mL of Et<sub>2</sub>O). Immediately colour change was observed from light to dark yellow. After stirring the reaction at room temperature overnight the insoluble impurities filtered off and the solvent was removed *in vacuo* to afford 188 mg (0.26 mmol, 66%) of a yellow solid. Crystals of the title compound suitable for X-ray diffraction were grown after a pentane solution was cooled to 0 °C for 3 days. <sup>1</sup>H NMR (CDCl<sub>3</sub>, 400 MHz, rt)  $\delta$  7.19-7.05 (6H, m, CH<sub>Ar</sub>), 5.79 (2H, t, <sup>3</sup>J<sub>HH</sub> = 1.6, =CH-), 5.18 (1H, s, CH<sub>acac</sub>), 3.96 (2H, t, <sup>3</sup>J<sub>HH</sub> = 12.4, NCH<sub>2</sub>), 3.44 (2H, q, <sup>3</sup>J<sub>HH</sub> = 6.7, CH(CH<sub>3</sub>)<sub>2</sub>), 3.19 (6H, m, CH(CH<sub>3</sub>)<sub>2</sub>+NCH<sub>2</sub>), 3.05 (2H, d, <sup>3</sup>J<sub>HH</sub> = 9.0, NCH<sub>2</sub>CH), 2.73 (2H, s, =CHCH-), 1.88 (3H, s, CH<sub>3acac</sub>), 1.68 (3H, s, CH<sub>3acac</sub>), 1.48 (1H, m, CHCH<sub>2</sub>CH), 1.33 (6H, d, <sup>3</sup>J<sub>HH</sub> = 6.7, CH(CH<sub>3</sub>)<sub>2</sub>), 1.16 (6H, d, <sup>3</sup>J<sub>HH</sub> = 6.8, CH(CH<sub>3</sub>)<sub>2</sub>), 1.12 (6H, d, <sup>3</sup>J<sub>HH</sub> = 6.9, CH(CH<sub>3</sub>)<sub>2</sub>), 1.01 (6H, d, <sup>3</sup>J<sub>HH</sub> = 6.6, CH(CH<sub>3</sub>)<sub>2</sub>); <sup>13</sup>C NMR (CDCl<sub>3</sub>, 100 MHz, rt):  $\delta$  213.4 (d, <sup>1</sup>J<sub>RhC</sub> = 41.0, NCN), 191.2 (d, <sup>1</sup>J<sub>RhC</sub> = 68.0, CO), 186.2 (s, CCH<sub>3</sub>), 183.9 (s, CCH<sub>3</sub>), 147.9 (s, C<sub>Ar</sub>), 144.7 (s, C<sub>Ar</sub>), 144.4 (s, C<sub>Ar</sub>), 134.4 (s, =CH-), 127.9 (s, *p*-CH<sub>Ar</sub>), 124.8 (s, *m*-CH<sub>Ar</sub>), 124.2 (s, *m*-CH<sub>Ar</sub>), 99.7 (s, CH<sub>acac</sub>), 57.2 (s, NCH<sub>2</sub>), 50.8 (s, CHCH<sub>2</sub>CH), 47.3 (s, =CHCH-), 40.4 (s, NCH<sub>2</sub>CH), 28.9 (s, CH(CH<sub>3</sub>)<sub>2</sub>), 28.6 (s, CH<sub>3acac</sub>), 28.5 (s, CH<sub>3acac</sub>), 27.1, 25.9, 23.7 and 22.7 (s, CH(CH<sub>3</sub>)<sub>2</sub>); IR:  $\nu(\text{CO}) = 1947.7 \text{ cm}^{-1}$ . MS (ES):  $m/z$  713.3192 ([M + H]<sup>+</sup>; C<sub>40</sub>H<sub>54</sub>N<sub>2</sub>O<sub>3</sub>Rh requires 713.3189).

**Compound 5.18.**

Compound **5** (15 mg, 0.023 mmol) was dissolved in 5 ml of deuterated chloroform and stirred for 24h under a hydrogen atmosphere (2 bar) to give a brown suspension. The suspension was filtrated to afford a yellow solution. Compound **7** was isolated in a 79% yield (12 mg, 0.018) as a yellow solid after evaporation

of the solvent under reduced pressure.  $^1\text{H}$  NMR ( $\text{CDCl}_3$ , 400 MHz, rt):  $\delta$  6.84 (4H, s,  $m\text{-CH}_{\text{Mes}}$ , i1+i2), 6.74 (2H, s,  $m\text{-CH}_{\text{Mes}}$ , i1+i2), 6.72(2H, s,  $m\text{-CH}_{\text{Mes}}$ , i1+i2), 5.07 (1H, s,  $\text{CH}_{\text{acac}}$ ), 5.00 (1H, s,  $\text{CH}_{\text{acac}}$ ), 4.48 (4H, bq,  $^3J_{\text{HH}} = 13.9$ ,  $\text{NCH}_2$ , i1+i2), 3.08 (4H, bd,  $^3J_{\text{HH}} = 13.9$ ,  $\text{NCH}_2$ , i1+i2), 2.68 (4H, m,  $\text{NCH}_2\text{CH}$ , i1+i2) 2.10-2.32 (40H, m,  $\text{CH}_3_{\text{Mes}}+\text{CH}_2\text{CH}_2\text{CH}$ , i1+i2), 1.78 (3H, s,  $\text{CH}_3_{\text{acac}}$ , i1), 1.74 (3H, s,  $\text{CH}_3_{\text{acac}}$ , i2), 1.65 (3H, s,  $\text{CH}_3_{\text{acac}}$ , i1), 1.63 (3H, s,  $\text{CH}_3_{\text{acac}}$ , i2), 1.47 (4H, m,  $\text{CHCH}_2\text{CH}$ , i1+i2), 1.33-1.18 (8H, m,  $\text{CH}_2\text{CH}_2\text{CH}$ , i1+i2).  $^{13}\text{C}$  NMR ( $\text{CDCl}_3$ , 400 MHz, rt):  $\delta$  206.9 (d,  $^1J_{\text{RhC}} = 53.6$ ,  $\text{NCN}$ , i1), 206.7 (d,  $^1J_{\text{RhC}} = 54.3$ ,  $\text{NCN}$ , i2), 190.5 (d,  $^1J_{\text{RhC}} = 49.5$ , CO, i1), 189.6 (d,  $^1J_{\text{RhC}} = 49.4$ , CO, i2), 185.7 (s,  $\text{CCH}_3_{\text{acac}}$ , i1), 185.6 (s,  $\text{CCH}_3_{\text{acac}}$ , i1), 182.0 ( $\text{CCH}_3_{\text{acac}}$ , i1 and i2), 145.0 (s,  $\text{C}_{\text{Ar}}$ , i1), 144.7 (s,  $\text{C}_{\text{Ar}}$ , i1), 135.2 (s,  $\text{C}_{\text{Ar}}$ , i1 and i2), 134.3 (s,  $\text{C}_{\text{Ar}}$ , i1 and i2), 133.8 (s,  $\text{C}_{\text{Ar}}$ , i1 and i2), 133.1 (s,  $\text{C}_{\text{Ar}}$ , i1 and i2), 128.6 (s,  $m\text{-CH}$ ), 128.5 (s,  $m\text{-CH}$ ), 128.3 (s,  $m\text{-CH}$ ), 128.0 (s,  $m\text{-CH}$ ), 98.7 (s,  $\text{CH}_{\text{acac}}$ , i1 and i2), 52.8 and 52.7 (s,  $\text{NCH}_2$ , i1 and i2), 40.1, 39.7 and 39.6 (s,  $\text{NCH}_2\text{CH}+\text{CH}_2\text{CH}_2\text{CH}$ , i1+i2), 39.5 (s,  $\text{CHCH}_2\text{CH}$ , i1 and i2), 26.5 25.8 and 25.5 (s,  $\text{CH}_3_{\text{acac}}$ , i1 and i2), 21.5 ( $\text{CH}_2\text{CH}_2\text{CH}$ , i1+i2) 20.0 (s,  $p\text{-CH}_3$ , i1 and i2), 18.0 and 17.8 (s,  $o\text{-CH}_3$ , i1 and i2). IR:  $\nu(\text{CO}) = 1943.9 \text{ cm}^{-1}$ .

## Chapter 6 Catalytic hydrogenation and transfer hydrogenation reactions

# Chapter



The reduction of ketones or aldehydes is the most common carbonyl reduction reaction in organic synthesis, and is a key reaction in organic synthesis.

The most commonly used methods for reduction of ketones are metal hydride reduction, catalytic hydrogenation and transfer hydrogenation. The latter represents a powerful

### Catalytic hydrogenation and transfer hydrogenation reactions

Catalytic hydrogenation is a variant of hydrogenation, where the source of hydrogen is not molecular hydrogen, but the reaction is the presence of a catalyst (Scheme 6.1). The most

<b>6.1. Introduction</b> .....	<b>182</b>
6.1.1. Reduction of ketones.....	182
6.1.1.1. Direct hydrogen transfer.....	183
6.1.1.2. Hydridic route.....	183
6.1.2. Reduction of alkenes.....	186
<b>6.2. Results and discussion</b> .....	<b>188</b>
6.2.1. Transfer hydrogenation.....	188
6.2.2. Catalytic hydrogenation of alkenes.....	192
<b>6.3. Experimental</b> .....	<b>195</b>

W. H. Glaze, *Catalytic Hydrogenation*, Butterworths, London, 1957; (b) J. H. Goldstein, *Catalytic Hydrogenation*, Wiley, New York, 1958; (c) K. Hariguchi, *Catalytic Hydrogenation*, Wiley, New York, 1997; (d) P. M. Collins, *Catalytic Hydrogenation*, Wiley, New York, 1997; (e) P. M. Collins, *Catalytic Hydrogenation*, Wiley, New York, 1997; (f) P. M. Collins, *Catalytic Hydrogenation*, Wiley, New York, 1997; (g) P. M. Collins, *Catalytic Hydrogenation*, Wiley, New York, 1997; (h) P. M. Collins, *Catalytic Hydrogenation*, Wiley, New York, 1997; (i) P. M. Collins, *Catalytic Hydrogenation*, Wiley, New York, 1997; (j) P. M. Collins, *Catalytic Hydrogenation*, Wiley, New York, 1997; (k) P. M. Collins, *Catalytic Hydrogenation*, Wiley, New York, 1997; (l) P. M. Collins, *Catalytic Hydrogenation*, Wiley, New York, 1997; (m) P. M. Collins, *Catalytic Hydrogenation*, Wiley, New York, 1997; (n) P. M. Collins, *Catalytic Hydrogenation*, Wiley, New York, 1997; (o) P. M. Collins, *Catalytic Hydrogenation*, Wiley, New York, 1997; (p) P. M. Collins, *Catalytic Hydrogenation*, Wiley, New York, 1997; (q) P. M. Collins, *Catalytic Hydrogenation*, Wiley, New York, 1997; (r) P. M. Collins, *Catalytic Hydrogenation*, Wiley, New York, 1997; (s) P. M. Collins, *Catalytic Hydrogenation*, Wiley, New York, 1997; (t) P. M. Collins, *Catalytic Hydrogenation*, Wiley, New York, 1997; (u) P. M. Collins, *Catalytic Hydrogenation*, Wiley, New York, 1997; (v) P. M. Collins, *Catalytic Hydrogenation*, Wiley, New York, 1997; (w) P. M. Collins, *Catalytic Hydrogenation*, Wiley, New York, 1997; (x) P. M. Collins, *Catalytic Hydrogenation*, Wiley, New York, 1997; (y) P. M. Collins, *Catalytic Hydrogenation*, Wiley, New York, 1997; (z) P. M. Collins, *Catalytic Hydrogenation*, Wiley, New York, 1997.

## Chapter 6. Catalytic hydrogenation and transfer hydrogenation reactions.

### 6.1. Introduction.

#### 6.1.1. Reduction of ketones.

The reduction of ketones or aldehydes is the most successful approach to the synthesis of alcohols with respect to industrial applications<sup>1</sup> and is a key reaction in organic synthesis.<sup>2</sup> The most commonly used methods for reduction of ketones are: metal hydride reduction, catalytic hydrogenation and transfer hydrogenation. The latter represents a powerful strategy due to the wide number of alcohols accessible and mild reaction conditions (no need for hydrogen pressure), which makes this type of reactions economic and environmentally friendly.<sup>3</sup>

Transfer hydrogenation is a variant of hydrogenation, where the source of hydrogen is not molecular H<sub>2</sub> but a hydrogen donor in the presence of a catalyst (Scheme 6.1). The most commonly used hydrogen donor is isopropanol, which is employed as a solvent (a large excess is needed in order to overcome the unfavourable equilibrium<sup>4</sup>) with potassium hydroxide or potassium *tert*-butoxide as a base.

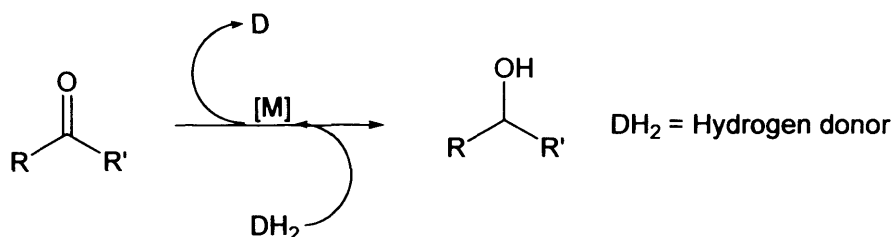
---

<sup>1</sup> Enthaler, Stephan; Jackstell, Ralf; Hagemann, Bernhard; Junge, Kathrin; Erre, Giulia; Beller, Matthias *J. Organomet. Chem.* **2006**, *691*, 4652.

<sup>2</sup> (a) Noyori, R. *Asymmetric Catalysis in Organic Synthesis*; John Wiley: New York, 1994. (b) *Catalytic Asymmetric Synthesis*; Ojima, I., Ed.; VCH: Berlin, 1993.

<sup>3</sup> (a) Gladiali, S.; Alberico, E. *Chem. Soc. Rev.* **2006**, *35*, 226; (b) Zassinovich, G.; Mestroni, G.; Gladiali, S. *Chem. Rev.* **1992**, *51*, 1051; (c) Noyori, R.; Hashiguchi, S. *Acc. Chem. Res.* **1997**, *30*, 97; (d) Gladiali, S.; Mestroni, G. in: Beller, M.; Bolm, C. (Eds.) *Transition Metals for Organic Synthesis, second ed.*, Wiley-VCH, Weinheim, **2004**, 145; (e) Blaser, H.-U.; Malan, C.; Pugin, B.; Spindler, F.; Studer, M. *Adv. Synth. Catal.* **2003**, *345*, 103.

<sup>4</sup> (a) Palmer, M. J.; Wills, M. *Tetrahedron: Asymmetry* **1999**, *10*, 2045 (b) Adkins, H.; Eloffson, R. M.; Rossow, A. G.; Robinson, C. C. *J. Am. Chem. Soc.* **1949**, *71*, 3622.



**Scheme 6.1.** Schematic representation of a transfer hydrogenation.

In most cases, two discrete reaction mechanisms are accepted for metal catalysed transfer hydrogenation of ketones: (a) direct hydrogen transfer; and (b) *via* an M-H hydridic route.<sup>1,4a</sup>

#### 6.1.1.1. Direct hydrogen transfer.

This is a concerted process, which entails the formation of a six-membered cyclic transition state composed of the hydrogen donor (*i*PrOH) and hydrogen acceptor (ketone) and the metal centre (Figure 6.1). This mechanism is similar to that proposed for the Meerwein–Ponndorf–Verley (MPV) reduction or for the Oppenaur oxidation.<sup>5</sup>

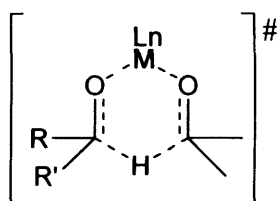


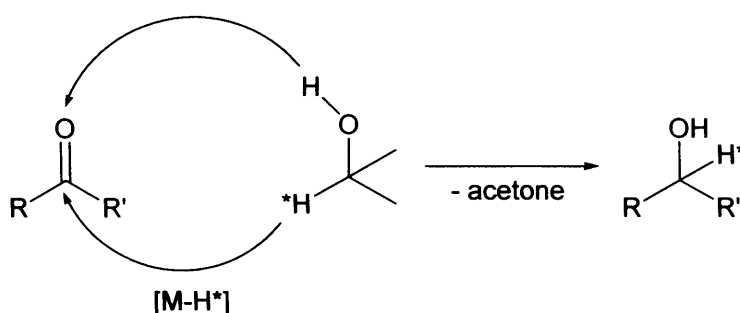
**Figure 6.1.** Transition state for a direct hydrogen transfer.

#### 6.1.1.2. Hydridic route.

This mechanism is the generally observed for transition metal complexes and entails the formation of a metal hydride as an intermediate species in the catalytic process. Depending on the type of intermediate the hydridic route shows two possible pathways, the

<sup>5</sup> (a) Hach, V. *J. Org. Chem.* **1973**, *38*, 293. (b) de Graauw, C. F.; Peters, J. A.; van Bekkum, H.; Huskens, J. *Synthesis* **1994**, 1007. (c) Boronat, Mercedes; Corma, Avelino; Renz, Michael *J. Phys. Chem. B* **2006**, *110*, 21168.

monohydride or dihydride mechanism.<sup>6</sup> The former entails the formation of a metal monohydride by donation of hydrogen from the isopropanol's C-H, which then undergoes hydride transfer to the carbonylic carbon at the coordinated ketone. It is worth noting that this mechanism can be either concerted or stepwise if the hydrogen transfer occurs in the outer-sphere of the metal (no coordination of the ketone); however, when the hydrogen transfer takes place in the inner-sphere (coordination of the ketone) the mechanism is always stepwise and involves the formation of an alkoxide followed by  $\beta$ -hydride elimination. Interestingly, the hydride and the proton keep their identity, *i.e.* the C-H from the isopropanol molecule ends up as a C-H in the resulting alcohol and the proton from the O-H in the transfer agent as the O-H in the final product (Scheme 6.2).



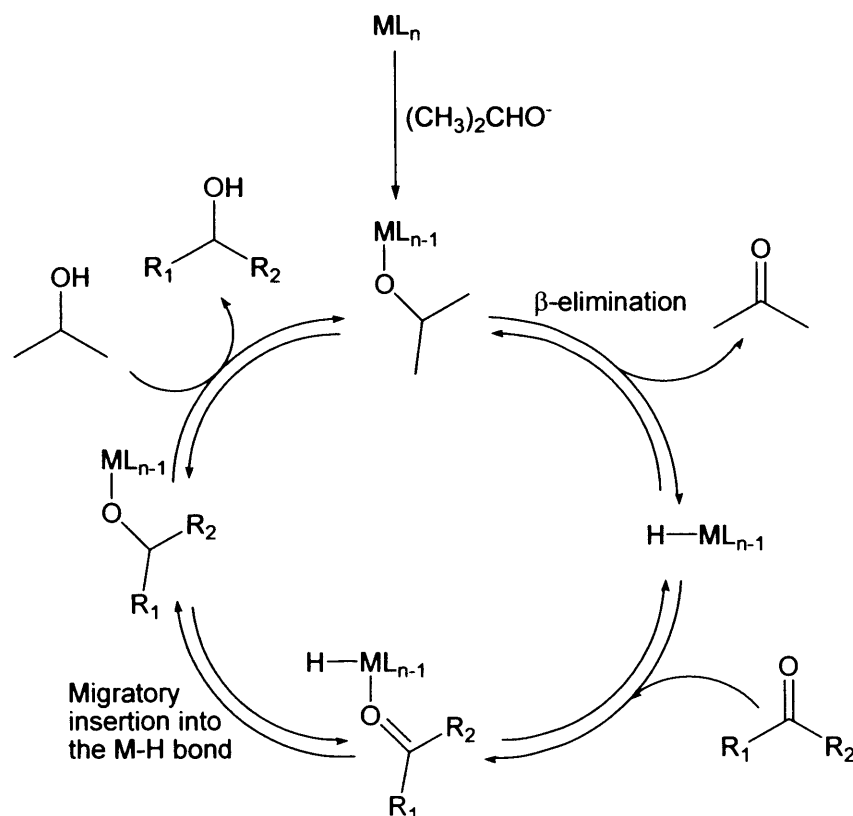
**Scheme 6.2.** Schematic representation of a hydride transfer (monohydride route).

Theoretical studies on rhodium-catalysed transfer hydrogenations, where the active species is a Rh-COD-diamine complex, concluded that the mechanism takes place *via* the monohydride route in a stepwise hydrogen transfer<sup>7</sup> (Scheme 6.3). Interestingly, the  $\beta$ -

<sup>6</sup> (a) Pàmies, O.; Bäckvall, J.E. *Chem. Eur. J.* **2001**, 5052. (b) Aranyos, A.; Csajnyik, G.; Szabó, K.J.; Bäckvall, J.E. *Chem. Commun.* **1999**, 351. (c) Almeida, M.L.S.; Beller, M.; Wang, G.Z.; Bäckvall, J.E. *Chem. Eur. J.* **1996**, 1533. (d) Wang, G.Z.; Bäckvall, J.E. *J. Chem. Soc. Chem. Commun.* **1992**, 337. (e) Wang, G.Z.; Bäckvall, J.E. *J. Chem. Soc. Chem. Commun.* **1992**, 980. (f) Chowdhury, R.L.; Bäckvall, J.E. *J. Chem. Soc. Chem. Commun.* **1991**, 1063. (g) Samec, J.S.M.; Bäckvall, J.E.; Andersson, P.G. P. Brandt, *Chem. Soc. Rev.* **2006**, 35, 237.

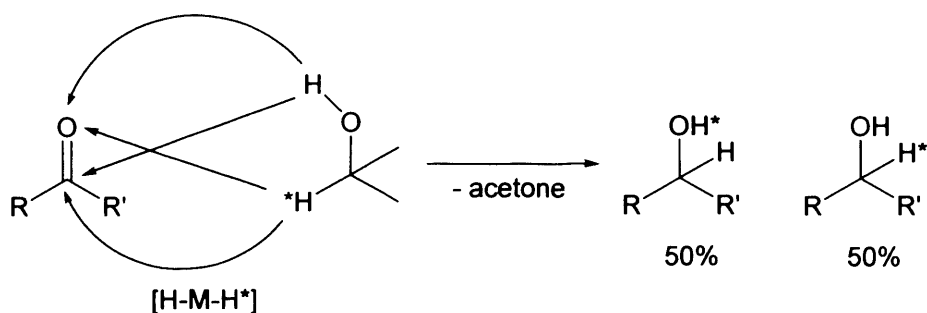
<sup>7</sup> (a) Bernard, M.; Guiral, V.; Delbecq, F.; Fache, F.; Sautet, P.; Lemaire, M. *J. Am. Chem. Soc.* **1998**, 120, 1441; (b) Guiral, V.; Delbecq, F.; Sautet, P. *Organometallics* **2000**, 19, 1589; (c) Bernard, M.; Delbecq, F.; Sautet, P.; Fache, F.; Lemaire, M. *Organometallics* **2000**, 19, 5715; (d) Guiral, V.; Delbecq, F.; Sautet, P. *Organometallics* **2001**, 20, 2207.

elimination of the alkoxide's C-H, which leads to formation of the Rh-hydride complex is the rate determining step.



**Scheme 6.3.** Generic catalytic cycle for the reduction of ketones *via* the monohydride route.

On the contrary, when the catalyst operates through the dihydride mechanism, the protons at the C-H and O-H of the hydrogen donor lose their identity due to the formation of the metal dihydride (Scheme 6.4).



**Scheme 6.4.** Schematic representation of a hydride transfer (dihydride route).

The mechanism that takes place in a given system depends on the metal catalyst, hydrogen donor and substrate. For transition metals, hydridic routes are by far the most common.

Within transition metals, the most common route for rhodium and iridium catalysts is the monohydride while for ruthenium catalysts the mechanism depends on the ligand system.<sup>6g</sup>

### 6.1.2. Reduction of alkenes via direct and transfer hydrogenation.

Since the synthesis of Wilkinson's hydrogenation catalyst<sup>8</sup>  $\text{Rh}(\text{PPh}_3)_3\text{Cl}$ , a great deal of rhodium and iridium complexes bearing bulky phosphines first,<sup>9</sup> and more recently N-heterocyclic carbenes have proven to be active catalysts for alkene hydrogenation using molecular hydrogen.<sup>10</sup>

The first rhodium carbene complexes tested in catalytic hydrogenation of alkenes were those of the type  $[\text{Rh}(\text{L})(\text{COD})\text{Cl}]$  and  $[\text{Rh}(\text{L})(\text{CO})_2\text{Cl}]$  (L = carbene ligand). The latter are inactive because of the unfavourable electronic effects. The good donor ability of carbenes makes the metal more electron rich, which results in the strengthening of the M-CO bond.

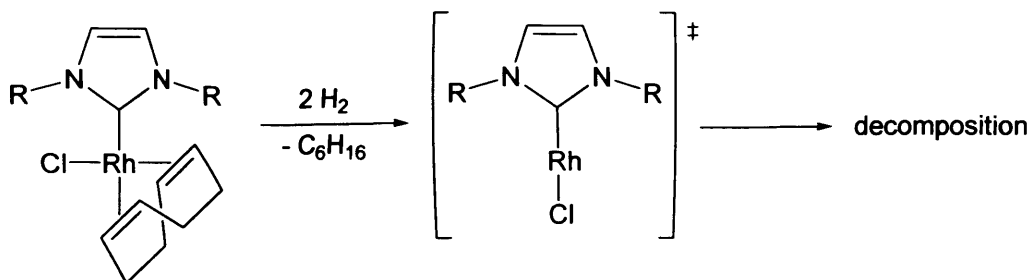
The former complexes are not useful for the hydrogenation of alkenes because of decomposition during the reaction or low activity. Herrmann *et al.* proposed that due to the presumably high stability of the carbene-metal bond, the olefinic chelating ligand (COD) may be reduced under the reaction conditions to an alkane forming a linear Rh intermediate (Scheme 6.4). The resulting complex is unstable and decomposes to give rhodium particles.<sup>8, 10b</sup>

<sup>8</sup> (a) Osborn, J. A.; Jardine, F. H.; Young, J. F.; Wilkinson, G. *J. Chem. Soc. (A)* **1966**, 1711. (b) Wilkinson, G. *German Patent* DE 1816063 A1, **1969**.

<sup>9</sup> (a) Evans, D. A.; Fu, G. C.; Hoveyda, A. H. *J. Am. Chem. Soc.* **1992**, 114, 6671. (b) Stork, G.; Kahne, D. E. *J. Am. Chem. Soc.* **1983**, 105, 1072. (c) Crabtree, R. H.; Davis, M. W. *Organometallics* **1983**, 2, 681.

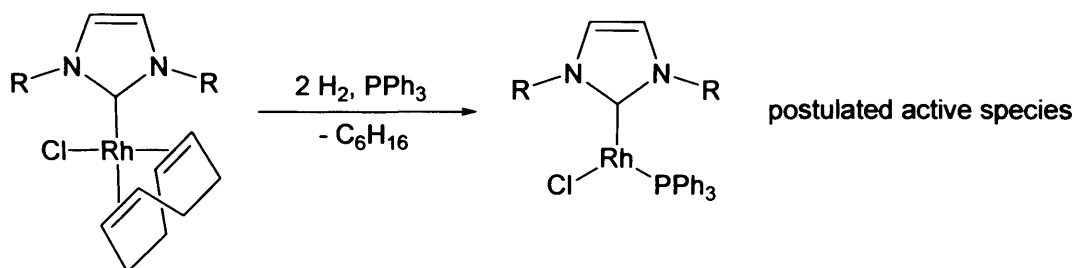
<sup>10</sup> (a) Vazquez-Serrano, Leslie D.; Owens, Bridget T.; Buriak, Jillian M. *Inorganica Chimica Acta* **2006**, 359, 2786. (b) Herrmann, Wolfgang A.; Frey, Guido D.; Herdtweck, Eberhardt; Steinbecka, Martin *Adv. Synth. Catal.* **2007**, 349, 1677. (c) Allen, D. P.; Crudden, C. M.; Calhoun, L. A.; Wang, R. *J. Organomet. Chem.* **2004**, 689, 3203. d) Allen, D. P.; Crudden, C. M.; Calhoun, L. A.; Wang, R.; Decken, A. *J. Organomet. Chem.* **2005**, 690, 5736. (e) Herrmann, W. A.; Baskakov, D.; Herdtweck, E.; Hoffmann, S. D.; Bunlaksananusorn, T.; Rampf, F.; Rodefeld, L. *Organometallics* **2006**, 25, 2449.





**Scheme 6.4.** Possible decomposition pathway of Rh(NHC)(COD)Cl complexes.

Addition of PPh<sub>3</sub> to the reaction mixture stabilised the active species by formation of tricoordinated complex (Scheme 6.5). This avoids the decomposition of the catalyst and, consequently, improves its activity.<sup>11</sup>



**Scheme 6.5.** Stabilisation of the active species.

The activity of rhodium and iridium carbene complexes for catalytic hydrogenation and transfer hydrogenation was dramatically improved by the use of chelating bis-carbenes. Peris and co-workers synthesized the first Rh(III) bis-carbene chelating species [Rh(III)(biscarbene)(OAc)<sub>2</sub>],<sup>12</sup> which were followed by the same type of Ir(III) complexes published by Crabtree *et al.*<sup>13</sup> Contrary to what is observed for phosphines, Ir complexes are more active than their Rh analogues for transfer hydrogenation and catalytic hydrogenation.<sup>10a, 13, 14</sup>

<sup>11</sup> Neveling, A.; Julius, G. R.; Cronje, S.; Esterhuysen, C.; Raubenheimer, H. G. *J. Chem. Soc., Dalton Trans.* **2005**, 181.

<sup>12</sup> Albrecht, M.; Crabtree, R. H.; Mata, J.; Peris, E. *Chem. Commun.* **2002**, 32.

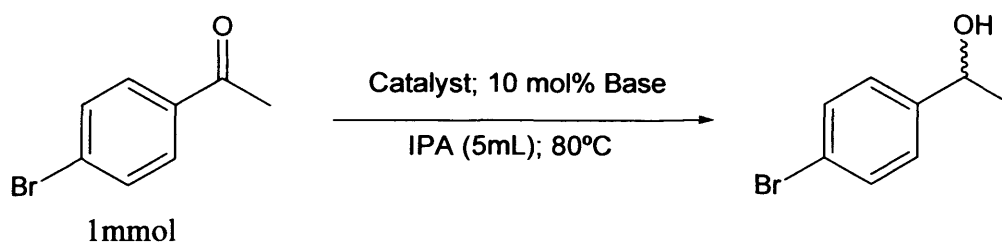
<sup>13</sup> Albrecht, Martin; Miecznikowski, J. R.; Samuel, Amanda; Faller, J. W.; Crabtree, R. H. *Organometallics*, **2002**, *21*, 3596.

<sup>14</sup> (a) Linn, D. E.; Halpern, G. *J. Am. Chem. Soc.* **1987**, *109*, 2969. (b) Zassinovich, G.; Mestroni, G.; Gladiali, S. *Chem. Rev.* **1992**, *92*, 1051. (c) Gladiali, S.; Mestroni, G. In *Transition Metals for*

The work presented in this chapter is focused on the catalytic activity of the previously presented rhodium and iridium complexes (*Chapter 4*) towards hydrogenation with molecular hydrogen and transfer hydrogenation.

## 6.2. Results and discussion.

### 6.2.1. Ketone transfer hydrogenation.



**Scheme 6.6.** Catalytic hydrogen transfer of 4-bromoacetophenone.

The activity of rhodium (I) and iridium (I) carbene complexes  $[\text{M}(\text{NHC})(\text{COD})\text{Cl}]$  presented in *Chapter 4* was tested at different catalyst concentrations. This allowed a direct comparison between Rh and Ir complexes of expanded carbenes and also a study of the effects of alkyl and aromatic carbene N-substituents (Table 6.1).

The Ir and Rh complexes,  $[\text{M}(7\text{-Cy})(\text{COD})\text{Cl}]$ , catalyse the reduction of 4-bromoacetophenone to the racemic mixture of the corresponding alcohol at  $80^\circ\text{C}$  via hydrogen transfer from *i*PrOH with potassium *tert*-butoxide as the base (Scheme 6.6). The iridium complex  $[\text{Ir}(7\text{-Cy})(\text{COD})\text{Cl}]$  shows a higher activity than its rhodium analogue, as has been previously reported for carbene based catalysts.<sup>10a</sup>

On the other hand, rhodium (I) complexes of saturated carbenes with aromatic N-substituents  $[\text{Rh}(7,6,5\text{-Mes})(\text{COD})\text{Cl}]$  show no activity whatsoever towards transfer hydrogenation under the previously described conditions.

The significant effect of the N-substituents on the activity of the catalyst suggests a hydride mechanism, similar to the one proposed by Noyori and co-workers.<sup>15</sup> This mechanism

---

*Organic Synthesis*; Beller, M., Bolm, C., Eds.; Wiley-VCH: Weinheim, Germany, 1998; Vol. 2, pp 97-119. (d) Noyori, R.; Hashiguchi, S. *Acc. Chem. Res.* **1997**, *30*, 97.

<sup>15</sup> (a) Yamakawa, M.; Ito, H.; Noyori, R. *J. Am. Chem. Soc.* **2000**, *122*, 1466. (b) Hillier, Anna C.; Lee, Hon Man; Stevens, Edwin D.; Nolan, S. P. *Organometallics* **2001**, *20*, 4246

implies the coordination of the substrate previous to its reduction by the hydride. Therefore, the steric properties of the carbene play an important role on the selectivity and reactivity of the system. Although **7-Mes** and **7-Cy** rhodium complexes do not show appreciable electronic differences, the **7-Mes** are significantly more sterically hindered than their **Cy** counterparts. A proof of this is that the carbene ligand in complex [Rh(**7-Cy**)(CO)<sub>2</sub>Cl] rotates at ambient temperature, whereas **7-Mes** does not, indicating that the aromatic N-substitution affords a more encumbered ligand as previously explained in section 4.2.2.1.

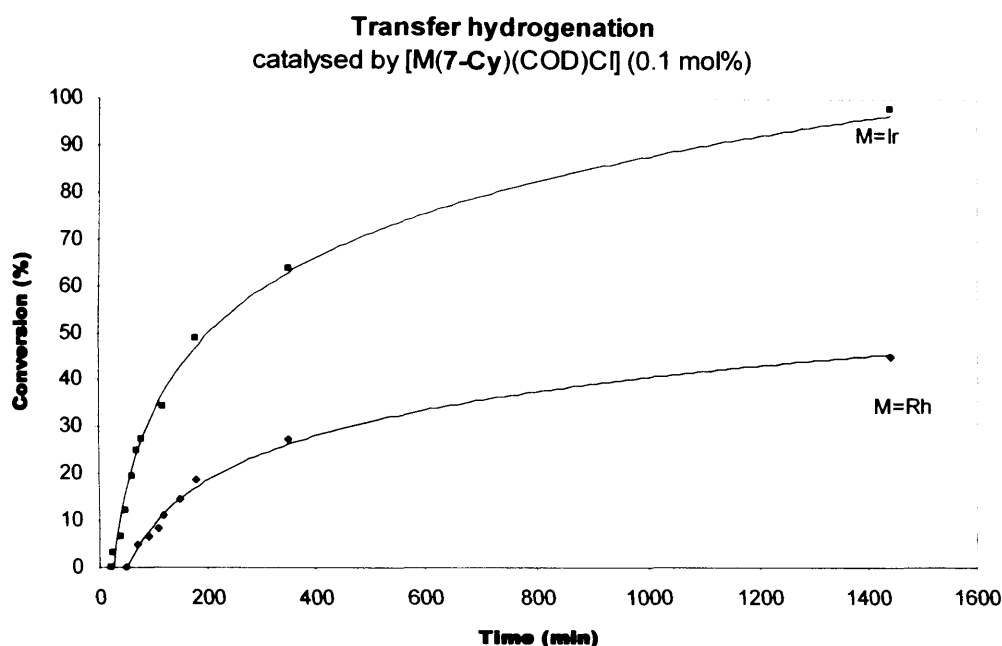
**Table 6.1.** Reaction conditions: 10 mol% base,  $t = 80^\circ\text{C}$ , 24 h, 5 mL of <sup>i</sup>PrOH per 1 mmol of substrate; conversion calculated by <sup>1</sup>H NMR.

Catalyst (mol %)	Solvent/base	Conversion [%]	TON
Ir( <b>7-Cy</b> )(COD)Cl (0.1)	<sup>i</sup> PrOH/K <sup>t</sup> BuO	99	990
Ir( <b>7-Cy</b> )(COD)Cl (0.01)	<sup>i</sup> PrOH/K <sup>t</sup> BuO	61	6100
Ir( <b>7-Cy</b> )(COD)Cl (0.001)	<sup>i</sup> PrOH/K <sup>t</sup> BuO	54	54000
Ir( <b>7-Cy</b> )(COD)Cl (0.0001)	<sup>i</sup> PrOH/K <sup>t</sup> BuO	11	110000
Rh( <b>7-Cy</b> )(COD)Cl (1)	<sup>i</sup> PrOH/K <sup>t</sup> BuO	63	63
Rh( <b>7-Cy</b> )(COD)Cl (0.1)	<sup>i</sup> PrOH/K <sup>t</sup> BuO	47	470
Rh( <b>7-Cy</b> )(COD)Cl (0.01)	<sup>i</sup> PrOH/K <sup>t</sup> BuO	26	2600
Rh( <b>7-Cy</b> )(COD)Cl (0.001)	<sup>i</sup> PrOH/K <sup>t</sup> BuO	25	25000
Rh( <b>7-Mes</b> )(COD)Cl (1)	<sup>i</sup> PrOH/K <sup>t</sup> BuO or K[HMDS]	0	-
Rh( <b>7-Mes</b> )(COD)Cl (0.1)	<sup>i</sup> PrOH/K <sup>t</sup> BuO or K[HMDS]	0	-
Rh( <b>6-Mes</b> )(COD)Cl (1)	<sup>i</sup> PrOH/K <sup>t</sup> BuO or K[HMDS]	0	-
Rh( <b>6-Mes</b> )(COD)Cl (0.1)	<sup>i</sup> PrOH/K <sup>t</sup> BuO or K[HMDS]	0	-
Rh( <b>5-Mes</b> )(COD)Cl (1)	<sup>i</sup> PrOH/K <sup>t</sup> BuO or K[HMDS]	0	-
Rh( <b>5-Mes</b> )(COD)Cl (0.1)	<sup>i</sup> PrOH/K <sup>t</sup> BuO or K[HMDS]	0	-

The time dependence of the transfer hydrogenation of 4-bromoacetophenone using 0.1 mol% [Ir(**7-Cy**)(COD)Cl] or [Rh(**7-Cy**)(COD)Cl] as catalysts and 10 mol% of K<sup>t</sup>BuO is shown in plot 6.1. The solid lines correspond to a pseudo-first-order fit with  $k = 0.0032 \pm 0.0001 \text{ min}^{-1}$  for [Ir(**7-Cy**)(COD)Cl] and  $k = 0.0004 \pm 0.0001 \text{ min}^{-1}$  for [Rh(**7-Cy**)(COD)Cl] (values obtained from plots 6.2.a and 6.2.b). At early times the plots show a

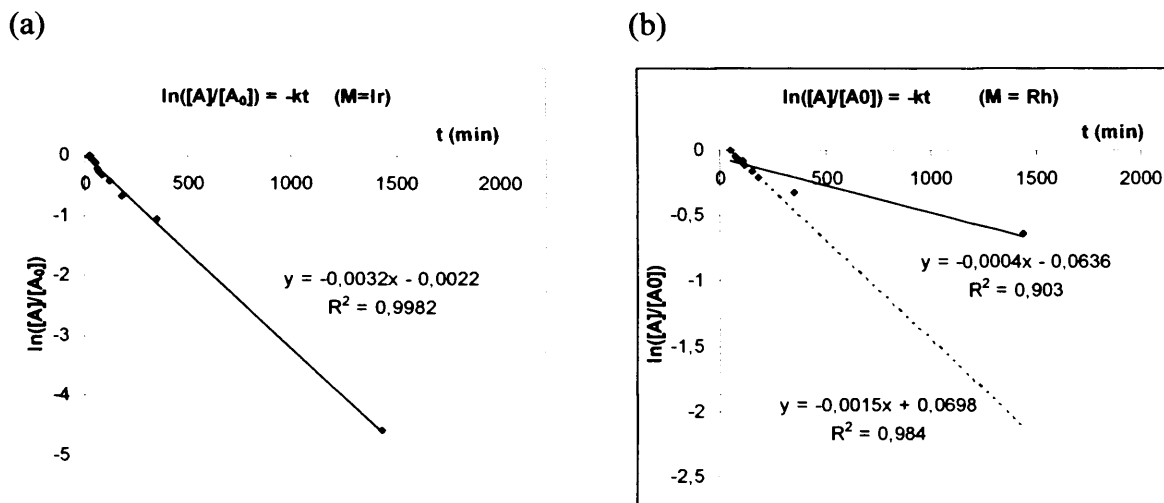
delay in the initiation of the catalytic process, probably caused by the low catalytic activity at low temperatures.

The TON and TOF obtained after 3h are, respectively, 490 and 163 h<sup>-1</sup> for [Ir(7-Cy)(COD)Cl] and 190 and 63 h<sup>-1</sup> for [Rh(7-Cy)(COD)Cl].



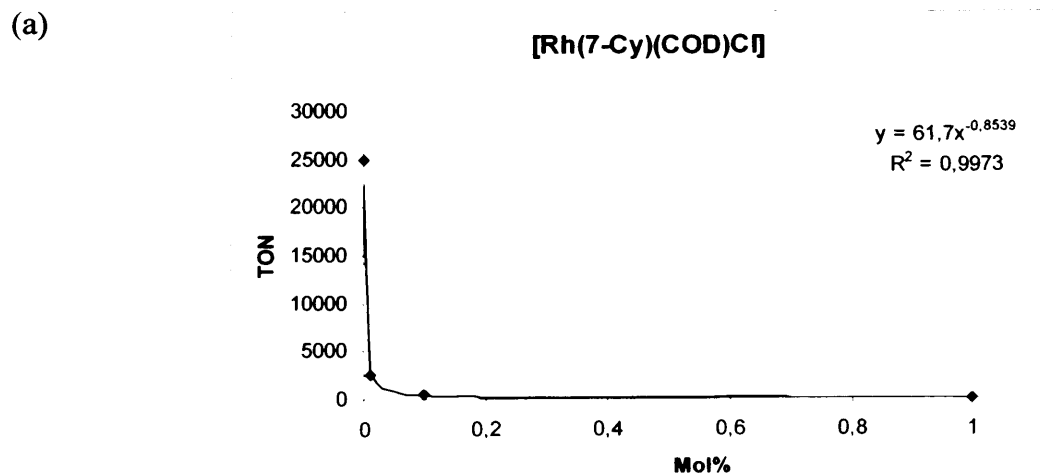
**Plot 6.1.** Time dependence of the transfer hydrogenation of 4-bromoacetophenone using 0.1 mol % of [Ir(7-Cy)(COD)Cl] and [Rh(7-Cy)(COD)Cl] at 80°C with an excess of K<sup>t</sup>BuO.

Plots 6.2.a and 6.2.b show the change of the concentration of 4-chloroacetophenone with time. The fact that the plot of the concentration against the reaction time is a straight line reveals a pseudo-first-order behaviour in the case of the iridium catalyst. Conversely, the plot that corresponds to the rhodium catalyst (graphic 6.2.b) deviates from a straight line at long reaction times, but the data collected during the first 180 minutes of reaction does fit with a straight line, suggesting a loss of activity of the catalyst at long reaction times due to decomposition of the rhodium complex (a suspension of rhodium black is recovered after 24h of reaction). Taking into account only the data collected during the 180 min, the rate constant ( $k$ ) obtained for [Rh(7-Cy)(COD)Cl] is  $0.0015 \pm 0.0001 \text{ min}^{-1}$ .

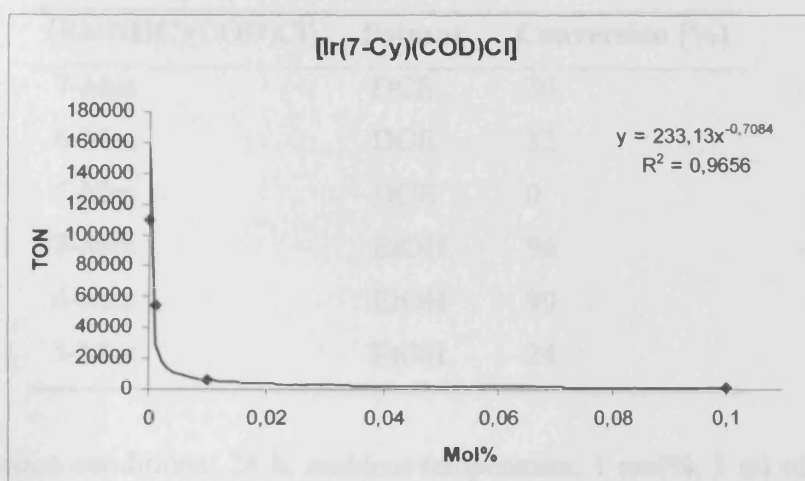


**Plots 6.2.a and 6.2.b.** Graphic determination of the rate constant ( $k$ ).  $[A]$  and  $[A_0]$  represent the concentration of 4-chloroacetophenone at a specific time and at  $t = 0$ , respectively. The dotted line represents the trend line taking into account only the data collected during the first 180 minutes of reaction.

The representation of the TON after 24h of reaction against the mol% of catalyst used in the reaction shows an exponential increase of the catalytic activity of the Rh and Ir complexes when their concentration decreases (plots 6.3.a and 6.3.b respectively).



(b)



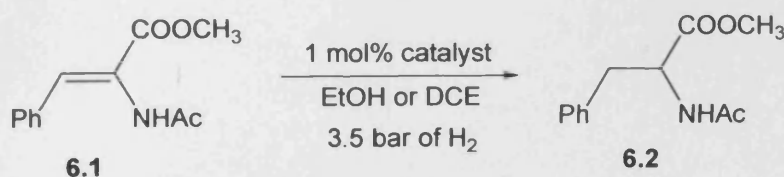
**Plots 6.3.a and 6.3.b.** Representation of the TON after the 24h (Y axis) against the concentration of the Rh (a) and Ir (b) catalysts in mol% (X axis).

### 6.2.2. Catalytic hydrogenation of alkenes with molecular hydrogen.

As mentioned in the introduction of this chapter when  $[\text{Rh}(\text{NHC})(\text{COD})\text{Cl}]$  complexes are used as catalysts in the catalytic hydrogenation of alkenes, the active species involved is assumed to be a linear  $\text{NHC-Rh-Cl}$ . Due to the lack of stabilisation this linear complex undergoes decomposition to rhodium particles. Therefore, a ligand capable of providing a better steric protection of the metal centre, such as expanded carbenes, would enhance the catalytic performance of this type of complexes by avoiding the decomposition of the active species.

As previously mentioned, the effect of the opening of the  $\text{N-C}_{\text{NHC}}\text{-N}$  angle in expanded carbenes is to twist the N-substituents towards the metal centre effectively blocking two faces of the metal coordination sphere. Consequently, the use of expanded carbenes in catalytic hydrogenation should render active species more reluctant to decompose.

In order to explore the above postulate  $[\text{Rh}(\text{NHC})(\text{COD})\text{Cl}]$  complexes with 5, 6 and 7-membered carbenes were tested in the catalytic hydrogenation of alkene **6.1** (Scheme 6.7).



**Scheme 6.7.** Catalytic hydrogenation of alkene **6.1**.

[Rh(NHC)(COD)Cl]	Solvent	Conversion [%]
7-Mes	DCE	30
6-Mes	DCE	32
5-Mes	DCE	0
7-Mes	EtOH	96
6-Mes	EtOH	99
5-Mes	EtOH	24

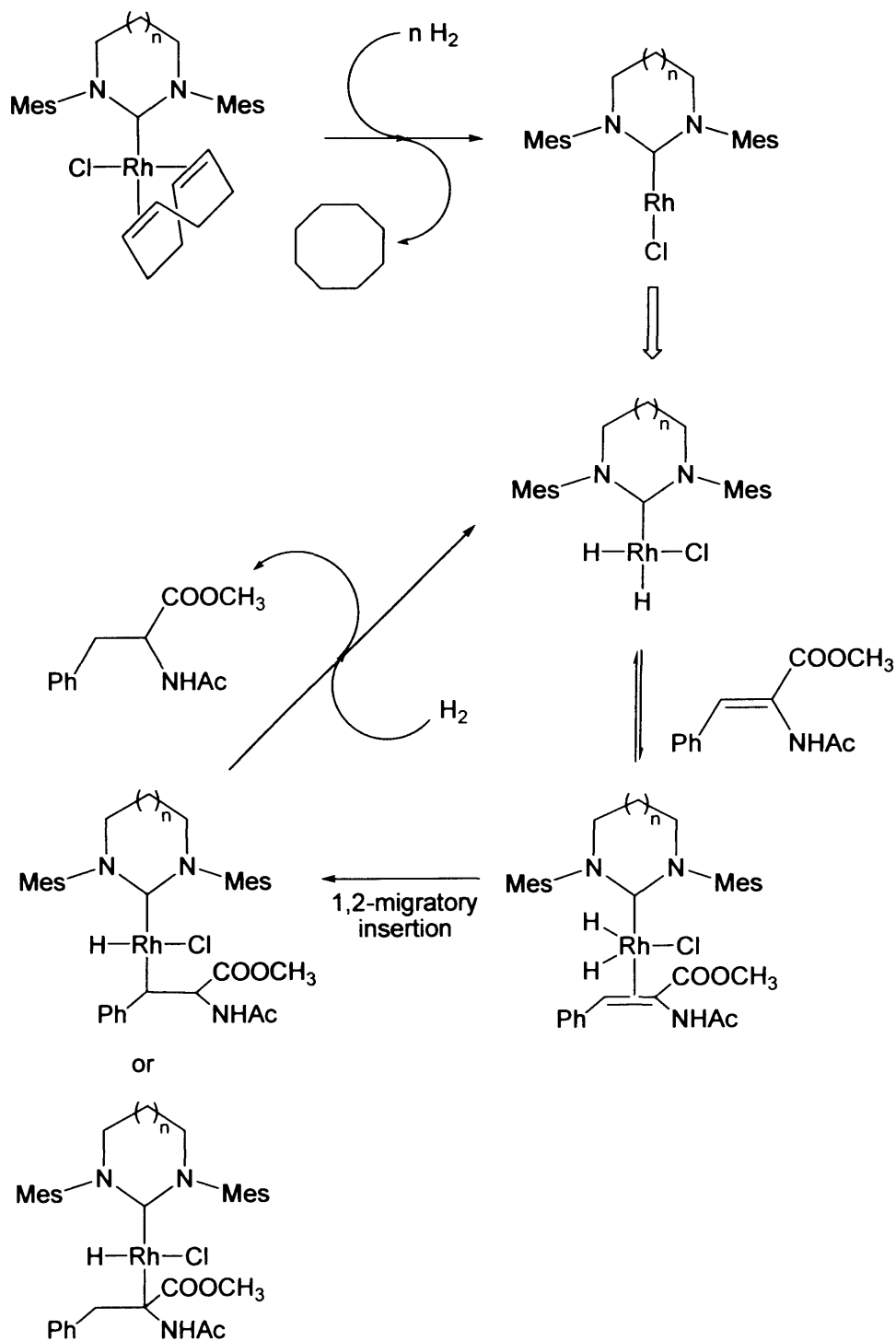
**Table 6.2.** Reaction conditions: 24 h, ambient temperature, 1 mol%, 5 ml of EtOH or 10 ml of DCE per 1 mmol of alkene **6.1**; Conversion calculated by  $^1\text{H}$  NMR.

From the results obtained, summarised in Table 6.2, it can be concluded that 6- and 7-membered expanded carbenes show a higher activity than their five-membered equivalent. Of note is that no significant difference in activity was observed between the **6-Mes** and the **7-Mes** complexes, if so, maybe a lower activity for the 7-membered counterpart. The use of dichloroethane as solvent affords the alkane **6.2** in low yields, however, when this is changed to ethanol the conversion increases dramatically. This might be a consequence of the better solubility of molecular hydrogen in alcohol or the somewhat better stabilisation of the active species in a coordinating solvent.

In all cases rhodium particles were recovered instead of the catalyst, which suggests that the reaction times must be shorter than 24 hours.

In conclusion, the catalyst performance is remarkably enhanced by the expansion of the ring. This suggests that the active species involved in this catalytic system are linear intermediates of the type [NHC-Rh-Cl], which undergo oxidative addition of molecular hydrogen. A mechanism based on the work reported by Buriak *et al.*<sup>10a, 16</sup> on complexes of general formula [Ir(NHC)(COD)L]X is depicted in Scheme 6.8.

<sup>16</sup> Vazquez-Serrano, L.D.; Owens, B.T.; Buriak, J.M. *Chem. Commun.* **2002**, 2518.



**Scheme 6.8.** Proposed mechanism for the hydrogenation of 6.1.



### 6.3. Experimental.

**General remarks.** All air sensitive experiments were performed under a nitrogen atmosphere in an MBraun glove box or under argon by standard Schlenk techniques. Ethanol, isopropanol and dichloroethane were distilled from calcium hydride under N<sub>2</sub> atmosphere. [Rh(NHC)(COD)Cl] complexes were synthesised according to the experimental procedure describe in *Chapter 4*. <sup>1</sup>H spectra were recorded using a Bruker Advance DPX<sub>400</sub> spectrometer.

#### **Transfer hydrogenation.**

The Rh/Ir catalyst precursor was dissolved in a solution of K<sup>t</sup>BuO (0.01 mmol) in 2-propanol (5 mL) and 4-bromoacetophenone (1mmol) in a Schlenk tube. The solution was heated to 353 K for 24 hours, volatiles were evaporated and the final conversion calculated by <sup>1</sup>H NMR.

The reaction progress was monitored by GC-MS analysis in order to calculate the time dependence of the transfer hydrogenation of 4-bromoacetophenone. Aliquotes of 0.1 ml were taken every 5 minutes for the first 30 minutes, every 10 minutes the next 90 minutes, every 30 minutes for the next hour, and finally another two samples were taken after 350 minutes and a final one after 24h. The samples were filtered through a short pad of silica, and the silica was washed with DCM.

#### **Description of GC/MS analysis**

Yields and substrate identities were determined by GC-MS analysis of reaction mixtures using an Agilent Technologies 6890N GC system with an Agilent Technologies 5973 inert MS detector with MSD. Column: Agilent 190915-433 capillary, 0.25 mm x 30 m x 0.25 μm. Capillary: 30 m x 250 μm x 0.25 μm nominal. Initial temperature at 50 °C, held for 4 minutes, ramp 5 °C/minute next 100 °C, ramp 10 °C/minute next 240 °C hold for 15 minutes. The temperature of the injector and the detector were held at 240 °C.

The retention times for analytes (in minutes), 4-bromoacetophenone 18.3 and 1-(4-bromophenyl)ethanol 18.7.

**General protocol for catalytic hydrogenation.**

The catalyst (0.01 mmol) and the substrate (1 mmol) were dissolved in 5 ml of the ethanol or 10 ml of dichloroethane and transferred to a glass autoclave. The autoclave was put under vacuum and finally pressurized with hydrogen (3.5 bar). The solution was stirred at ambient temperature for 24 hours. At the end of the reaction the solid impurities were filtered off, the volatiles were evaporated and the yield calculated by  $^1\text{H}$  NMR.

